PROPERTIES OF CROSSLINKED PHEMA HYDROGELS

A thesis submitted for the degree of
Doctor
of Philosophy in the Departments of
Physical and Inorganic Chemistry and
Chemical Engineering.
The University of Adelaide, May 1991.

Darrell Jonathan Bennett B.Sc.(Hons).

Table of Contents

SUMMARY

Poly (2-hydroxy ethyl methacrylate) (PHEMA) and a series of copolymers of PHEMA with various oligo (ethylene glycol) dimethacrylates, with the number of ethylene glycol units varying between one and nine, were prepared. The effect of sorbed water and the degree of crosslinking on the dynamic mechanical properties of these polymers, and the nature and state of water in the polymer was investigated using a variety of techniques. Polymer samples of varying hydration were prepared by conditioning at different relative humidities. The kinetics of sorption and desorption were also studied.

The amounts of freezing and non-freezing water in the polymer samples were determined using differential scanning calorimetry. Some fine structure to the melting endotherm was observed. The size and structure of the endotherm was found to be dependent on a number of factors including the time frozen, the temperaure at which the sample was frozen and the immediate past history of the sample. Crosslinking led to a large decrease in the relative amount of freezing water. ^{1}H solution NMR was also used to measure the relative amounts of mobile and bound water at differing temperatures. The decrease in mobile water at 258 K was measured with time and found to decrease in an exponential manner.

Proton enhanced magic angle spinning ^{13}C NMR was used to measure both the ^{13}C relaxation in the rotating frame, $T_{1\rho}(C)$, and the spin lock cross polarisation time, T_{SL}. $T_{1\rho}(C)$ values decreased with increasing amounts of sorbed water,especially when the sample Tg fell below the measuring temperature. This was most noticeable for the carbonyl and quaternary carbons. The carbonyl T_{SL} also showed a decrease as sorbed water increased.

Mechanical properties were measured using a free oscillation torsion pendulum. The greatest effect noted being a decrease in the glass transition

temperature, Tg, with increasing water sorption. β, γ and water induced transitions were also noted and found to vary with copolymer type and water content. A number of equations were used in order to try and predict the change in Tg due to sorbed water and crosslinking. These met with varying success.

Statement

The candidate, Darrell Jonathan Bennett, declares that (a) this thesis contains no material which has been accepted for the award of any other degree or diploma in any Univerity and that, to the best of the candidates knowledge and belief, the thesis contains no material previously published or written by another person except where due reference is made in the text of the thesis; and (b) the author consents to the thesis being made available for photocopying and loan if applicable if accepted for the award of the degree.

Darrell Jonathan Bennett, May 1991.

Acknowledgements

I would like to thank my supervisors, Dr P.E.M.Allen and Dr D.R.G.Williams for their help and assistance throughout the course of my postgraduate studies.

Thanks must also go to Mrs A.Hounslow for obtaining the solid state NMR spectra and also to Stan Hagias for teaching me how to use the WP-80 NMR spectrometer and for his assistance in the early part of this project. Mention must also be made of the assistance of the workshop staff in both departments.

Tony Clayton, Lai Chee Hoong and Darren Miller should also be ackowledged for their part in making life in the lab a bit more interesting.

I would also like to thank my parents for their support and finally special thanks to Jane for her help and love, especially in the latter stages of this work.

ABBREVIATIONS

DiEGDMA	di (ethylene glycol) dimethacrylate.
DSC	differential scanning calorimetry
EGDMA	ethylene glycol dimethacrylate
EWC	equilibrium water content
MMA	methyl methacrylate
NMR	nuclear magnetic resonance
OED	oligo (ethylene glycol) dimethacrylate
PEMAS	proton enhanced magic-angle-spinning
PHEMA	poly(2-hydroxy ethyl methacrylate)
P400	poly400 (ethylene glycol) dimethacrylate
TBO	t-butyl per-2 ethyl hexanoate
TEGDMA	tetra (ethylene glycol) dimethacrylate
T_g	glass transition temperature
TP	torsion pendulum

CHAPTER ONE

INTRODUCTION

The preparation and possible biological uses of poly(2-hydroxy ethyl methacrylate) (PHEMA) were first described by Wichterle and Lim (1,2) in the early 1960s. HEMA monomer has the formula;

$$H_2C=C(CH_3)COOCH_2CH_2OH$$

The polar hydroxy group enables PHEMA to absorb large amounts of water, up to 40-45% in some cases, of the total weight of the hydrogel (3-6). This also has the effect of substantially lowering the glass transition temperature (T_g) (7-8) of the polymer making it rubbery at room temperature. Polymers of this type are usually classified as hydrogels.

The term gel can cover a variety of soft coherent substances ranging from lamellar mesophases, clays, amorphous vanadium pentoxide, phospholipids and also three dimensional or network polymers (9). Polymeric gels are capable of absorbing large amounts of water or other liquids while still still retaining such essential properties of solids as finite shear and compression moduli. For the purpose of this thesis the most useful definition of polymeric hydrogels is that of Aharoni and Edwards (9): a system consisting of a polymer network swollen with solvent, in this case water, where polymer network refers to the three dimensional polymeric structure excluding the occluded solvent.

The nature of synthetic hydrogels makes them suitable for such potential medical applications as soft contact lenses (10), reverse osmosis membranes (11-13), kidney dialysis membranes (14-16) and drug delivery systems (17-23). For many of these possible applications it is desirable to be able to manipulate the physical properties of the hydrogel in order to affect the transport or release of drugs or other chemicals through the hydrogel. PHEMA hydrogels are particularly useful for biomedical

applications as they exhibit a high degree of chemical stability and mechanical integrity. They have also been shown to be resistant to acid hydrolysis and reactions with amines (24), and incur alkaline hydrolysis only at high temperature and pH (25).

A number of techniques, such as differential scanning calorimetry (DSC) and nuclear magnetic resonance (NMR), are available for investigating the behaviour of water in polymers. This has led to a proliferation of terms used to describe the state of the water in the polymer (26-42) including terms such as primary and secondary, bound, interfacial, bulk, free and freezing and non-freezing. The techniques used and hysteresis effects can also change the types and amounts of water found.

The concept of hydration shells (43) has been used to describe the nature of the water binding process in hydrogels with non-freezing water molecules hydrogen bonded directly to the hydrophilic groups on the polymer with successive hydration shells of freezing water molecules surrounding the inner hydration shell. It has been proposed (44), in the case of PHEMA, that less than 20 wt % of water is strongly bound to the polymer, corresponding to two water molecules per polymer repeat unit. The so-called interfacial water accounts for a further 15%. It is believed to be bound by dipole-dipole interactions with hydroxy groups or hydrophobic interactions. The remaining water is freely diffusable.

It has been observed (45-46) that the water uptake of PHEMA is relatively insensitive to low degrees of crosslinking. This has been taken as an indication of a secondary, non-covalent network existing along with the primary, covalently bonded crosslink network. This secondary structure has been proposed to be due to hydrophobic interactions between either α-methyl groups or chain backbones (47) or hydrogen bonded hydroxy groups probably stabilised by the exclusion of water from the regions containing the bonds (48). Other studies indicate the possibility of interactions involving both hydroxy and carboxyl groups (49). This secondary structure

effectively crosslinks the polymer, controlling the swelling behaviour of the hydrogel. While low degrees of crosslinking have little effect on the water uptake this is not true for higher degrees of crosslinking which lead to a reduced water content (43).

Previous swelling work (37-41) has indicated that the maximum water content in homogeneous PHEMA hydrogels is approximately 40 wt%. This is the limiting water content for a transparent hydrogel. Above this the gels are heterogeneous and cloudy. A high water content for hydrogels in general has been found to be beneficial with respects to better transport and interfacial properties but unfortunately at the same time it tends to have an adverse effect on the mechanical properties (50-51). Alternatively the absence of "free water" has been reported as desirable for high salt rejection in the case of membranes used for desalination by reverse osmosis (52).

Much of the work here involves investigating the effect of crosslinking on the PHEMA hydrogel. PHEMA generally contains a small amount of crosslinking in its original form as a result of impurities in the HEMA left over from the production process. This impurity usually consists of ethylene glycol dimethacrylate (EGDMA). Even a small amount of EGDMA in the HEMA monomer has the effect of creating a network polymer which is insoluble in water.

EGDMA, however, is only the first in a series of oligo (ethylene glycol) dimethacrylates (OED) which have the general formula :

$$H_2C=C(CH_3)COO(CH_2CH_2O)_nCOC(CH_3)=CH_2$$

where the value of n regulates the length and flexibility of the oxyethylene (OE) backbone, both increasing as n increases.

OEDs with values of n ranging from one to nine were used in the preparation of crosslinked copolymers of PHEMA. The naming of the OEDS generally follows that of the n value initially so that OEDs with n=1,2,and 4 are called EGDMA, di-(ethylene glycol) dimethacrylate (DiEGDMA) and tetra-(ethylene glycol) dimethacrylate (TEGDMA)

respectively. When n>4, the name is based on the average molecular weight of the OE chain between methacrylate groups, so for (poly 400 ethylene glycol) dimethacrylate (P400) the mean value of n is approximately nine.

Varying the type and amount of OED used as as a crosslinking agent enables a number of different parameters to be varied. The EGDMA homopolymer is an extremely brittle glassy polymer with a very high T_g (53). As the OE length increases, however, the T_g of the respective OED homopolymers falls, with P400 having a T_g of 268 K(53). This property of the OEDs enables copolymers with HEMA to be formed that have a wide range of glass transition temperatures. It has also been noted (53) that the increase in polarity of the OEDs as n increases, due to the increasing number of ether groups, cause differences in water sorption properties with P400 absorbing much larger amounts of water than EGDMA . The choice of crosslinking agent used therefore presents the possibility of being able to control both the hydrophilicity of the crosslinked HEMA copolymer and therefore its water absorption properties, and also some of the bulk mechanical properties, such as its T_g.

Although the kinetics of water sorption into PHEMA has been previously studied (54-57) much of this was concerned with the effect that the amount of water in the initial polymerisation mixture had on the diffusion constant. Similarly little work has been done on the diffusion rate of water into crosslinked PHEMA copolymers. From the work that has been carried out it is apparent that the uptake of water into PHEMA can be described as a square root function of time and could therefore be modelled using Fickian kinetics (58-60). However the existence of separate water sorption fronts has been taken as an indication that it is not true Fickian sorption (58). Copolymerising HEMA with a crosslinking agent also changes the sorption kinetics and the hope has been expressed (60) that with the judicious use and selection of crosslinking agents it might be possible to

advantageously modify the rate of diffusion of water into the polymer. This possibility has been further explored in this thesis.

The desorption of water from these systems appears to have been neglected, despite its possible relevance to rates of drug release, so the desorption of water from the various copolymers has also been investigated.

Previous dynamic mechanical measurements of PHEMA hydrogels have indicated the existence of three relaxations in the dry polymer (7). The lowest temperature relaxation (140K) is presumed (7) due to internal rotations of the hydroxy side chain. A further relaxation observed at 300K has been ascribed to partial rotation of the $COOCH_2CH_2OH$ group while the high temperature relaxation (376K) (7) is due to large scale main chain motion occurring as the polymer changes from glassy to rubbery.

The addition of small molecules, including water, has been found to have an effect on all three of these transitions, with perhaps the greatest noted being its plasticising effect. Water and other solvents are also responsible for the appearance of a peak occurring at approximately 170K which has been presumed due to water interfering with polymer-polymer interactions and replacing them with polymer-solvent interactions (7). Dynamic mechanical testing has been carried out on various crosslinked PHEMA copolymers in order to determine the effect the degree of hydration and crosslinking has on the dynamic mechanical properties of these copolymers.

The origins of the bulk mechanical properties of polymers must lie in the molecular dynamics of the macromolecules and the segments of the macromolecules (61). It was thought that with the use of solid state NMR techniques, that are able to provide direct information on the molecular motions and relaxations of the carbons that make up the repeat units in the polymer, it might be possible to find a correlation between changes in the bulk mechanical properties, such as those measured by a torsion pendulum, and the changes observed by NMR methods as both the degree of hydration

of the polymer changes and as HEMA is copolymerised with other monomers. NMR pulse sequences were used that are capable of detecting changes in both near static motion and motion in the mid kHz range of the polymer carbons.

^{1}H NMR has also been used to study the behaviour of water in hydrogels. Smyth et al. used ^{1}H NMR to investigate water in a number of partially hydrated PHEMA samples over a wide temperature range measuring a variety of different relaxation parameters (44). They found that, for a 53 wt% water/PHEMA sample, the bulk of the water present is bound water which is rendered mobile at ≈180K and has the characteristics of a glass. 10 % of this low temperature mobile water eventually froze i.e.formed a crystalline phase.

^{1}H NMR work here was carried out primarily to study the effect that crosslinking has on the water in fully saturated hydrogels and how the different types of water observed in the hydrogel change as the sample is frozen. HEMA was also copolymerised with MMA to see what effect a hydrophobic non-crosslinking copolymer would have.

DSC studies were carried out in conjunction with the ^{1}H NMR work to see what effect copolymerisation had on the relative proportions of freezing and non freeing water.

It was hoped that by making use of a variety of experimental techniques a fuller understanding could be obtained both of the effect water and crosslinking have on the dynamic mechanical properties of hydrogels and the environments in which water exists in the hydrogel.

CHAPTER TWO

EXPERIMENTAL TECHNIQUES

2.1 Sample Sources

HEMA was obtained from Mitsubishi Chemicals, courtesy of SOLA Optical, and contained 50 ppm hydroquinone monomethyl ether as inhibitor. EGDMA, DiEGDMA, TEGDMA and P400 from Fluka and PMMA from Polyscience. The peroxide initiator used was t-butyl per-2-ethyl hexanoate (TBO), (Interox, Australia) with the structural formula

$$H_3CC(CH_3)_2OOCOCH(C_2H_5)CH_2CH_2CH_2CH_3$$

2.2 Sample Preparation

All monomers were dried over anhydrous magnesium sulphate and then stored over activated 3Å molecular sieves at -15°C until required. The initiator was used as supplied and at the concentration in monomer of 0.2% V/V. To prevent inhibition of the polymerisation by oxygen high purity dry nitrogen was bubbled through the monomer for 15-20 minutes immediately prior to casting. Monomers were cast between two glass sheets using silastic tubing (Dow Corning) as a gasket in the manner described by Cowperthwaite(1). The resultant casts were between 0.5 and 2 mm thick depending on the thickness of the gasket used.

Due to the strong adhesion of PHEMA to glass it was necessary to treat the surface of the glass sheets with trimethylchlorosilane (TMCS) prior to casting any monomer mixtures containing HEMA. The TMCS reacts with the silanol groups on the glass surface preventing the hydroxy group of HEMA bonding to the surface. This facilitated the easy removal of the polymer from the mould. Some PHEMA samples were also prepared by polymerising between two teflon sheets. HEMA was cured at 60°C until gelation occurred after approximately 2 hours, after which the temperature

was raised in 10°C steps every hour up to 110°C and kept at that temperature for 12 hours. The temperature was then slowly reduced over a period of 4-5 hours to ambient temperature. Similar cure profiles were used for copolymers of HEMA with the oligo-(ethylene glycol) dimethacrylates and MMA, although for high concentrations of EGDMA and DiEGDMA a further post cure was required at 120°C for one hour in order to ensure that the full possible cure could be reached. The resulting casts were all clear and transparent. Curing for any length of time above these temperatures led to some degradation of the cast indicated by a brown discolouration appearing. Copolymer composition is generally specified in terms of mole % of the OED used.

The extent of cure of all samples was checked by differential scanning calorimetry (DSC) using a Perkin Elmer DSC 2. Full cure was assumed to occur when no exotherm, due to monomer polymerising, was noticeable on the DSC thermogram. It must be noted however, that previous work(2-6) has shown that polymers of EGDMA, DiEGDMA and TEGDMA have some remaining unsaturation, even at full attainable cure, that cannot be measured by DSC. This unsaturation occurs in the form of trapped monomer and unreacted pendant double bonds. This should have little effect on copolymers containing only small amounts of these monomers but at high concentrations there may be some effect on the properties of the copolymer. Copolymers containing greater than 60 mol% EGDMA tended to crack and craze extensively and samples larger than approximately one cm^2 could not be produced.

NMR measurements (7) indicated the presence of 0.3 mol% EGDMA in the HEMA monomer. This results in a three dimensional network polymer which is insoluble in water. The monomers were not deinhibited. It has been found that deinhibiting TEGDMA by passing through an activated alumina column had little or no effect on the properties of the polymer (8)

PMMA sheets were formed either by polymerisation of MMA or by compression moulding of PMMA beads. The beads were molded at 180°C for one hour and then allowed to cool slowly over a period of 7-8 hours, to ambient temperature.

2.3 Sample Hydration

All DSC, NMR, absorption and mechanical tests were carried out on samples prepared from casts produced as described above. Samples were initially dried to a constant weight in a vacuum oven at 50°C which took approximately one week to achieve. Appropriately sized samples were then fashioned from the dried casts. In the case of torsion pendulum samples care was taken to ensure that the sides were smooth and parallel. To achieve partially hydrated samples the polymers were either placed in deionised water or stored at different relative humidities obtained using saturated salt solutions in sealed containers at a constant temperature (9,10). The salt solutions used along with their respective relative humidities are shown in Table 2.1. Constant temperature water baths were used which maintained the desired temperature to ±1°C. Previous measurements (11) have shown that humidities obtained in this way are within ±3% of the published values.

Table 2.1
List of salts used to obtain different relative humidities at the temperatures listed.

Salt	Temp (°C)	%R.H.
NaOH	25	6
MgCl	25	33
NH_4CL	25	79
KBr	20	84
NA_2SO_4	20	93
$PbNO_3$	25	98

2.4 Differential Scanning Calorimetry

A Perkin Elmer DSC II was used for all DSC measurements. Measurements above ambient temperature were carried out using high purity dry nitrogen as the purge gas and the instrument was calibrated with Indium (m.p. 429.78 K, ΔH_f=6.8 cal/g) and Lead (m.p. 600.65K, ΔH_f=5.5 cal/g). Below ambient temperature, water and n-octane (m.p. 216.4 K) were used as calibration standards. Melting point temperatures were measured using the method shown in Figure 2.1(a). Liquid nitrogen was used as the coolant which enabled temperatures down to 100 K to be reached. At temperatures below 258 K helium was used as the purge gas. It was necessary to enclose the head of the DSC in a dry box to prevent condensation on the samples or sample holders whenever temperatures below ambient were required.

All calibrations were carried out at the same heating rate as that at which the sample was scanned.This was usually either 20 K/min or 10 K/min.

2.4(a) Measurement of Freezing Water

Hydrated polymer samples were enclosed in volatile-sample pans, (P.E. No219-0062), to minimise water loss during measurement, after first removing any surface water with absorbent paper. The amount of freezing water was calculated by measuring the area under the peak produced on the DSC thermogram when the water in the sample melted to the area produced by the melting of a known weight of water.

2.4(b) Glass Transition Temperature

Several methods can be used to obtain the glass transition temperature T_g from a DSC thermogram (12). In this work the midpoint method, shown in Figure 2.1b, was used.

All samples were enclosed in volatile sample pans. Samples were weighed before and after the run to determine any water loss.

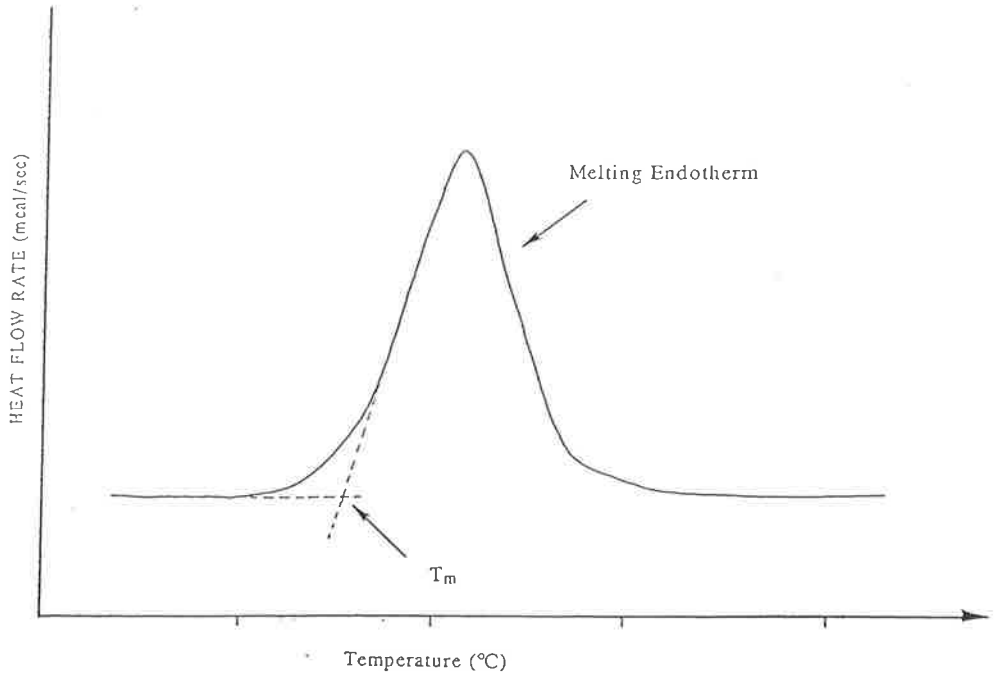

Figure 2.1(a) Method used for determining transition temperatures from DSC thermograms, in this case melting points. T_m is taken to be the melting point temperature. Temperature increases to the right.

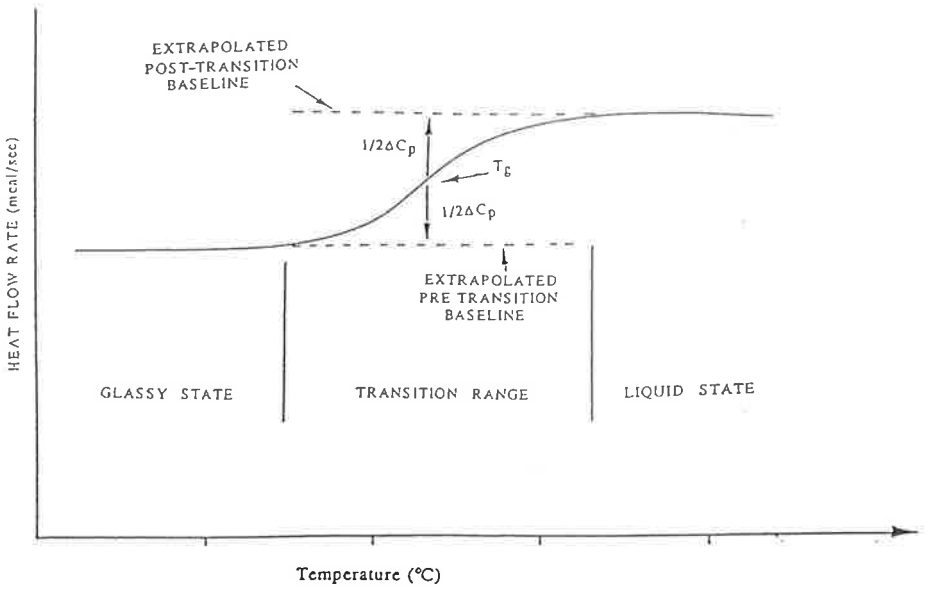

Figure 2.1(b) An example of the midpoint method used here for obtaining glass transition temperatures from DSC thermograms. Tg is taken as the temperature at which the heat capacity change is half that of the total change from the glassy state to the rubbery state.

2.5 Dynamic Mechanical Measurements

Dynamic mechanical measurements of the relaxation properties of polymers with varying water content were made using a free oscillation torsion pendulum (TP). The sample was counterbalanced to ensure that there was no strain on the sample and mounted on a fixed base with an inertial arm connected to the sample which was able to be pulsed by an electromagnet. The resultant sinusoidal decay was monitored by a mirror, light and photoresistor and the resulting output recorded on a chart recorder.

From this the log decrement, Δ, can be calculated using Equation 2.1;

$$\Delta = \ln \frac{A(n)}{A(n+1)} \qquad \text{Equation 2.1}$$

where A(n) is the reference peak amplitude and A(n+1) is the amplitude one cycle later. P, the period of oscillation, can also be calculated. These two parameters can then be used to calculate the in-phase shear or storage modulus, G', and the out-of-phase shear or loss modulus, G", using the appropriate equations (13). G' is a measure of the energy stored in the specimen due to the applied strain while G" is a measure of the energy loss from the specimen. The ratio of G' to G", defined as the loss tangent, tan δ, can be used to characterise the energy dissipation, where

$$\tan \delta = \frac{G''}{G'} \approx \frac{\Delta}{\pi} \qquad \text{Equation 2.2}$$

G', G" and tan δ can give information on transitions occurring in the sample, eg. from glassy to rubbery.

Previous experiments on this instrument (8,14) indicate errors in T_g of ±3 K, for Δ of 4.7%, and for G' of 4.73% which are comparable to other torsion pendulum systems (15).

Measurements were made on samples approximately 10x1.0x30 mm. Subambient temperatures were attained by cooling the sample chamber with liquid nitrogen and then raising the temperature using a heating tape which gave a heating rate of approximately 2 K/min. Superambient temperatures required a thermostatted air circulation heater. Combining these two methods gave a temperature range between 123 K to 473 K. All measurements were made with the sample enclosed in a high purity nitrogen atmosphere. The temperature was measured to ±1K using previously calibrated copper-constantan thermocouples placed at each end of the sample. At extremely low temperatures (< 100 K) there was a slight variation of approximately 2 K along the length of the sample; when this occurred the average temperature of the two thermocouples was used.

2.6 Nuclear Magnetic Resonance

2.6(a) Solution NMR

A Brüker WP80 Fourier Transform NMR spectrometer with a variable temperature (VT) accessory was used to obtain the ^1H spectra of water in PHEMA and PHEMA copolymers. A fully saturated polymer sample was cut into small pieces of approximately one mm^3 and packed firmly into a 5mm diameter NMR tube (Wilmad 507-PP) which contained a sealed 2.5 mm diameter capillary tube (Wilmad WG-1364-2.5A) filled with deuterated acetone, (m.p. -95.4 C), which acted as an external lock. The NMR tube was sealed securely to minimise water loss.

Spectra were collected at various temperatures and under identical conditions, (eg. the same number of scans collected). This enabled the change in the amount of mobile water to be monitored as a function of time and/or temperature. The linewidth at half peak height, $W_{1/2}$, which is

related to T_2 by Equation 2.3, also gives some information on molecular mobility

$$T_2 \approx \frac{1}{\pi W_{1/2}} \qquad \text{Equation 2.3}$$

The temperature was measured using a copper-constantan thermocouple. The accuracy of the temperature displayed on the VT accessory was verified using the Van Geet equation, Equation 2.4(16);

$$T_{act} = 403 - \frac{29.5}{M}(\Delta\nu) - \frac{23.81}{M^2}(\Delta\nu)2 \qquad \text{Equation 2.4}$$

where M=frequency of the spectrometer, T_{act} is the actual temperature and $\Delta\nu$ is the difference in frequency between the hydroxy and methyl protn resonances of methanol. The temperature indicated was found to be correct to ±1°C

The spectrometer operated at 80 MHz for ^1H nuclei. Standard techniques were used for measurement; (^1H pulse-1.2μs/45°C), 16K data table, phase alternating pulse sequence (PAPS) and quadrature signal detection.

2.6(b) Solid State NMR

The use of high resolution NMR for studying solid polymers can provide detailed information on various types of molecular motions. It can be sensitive to a wide range of motional frequencies from 0.01 -10^{10} Hz. Two frequency ranges chosen here are characterised by $T_{1\rho}(C)$, the ^{13}C relaxation time in the rotating frame, sensitive to motions in the kilohertz range and T_{SL}, the spin-lock cross polarisation time, sensitive to near static motions. In the process of calculating T_{SL} $T_{1\rho}(H)$, the ^1H relaxation in the rotating frame , can also obtained.

To achieve a high resolution ^{13}C spectrum it is necessary to remove line broadening which occurs due to dipolar interactions between ^{13}C and

proton nuclei and chemical shift anisotropy (CSA), due to the asymmetry of the electron cloud shielding the carbon nucleus. Dipolar broadening can be reduced by using a high powered decoupling field, analogous to proton decoupling used in ^{13}C NMR of liquids to remove carbon-proton spin -spin coupling, but normally some ten times larger. CSA can be removed by spinning at the magic angle (54.7°) as the degree of shielding that a nucleus experiences is dependant on the orientation of the molecule to B_o, the magnetic field. This has a $3\cos^2\beta$-1 dependance, where β is the angle between the bond axis and the B_o field. At the magic angle this term becomes zero. Sample spinning rates must be of the order of the CSA linewidth, (1-5 kHz), to remove CSA.

In addition to these two methods cross polarisation (CP) or proton enhancement was used. This process helps eliminate two problems associated with ^{13}C NMR. Firstly, the low natural abundance of ^{13}C nuclei, (1.11% compared to 99.9% for ^{1}H nuclei), and secondly the long T_1 values of ^{13}C nuclei in solids as it is necessary to use data acquisition times similar to T_1 in order to prevent signal saturation.

Cross polarisation occurs when the smaller "hotter" ^{13}C reservoir is brought into contact with the larger "cooler" ^{1}H reservoir and magnetisation is transferred from the proton reservoir to the ^{13}C nuclei. This occurs when the Hartmann-Hahn condition is satisfied:

$$\gamma_C B_C^1 = \gamma_H B_H^1 \qquad \text{Equation 2.5}$$

where γ_C and γ_H are the ^{13}C and ^{1}H gyromagnetic ratios and B_C^1 and B_H^1 are the magnitudes of the carbon and proton field respectively. With this condition met proton and carbon levels are brought to lower matching levels and energy conserving spin flips can now occur between carbon and proton spins. This has the effect of reducing the T_1 values and, under ideal

conditions, enhancing the ^{13}C signal approximately four times. The time constant describing the rate of magnetisation transfer is T_{SL} or T_{CH} and it is possible to measure this using the following pulse sequence (17). Firstly the proton spins are polarised in a field B_o followed by placing them in a rotating field by a 90° pulse followed by a 90° phase shift and continued irradiation by a strong H field. The ^{13}C spins are then placed in the rotating frame such that the Hartmann-Hahn condition is obeyed and contact established with the proton nuclei for a variable time. As cross polarisation occurs through static dipolar coupling of the carbon and proton nuclei this provides information on near static components of motion. The pulse sequence is shown in Figure 2.2.

T_{SL} values can then be calculated from the varying intensities of the ^{13}C nuclei with varying contact times, τ. An equation has been developed (18) relating intensity to τ

$$I=I_o\lambda^{-1}\left[1 - \exp\left(\frac{-\lambda\tau}{T_{SL}}\right)\right]\exp\left(\frac{\tau}{T_{1\rho}(H)}\right)\right] \qquad \text{Equation 2.6a}$$

where

$$\lambda=1 + \frac{T_{SL}}{T_{1\rho}(C)} - \frac{T_{SL}}{T_{1\rho}(H)} \qquad \text{Equation 2.6b}$$

and I = peak intensity after cross polarisation contact time τ and T_{SL}, $T_{1\rho}(C)$ and $T_{1\rho}(H)$ are as defined previously. Since $T_{1\rho}(C)$ is usually much greater than T_{SL} the ratio $T_{1\rho}(C)/T_{SL}$can be assumed to be zero and equation 2.6a simplifies to

$$I=\frac{I_o}{T_{SL}}\left[\exp\left(\frac{-\tau}{T_{1\rho}(H)}\right) - \exp\left(\frac{-\tau}{T_{SL}}\right)\right]\left(\frac{1}{T_{SL}} - \frac{1}{T_{1\rho}(H)}\right) \qquad \text{Equation 2.7}$$

The data obtained was then fitted to this equation using a non linear least squares regression method via a program DATAFT (19) and T_{SL} and $T_{1\rho}(H)$ values obtained.

$T_{1\rho}(C)$ values were also measured, again using a pulse sequence described by Schaefer (17). Spin contact is established for a variable time, τ, which is then terminated by switching off the proton rotating field. The carbon spins are then held in their rotating field for a variable time and data is then collected with dipolar decoupling on. This sequence is illustrated in Figure 2.3.

All magic angle spectra were acquired on a Brüker CXP-300 spectrometer with a frequency of 75.47 MHz, a proton decoupling field of 61 kHz (1.36G), and a carbon spin-lock field of 60 kHz (53G). The recycle time was five seconds and the $\pi/2$ carbon pulse size approximately 4.2 μs. All cross polarisation experiments were conducted with spin temperature alternation and received phase cycling (CYCLOPS) to remove quad images. The probe temperature was 298±3 K. For T_{SL} measurements τ times were in the range 0.05-7ms and for $T_{1\rho}(C)$ delay times ,τ, between 0.2-18ms before acquisition were used.

PHEMA and PHEMA copolymers were crushed to a granular powder, dried in a vacuum oven at 50° C and then allowed to rehydrate at different relative humidities. The rotor used was a zirconia double bearing rotor which allowed spinning speeds of approximately 3.6 kHz. A hole in the end cap of the rotor was sealed using silicon sealant in order to prevent excessive water loss during the experiment. PMMA samples were cut into disks, dried and rehydrated as above. These were run in an Andrews - Beams type rotor, made of boron nitride, at a spinning speed of 2-3kHz. After completion of the experiment the samples were removed from the rotor, weighed and then dried to determine any water loss.

2.7 Diffusion Measurements

Diffusion of water into the samples was measured either by placing the dry sample in deionised water at 25±1°C or in different relative humidities and weighing at appropriate intervals after first removing any

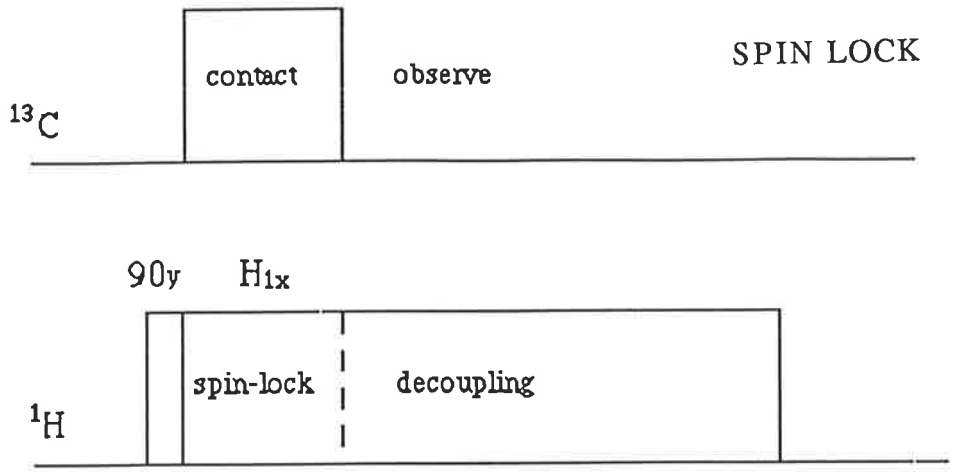

Figure 2.2 Schematic of the pulse sequence used to obtain T_{SL} times. ^{13}C magnetisation builds up during contact . The ^{13}C signal is then aquired after turning off the matching radiofrequency field, but with high power proton decoupling. See text for details.

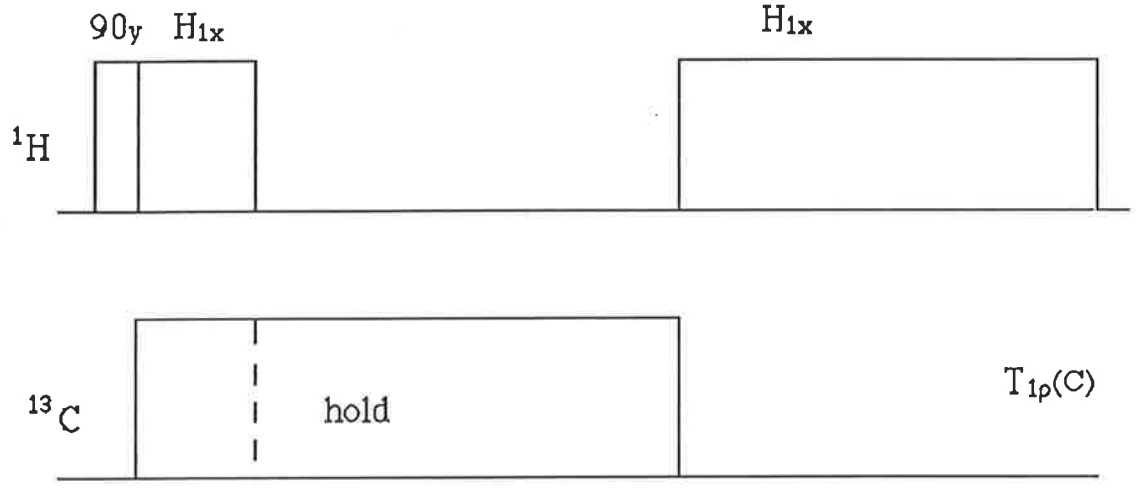

Figure 2.3 Schematic of the pulse sequence used to obtain $T_{1\rho}(C)$ times. Main features are the initial establishment of the Hartmann-Hahn condition. The carbons are held in their rotating frames with no CP contact for various lengths of time. The ^{13}C signal is then acquired with dipolar decoupling of the protons.

surface water. The amount of water absorbed into the polymer can be defined in a number of different ways. The two methods most commonly used are to either express the water content as a percentage of its dry weight using Equation 2.8;

$$\%H_2O=\frac{W_W - W_D}{W_D}x100\% \qquad \text{Equation 2.8}$$

where W_W is the weight of the wet polymer and W_D is the weight of the dry polymer, or to express it as a function of its wet weight, most commonly termed the Equilibrium Water Content (EWC) or in some cases the Equilibrium Swelling Content (ESC), using Equation 2.9;

$$EWC=\frac{W_W - W_D}{W_W}x100\% \qquad \text{Equation 2.9}$$

In this work the latter method is used unless otherwise specified.

Desorption measurements were carried out by placing the wet samples in dry atmospheres achieved using silica gel.

The size of voids in the samples was determined by the method described by Turner (20). The sample was suspended by a silk thread from a balance into a beaker of water. Corrections were made for the mass and sorption properties of the thread.

In all cases a Mettler AE166 digital electronic balance accurate to ±0.1 mg was used.

CHAPTER THREE

WATER SORPTION AND DESORPTION

3.1 Introduction

In this chapter the sorption and desorption of water in PHEMA and PHEMA crosslinked with varying amounts of EGDMA, DiEGDMA, TEGDMA and P400 has been studied at three different relative humidities (33%,79% and 100%) and in water, all at 25°C. Once the samples had reached equilibrium in their respective environments (i.e. no weight change over approximately a week), they were placed in a dry atmosphere and desorption allowed to take place, with subsequent measurements being made.

The term sorption (1-2) used here, is a generalised term and is used to describe the penetration and dispersal of molecules of a gas, vapour or liquid onto and throughout a polymeric solid to form a mixture. It includes adsorption onto external and internal molecular surfaces such as those of capillary pore systems and absorption of the sorbate into the bulk structure of the polymer.

The inclusion of the different oligo(ethylene glycol) dimethacrylates (OEDs) meant that three possible situations could occur. The copolymers could start off glassy and remain glassy at maximum EWC, as with Poly(HEMA/EGDMA) copolymers where the EGDMA content was above 14 mole%,they could be initially glassy and become rubbery, as with straight PHEMA, or they could be rubbery initially and become increasingly more so, as with copolymers containing large amounts of P400.

3.2 The Kinetics of Diffusion

The mathematical concept of "holes" in polymers where solvent molecules can reside has been used to interpret the diffusion of solvents

into polymers. A solvent molecule has a greater chance of diffusing between holes in regions of low solvent concentration since there are a greater number of unoccupied holes and therefore the concentration gradient can be viewed as the driving force behind diffusion.

Diffusion of water or solvents into polymers is generally found to occur between two limiting cases, the first being Fickian diffusion and the second, termed Case II diffusion.

Fickian diffusion is that which occurs according to Fick's Law

$$J = -D\frac{dc}{dx} \qquad \text{Equation 3.1}$$

where J is the diffusion flux (mass per cross-sectional area per unit time), D is the diffusion coefficient (cm^2sec^{-1}) and dc/dx is the concentration gradient. A solution to Fick's Law for thin sheets in which diffusion through the sheet edge is assumed to be negligible is given by Equation 3.2 (3),

$$\frac{Mt}{M_\infty} = 1 - \frac{8}{\pi}\sum_{n=0}^{\infty}\frac{1}{(2n+1)^2}\exp\left(\frac{-(2n+1)^2\pi^2 Dt}{4l^2}\right) \qquad \text{Equation 3.2}$$

where 2l is the sample thickness, Mt is the mass uptake (in this case of water) at time t (secs), M_∞ is the mass uptake at infinite time and D is the diffusion coefficient. In the case of desorption measurements Mt is the weight loss at time t, and M_∞ is the total weight loss. For $Mt/M_\infty < 0.5$ then Stefan's approximation (4), Equation 3.3, is often used to calculate D.

$$\frac{Mt}{M_\infty} = 2\left(\frac{Dt}{\pi l^2}\right)^{1/2} \qquad \text{Equation 3.3}$$

At higher sorption levels a further approximation, Equation 3.4, can be used(16).

$$Ln\left(1-\frac{Mt}{M_\infty}\right) = Ln\left(\frac{8}{\pi^2}\right) - \frac{\pi^2 Dt}{4l^2} \qquad \text{Equation 3.4}$$

Both of these equations have been used here to calculate D for individual points and in some cases to find the initial diffusion coefficient. The data was also fitted to the first eleven terms of Equation 3.2 (i.e n = 0 to 10) using the DATAFT program (Chapter Two). A common representation of data from diffusion experiments is to plot Mt/M_∞ against $t^{1/2}$ where l and t are as before. This is referred to as the reduced sorption curve.

Diffusion is said to be Fickian (5) if the following three criteria are obeyed,

(1) Mt/M_∞ vs $t^{1/2}$ gives linear sorption and desorption curves to Mt/M_∞ =60% or greater.

(2) Above the linear region sorption and desorption curves are concave to the x axis.

(3) The reduced sorption curve lies above the reduced desorption curve.

The other case mentioned is that of Case II diffusion. For Case II diffusion the basic parameter is the constant velocity of the advancing front which marks the boundary between the swollen gel and the glassy core of the polymer. It is also characterised by a weight gain which is linear with sorption time. Frisch proposed (6) that the equation, Equation 3.5,

$$\frac{Mt}{M_\infty} = k\, t^n \qquad \text{Equation 3.5}$$

where k is a constant characteristic of the system and n is an exponent characteristic of the type of diffusion, could be used as a simple way of analysing solvent transport. It can be seen that if n = 1/2 then Equation 3.5 is equivalent to Equation 3.3 and the diffusion follows a Fickian mechanism, while if n = 1 Case II diffusion is indicated. The value of n was derived from a log - log plot of Mt/M_∞ against t. Correlation factors r calculated from the fit of the data to the Equation 3.5 were usually greater than 0.99 for all the systems studied.

Vrentas and Duda (7-8) have also made use of the diffusional Deborah number, De, as an indication of Fickian or non-Fickian diffusion. De is defined as the ratio of the characteristic relaxation time to the characteristic diffusion time. If De $\approx$1 then relaxation controls the transport process and it is non-Fickian. If De<<1 or De>>1 then diffusion becomes Fickian.

Previous experiments on PHEMA (9-11) have found that the kinetics of linear swelling do not follow the same functional form as the kinetics of water uptake (12) and the hypothesis of voids has been used to explain these results. It has been suggested that these voids fill with water first before any linear expansion takes place. A similar concept has been used to describe the sorption of gases by glassy polymers like polyethylene terepthalate (13) and polystyrene (14).

Turner (15) has used this concept of voids to explain the behaviour of water sorption into PMMA. Turner used a conclusion reached by Bueche (16) that recognized that sorption into voids, or zero density regions, should cause an increase in density whereas sorption that causes swelling should not change the density. Turner then determined the amount of water in the voids by weighing the samples in water and air and using Equation 3.6,

$$\% \text{ in Voids} = \frac{(W_{w,t}-W_{w,o})}{(W_{a,t}-W_{a,o})} \times 100 \qquad \text{Equation 3.6}$$

where $W_{w,t}$ is the weight in water at time t and $W_{a,t}$ is the weight in air at time t.

Turner proposed that as water initially enters the surface zone of the polymer both swelling takes place and voids are filled, with the former process continuing to contribute to water uptake even after the wetting front, as determined by water moving into voids, has moved on. This causes an increase in D which continues until the swelling in the surface zone has reached equilibrium. After this the swelling zone and the wetting front keep pace and a constant D is achieved once the voids are full. Turner

assumed that this described the non - Fickian water sorption he found in PMMA as a case of Fickian sorption with a small contribution from Case II sorption. Similar systems having both a Fickian and non-Fickian contribution have been observed in a number of other crosslinked polymer systems.(17-19)

Other evidence for the existence of voids comes from the fact that the properties of some polymers are found not to change greatly with the sorption of small amounts of diluents leading to the conclusion that they have been absorbed into voids (20-21).

It is important not to confuse the concept of voids with the mathematical "hole" theory which was mentioned earlier with respect to modelling diffusion through polymers. The voids referred to here are presumed to be due to the inhomogeneous packing of polymer chains, frozen in below T_g (15,21-23)

3.3 Results

3.3.1 Sorption at 33% Relative Humidity

Table 3.1 shows the EWC, sorption and desorption coefficients D_s and D_d and n_s and n_d - the exponents calculated from Equation 3.5. The subscripts s and d refer to sorption and desorption respectively. The reduced sorption and desorption curves for the copolymers are shown in Figures 3.1a-h. The reduced sorption and desorption curves for PHEMA are shown in Figure 3.2. The correlation factor r calculated from the linear log-log plot used to calculate n from Equation 3.5 was generally greater than 0.99 for these and subsequent n values.

It is apparent from the observed n_s values, which are all close to 0.5 for the majority of the copolymers, that sorption at 33% relative humidity can be described by a Fickian mechanism, although there is some slight increase for HEMA copolymerised with between 3 and 14 mol% OED followed by a decrease as the OED content increases. The Fickian sorption

behaviour is further reflected in the reduced sorption curves which show linearity for all samples up to at least $M_t/M_\infty = 0.8$. It was also evident in the close fit obtained when calculating D_s from Equation 3.2, up to $M_t/M_\infty \approx 1$ in most cases , an example of which can be seen in Figure 3.3.

TABLE 3.1

Sorption and desorption results for PHEMA and PHEMA copolymers initially equilibrated at 33% Relative Humidity. E, Di and T represent EGDMA, DiEGDMA and TEGDMA respectively. The number in brackets in the D_s and D_d columns represents the standard error given by the DATAFT program.

Mole % OED	EWC	Calculated EWC	$D_s x 10^8$ $cm^2 sec^{-1}$	$D_d x 10^8$ $cm^2 sec^{-1}$	n_s	n_d
0	4.4	4.45	0.15	0.22	0.53	0.55
3E	4.2		0.22(0.01)	0.20(0.01)	0.51	0.49
6E	3.7		0.27(0.03)	0.19(0.01)	0.54	0.52
14E	3.8		0.28(0.03)	0.19(0.01)	0.53	0.53
30E	2.6		0.40(0.01)	0.28(0.01)	0.52	0.50
50E	1.9		0.66(0.02)	0.39(0.06)	0.48	0.52
3Di	4.1	4.0	0.27(0.01)	0.19(0.01)	0.54	0.52
6Di	3.7	3.8	0.34(0.01)	0.21(0.01)	0.54	0.65
14Di	3.4	3.5	0.28(0.01)	0.20(0.01)	0.59	0.55
30Di	2.9	2.9	0.30(0.01)	0.20(0.01)	0.57	0.54
50Di	2.2	2.2	0.37(0.01)	0.22(0.01)	0.49	0.57
70Di	1.7	1.6	0.48(0.03)	0.79(0.20)	0.55	0.43
100Di	0.9	0.9	0.99(0.05)	0.58(0.02)	0.52	0.54
3T	4.1	4.0	0.33(0.06)	0.21(0.06)	0.55	0.48
6T	3.4	3.8	0.61(0.05)	0.17(0.05)	0.57	0.53
14T	3.2	3.2	0.39(0.07)	0.24(0.06)	0.48	0.54
30T	3.1	2.9	0.37(0.07)	0.26(0.08)	0.50	0.56
50T	2.4	2.3	0.69(0.03)	0.37(0.01)	0.53	0.54
70T	1.8	1.6	0.73(0.04)	0.50(0.02)	0.49	0.48
100T	1.0	1.0	1.63(0.01)	0.81(0.04)	0.50	0.51
3P400	4.0	3.9	0.43(0.02)	0.23(0.01)	0.58	0.59
6P400	3.7	3.7	0.43(0.01)	0.29(0.01)	0.55	0.55
14P400	3.3	3.2	0.74(0.05)	0.41(0.03)	0.57	0.54
30P400	3.2	2.7	1.16(0.01)	0.61(0.03)	0.49	0.53
50P400	2.6	2.2	2.54(0.03)	1.11(0.07)	0.50	0.38
70P400	2.0	1.9	4.06(0.05)	1.6(0.2)	0.46	0.30
100P400	1.7	1.7	5.18(0.07)	1.8(0.1)	0.48	0.43

From Table 3.1 it can be seen that the initial effect of copolymerising HEMA with the crosslinking OEDs is to reduce the total

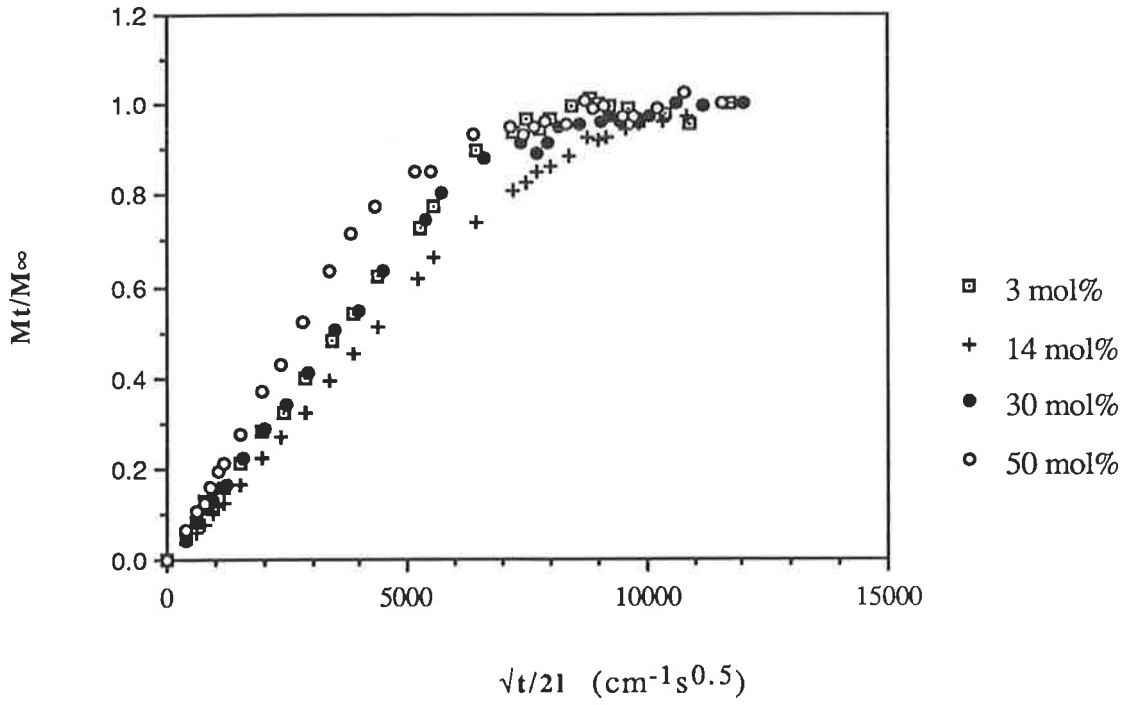

Figure 3.1a Reduced sorption curves for copolymers of HEMA containing EGDMA in the proportions given above. Samples equilibrated at 33% RH. In this plot and those that follow only some of the copolymer reduced sorption curves have been included for reasons of clarity.

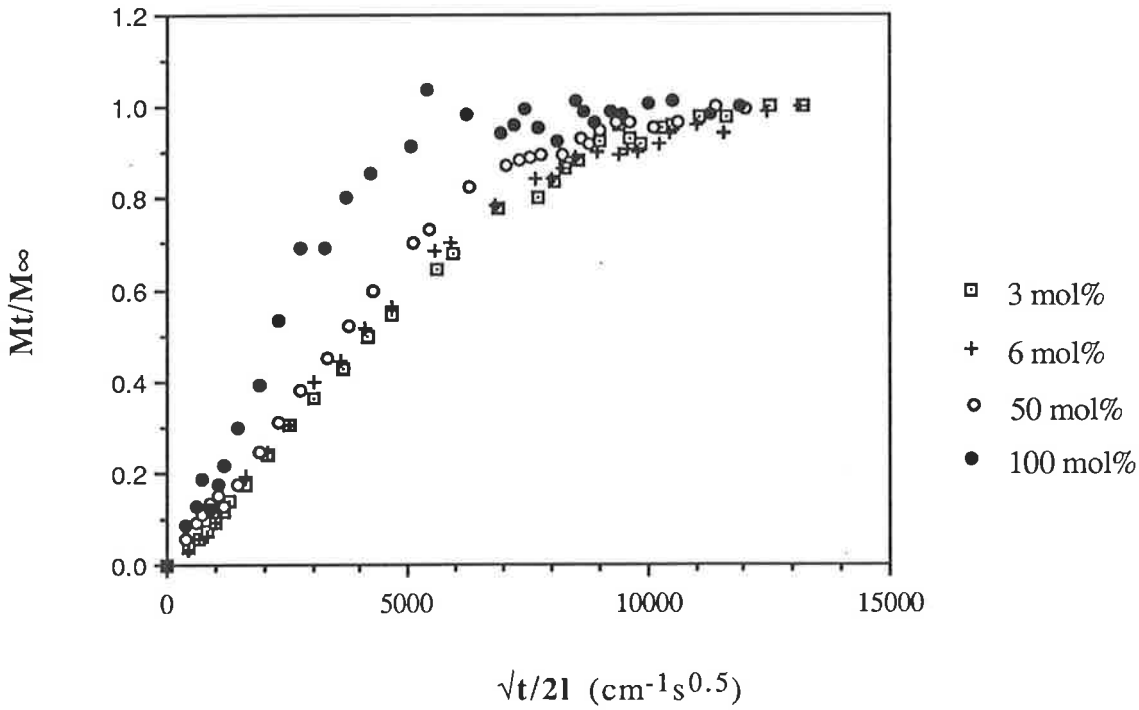

Figure 3.1 b Reduced sorption curves for copolymers of HEMA containing DiEGDMA in the proportions given above. Samples equilibrated at 33% RH

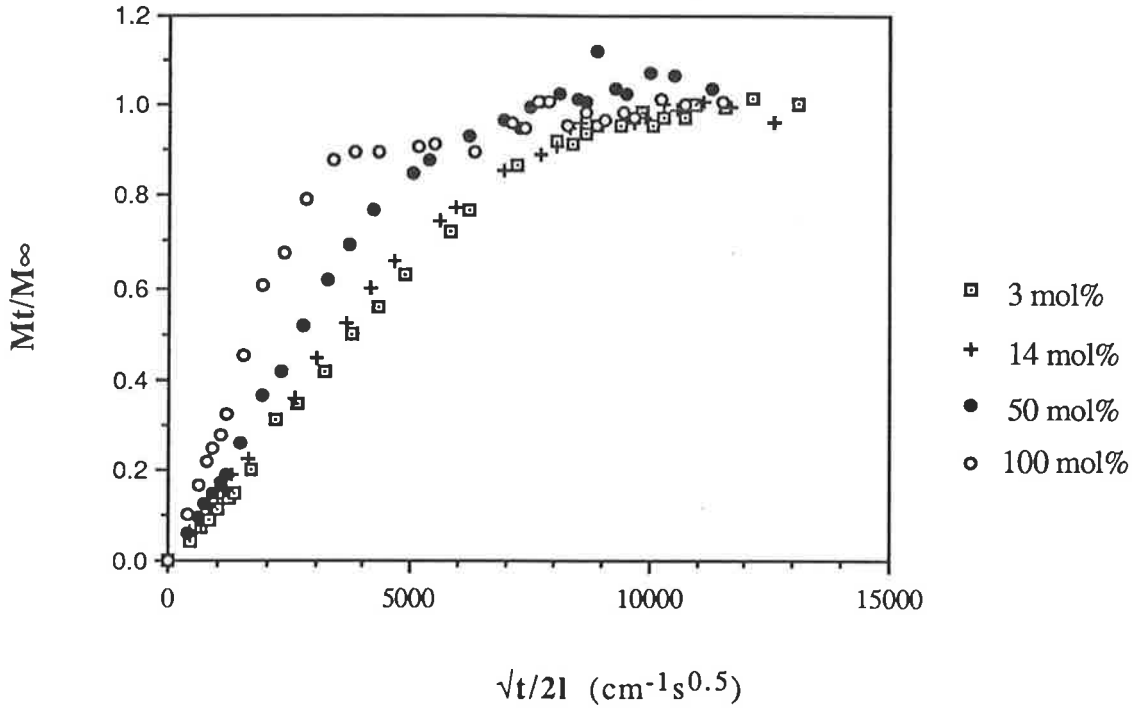

Figure 3.1c Reduced sorption curves for copolymers of HEMA containing TEGDMA in the proportions given above. Samples equilibrated at 33% RH

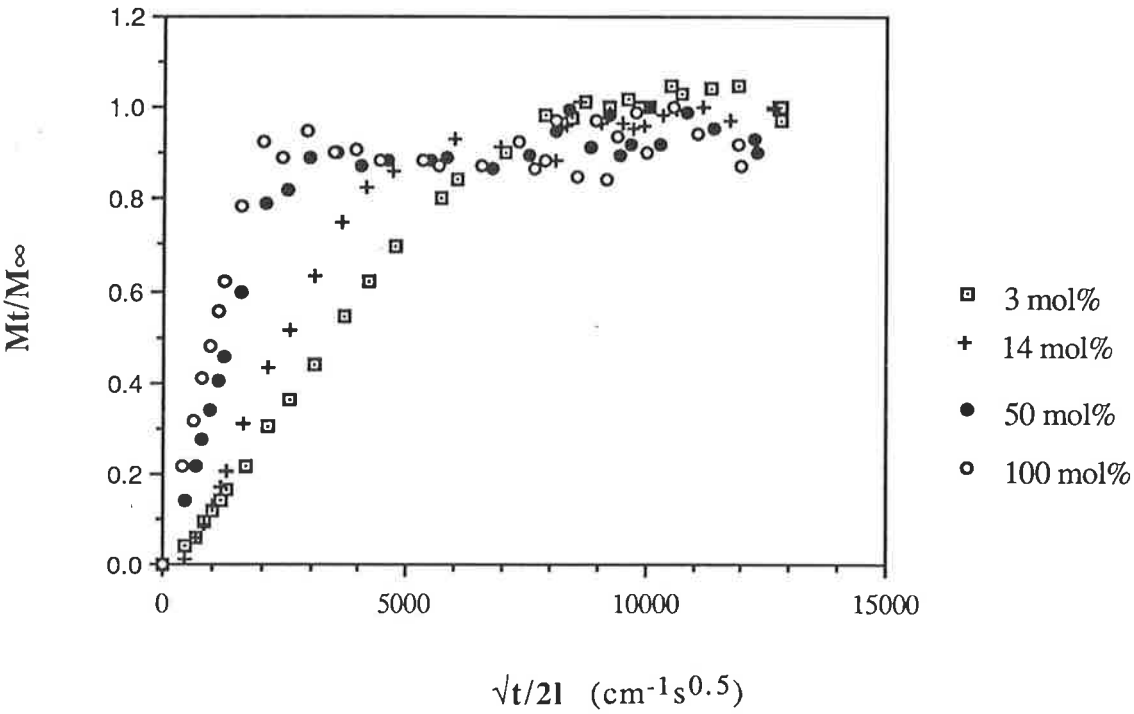

Figure 3.1d Reduced sorption curves for copolymers of HEMA containing P400 in the proportions given above. Samples equilibrated at 33% RH

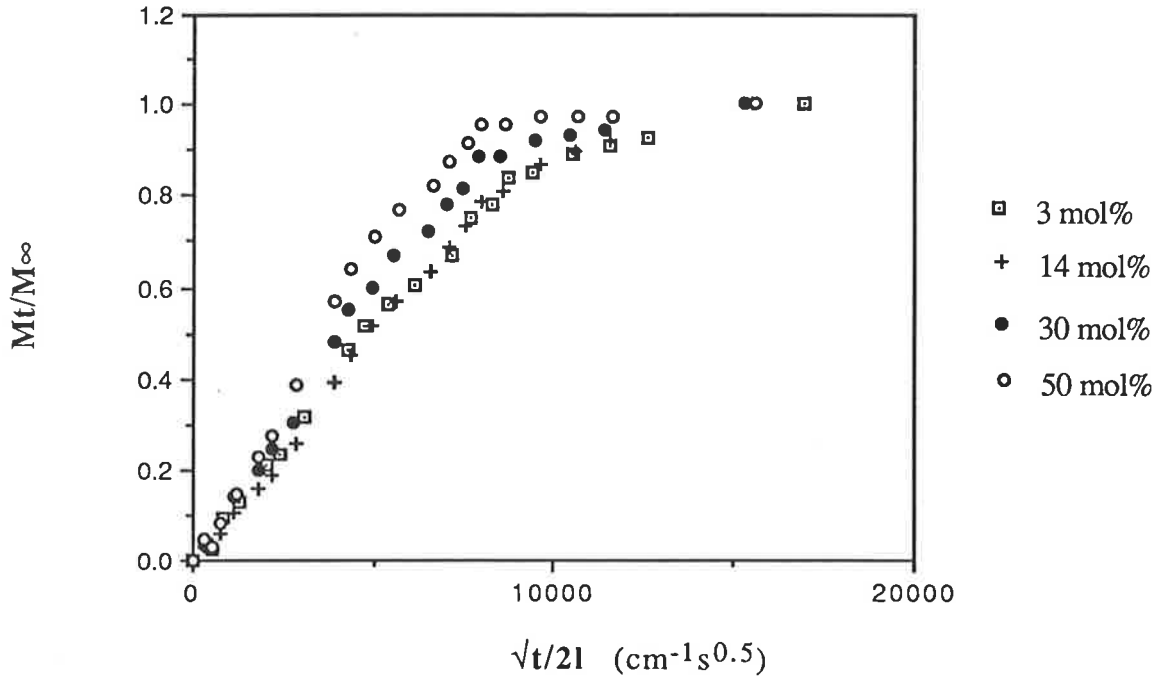

Figure 3.1e Reduced desorption curves for copolymers of HEMA containing EGDMA in the proportions given above. Samples initially conditioned at 33 % RH.

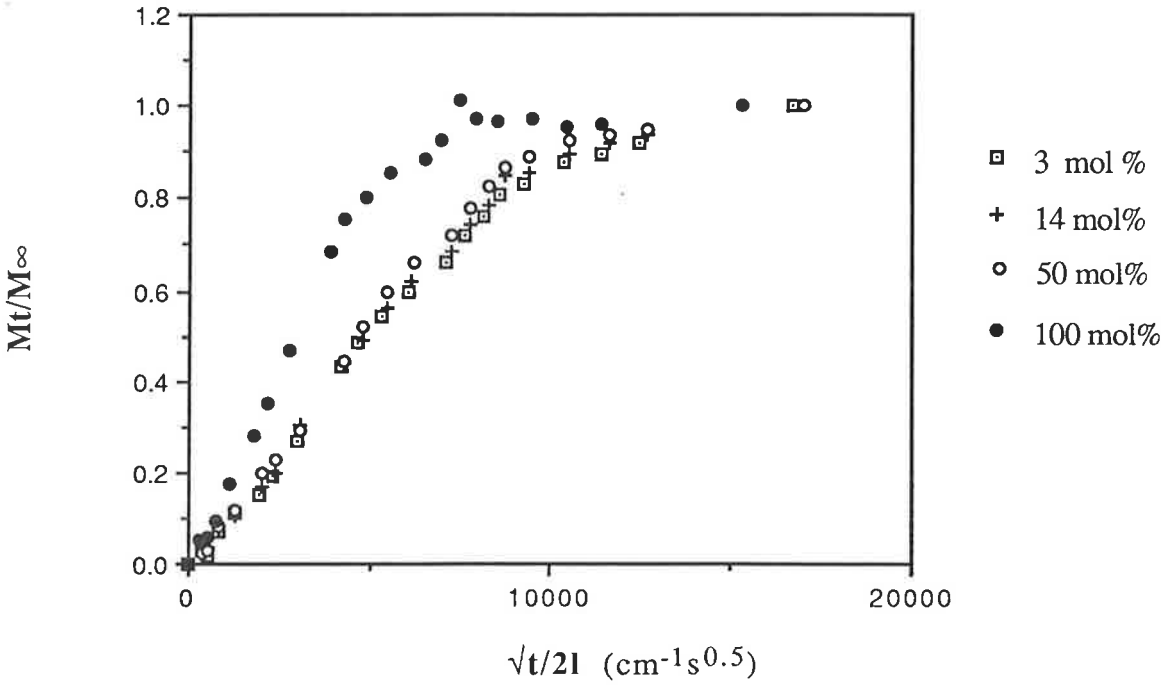

Figure 3.1f Reduced desorption curves for copolymers of HEMA containing DiEGDMA in the proportions given above. Samples initially conditioned at 33 % RH.

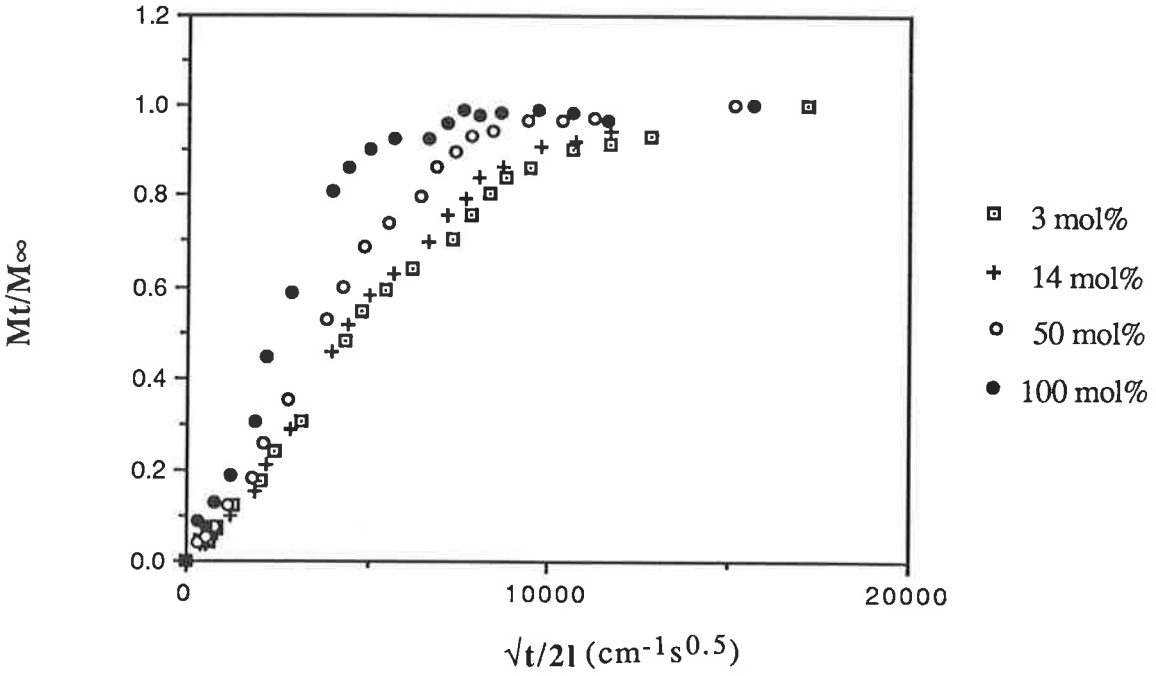

Figure 3.1g Reduced desorption curves for copolymers of HEMA containing TEGDMA in the proportions given above. Samples initially conditioned at 33 % RH.

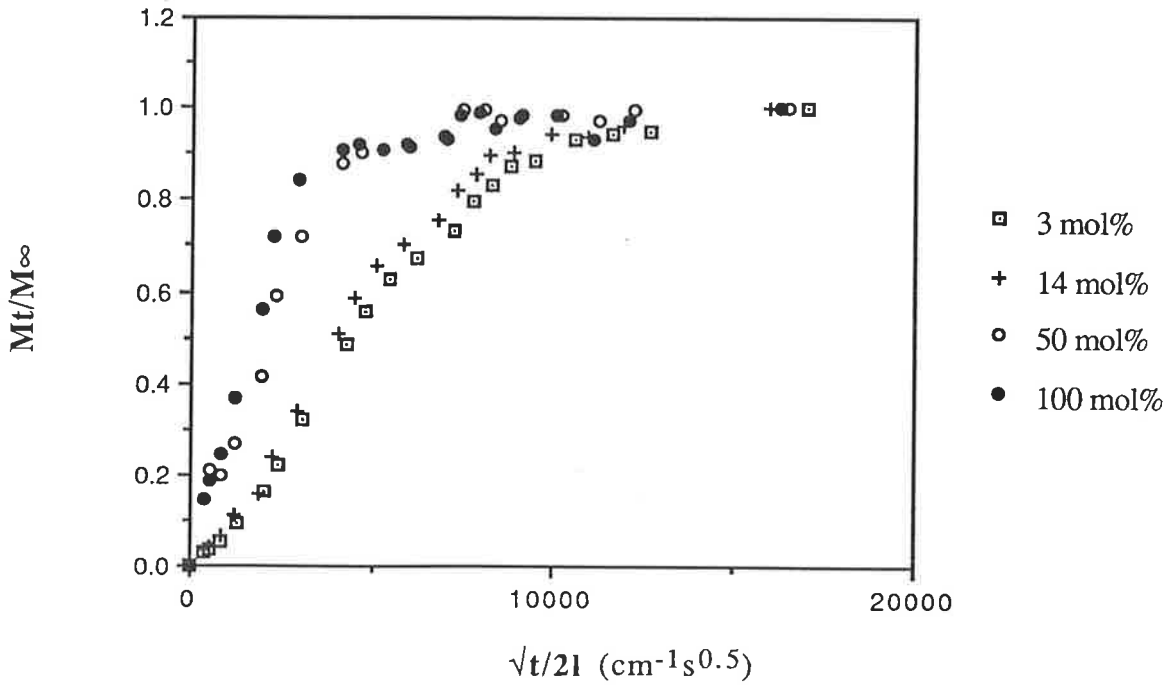

Figure 3.1g Reduced desorption curves for copolymers of HEMA containing P400 in the proportions given above. Samples initially conditioned at 33 % RH.

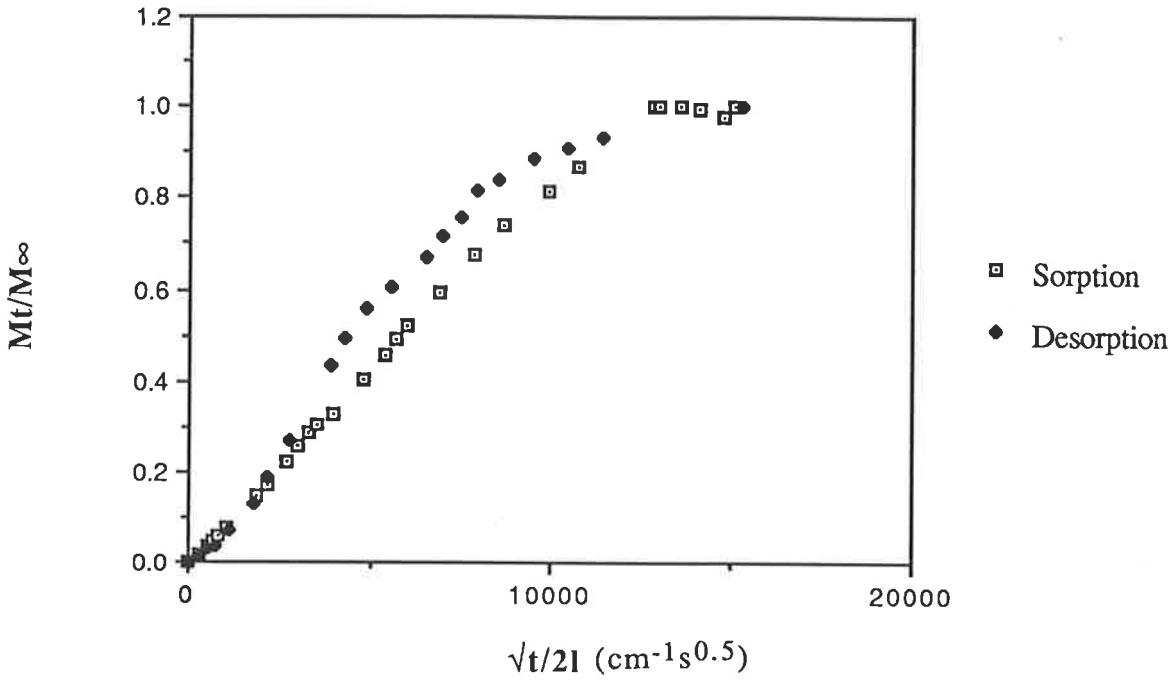

Figure 3.2 Reduced sorption and desorption curves for PHEMA initially equilibrated at 33 % RH.

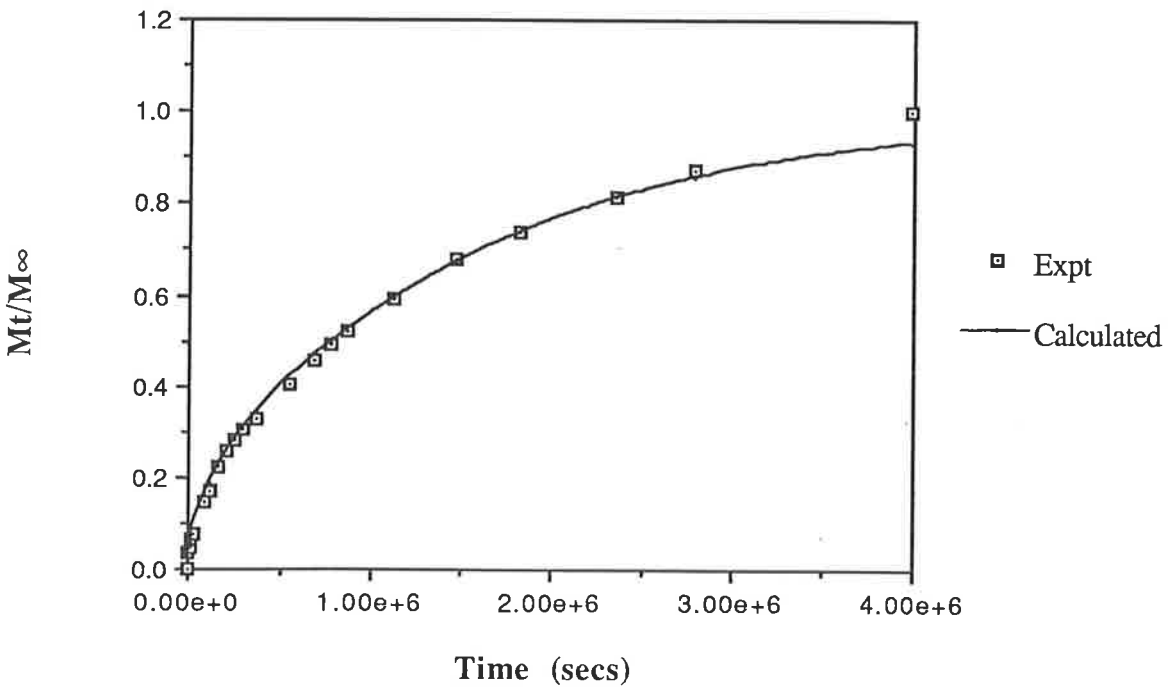

Figure 3.3 Comparison between calculated and experimental values for water sorption by PHEMA at 33 % RH using Equation 3.2.

uptake of water. The addition of 50 mol% EGDMA more than halves the EWC and similar results are obtained for the other dimethacrylates. Water uptake in the dimethacrylates themselves seems to be very dependent on the number of the ethylene glycol units in the homopolymer with P400 having the largest EWC and DiEGDMA the smallest.

The EWC of EGDMA was not able to be measured due to the inability to cast regular, planar sheets which had not cracked or crazed at high degrees of polymerisation. This increase in water uptake with increasing oxyethylene chain length can no doubt be attributed, in part, to the increasing number of polar units in the polymer.

The theoretical EWC for the copolymers was calculated by assuming that the EWC of the polymer did not change on copolymerisation and was simply additive. No EWCs could be calculated for EGDMA copolymers. The calculated EWCs for the DiEGDMA copolymers are slightly greater than the experimental values except for the 70 mol % DiEGDMA copolymer. For the TEGDMA samples the predicted values are reasonably close up to 14 mol% but then decrease below experimental values. All the calculated values for P400 copolymers are less than actual values.

The D_s values for the copolymers show an increase from the PHEMA value and in most cases the increase continues with increasing crosslinking, in fact the D_s values for the OED homopolymers are all higher than those of PHEMA and increase with increasing OE chain length.

D_d values for the copolymers are generally less than the D_s values except for PHEMA which has a slightly greater D_d value. n_d values follow a similar trend to that observed for sorption.

3.3.2 Sorption at 79% Relative Humidity

Table 3.2 shows the EWCs, sorption and desorption coefficients and n_s and n_d values for PHEMA copolymers. The reduced sorption curves are shown in Figures 3.4a-d. PHEMA sorption and desorption curves are

shown in Figure 3.5. The reduced desorption curves were similar to those obtained previously.

The calculated n_s value for PHEMA is again approximately 0.5 indicating possible Fickian diffusion but with the addition 3 mol% OED there is an immediate increase in n_s. The n_s values increase for all copolymers systems up to the addition of 14-30 mol% crosslinker and then decrease as OED content increases.

Despite the increase in the n_s values reasonable fits to Equation 3.2 could still be made up to $n_s = 0.85$, above this they deteriorated, as would be expected, with the worst fit being obtained with a HEMA copolymer containing 6 mol% DiEGDMA, with $n_s = 0.8$, shown in Figure 3.10, which had the highest n_s value. For this copolymer experimental points begin to deviate from the calculated Fickian diffusion curve at $Mt/M_\infty \approx 0.80$ and increase above the theoretical curve. The n_d values show a different trend with the majority of the values varying being between 0.4 and 0.5.

When the data was fitted to Equation 3.2 a similar trend was observed for most of the other copolymers. The copolymers with low amounts of crosslinker tended to diverge from the theoretical uptake at $Mt/M_\infty \approx 0.90$. As the amount of crosslinker increased the fit to the data improved with good fits being obtained for all copolymer systems which had greater than 50 mol% crosslinker. There appears to be no discernible trend for the D_s values for either the EGDMA or DiEGDMA systems. The D_s values for the TEGDMA system appear constant with a sharp increase for the straight TEGDMA sample. The P400/HEMA copolymer values increase up to 50 mol% P400 from $0.49 \times 10^{-8} cm^2 sec^{-1}$ to 1.36×10^{-8} $cm^2 sec^{-1}$ and then decrease to 1.02×10^{-8} $cm^2 sec^{-1}$ for 100% P400. The desorption coefficients for the EGDMA and DiEGDMA systems again appear to follow no discernible trend, while for the TEGDMA copolymers D_d follows a similar trend to that of the sorption coefficients. The P400 values increase

monotonically from 0.45×10^{-8} $cm^2 sec^{-1}$ at 3 mol% to 2.55×10^{-8} $cm^2 sec^{-1}$ for straight P400

TABLE 3.2

Sorption and desorption results for PHEMA and PHEMA copolymers initially equilibrated at 79% Relative Humidity. E, Di and T represent EGDMA, DiEGDMA and TEGDMA respectively. The number in brackets in the D_s and D_d columns represents the standard error given by the DATAFT program.

Mole % OED	EWC	Calculated EWC	$D_s x 10^8$ $cm^2 sec^{-1}$	$D_d x 10^8$ $cm^2 sec^{-1}$	n_s	n_d
0	11.9	11.88	1.31(0.08)	0.43(0.03)	0.52	0.41
3E	10.7		0.68(0.05)	0.47(0.03)	0.66	0.40
6E	11.5		0.59(0.1)	0.45(0.03)	0.70	0.45
14E	8.5		0.33(0.05)	0.35(0.01)	0.77	0.56
30E	7.1		0.52(0.03)	0.41(0.02)	0.65	0.49
50E	4.7		0.60(0.03)	0.44(0.02)	0.62	0.51
3Di	12.2	11.4	0.48(0.06)	0.47(0.03)	0.66	0.42
6Di	11.6	11.0	0.63(0.06)	0.43(0.03)	0.80	0.43
14Di	10.6	10.2	0.56(0.04)	0.45(0.03)	0.71	0.40
30Di	8.6	8.4	0.44(0.02)	0.39(0.02)	0.67	0.44
50Di	6.0	6.6	0.37(0.02)	0.37(0.1)	0.62	0.47
70Di	4.5	4.7	0.42(0.02)	0.39(0.02)	0.63	0.50
100Di	2.7	2.7	0.62(0.03)	0.59(0.02)	0.60	0.50
3T	11.5	11.5	0.65(0.04)	0.46(0.02)	0.59	0.43
6T	11.2	11.1	0.62(0.03)	0.46(0.03)	0.63	0.44
14T	9.9	9.5	0.59(0.04)	0.48(0.02)	0.65	0.43
30T	9.4	8.6	0.55(0.04)	0.44(0.02)	0.72	0.46
50T	8.1	6.9	0.56(0.03)	0.50(0.02)	0.70	0.47
70T	5.8	5.1	0.56(0.03)	0.59(0.02)	0.64	0.49
100T	3.3	3.3	0.83(0.05)	0.82(0.04)	0.66	0.45
3P400	12.7	11.6	0.49(0.06)	0.45(0.02)	0.72	0.42
6P400	12.5	11.3	0.74(0.07)	0.54(0.02)	0.79	0.46
14P400	12.3	10.8	0.71(0.09)	0.78(0.03)	0.77	0.42
30P400	12.3	10.2	0.9(0.08)	1.17(0.05)	0.72	0.40
50P400	10.8	9.6	1.3(0.06)	1.71(0.06)	0.72	0.45
70P400	10.3	9.3	1.3(0.06)	2.29(0.07)	0.60	0.45
100P400	9.0	9.0	1.0(0.05)	2.55(0.09)	0.66	0.41

Again the EWC decreased with the addition of crosslinker and the EWC increased with increasing molecular weight of OED monomer. The predicted EWCs for the DiEGDMA system are reasonably close but the

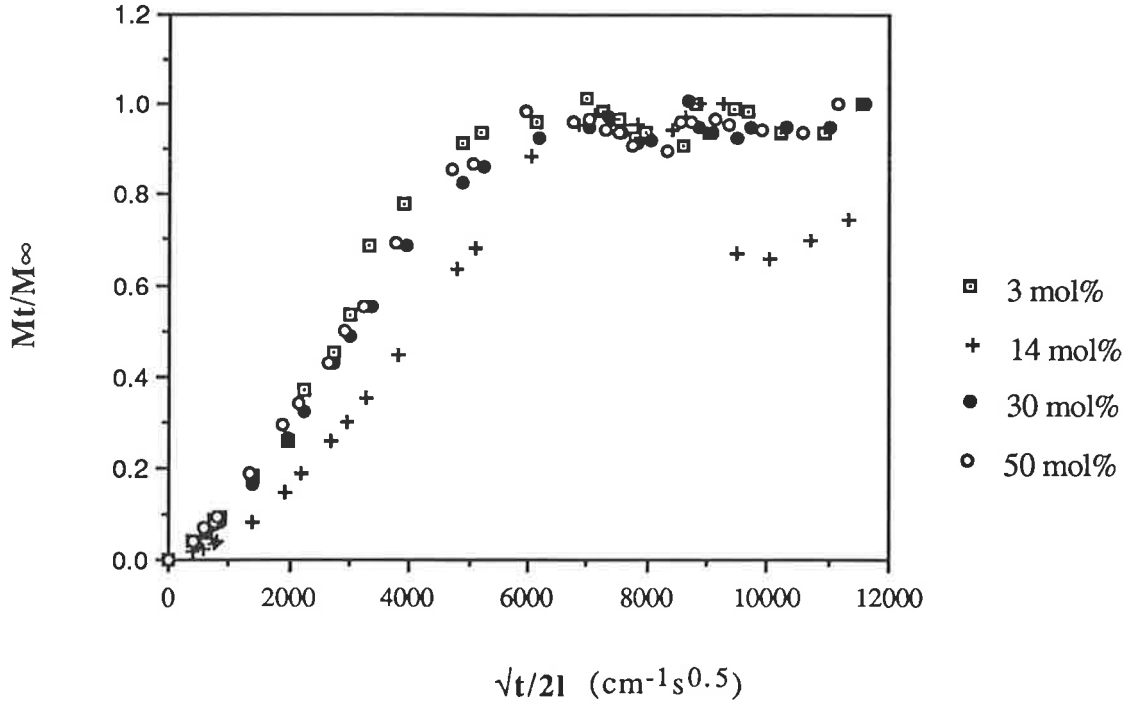

Figure 3.4a Reduced sorption curves for copolymers of HEMA containing EGDMA in the proportions given above. Samples equilibrated at 79% RH

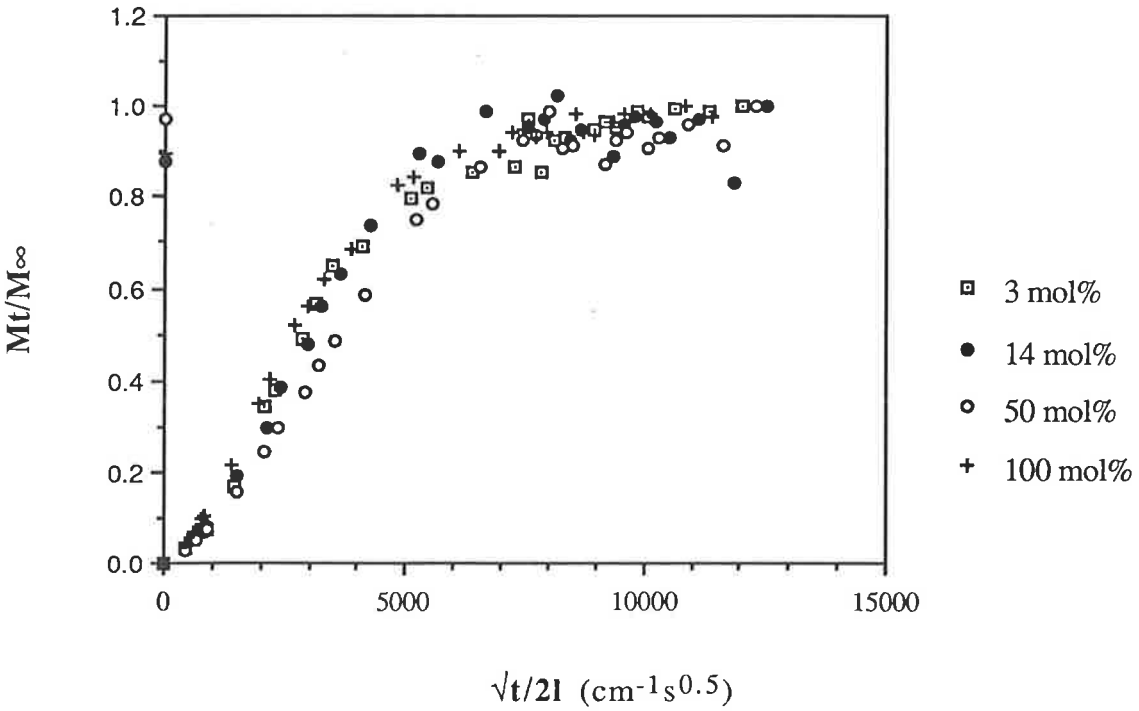

Figure 3.4b Reduced sorption curves for copolymers of HEMA containing DiEGDMA in the proportions given above. Samples equilibrated at 79% RH

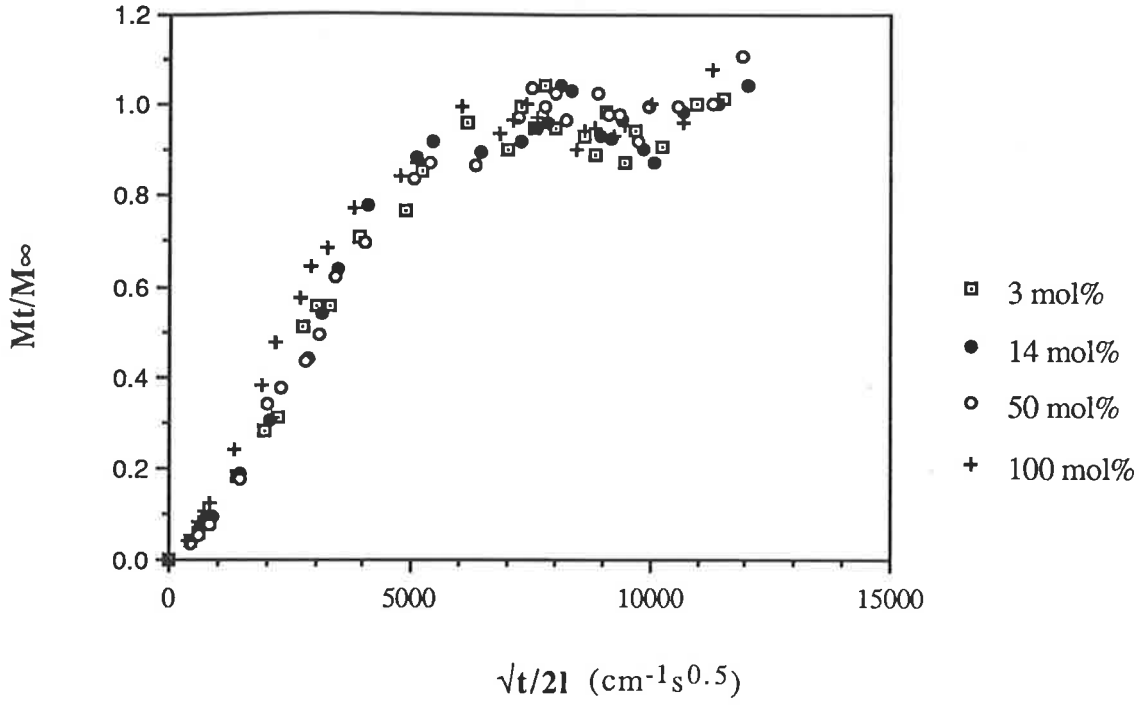

Figure 3.4c Reduced sorption curves for copolymers of HEMA containing TEGDMA in the proportions given above. Samples equilibrated at 79% RH

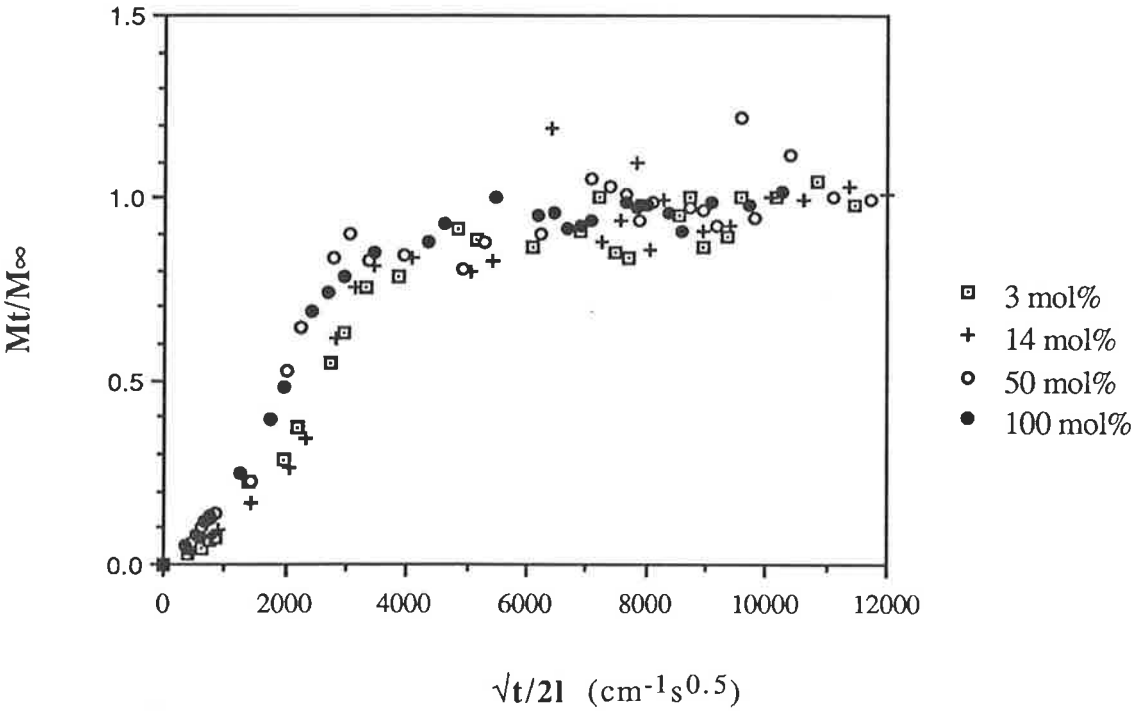

Figure 3.4d Reduced sorption curves for copolymers of HEMA containing P400 in the proportions given above. Samples equilibrated at 79% RH

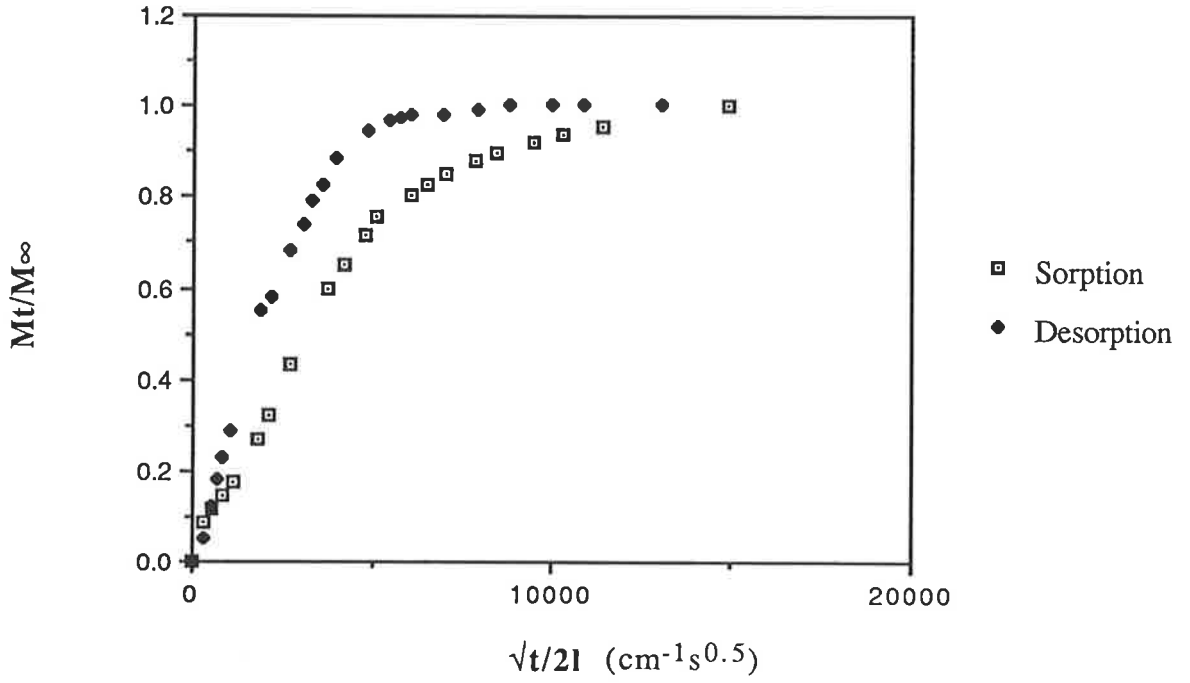

Figure 3.5 Reduced sorption and desorption curves for PHEMA initially equilibrated at 79 % RH.

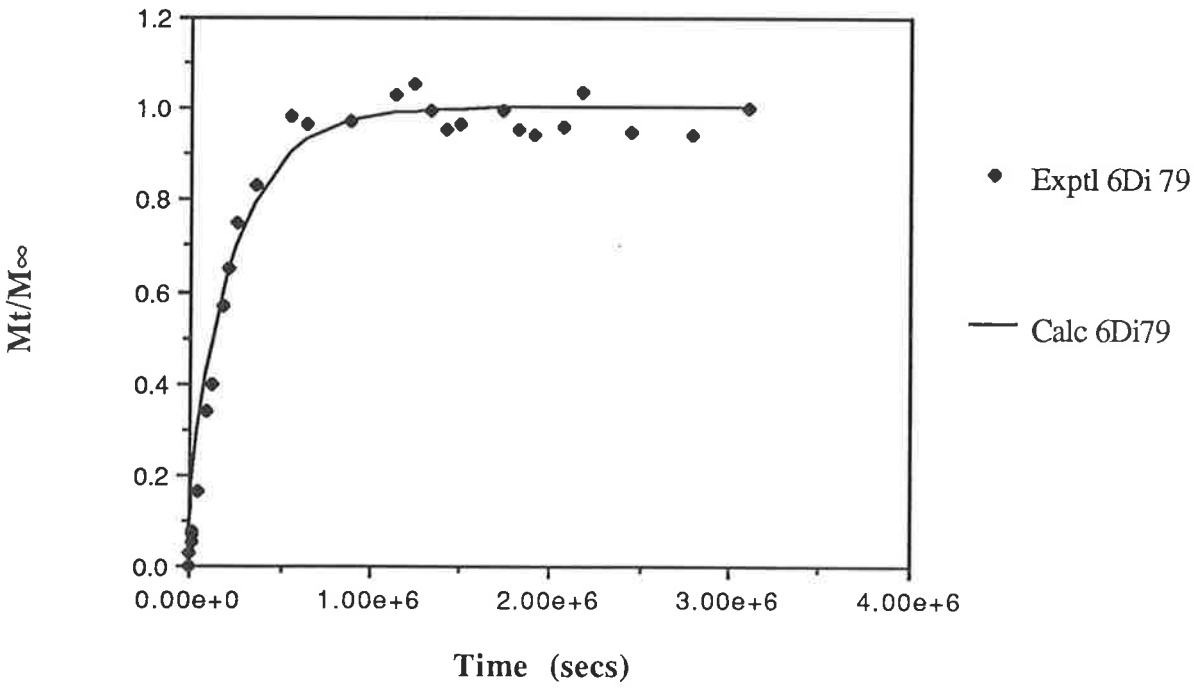

Figure 3.6 Comparison between calculated and experimental values for HEMA copolymerised with 6 mol% DiEGDMAand equilibrated at 79 % RH.

predicted values for the TEGDMA and P400 systems are all less than the actual EWC.

In general the D_d values are less than the D_s values for the EGDMA, DiEGDMA and TEGDMA systems and markedly less for PHEMA alone. For the P400 system, however, the D_d values exceed D_s for all copolymers except the 3 and 6 mol % P400 samples.

3.3.3 Sorption at 100% Relative Humidity

Reduced sorption curves for the four copolymer systems are shown in Figues 3.7 a-d. Table 3.3 gives the values obtained for the EWC, D_s and D_d values, and n_s and n_d values . Figure 3.8 shows the reduced sorption and desorption curve for straight PHEMA. The reduced sorption curves were similar to those observed previously

It was not possible to measure desorption values for all copolymers, as copolymers containing more than 14 mol% EGDMA, 30 mol% DiEGDMA and 6 mol% P400 began cracking and breaking up soon after desorption started.

The reduced sorption curves for the EGDMA and DiEGDMA systems show reasonable linearity up to $M_t/M_\infty=0.5$. The TEGDMA and P400 copolymers, however, show a different pattern with the slope increasing from $M_t/M_\infty=0$ to $M_t/M_\infty=0.1$ and then remaining constant up to $M_t/M_\infty=0.75$.

All copolymers exhibited a water sorption curve that increased above M_∞ before decreasing to their eventual equilibrium value. This "overshoot" tended to decrease with increasing OED content but for some copolymers reached as high as $M_t/M_\infty=1.2$

The n_s value for PHEMA is 1.0 indicating the possibility of Case II diffusion according to the criteria proposed by Frisch (7). Figure 3.9 shows the fit obtained between experimental and calculated values for PHEMA For the copolymers these values vary. The EGDMA copolymers

have n_s values of approximately 0.6. The DiEGDMA system shows a decrease from a 3 mol% value, n_s=0.92, to that of straight DiEGDMA with n_s = 0.64. The TEGDMA values vary from 0.64 for TEGDMA to 0.84 for 6 mol % TEGDMA and then decrease as the TEGDMA copolymer content increases. The P400 system has values of around 0.8.

TABLE 3.3

Sorption and desorption results for PHEMA and PHEMA copolymers initially equilibrated at 100% Relative Humidity. E, Di and T represent EGDMA, DiEGDMA and TEGDMA respectively. The number in brackets in the D_s and D_d columns represents the standard error given by the DATAFT program..

Mole % OED	EWC	Calculated EWC	$D_s x 10^8$ $cm^2 sec^{-1}$	$D_d x 10^8$ $cm^2 sec^{-1}$	ns	nd
0	31.7		1.85(0.07)	4.01(0.05)	1.01	0.36
3E	22.8		1.97(0.09)	1.8(0.02)	0.63	0.39
6E	19.2		1.72(0.5)	1.07(0.08)	0.61	0.39
14E	12.4		1.1(0.1)	0.99(0.08)	0.63	0.36
30E	8.8		0.7(0.1)		0.62	
50E	6.5		0.61(0.06)		0.59	
3Di	26.1	30.7	0.70(0.08)	3.2(0.4)	0.92	0.36
6Di	23.5	29.7	1.04(0.06)	1.9(0.1)	0.75	0.38
14Di	19.8	27.6	0.64(0.08)	1.53(0.07)	0.78	0.35
30Di	13.4	22.8	0.70(0.02)	1.16(0.04)	0.74	0.39
50Di	9.3	17.4	0.60(0.06)		0.69	
70Di	6.4	11.2	0.53(0.04)		0.71	
100Di	4.0	4.0	0.56(0.02)		0.64	
3T	29.5	30.8	0.37(0.03)	3.4(0.5)	0.78	0.28
6T	24.0	29.9	0.8(0.2)	2.6(0.3)	0.84	0.29
14T	17.3	25.9	1.1(0.3)	1.60(0.2)	0.80	0.36
30T	18.2	23.8	0.77(0.08)	1.25(0.09)	0.83	0.45
50T	14.9	19.0	0.58(0.07)	1.17(0.06)	0.77	0.41
70T	11.7	13.7	0.58(0.05)	0.88(0.03)	0.75	0.41
100T	7.6	7.6	0.55(0.05)	1.10(0.02)	0.67	0.41
3P400	31.1	31.2	1.04(0.09)	2.7(0.3)	0.75	0.37
6P400	25.9	30.7	1.27(0.06)	3.8(0.5)	0.84	0.37
14P400	25.0	29.6	1.13(0.04)		0.76	
30P400	22.7	27.4	1.69(0.07)		0.83	
50P400	21.0	25.0	1.51(0.05)		0.79	
70P400	20.3	22.5	1.68(0.07)		0.79	
100P400	19.8	19.8	1.22(0.04)		0.81	

Despite the relatively high n_s values most systems gave a good fit to Equation 3.2 up to M_t/M_∞ = 0.8, although the standard error calculated was

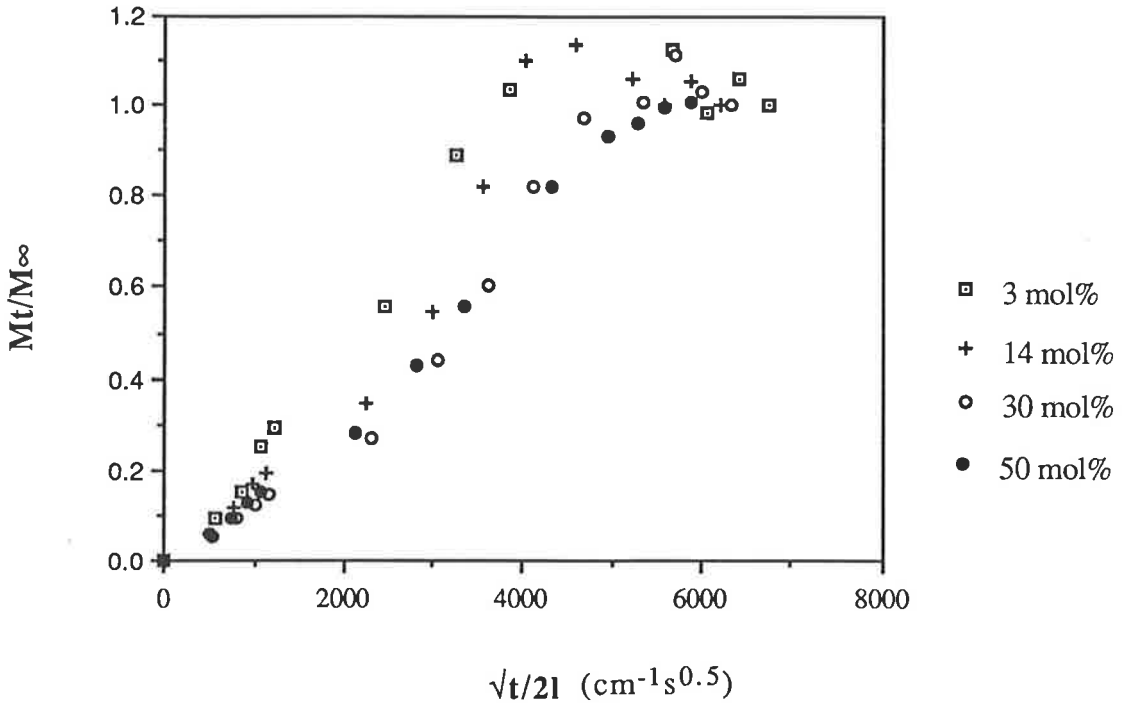

Figure 3.7a Reduced sorption curves for copolymers of HEMA containing EGDMA in the proportions given above. Samples equilibrated at 100% RH

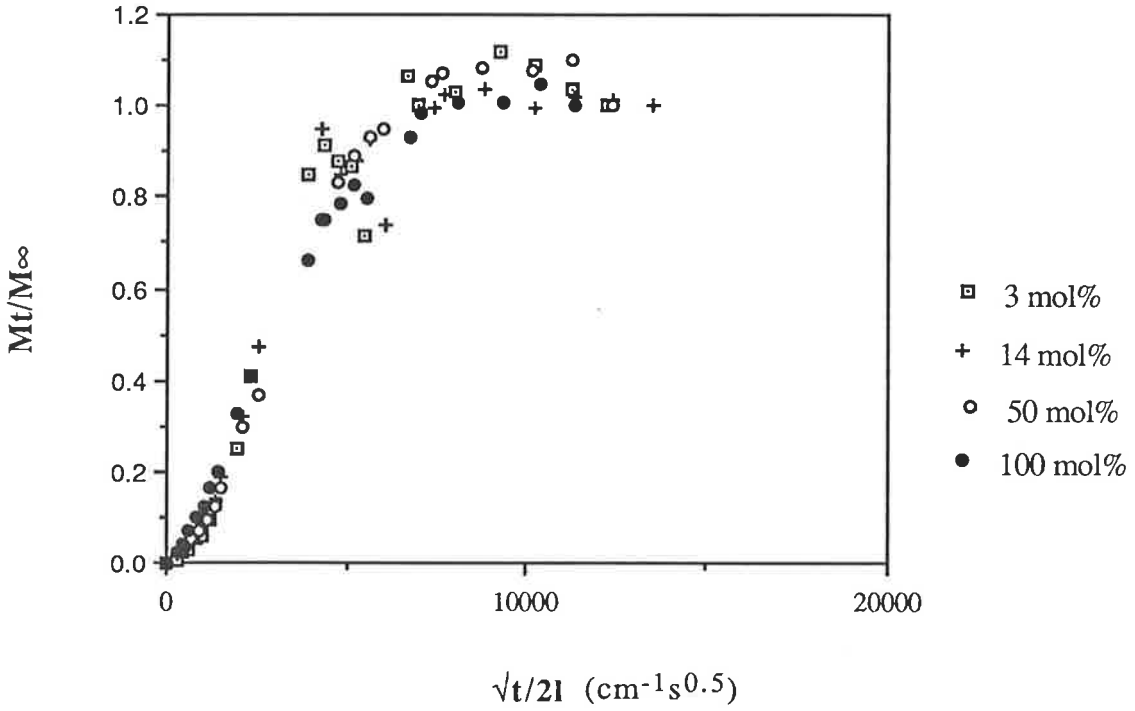

Figure 3.7b Reduced sorption curves for copolymers of HEMA containing DiEGDMA in the proportions given above. Samples equilibrated at 100% RH

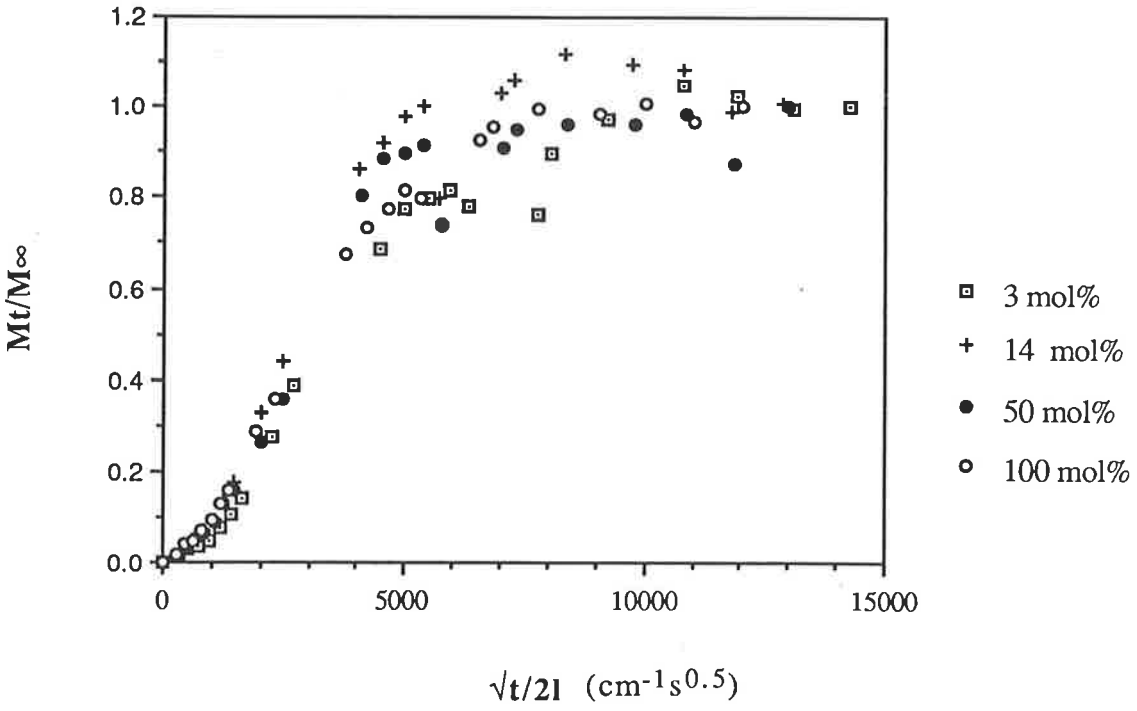

Figure 3.7c Reduced sorption curves for copolymers of HEMA containing TEGDMA in the proportions given above. Samples equilibrated at 100% RH

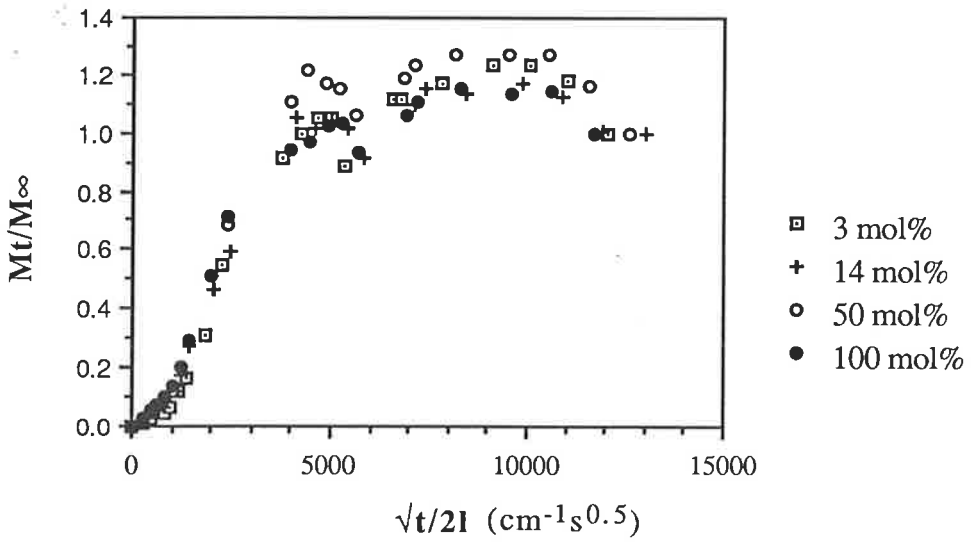

Figure 3.7d Reduced sorption curves for copolymers of HEMA containing P400 in the proportions given above. Samples equilibrated at 100% RH

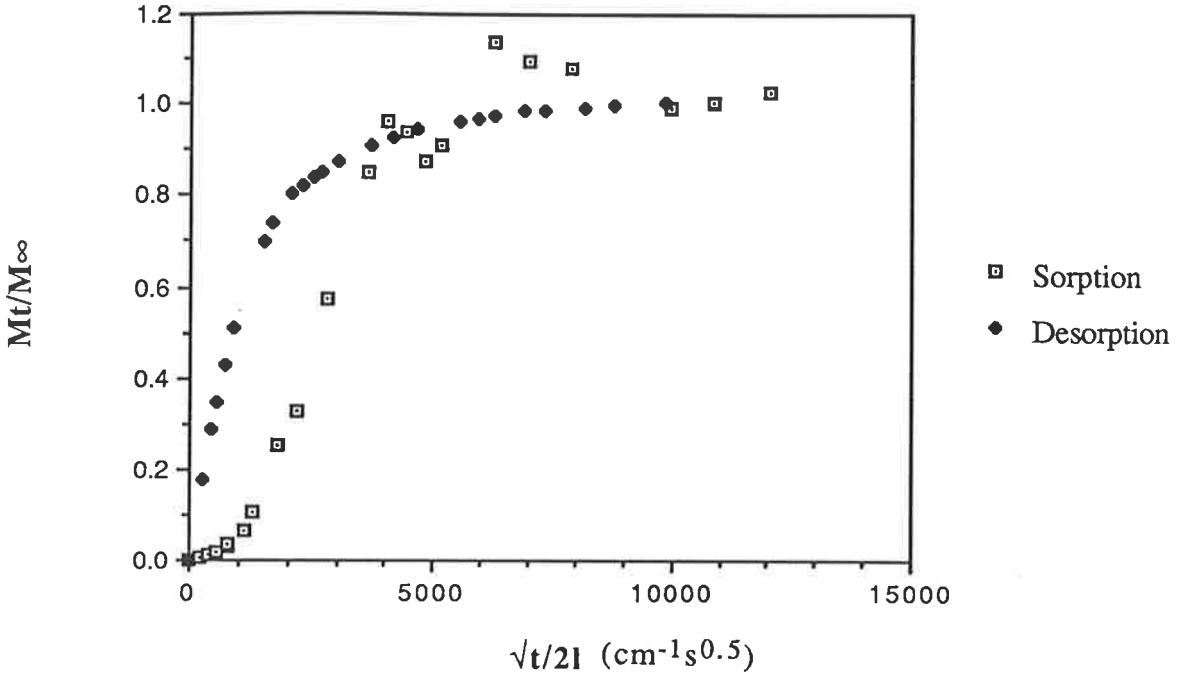

Figure 3.8 Reduced sorption and desorption curves for PHEMA initially equilibrated at 100% RH.

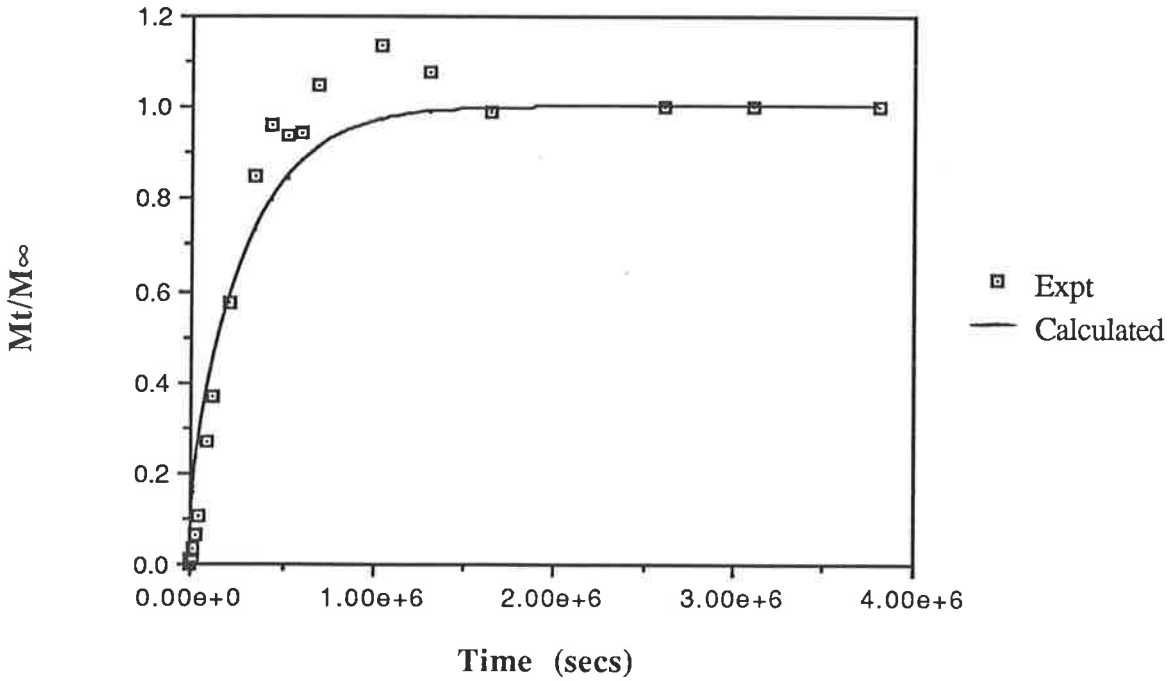

Figure 3.9 Comparison between calculated and experimental sorption values for PHEMA equilibrated at 100 % RH using Equation 3.2.

greater than for previous results at 33% and 79 % RH. This could in part, however, be due to the water overshoot above the final EWC. Better fits were obtained from the desorption curves as evidenced by a lower percentage standard error.

The n_d values are all significantly lower with PHEMA having n_s=0.36 and the copolymers having values ranging between 0.35 to 0.4 in most cases.

The diffusion coefficient, D_s, for PHEMA is 1.85×10^{-8} $cm^2 sec^{-1}$, higher, as would be expected, than the previous values obtained at 33% and 79% RH. For the EGDMA system D_s shows a decrease with the addition of crosslinker from 1.97×10^{-8} $cm^2 sec^{-1}$ to 0.61×10^{-8} $cm^2 sec^{-1}$. The other copolymer systems tend to show a larger D_s for intermediate copolymer ratios decreasing for low and high mol% of OED. This is most obvious with the P400 system, starting initially at 1.04×10^{-8} $cm^2 sec^{-1}$ for 3 mol% P400, rising to 1.69×10^{-8} $cm^2 sec^{-1}$ for 30 mol% P400 and then decreasing to 1.22×10^{-8} $cm^2 sec^{-1}$ for straight P400.

The D_d value for PHEMA is considerably larger than the D_s value, at 4.0×10^{-8} $cm^2 sec^{-1}$ being more than two times greater. The other copolymers, apart from the EGDMA system, all have D_d much greater than D_s. These values tend to decrease as crosslinking increases.

It is also apparent that the calculated EWCs are greater than the experimental EWCs unlike the results found for the samples equilibrated at 33% and 79 % RH

3.3.4 Sorption in Water

The reduced sorption curves for the copolymer systems are shown in Figure 3.10 a-d. Table 3.4 gives the EWCs, D_s, D_d, n_s and n_d values obtained from the appropriate equations. There was again a problem with samples breaking up on desorption and it was not possible to obtain values for desorption for samples containing greater than 14 mol% EGDMA, 30

mol% DiEGDMA and 3 mol% P400. Figure 3.11 shows the reduced sorption and desorption curves for PHEMA.

TABLE 3.4

Sorption and desorption results for PHEMA and PHEMA copolymers initially equilibrated in water. E, Di and T represent EGDMA, DiEGDMA and TEGDMA respectively. The number in brackets in the D_s and D_d columns represents the standard error given by the DATAFT program.

Mole% OED	EWC	Calculated EWC	$D_s x10^8$ cm^2sec^{-1}	$D_d x10^8$ cm^2sec^{-1}	n_s	n_d
0	39.2		8.6(0.3)	4.12(0.4)	0.51	0.48
3E	28.0		5.2(0.4)	5.1(0.2)	0.52	0.41
6E	23.7		4.31(0.5)	5.4(0.9)	0.55	0.44
14E	18.5		2.11(0.2)	2.3(0.3)	0.58	0.40
30E	11.1		0.57(0.05)		0.63	
50E	7.49		0.08(0.01)		0.55	
3Di	33.0	38.1	8.4(0.3)	5.8(0.7)	0.51	0.39
6Di	27.9	36.9	6.4(0.4)	4.3(0.5)	0.53	0.37
14Di	21.4	34.4	5.5(0.4)	3.3(0.5)	0.51	0.41
30Di	14.9	28.8	1.00(0.07)	1.4(0.1)	0.57	0.41
50Di	9.7	22.1	0.84(0.04)		0.62	
70Di	7.3	18.4	0.60(0.01)		0.57	
100Di	4.2	4.2	0.68(0.03)		0.44	
3T	33.7	38.1	8.8(0.3)	6.6(0.7)	0.52	0.49
6T	29.9	37.1	7.6(0.2)	5.2(0.6)	0.52	0.52
14T	21.9	32.2	4.5(0.2)	2.5(0.3)	0.56	0.37
30T	18.4	29.6	2.3(0.1)	1.8(0.2)	0.56	0.38
50T	15.4	23.6	1.9(0.1)	1.6(0.1)	0.58	0.36
70T	12.0	16.5	1.15(0.04)	1.25(0.06)	0.57	0.44
100T	7.9	7.9	0.96(0.08)	1.44(0.02)	0.51	0.48
3P400	34.5	38.6	8.5(0.2)	5.0(0.6)	0.51	0.52
6P400	31.6	37.9	9.6(0.4)		0.52	
14P400	29.7	36.7	6.1(0.3)		0.57	
30P400	27.4	33.9	6.5(0.2)		0.56	
50P400	25.8	30.9	8.8(0.2)		0.55	
70P400	24.3	27.7	8.6(0.2)		0.57	
100P400	24.1	24.1	7.9(0.1)		0.57	

It can be observed from the reduced sorption curves that these are noticeably different from those obtained from the samples conditioned at 100 % RH. These curves tend to be linear up to $M_t/M_\infty = 0.9$ without the inflexion noticeable in the earlier sorption work. They also tend to reach their equilibrium EWC much more rapidly than the previous examples. Again, a water overshoot is evident, as with the samples equilibrated at 100

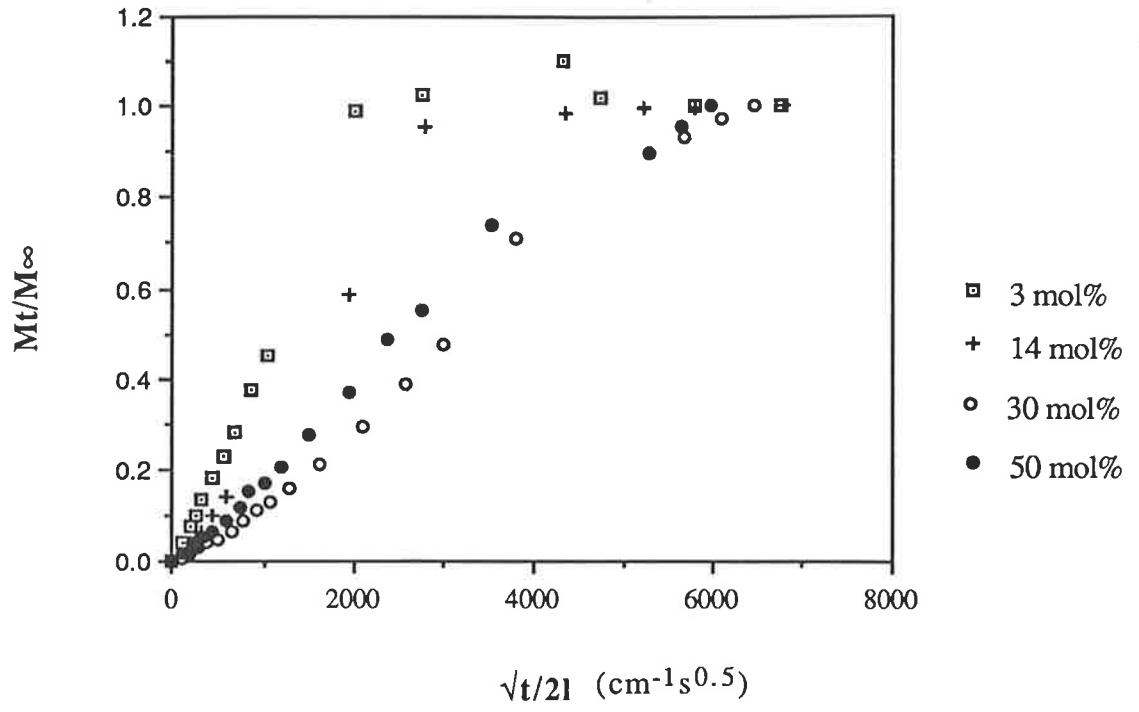

Figure 3.10a Reduced sorption curves for copolymers of HEMA containing EGDMA in the proportions given above. Samples equilibrated in water.

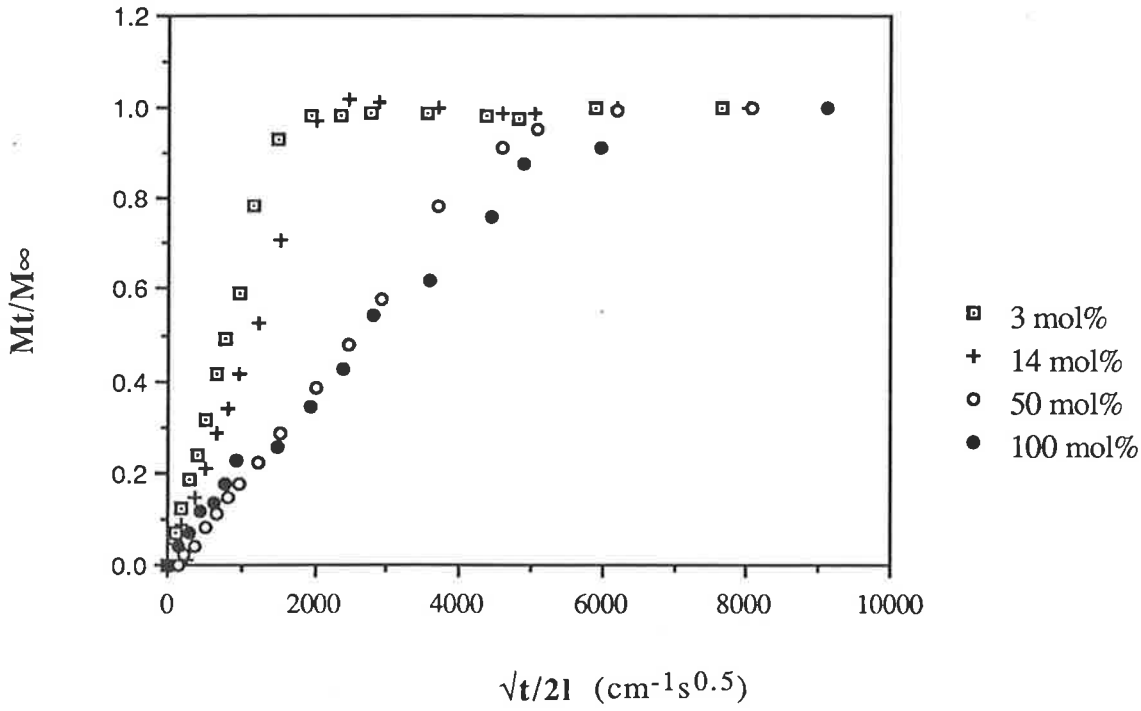

Figure 3.10b Reduced sorption curves for copolymers of HEMA containing DiEGDMA in the proportions given above. Samples equilibrated in water.

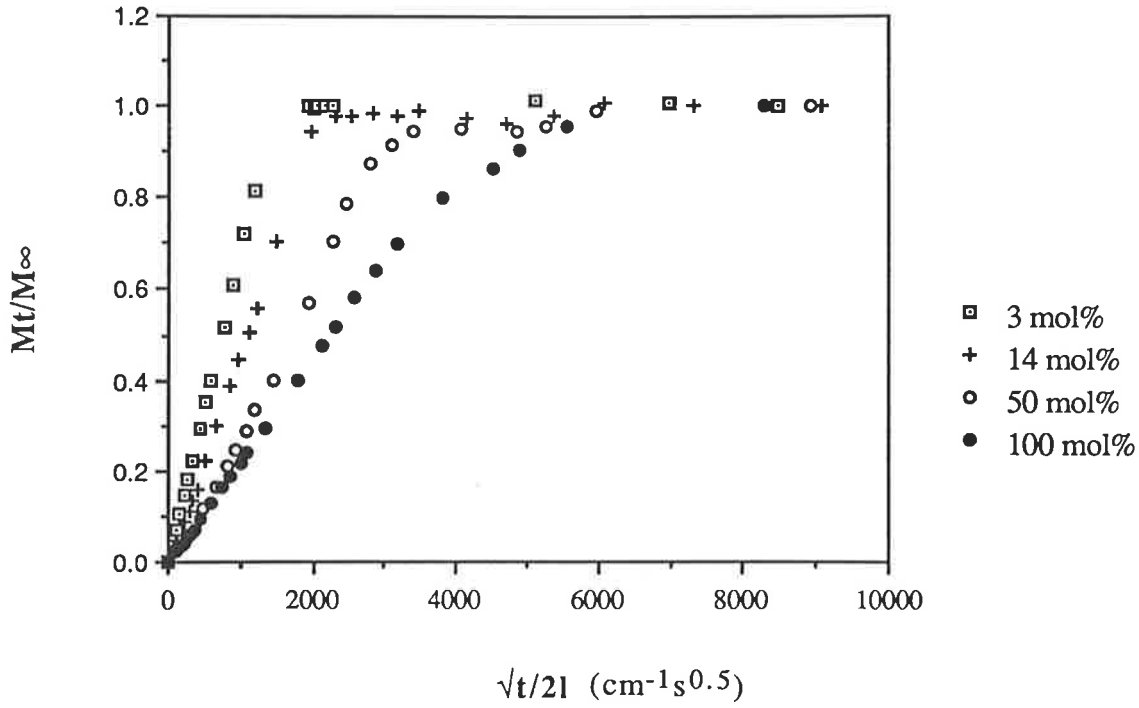

Figure 3.10c Reduced sorption curves for copolymers of HEMA containing TEGDMA in the proportions given above. Samples equilibrated in water

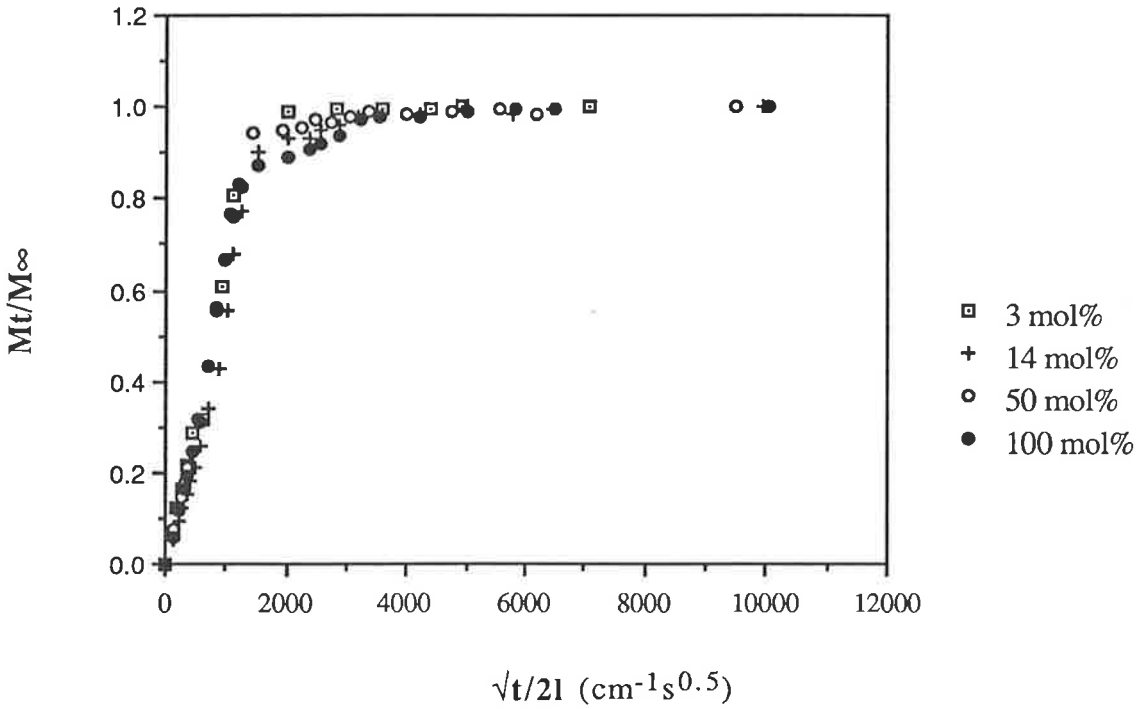

Figure 3.10d Reduced sorption curves for copolymers of HEMA containing P400 in the proportions given above. Samples equilibrated in water

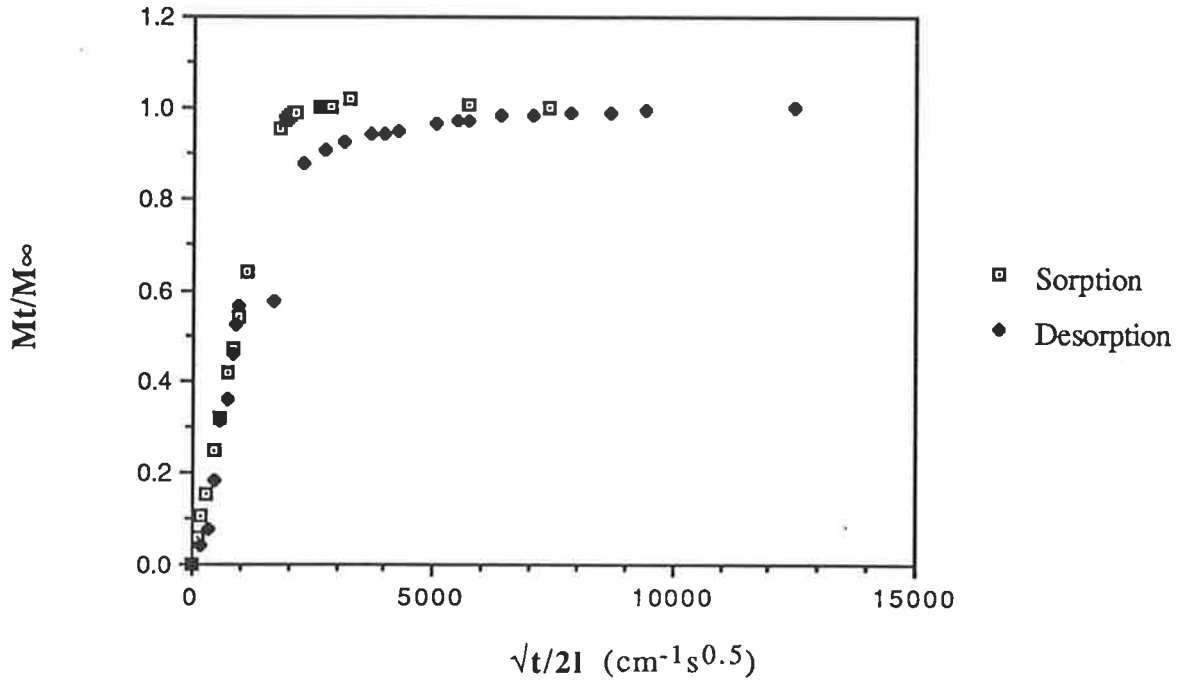

Figure 3.11 Reduced sorption and desorption curves for PHEMA initially equilibrated in water.

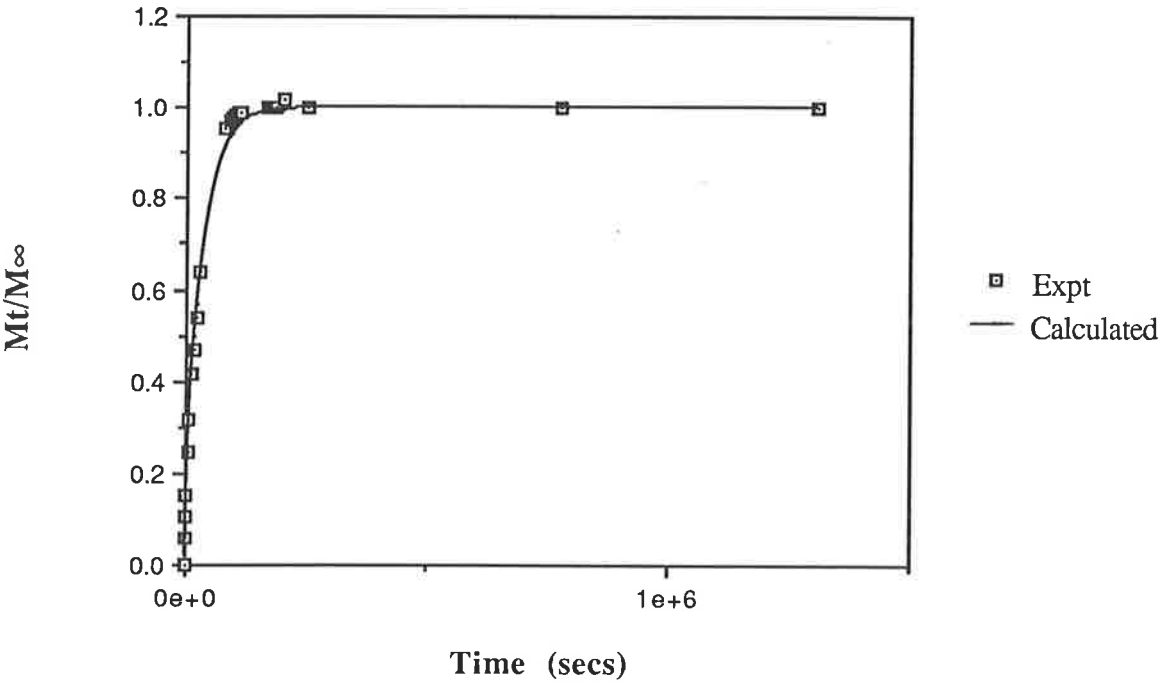

Figure 3.12 Comparison between calculated and experimental values for water sorption into PHEMA equilibrated in water.

% RH, but it does not appear to occur to the same extent as found for those samples.

The n_s values calculated here are much less than at 100% RH, with PHEMA having n_s=0.51. The copolymers also exhibit values generally between 0.5 and 0.6, with a tendency to increase slightly as the crosslinking concentration increases. The n_d values for the EGDMA and DiEGDMA systems, however, tend to be similar to those obtained for similar copolymers that were equilibrated at 100 % RH. TEGDMA copolymer values lie between 0.36 and 0.52, slightly higher than those in the previous section.

Good fits were obtained to Equation 3.2 for both the sorption and desorption curves, an example of which can be seen in Figure3.12. The D_s value for PHEMA is much greater than those calculated previously, at 8.6×10^{-8} $cm^2 sec^{-1}$. As crosslinking increases D_s decreases below that found for PHEMA with less of a decrease noted as the size of the OED copolymer used increases. D_d for PHEMA is less than D_s, with the D_d values of the copolymers following a similar trend to that of the D_s values. n_d values showed no obvious trend and varied between 0.37 and 0.52.

As with the samples equilibrated at 100% RH the calculated EWC is again greater than the experimental EWC.

3.3.5 Variation of Diffusion Coefficients with Sorption Time

Individual D_s and D_d values were calculated for PHEMA samples using Equations 3.3 and 3.4. and plotted as a function of M_t/M_∞. (Figures 3.13a-b). D_s for the 33 % RH conditioned sample shows a steady increase up to M_t/M_∞ =0.5 at which stage it levels off and remains constant. At 79 % RH D_s again shows an increase, levelling off at M_t/M_∞= 0.3 but decreases slightly at M_t/M_∞=0.5 and then decreases again, sharply, at M_t/M_∞ = 0.95. There is an almost linear increase in D_s at 100 % RH up to M_t/M_∞ =0.8 after which there is some scatter in the points. For samples

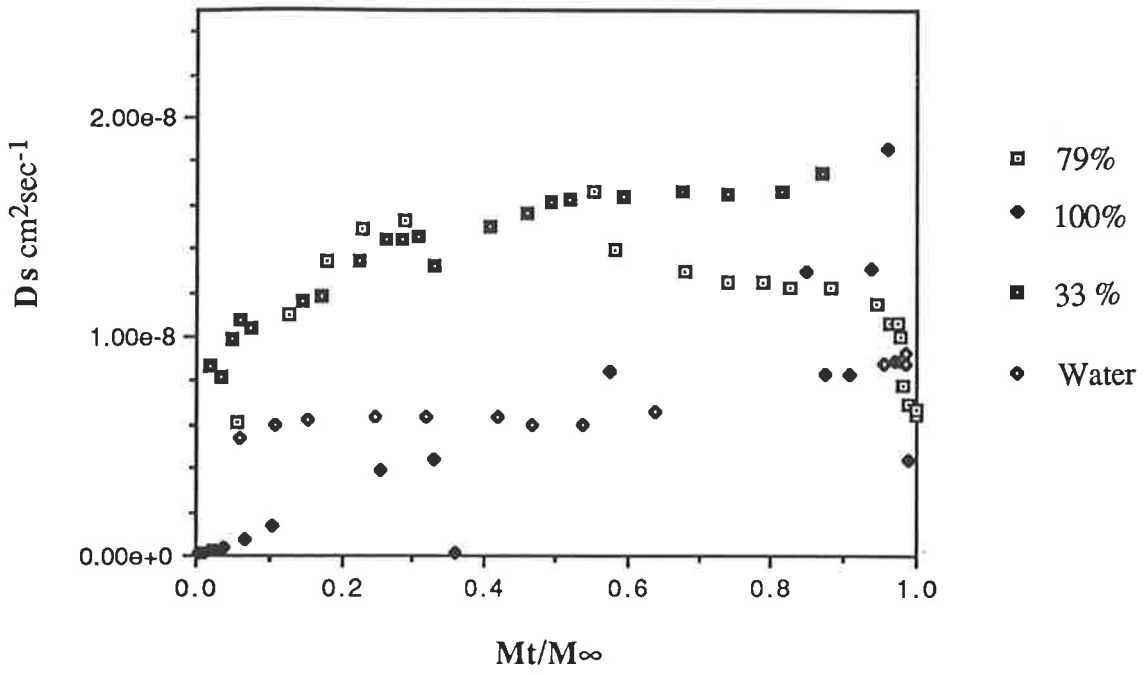

Figure 3.13a Variation in sorption coefficent, Ds, with water uptake for PHEMA samples equilibrated at different relative humidities and in water as above. Ds for the sample equilibrated at 33% Rh has been multiplied by 10. Ds for the sample equilibrated in water has been divided by 10.

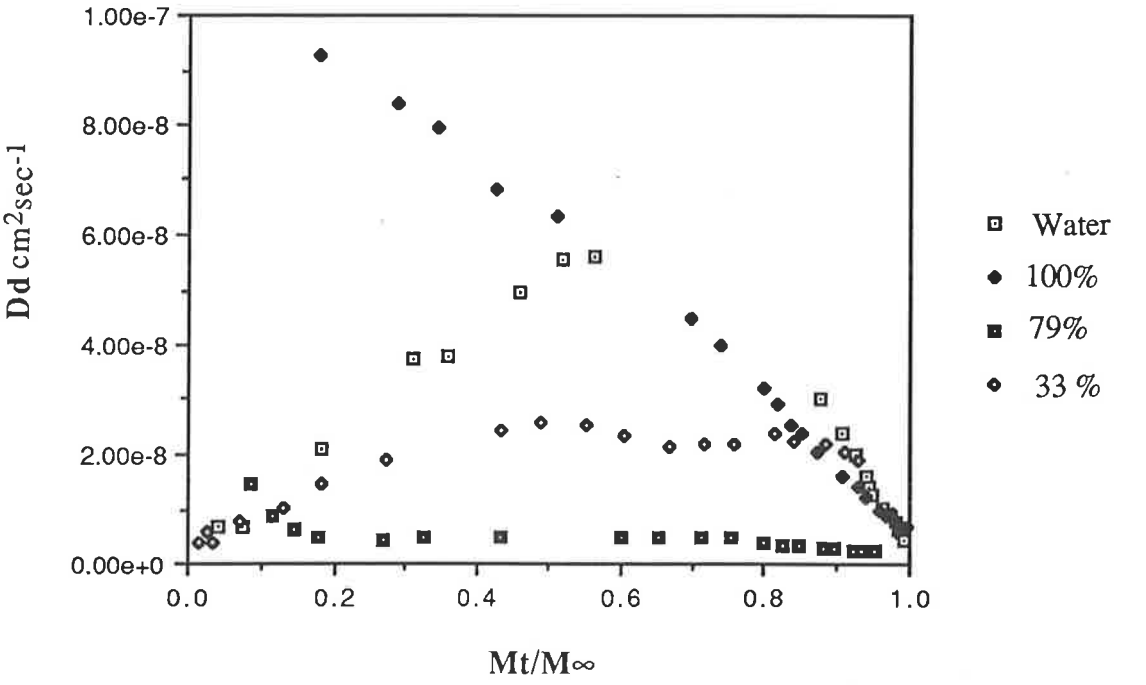

Figure 3.13 b Variation in desorption coefficients with water uptake for the desorption of PHEMA samples equilibrated at different RHs and in water.

sorbed in water D_s show a slight increase up to Mt/M_∞ = 0.2, levels off to Mt/M_∞ =0.75 after which it again increases

The D_d values for samples conditioned at 33 % RH are similar to the D_s values for the same RH. The desorption coefficient for samples conditioned at 79%, however, shows a different trend, starting off at a high value before decreasing. Similarly D_s for 100% conditioned samples shows an almost linear decrease. D_s values for saturated PHEMA shows an increase up to Mt/M_∞ =0.5 after which it decreases to nearly its starting value.

3.3.6 Water in Voids

Turner's method (15) has been used here to determine the amount of water residing in voids in PHEMA and the copolymers formed with the OEDs. The results are given in Table 3.5 The sample used was of a similar thickness to that used in the sorption work mentioned earlier. The amount of water entering voids initially shows a sharp rise (Figure 3.14) which peaks at 7.2% after thirty minutes and an EWC of 14 %. As sorption continues the percentage of water in voids decreases to a value, at the final equilibrium EWC, of approximately 3 %. Therefore the final percentage of water residing in zero density voids as a percentage of the hydrogel weight is approximately 1.2 %. From Table 3.5 it can be seen that the primary effect of copolymerising HEMA with OEDs is to increase the water present in voids. Surprisingly though, while the addition of 3 mol% OED, in general, causes only a small increase in void size from 3 % to 5% at full hydration, it is apparent from Figure 3.15 that there is a much greater difference in the sorption process. This shows the sorption of water into voids for HEMA copolymerised with 6 mol% of three different OEDs

The maximum amount of water found in voids again peaks at low EWC but is much greater than that found for PHEMA. For the 6 mol% EGDMA/HEMA copolymer the amount of water residing in voids peaks at an

EWC of just over 1% with 55% of the water in voids before this decreases to 5 % at full saturation. Similar results were obtained for HEMA copolymerised with 6 mol% TEGDMA and 6 mol%P400, with the amount of water found in voids peaking at approximately 3% EWC and reaching maximum values of 44 % and 28 % respectively.

Similar behaviour was observed for other copolymers with higher concentrations of OEDs, although the maximum amount of water found in voids did not exceed 70%. As the concentration of crosslinking increased the percentage of water found in voids also tended to increase. There is also a noticeable trend as the molecular weight of the OED increases. The EGDMA copolymers generally had a larger percentage of voids for similar mole ratio copolymers and this void percentage tended to decrease as the number of ethylene glycol units in the OED increased.

Simon (24) examined voids in TEGDMA and found that initially 60 % of the water entered voids, again peaking at low EWC, before decreasing to 30 % at full EWC. This was equivalent to 1.7 mass % of the water existing in voids and this was attributed to inhomogeneities in the polymer that arose due to an inhomogeneous, diffusion controlled crosslinking reaction. Similar results were obtained here for TEGDMA but the value at full EWC was slightly lower at 26 %

The amount of water residing in voids was also measured for PHEMA that had been conditioned at different relative humidities. For these samples it was necessary to rapidly weigh the sample in water before any significant diffusion of water into the sample could occur For PHEMA conditioned at 33 % RH it was found that 35 % of the sorbed water existed in voids. This corresponds to some 1.6 wt % of the hydrogel. This is slightly more than that found for saturated PHEMA and seems to imply that initially the majority of the water is absorbed into voids before swelling takes place. For the samples conditioned at 79% and 100% RH the amounts found in voids were 12.2 % and 4.3 % respectively. This corresponds to

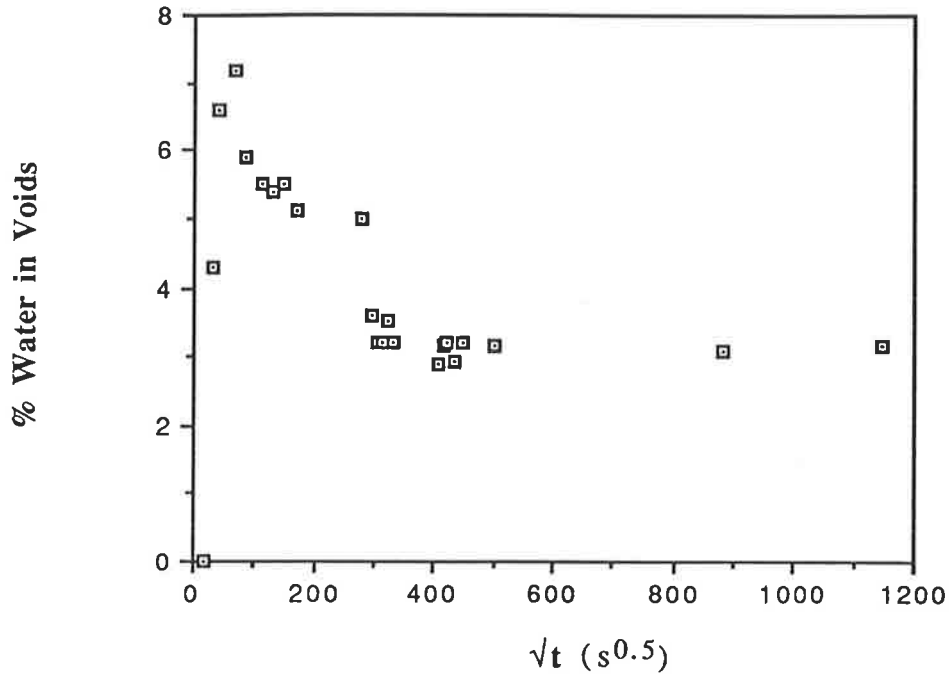

Figure 3.14 Percentage of water sorbed into voids in PHEMA.

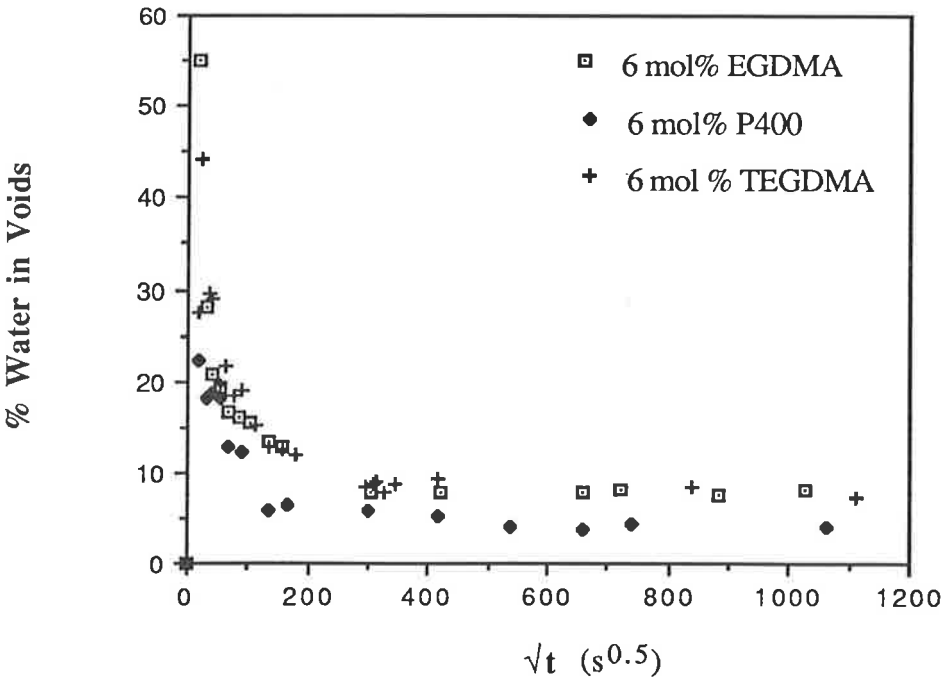

Figure 3.15 Percentage of water found in voids for three copolymers of HEMA with 6 mol % EGDMA, TEGDMA and P400 as above.

1.5 wt% and 1.4 wt% of the hydrogel respectively, which again seems to indicate that the voids tend to be filled first and then remain at a constant level.

TABLE 3.5
Percentage of water found to reside in the voids of PHEMA copolymers.

	Void size for copolymers of HEMA with			
Mole %	EGDMA	DiEGDMA	TEGDMA	P400
3	5.0	4.2	9.3	6.6
6	8.1	4.3	7.3	4.7
14	11.8	7.9	15.8	5.3
30	20.4	14.5	9.7	6.5
50	35.6	24.7	16.1	7.6
70		29.5	15.5	8.6
100		37.4	25.6	12.3

3.3.7 Density Measurements.

The density of the polymers used could be calculated by making use of Archimede's principle and by knowing the weights of the polymers in air and in water which have been previously measured in order to calculate the amount of water present in voids. The density of PHEMA was found to be 1.28±0.01 g/cm^3 which is comparable to that found by Wichterle and Chromecek of 1.274 g/cm^3 (46). The density of the copolymers is given in Table 3.6.

From the data presented in Table 3.6 it is apparent that in general the density of the copolymers decreases as the degree of crosslinking increases indicating perhaps that chain packing is more ordered and uniform in PHEMA.

TABLE 3.6
Density of copolymers of HEMA with EGDMA, DiEGDMA,TEGDMA and P400 given in g/cm^3.

Mol% OED	3	6	14	30	50	70	100
EGDMA	1.28	1.28	1.27	1.27	1.26		
DiEGDMA	1.28	1.28	1.27	1.26	1.25	1.24	1.23
TEGDMA	1.26	1.26	1.23	1.26	1.26	1.24	1.24
P400	1.24	1.27	1.26	1.24	1.22	1.22	1.22

3.4 Discussion

It is obvious from the data presented that the type of diffusion that occurs in the polymers studied is strongly dependent on a number of factors, including the type and degree of crosslinking and the conditions under which sorption was allowed to take place. It is also apparent from the reduced sorption and desorption curves for PHEMA (Figures 3.2, 3.5 and 3.8) at 33 % ,79 % and 100 % RH that one of the criterion mentioned earlier for Fickian diffusion is not obeyed and therefore sorption in these cases can not be said to be truly Fickian. The PHEMA sample sorbed in water, however, does seem to follow these three criteria.

The tendency for the polymer samples to absorb water above the final equilibrium value has been previously observed in a number of other systems (25,39) and has been analysed by Vrentas et al (26) and Smith and Peppas (27).

Kambour et al (28), Titow et al (29) and Overbergh et al (30) attributed this type of overshoot to crystallisation caused by the penetrant and assumed that ordered regions formed during sorption reject penetrant sorbed before these ordered regions had formed. Peppas and Urdahl (31), however, offer an alternative view for this phenomena. They studied penetrant overshoot occurring in crosslinked polystyrene/cyclohexane systems with varying crosslinking ratios. As crosslinked polystyrene does

not exhibit any substantial degree of crystallinity the above explanation could not suffice to explain the penetrant overshoot. They found that it was dependent on sample thickness, the degree of crosslinking and, to some extent, the temperature at which the experiment was carried out. It was observed that as the crosslinking density decreased the magnitude of the overshoot increased. Peppas and Urdahl (31) suggest that the greater mobility of the macromolecular chains, due to less crosslinking, tends to enhance the transport process since the mobility of the penetrant molecules in the swollen region increases. The change in solubility then arises from a slower reordering of the macromolecular chains and chain segments, which occurs on a longer timescale than the sorption process and subsequently leads to the rejection of some of the already sorbed penetrant

The overshoot here is much more evident for the samples conditioned at 100 % RH and appears only minimally for those samples sorbed in water, (i.e a maximum overshoot for copolymers sorbed in water of M_t/M_∞ = 1.02 compared to 1.43 for the 3 mol% EGDMA sample conditioned at 100% RH). The overshoot is shown graphically in Figure 3.16 for the 100 % RH conditioned copolymers. It can be seen that for all copolymers, and particularly for the EGDMA copolymers, that the overshoot tends to increase with decreasing crosslinking, tending to agree with the conclusions reached by Peppas and Urdahl about the reasons for the uptake of solvent above its final equilibrium value. It may also be possible that the tendency for the 100% RH conditioned samples to exhibit a larger overshoot is due to a much slower reordering of the macromolecular chains than that occurring in the samples sorbed in water due to less water sorption and therefore a smaller plasticising effect.

Some water sorption studies on Poly (HEMA/MMA) and Poly (HEMA/NVP) copolymers, in some cases crosslinked with 0.8 wt % EGDMA (32), and recently on copolymers of EGDMA, DiEGDMA , Tri EGDMA and TEGDMA copolymerised with 0, 30 and 50 mol% HEMA have

been conducted (25), with sorption taking place in water. Franson and Peppas (32) found n_s values for HEMA/MMA copolymers of 0.50 with the MMA content varying between 0 and 50 mol%. They also studied the motion of the penetrant front by taking a series of photomicrographs of cylindrical samples and, by utilizing polarizing filters, it was possible to see the stresses resulting from the transition from glassy to rubbery.

They found that for PHEMA homopolymers and copolymers with MMA there were three distinct zones. There was a penetrant front separating the rubbery and glassy polymer. Behind this there was a zone of varying thickness, depending on time of sorption and the hydrophilicity of the polymer, of significantly different refractive index where macromolecular relaxations are still prominent. From the back of this region and to the edge of the polymer was a swollen and rubbery gel, effectively at mechanical equilibrium (Figure 3.17). They found that it was not possible to fit the position of the two fronts to either a linear or square root function of diffusion time and concluded that water transport could not be strictly Fickian despite the n_s values found

Mardel (33) measured the diffusion rates of water into copolymers of HEMA with 5, 10, 15 and 20 wt% MMA in water and found both the EWC and D_s decreased as the percentage of MMA increased. The value of $9.36 \times 10^{-8} cm^2 sec^{-1}$ for 5 wt% MMA copolymer is comparable to values found here for PHEMA and slightly crosslinked PHEMA. Previous values found for PHEMA (34-37) vary between $5 \times 10^{-8} cm^2 sec^{-1}$ up to $3080 \times 10^{-8} cm^2 sec^{-1}$, although the last value measured by Refojo (37) was calculated from permeability measurements which could explain its large value. The other previous measurements were made on PHEMA samples that had been polymerised with water in situ and this has been found to effect the diffusion coefficient (34,36). Diffusion was found to conform to Ficks law in that it gave linearity when plotted according to Equation 3.3.

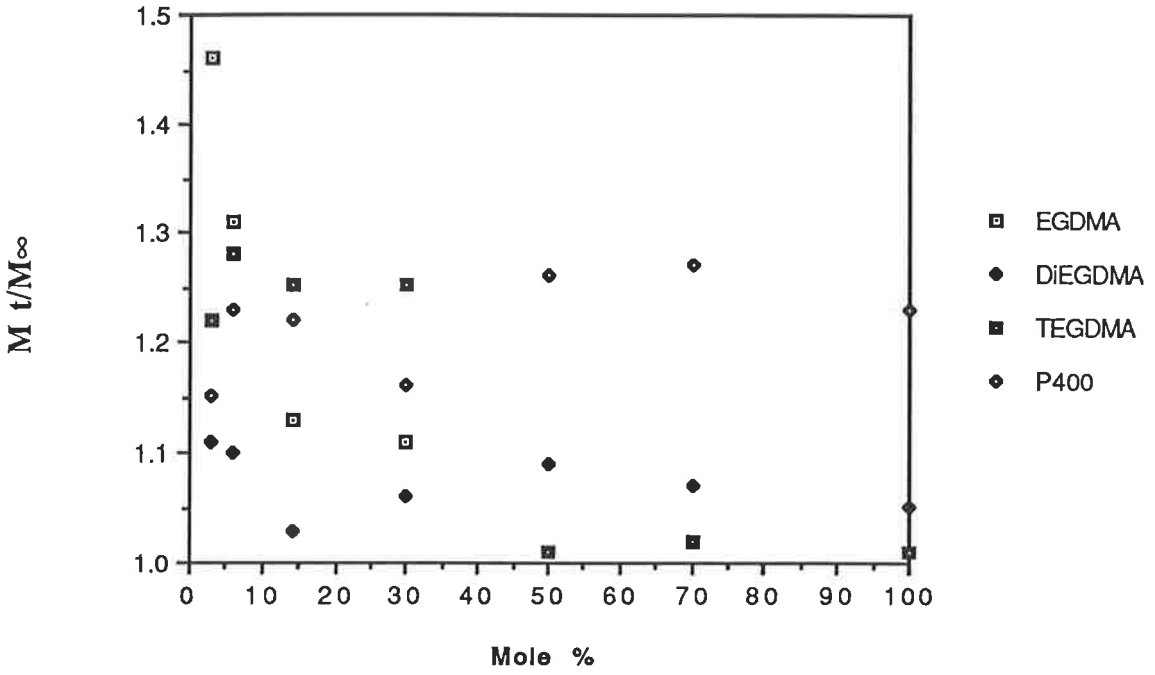

Figure 3.16 Water uptake overshoot for copolymers of HEMA with OEDs against mole % of OED

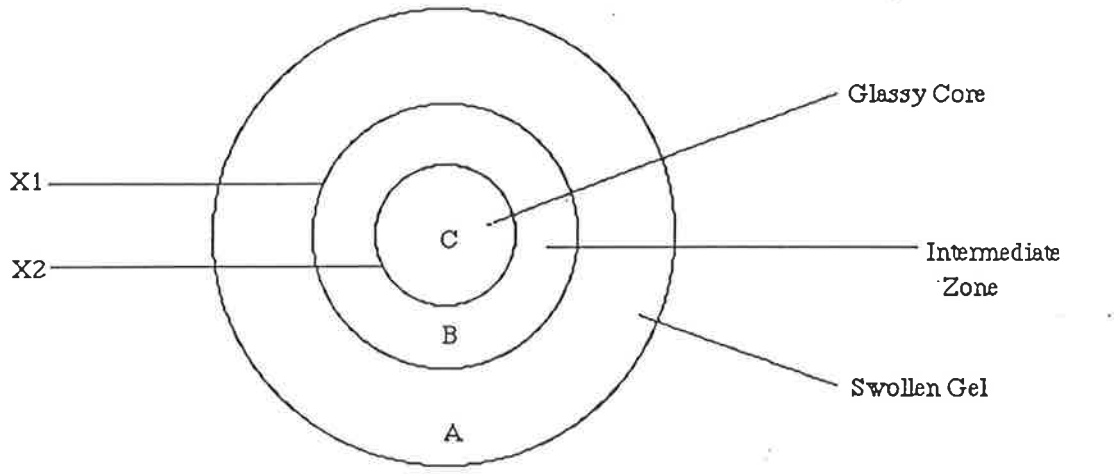

Figure 3.17 Schematic of the three zones and two penetration fronts found by Franson and Peppas (33) for sorption of water into PHEMA.

Robert, Buri and Peppas (38) have studied the diffusion of water into PHEMA microparticles, with diameters varying between 105 and 601 μm, crosslinked with up to 0.124 mol% EGDMA. They found a large departure from Fickian transport with n_s values increasing up to 0.85 for the highest crosslinked sample. They attributed this to two factors: (1) The effect of crosslinking on the relaxation time caused the diffusional Deborah number, De, to approach one, and (2) Diffusion of the penetrant decreasing more rapidly than the relaxation time as a function of the degree of crosslinking.

Walker and Peppas (25) studied the OED/HEMA system mentioned above. They gave n_s values only for the DiEGDMA and TriEGDMA (not studied here) copolymer systems and there is reasonably good agreement between their values and the values given in Table 3.4.(i.e n_s values of 0.41.0.59 and 0.59 for 100, 70 and 50 mol% DiEGDMA/HEMA compared to 0.44, 0.59 and 0.62 found here). They concluded that non-Fickian transport is observed as the percentage of HEMA in the copolymer is increased, due mainly to reduced crosslinking leading to greater relaxations. While their initial findings agree with the results here it must be noted that the n_s values tend to decrease as the percentage of OED fell below 50 mol% and diffusion seemed to conform more to a Fickian mechanism which is also in accord with the results found by Robert et al.(38) above.

From Tables 3.1-4 it has been observed that the n_s values often peak at intermediate crosslinking concentrations. This could be explained, by means of the De number, as competition between the change in characteristic relaxation with increasing crosslinking and a change in the characteristic diffusion time as the percentage of hydrophilic HEMA is decreased and the network becomes more crosslinked. This could cause De to approach a value of one at intermediate crosslinking concentrations and therefore for sorption to become less Fickian. This process would also be dependent on the hydrophilicity of the crosslinking agent as well as the flexibility of the crosslinker used. A similar approach could also be used to explain the

variation in n_s values as water vapour concentration increases. The characteristic diffusion time would tend to increase with increasing relative humidity, i.e. the samples reach full EWC quicker, and at 100 % RH, De ≈1 and sorption approaches Case II diffusion. Sorption in water occurs more rapidly and therefore De no longer has a value near one and sorption again becomes Fickian.

Some doubt, however,must be cast on the curing procedure used by Walker and Peppas (25). As has been mentioned previously, it has been found extremely difficult, if not impossible, to cure EGDMA to within its full possible cure without the sample breaking up, and extensive cracking and crazing occurring, and even at full attainable cure there still remains appreciable amounts of monomer, possibly up to 15% remaining unreacted (39-43,24) . As Walker and Peppas sliced uniform 0.3mm discs of EGDMA homopolymer without it cracking it seems unlikely the polymer had achieved its full attainable cure and it seems reasonable to assume that there were large amounts of unreacted monomer still residing in the polymer causing plasticisation. This residual monomer could also have an effect on the rates of diffusion, although a comparison of n_s values is not possible since Walker and Peppas (25) did not include these for the EGDMA/HEMA and TEGDMA/HEMA copolymers. This could also explain the relatively larger overshoot they found for the copolymers compared to that found here (up to M_t/M_∞ = 1.6 in some cases) as it could have been due to monomer leaching out of the polymer as it became increasingly rubbery. They also found unusually high T_gs (eg a dry 30 mol% TEGDMA/HEMA copolymer T_g of 280 °C while results here and elsewhere (44,24) give T_gs for PHEMA and TEGDMA of 100°C and 125°C respectively) The reason for this discrepancy seems hard to explain despite the different methods used to calculate the T_g.

It is also apparent that the diffusion coefficient does not remain constant during sorption (Figure 3.12a-b). The increase in D_s found initially could be explained by invoking the description Turner used (15) to

describe water sorption into PMMA. Water fills the voids in the polymer first and the wetting front moves on while swelling is continuing to take place behind it.. D_s therefore increases until the swelling in the surface zone has reached equilibrium. The differing rates and extents at which these processes occur under the different sorption conditions used could explain the changes found in D_s . The subsequent decrease found, in some cases, for D_s at high EWC could also be due to the rejection of some of the already sorbed water i.e. the overshoot phenomena.

The increasing percentage of voids as the crosslinking increases and as the molecular weight of the OEDs decreases possibly arises from greater inhomogeneity occurring during polymerisation. The relatively stiffer EGDMA prevents smooth packing of the polymer chains and therefore leads to larger inhomogeneities in the copolymer and hence a greater percentage void size, while the more flexible P400 copolymers allow more scope for rearrangement of the polymer chains and therefore fewer voids. This change in void composition with crosslinking will also presumably affect the rate of diffusion and could explain why PHEMA has a lower diffusion coefficient of sorption at 33 % RH than the crosslinked copolymers due to water filling voids first, with the copolymers having larger void sizes. The larger void size found as crosslinking increases may also explain why the 14 mol% EGDMA copolymer has a higher EWC than the 6 mol% EGDMA copolymer when equilibrated at 33 % RH. For samples equilibrated at higher RHs and in water the decrease in D_s with increasing OED content is probably due to the increase in crosslinking and a decrease in hydrophilicity of the hydrogel.

These results also show that desorption is not as greatly affected by crosslinking and the initial amount of water in the polymer. The reduced desorption curves were all similar to those found for desorption from 33% RH (Figure 3.1e-h) and all gave good fits to Equation 3.2 and linearity up to $M_t/M_\infty \approx 0.85$ with Equation 3.3.

3.5 Summmary

It was found that both changes in the relative humidity and changes in the type and degree of crosslinking affect the water sorption kinetics with sorption varying from Fickian sorption to, in the extreme case, Case II sorption for PHEMA equilibrated at 100% RH. The incorporation of a crosslinking agent into PHEMA in the form of the OEDs generally led to a reduced EWC, the reduction in EWC being greatest for the EGDMA copolymers and decreasing as the molecular weight of the OED used increased, for similar mole ratio copolymers. This is probably due both to the increase in hydrophilicity of the OED and an in increase in its flexibility leading to less tightly crosslinked networks as the OE chain lenghtens.

The change in hydrophilicity and flexibility of the copolymers also causes the change in sorption kinetics due to changes caused in the characteristic relaxation and diffusion times of the polymers, although desorption kinetics seemed to vary little.

The size of low or zero density voids in the copolymers also varied with copolymer composition and this would have an effect on water sorption due to the tendency for the voids to fill first.

CHAPTER FOUR

DYNAMIC MECHANICAL TESTING

4.1 Introduction

The effect on the mechanical properties of copolymerising HEMA with up to 14 mole percent of 3 different OEDs; EGDMA, TEGDMA and P400, was investigated for copolymers of varying hydration, using a free oscillation torsion pendulum (TP). The various EWCs of the samples were achieved by equilibrating the samples at the different relative humidities given in Chapter Two. Changes in G', G" and tan δ can be used to characterise the relaxation properties of a polymer and can give information on various transitions occurring due to changes in molecular motions (Section 2.5).

4.2 Results and Discussion

The results of the TP scans on samples of wet and dry PHEMA are given in Figures 4.1a-c. These show the change in tan δ, the loss modulus, log G" and the storage modulus, log G', as a function of temperature. From the tan δ temperature plot of the dry PHEMA sample it is possible to observe three distinct relaxations evidenced by peaks in the tan δ trace occurring at approximately -125°C, 30°C and 125°C. These three peaks are generally referred to as the γ,β and α relaxations in order of increasing temperature (1). The α peak is also usually taken to be an indication of the glass transition temperature, T_g.

4.2.1 The Glass Transition Region

4.2.1(a) PHEMA

A number of different parameters can be obtained from the TP data that can be used to characterise the glass transition region. These are the

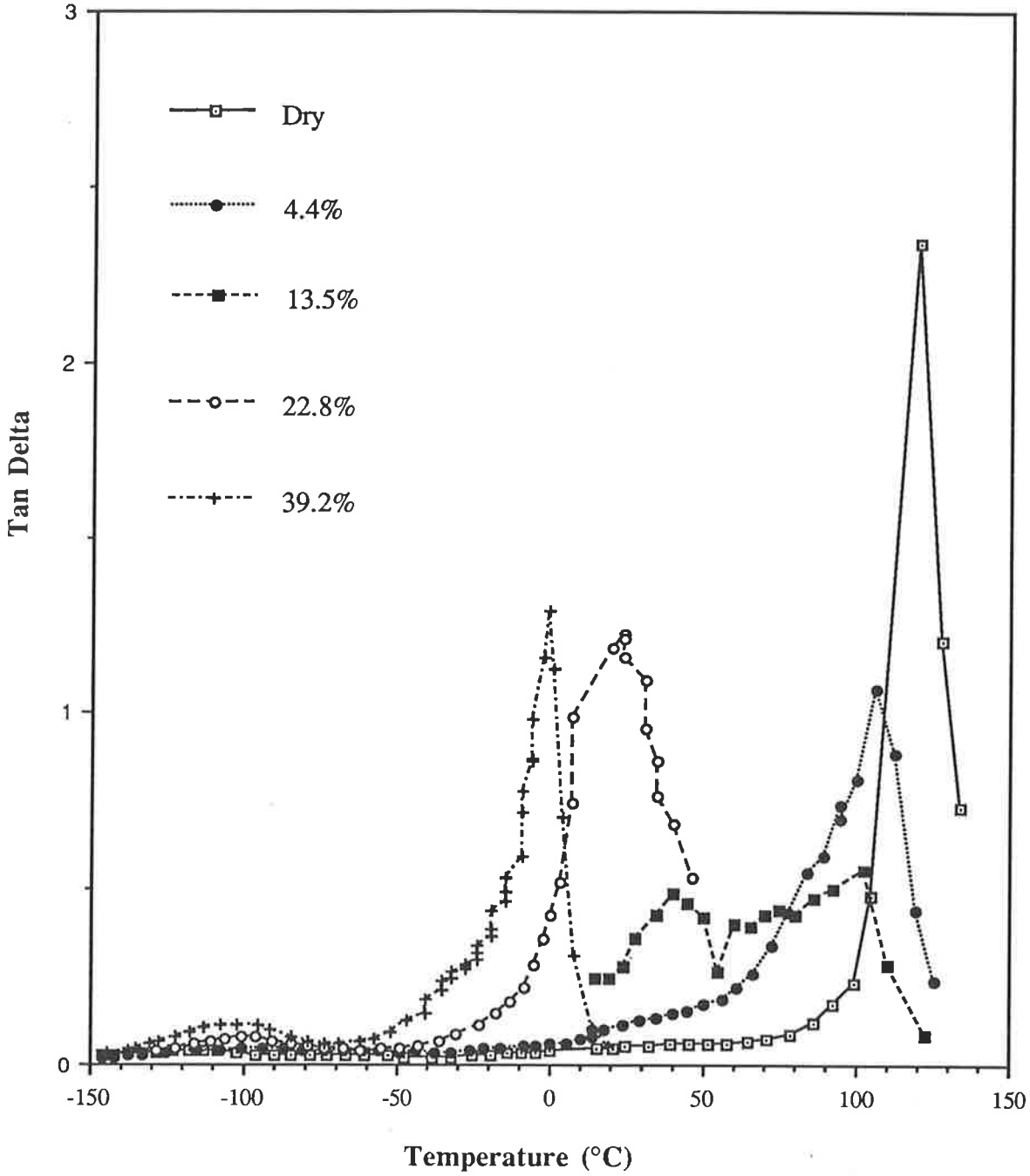

Figure 4.1a Tan δ-temperature plots for PHEMA at the EWCs given above.

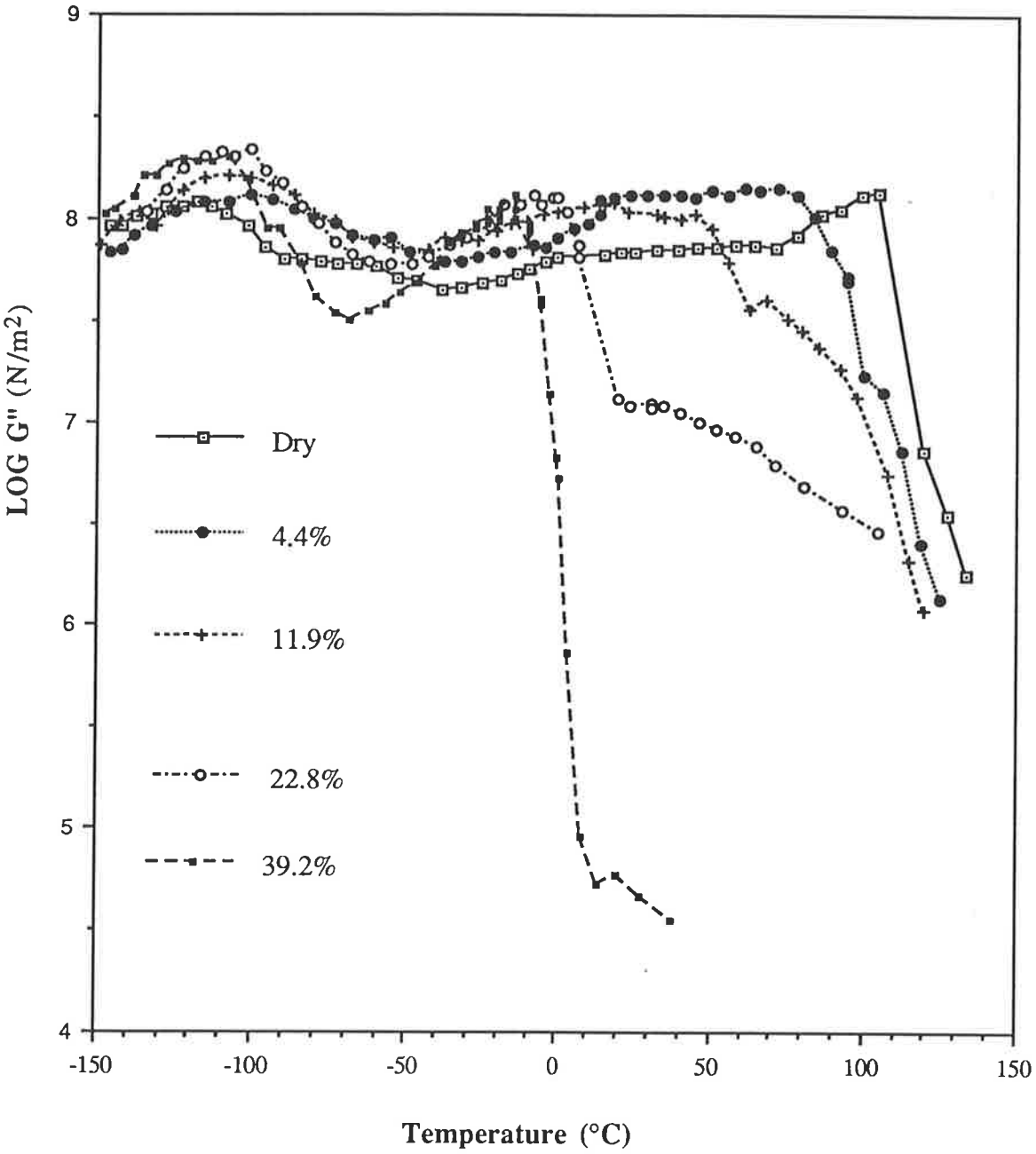

Figure 4.1b Log G"-temperature plots for PHEMA at the EWCS given above.

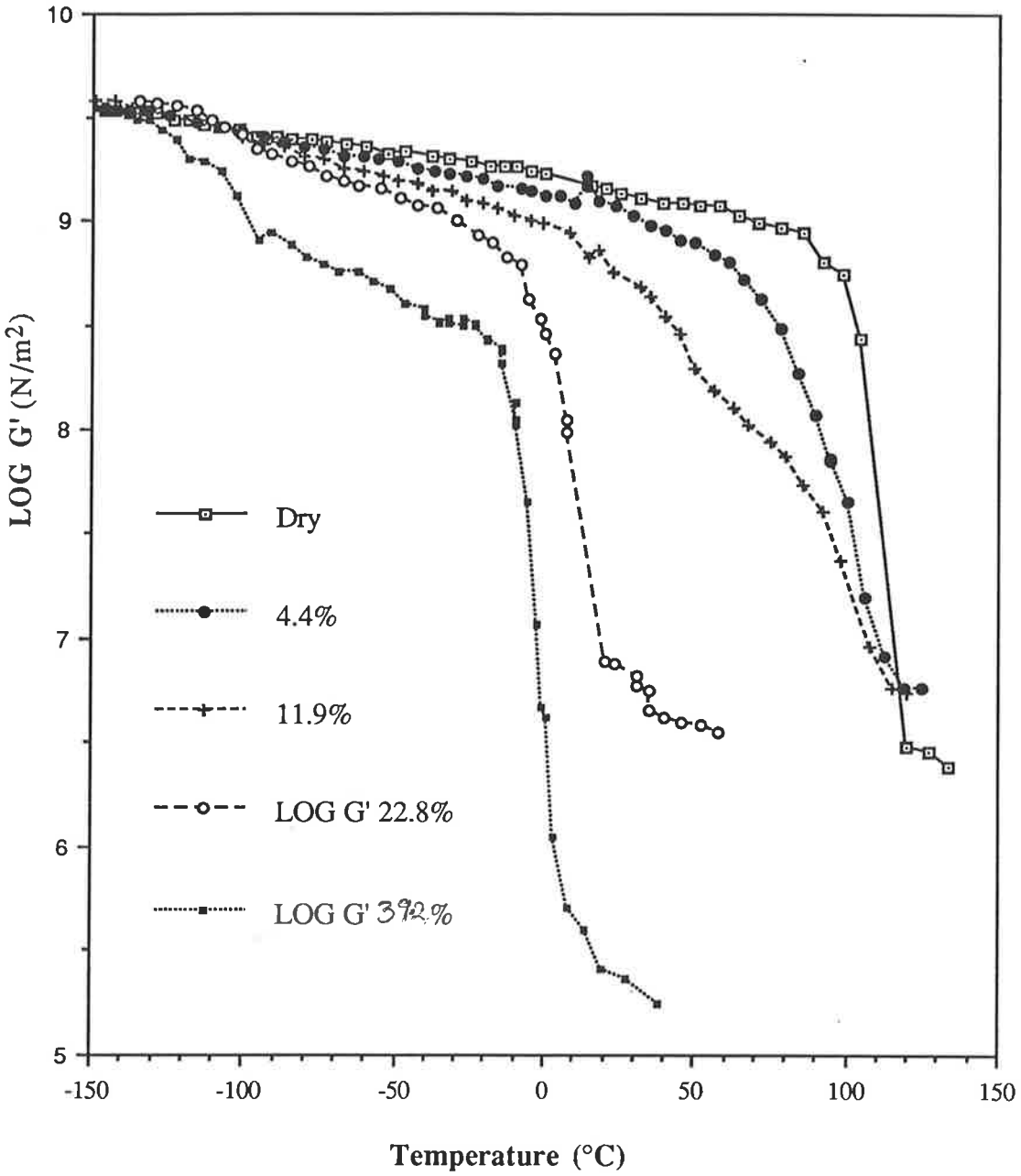

Figure4.1c Log G'-temperature plots for PHEMA at the EWCs given above.

height of the tan δ peak at the glass transition temperature, tan $\delta(T_g)$, and the half height peak width of the tan δ glass transition peak. The storage modulus at room temperature, Log G'(25°C), also provides some information on the stiffness of the polymer at room temperature, with a higher storage modulus generally indicating a stiffer polymer. The three peaks observed in the tan δ plot (Figure 4.1a) can also be seen in the log G"-temperature plot (Figure 4.1b) and and are usually given the same designations (i.e. α, β and γ). In some cases the high temperature log G" peak also has been used as a measure of the T_g and this temperature has also been noted and has been designated Tα. This data is presented in Table 4.1. It is doubtful, however if Tα is a true indication of T_g as it seems to give much lower glass transition temperatures, for some of the copolymers, compared to T_gs calculated from the tan δ plot, indicating in some cases that they would be above T_g at room temperature while they are still relatively stiff and glassy (eg for a fully hydrated 14 mol% EGDMA/HEMA copolymer the loss modulus peaked at 4°C but the sample was not rubbery at room temperature).

TABLE 4.1

Dynamic mechanical results for PHEMA at varying stages of hydration. The glass transition temperature, T_g, has been taken from the tan δ plot. T_α refers to the high temperature peak in the log G" trace. Peak height and width at 1/2 height refer to the tan δ glass transition peak

EWC	T_g (°C)	Log G' (25°C) G' in N/m^2	Peak Height	Width at 1/2 Height (°C)	Tα (°C)
0	125	9.12	2.35	21.1	112
4.4	107	9.04	1.1	30.2	70
11.8	50	8.77	0.48	38.6	20
13.5	41	7.83	0.52	25.4	13
22.8	20	6.83	1.24	25.2	-5
31.7	5	6.40	1.35	19.7	-12
39.2	0	5.43	1.45	14.03	-16

It can be seen from Table 4.1 that there is an initial drop in the tan δ (T_g) height as the EWC increases from 0 to 13.5%, after which it increases again to a value approximately 60 % of the original dry value. The half height peak width also increases initially, doubling up to 13.5% EWC, but then decreasing to a give a final half height peak width narrower than that of the dry sample. The log G'(25°C) values decrease uniformly with the addition of water. The water also has a very considerable plasticising effect with the T_g dropping by 125°C from the dry to fully hydrated polymer.

Water loss from the TP samples during testing was normally about 0.5 % to 2 % for samples of between 4 and 13.5% EWC respectively. For higher water content however, greater than 20 %EWC, water loss occurred much more rapidly above 25° C and so the runs were usually terminated as soon as it was obvious that the T_g had been exceeded.

From the 13.5% EWC samples it can be seen that the tan δ plot reveals the existence of two peaks with the low temperature peak occurring in approximately the area where it might be assumed that the glass transition temperature would lie. The two peaks occur at 43 °C and 103°C for the 13.5% EWC sample. The temperature of 103°C is approximately that found for the T_g of the 4.4% EWC sample. This could possibly be a result of water loss from the surface of the sample and the subsequent formation of a dry "skin" on the polymer surface resulting in a further T_g occurring at a higher temperature. To test this a polymer sample approximately 1.5 times thicker was run at the same heating rate. As the sample was thicker the water loss was slightly less at around 1.5% A comparison between the two scans are given in Figure 4.2. It can be seen that there is little difference in the two tan δ curves around the low temperature peak, but the second, higher temperature peak is slightly smaller for the thicker sample. Additionally some runs were repeated on samples that had just been scanned. The tan δ temperature plots for an initially 13.5% EWC sample are given in Figure 4.3. At the end of the first scan the sample had lost

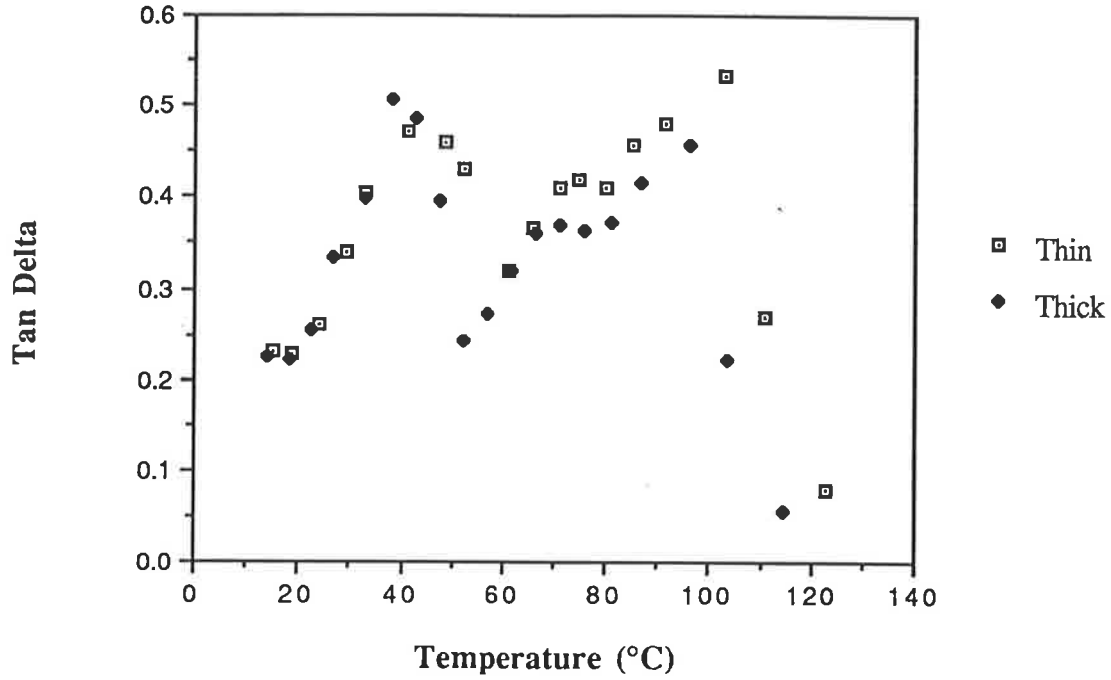

Figure 4.2 Comparison between tan δ–temperature plots for two PHEMA samples of 13.5% EWC but with different thicknesses.

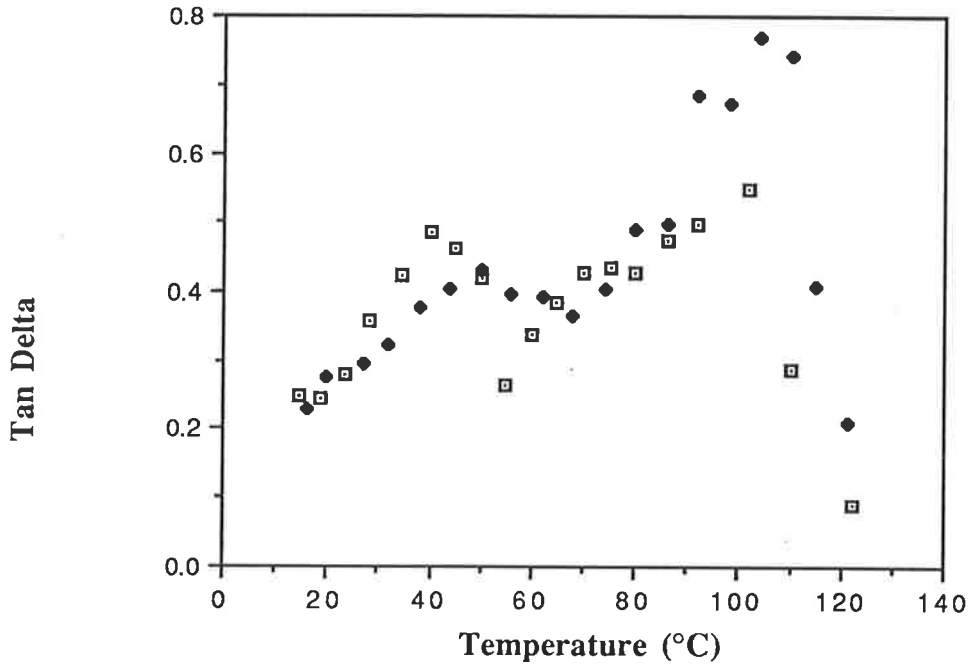

Figure 4.3 Repeat torsion pendulum run on 13.5 %EWC sample previously run.
▫ First run, ◆ Second run.

approximately 2 %EWC, it was then cooled and a repeat run was carried out immediately. The second plot shows that the low temperature peak had decreased in size and there was a concomitant increase in the higher temperature peak. This seems to imply that the appearance of the second peak is due to water loss from the sample. However it could be possible that the two peaks are due to some inhomogeneity in the sample or that there is some change in the organisational structure of the water in the polymer as the temperature increases, leading to the second higher temperature peak.

Measurements of water loss after the 13.5% EWC sample had reached 60 °C showed only a 1-2% EWC decrease with most of the water loss occurring after this temperature To test the effect of water loss on the height and width of the low temperature peak some runs were stopped after the sample had reached about 60°C, or after the lower temperature tan δ peak had just passed its maximum, and then immediately rescanned. The result is shown in Figure 4.4 and it is apparent that the loss of water has had little effect on this peak. It therefore seems reasonable to assume that the height of this peak, its temperature and peak width have not been altered to any great extent by water loss that has occurred up to 60°C. In the data presented the low temperature peak was generally taken as the glass transition peak. This was also confirmed by rapidly heating a partially hydrated sample to approximately 70 °C at which temperature it was obviously rubbery.

4.2.1(a) HEMA/EGDMA Copolymers

The tan δ-temperature scans for copolymers of HEMA with 3, 6 and 14 mol % EGDMA between -50°C and 175°C are shown in Figures 4.5a-c. The subambient tan δ plots will be considered later. Table 4.2 gives the values of the various parameters determined in the same way as those desrcibed previously for the PHEMA samples. The tan δ (T_g) of the dry copolymers decreases with increasing EGDMA content; the 14 mol% sample

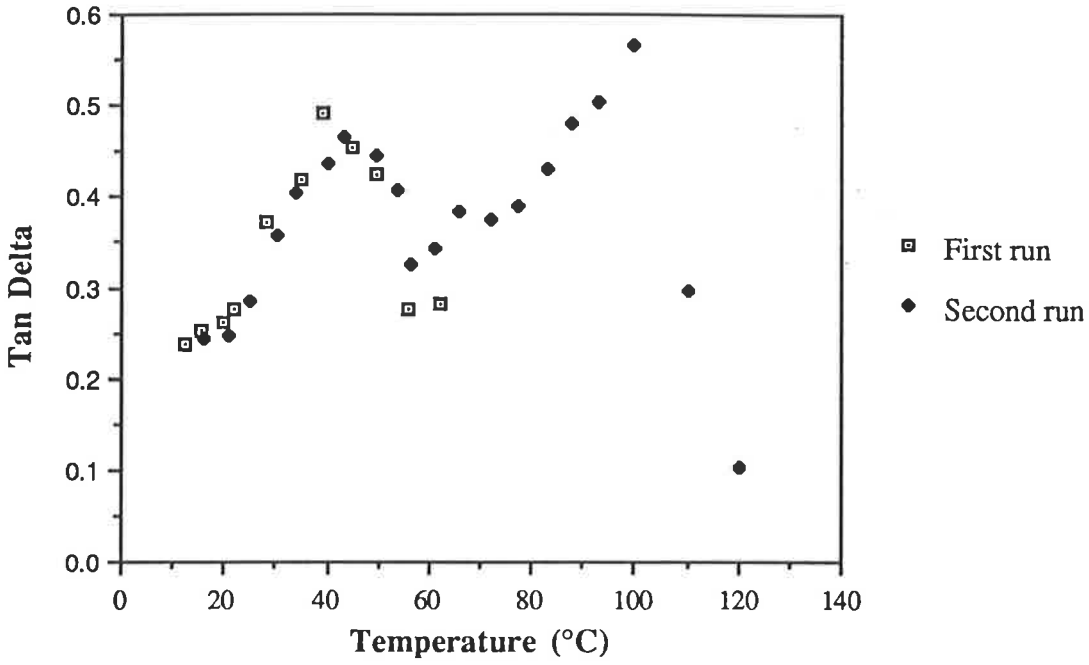

Figure 4.4 Tanδ-temperature plots for a PHEMA sample initially at 13.5%. The first run was stopped at 60°C, the sample was then cooled and a second run up to 120°C was made.

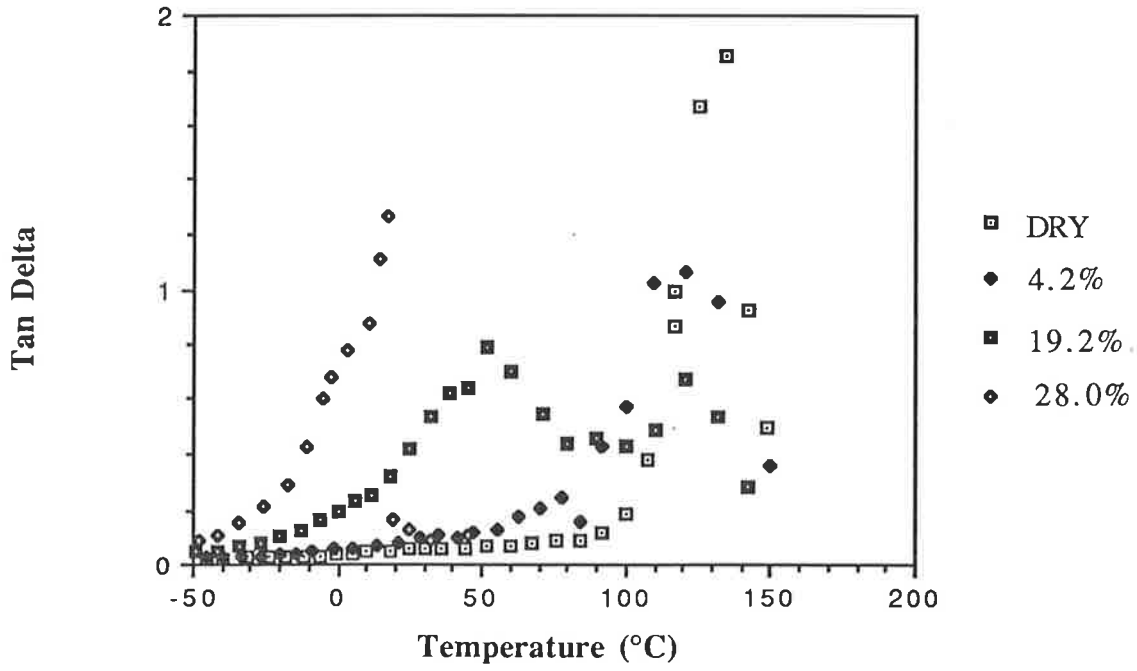

Figure 4.5a Tan δ-temperature plots for copolymers of HEMA containing 3 mol% EGDMA at EWCs as listed above

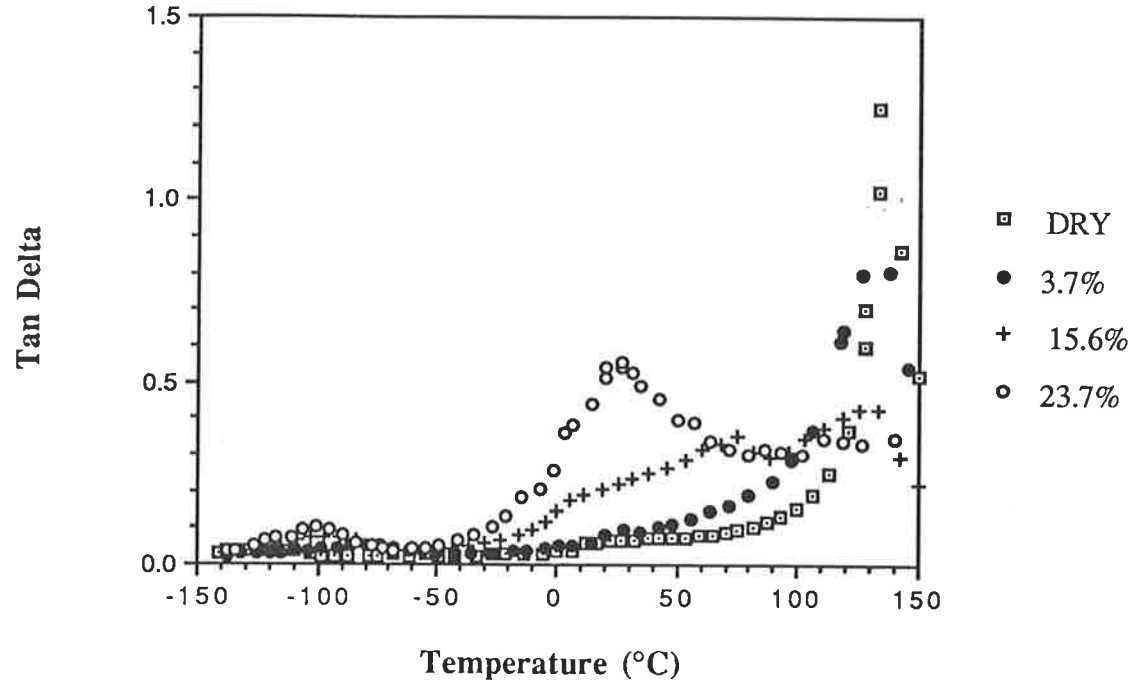

Figure 4.5b Tan δ–temperature plots for copolymers of HEMA containing 6 mol% EGDMA at EWCs as listed above.

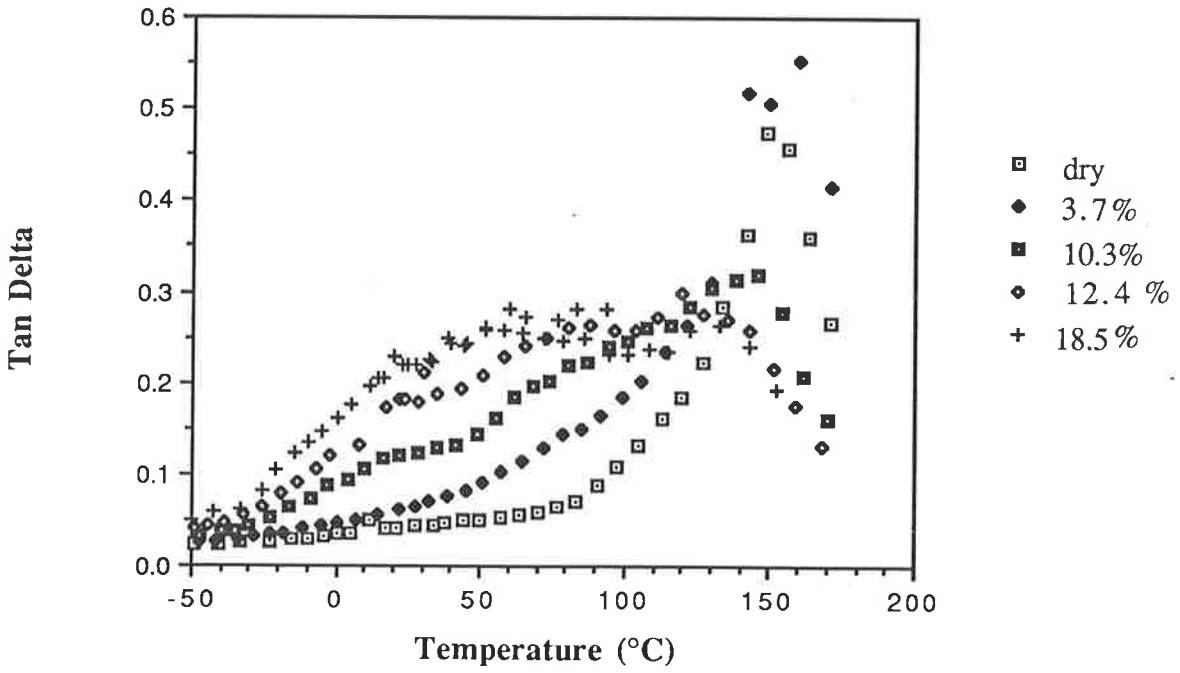

Figure 4.5c Tan δ-temperature plots for copolymers of HEMA with 14 mol% EGDMA at EWCs as listed above.

having a value approximately half that of PHEMA. The half height peak width increases monotonically with the addition of EGDMA along with a uniform increase in Log G' (25°C). Because of the high T_gs found for some of the copolymers it was not possible to measure them accurately due to considerable water loss from the sample at temperatures above 100°C. This can be observed in the tan δ-temperature plots as a large broadening of the T_g peak, especially for the 14 mole % EGDMA samples of intermediate water concentration. For high water content samples it was usually possible to measure the T_g as it occurred below 100°C and the run could be completed before there was appreciable water loss from the sample. Again there is evidence of dual peaks in some of the tan δ scans for copolymers of intermediate water content.

TABLE 4.2

Dynamic mechanical results for HEMA/EGDMA copolymers at varying stages of hydration. The glass transition temperature, T_g, has been taken from the tan δ plot. T_α refers to the high temperature peak in the log G" trace. Peak height and width at 1/2 height refer to the tan δ glass transition peak

Mole % EGDMA	EWC	T_g (°C)	Log G' (25°C) G' inN/m^2	Peak Height	Width 1/2 Height (°C)	Tα (°C)
3%	0	136.7	9.07	2.1	23.3	111
	4.2	123.3	9.02	1.1	50	77
	19.2	55.8	8.28	1.24	60.4	3
	28.0	13.9	6.18	0.79	18.6	-11
6%	0	143	9.16	1.34	17.0	122
	3.7	134	9.1	0.81	41.0	95
	11.5	107	8.87	0.43	111.4	65
	15.6	72	8.62	0.38	134.7	14
	23.7	25	7.71	0.57	71.9	-6
14%	0	158	9.20	0.55	35.5	124
	3.8	150	9.15	0.55	57	81
	18.5	83	8.58	0.28	190	4

4.2.2(c) HEMA/TEGDMA Copolymers

Tan δ–temperature curves are given for copolymers of HEMA with 3, 6 and 14 mol% TEGDMA in Figures 4.6a-c and Table 4.3 gives the data calculated from the respective loss modulus, storage modulus and tan δ plots (including data from some copolymers of HEMA with 9 mol% TEGDMA).

TABLE 4.3

Dynamic mechanical results for HEMA/TEGDMA copolymers at varying stages of hydration. The glass transition temperature, T_g, has been taken from the tan δ plot. T_α refers to the high temperature peak in the log G" trace. Peak height and width at 1/2 height refer to the tan δ glass transition peak.

Mole % TEGDMA	EWC	T_g (°C)	Log G' (25°C) G' inN/m^2	Peak Height	Width 1/2 Height (°C)	Tα (°C)
3%	0	127	9.13	1.8	20.5	118
	4.1	117	9.02	1.3	27.7	83
	11.5	53	8.79	0.45	53.6	
	18.4	44	8.01	0.77	66.5	0
	33.7	4	6.1	1.6	11.1	-16
6%	0	129	9.10	1.6	15.9	115
	3.4	121	9.08	1.2	33.1	83
	11.2	55	8.60	0.43	70.0	
	16.7	26	8.03	0.75	56.9	1
	29.9	2	6.42	1.25	17.2	-12
9%	0	119	9.08	1.08	23.5	111
	3.3	111	9.04	0.88	31.9	98
	16.4	40	8.23	0.48	80.6	2
	24.4	19	7.14	0.70	62.2	-15
14%	0	124	9.12	0.84	23.5	
	3.2	106	9.03	0.52	51.2	
	9.9	63	8.62	0.36	75.0	
	17.3	31	7.92	0.54	75.6	
	21.9	20	7.77	0.54	70.5	

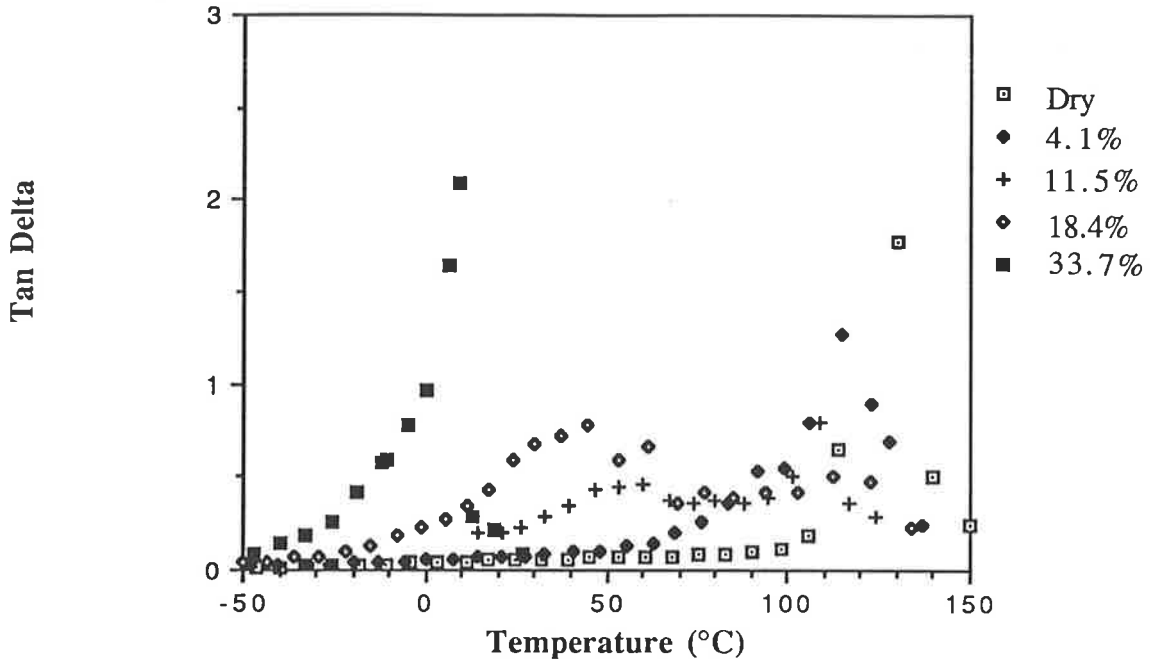

Figure 4.6a Tan δ–temperature plots for copolymers of HEMA with 3 mol% TEGDMA with EWCs as listed above.

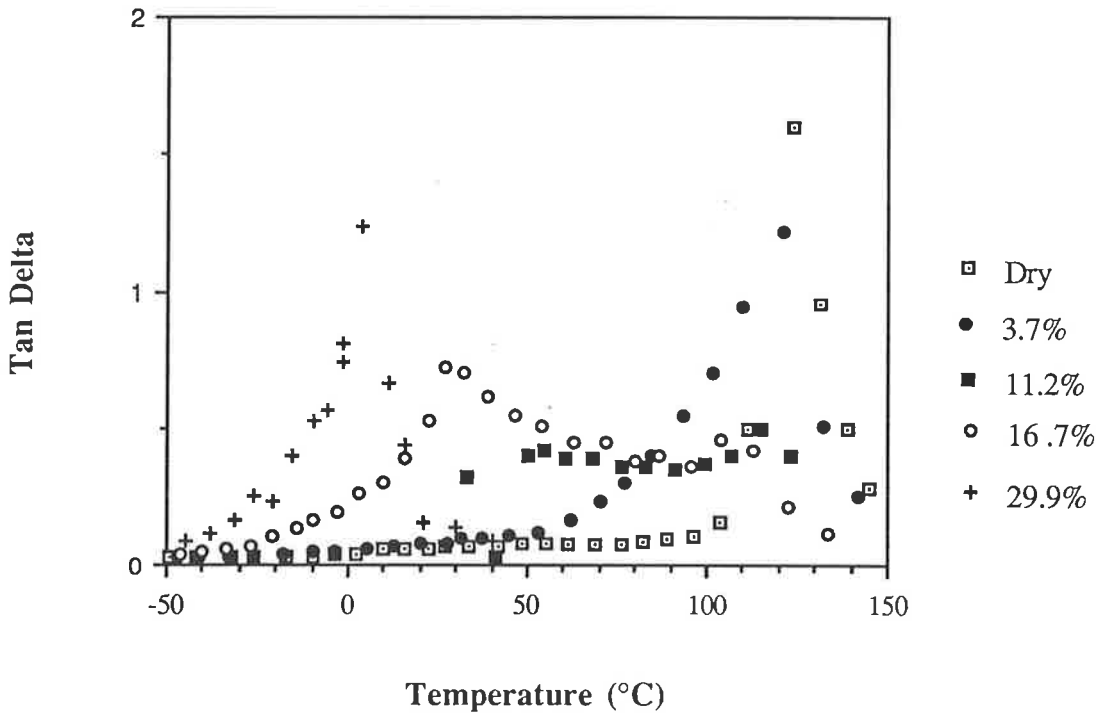

Figure 4.6b Tan δ–temperature plots for copolymers of HEMA with 6 mol% TEGDMA at EWCs as listed above.

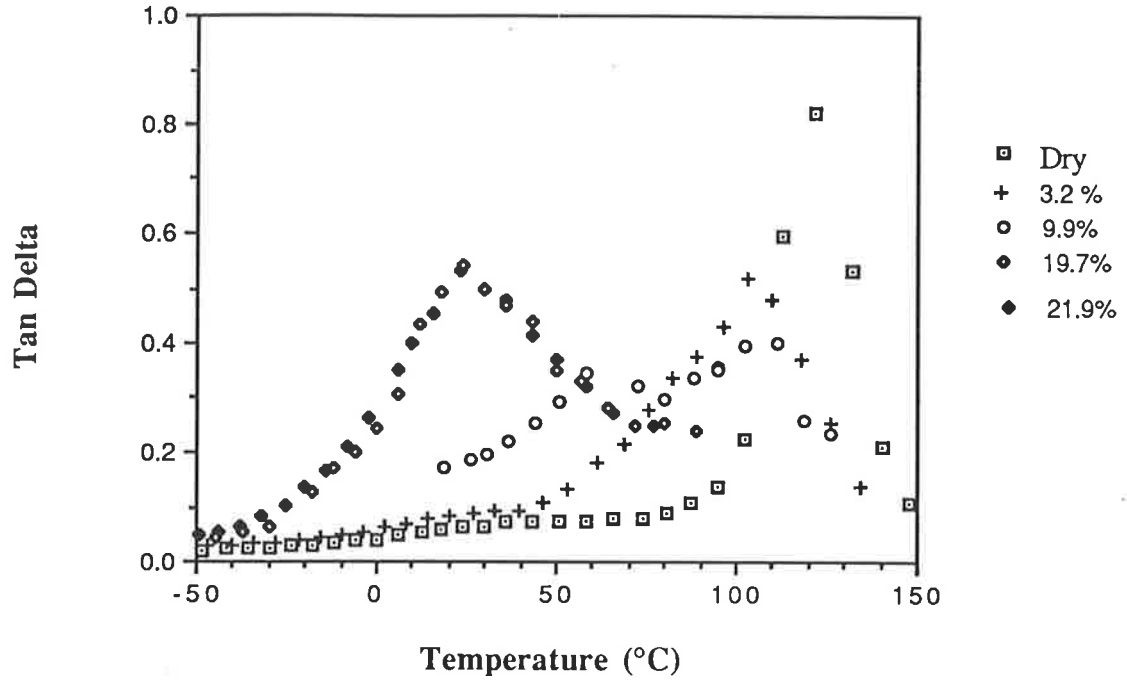

Figure 4.6c Tan δ-temperature plots for copolymers of HEMA with 14 mol% TEGDMA at EWCs as listed above.

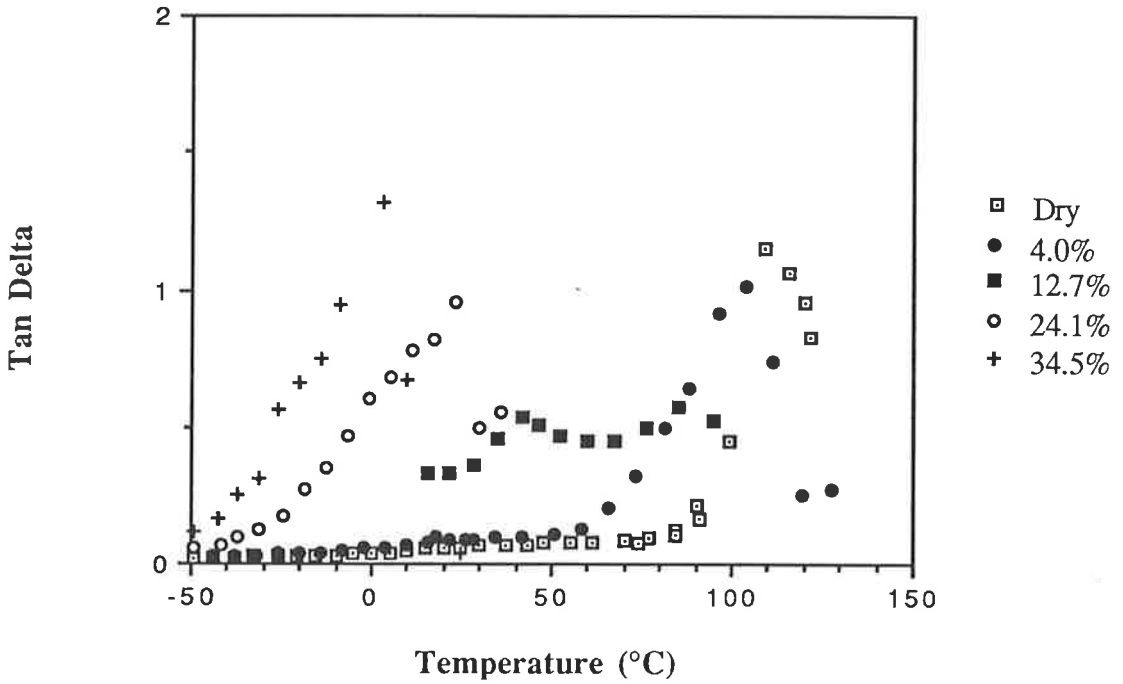

Figure 4.7a Tan δ-temperature plots for copolymers of HEMA with 3 mol% P400 at EWCs as listed above.

Addition of TEGDMA also causes a decrease in tan δ (T_g) with increasing TEGDMA content but not to the same extent as found with the EGDMA copolymers. The half height peak width of the glass transition peak and log G'(25°C) stay approximately the same with the addition of TEGDMA.

Water loss from the TEGDMA/HEMA copolymers was of the same order as that found for the wet PHEMA samples and it was therefore usually possible to observe the T_g reasonably accurately. Double peaks were again observed for samples of intermediate water content.

4.2.2(d) HEMA/P400 Copolymers

Tan δ scans for 3, 6 and 14 mol% P400/HEMA copolymers are given in Figures 4.7a-c. The results of the dynamic mechanical tests are presented in Table 4.4.

The copolymerisation of P400 with HEMA causes a decrease in the tan δ(T_g) value for the dry copolymers from 3 to 14% P400. The half peak width stays approximately the same but there is a decrease in the Log G'(25) value with increasing content of P400 for the dry samples.

The T_gs found for the P400 copolymers were lower than that of PHEMA and it was therefore possible to terminate the scan at a lower temperature so that the water loss from the samples was less. Again dual peaks are observable for the 3 and 6 mol % P400 copolymers of intermediate water content.

It can be observed from the log G'-temperature plot (Figure 4.1c) for PHEMA that the storage modulus drops steeply at about 0°C for the saturated sample and that the T_g indicated by the tan δ plot is also at 0°C. This was also found to be the case for copolymers of HEMA with TEGDMA and EGDMA at high EWC, with T_gs never falling below 0°C. Kolarik and Janacek (2) found similar results for log G' values of PHEMA and reasoned that on cooling only a fraction of the water in the system remains bonded to the PHEMA with the surplus water forming a crystalline phase on cooling

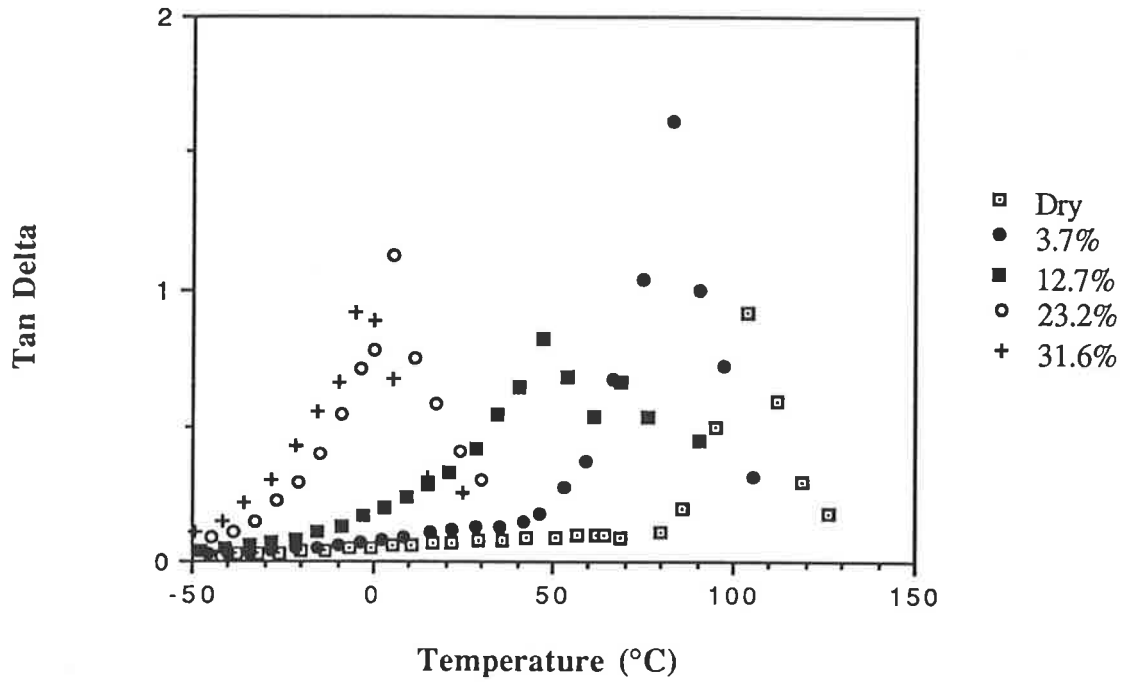

Figure 4.7b Tan δ-temperature plots for copolymers of HEMA with 6 mol% P400 at EWCs as listed above.

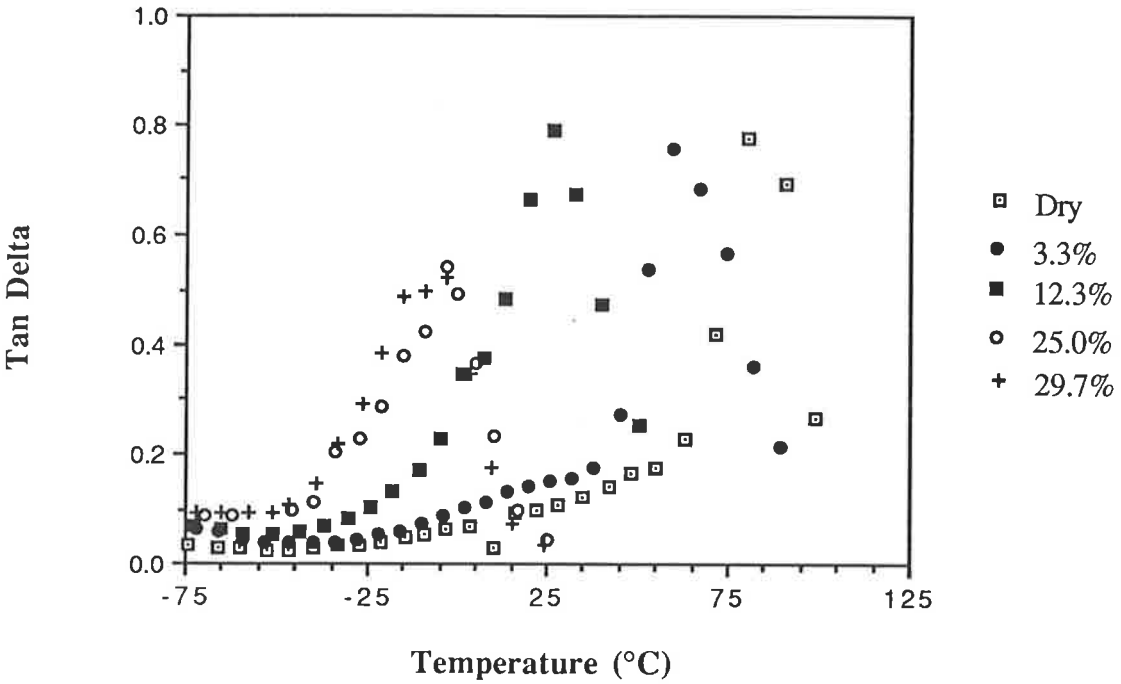

Figure 4.7c Tan δ-temperature plots for copolymers of HEMA with 14 mol% P400 at EWCs as given above.

and melting at 0°C causing the sharp decline in the log G' value. The high EWC copolymers containing 14 mol% P400 however show a storage modulus (Figure 4.8) that decreases sharply before 0°C and a T_g below 0°C indicating possibly that there is not enough surplus water to form a crystalline phase (i.e freeze) and thereby influence the glass transition temperature of the copolymer by melting at 0°C.

TABLE 4.4

Dynamic mechanical results for HEMA/P400 copolymers at varying stages of hydration. The glass transition temperature, T_g, has been taken from the tan δ plot. T_α refers to the high temperature peak in the log G" trace. Peak height and width at 1/2 height refer to the tan δ glass transition peak.

Mole % P400	EWC	T_g (°C)	Log G' (25°C) G' inN/m^2	Peak Height	Width 1/2 Height (°C)	Tα(°C)
3%	0	111	9.12	1.19	23.4	96
	4.0	104	9.01	1.02	34.1	76
	12.7	43	8.40	0.54	43.3	16
	24.1	22.5	7.03	0.97	37.7	-18
	34.5	5.7	6.85	1.31	27.3	-24
6%	0	109	9.04	1.02	19.4	93
	3.7	84	8.80	1.56	20.7	57
	12.5	50.8	8.32	0.89	52.6	4
	23.2	3.9	6.7	1.18	23.2	-24
	31.6	-2	6.59	0.92	29.5	-28
14%	0	84.1	8.88	0.88	21.3	64
	3.3	62.9	8.73	0.81	32.0	16
	12.3	27.4	7.58	0.79	34.5	-5
	25.0	-2.5	6.92	0.55	34.5	-31
	29.7	-6.1	6.8	0.56	32.8	-32

The effect of the inclusion of small molecules, including water, on PHEMA has been previously studied by Janacek and Kolarik (2,3). However, they carried out measurements on samples that had been polymerised with water in situ (4), and, has been previously noted,

(Chapter 3), the initial amount of water included in the polymerisation can have an effect on bulk properties, such as the diffusion coefficient, and could, therefore, conceivably effect the mechanical properties. Khozin et al.(59) found that varying the amount of solvent added to an epoxy prepolymer varied the size of inhomogeneities occurring in the cured polymer. It has also been noted that solvents can affect polymer structure by chain transfer (60). Both of the above effects might result in changes in the dynamic mechanical properties of the polymer. Janacek and Kolarik also did not give tan δ measurements for PHEMA although this can give useful information on the number and state of the molecules participating in particular molecular relaxations. It has been proposed (5) that the height of the glass transition peak in the tan δ-temperature plot is due to the number of kinetic units mobile enough to contribute to the transition with the breadth depending on the distribution of environments in which these units are located.

Allen et al. (6) found that the tan $\delta(T_g)$ peak height increased with increasing oxyethylene chain length for poly (oligo - ethylene glycol dimethacrylates) from tri-EGDMA up to P600EGDMA, with a corresponding increase in flexibility of the polymers. In turn the 1/2 height peak width of the glass transition peak decreased. Similarly, Andrady and Sefcik (7) found that the tan $\delta(T_g)$ peak height in crosslinked poly (propylene glycol) increased with increasing mean chain molecular weight between crosslinks which supports the proposed theory.

It can be seen from Tables 4.1-4 that, with the sorption of water into the copolymers, there is a general trend followed by most of the systems studied. Initially the tan $\delta(T_g)$ peak height decreases to a minimum at intermediate EWC and then subsequently increases at full hydration. Concomitantly there is an increase in 1/2 height peak width of the glass transition peak to a maximum folowed by a decrease at full EWC. This

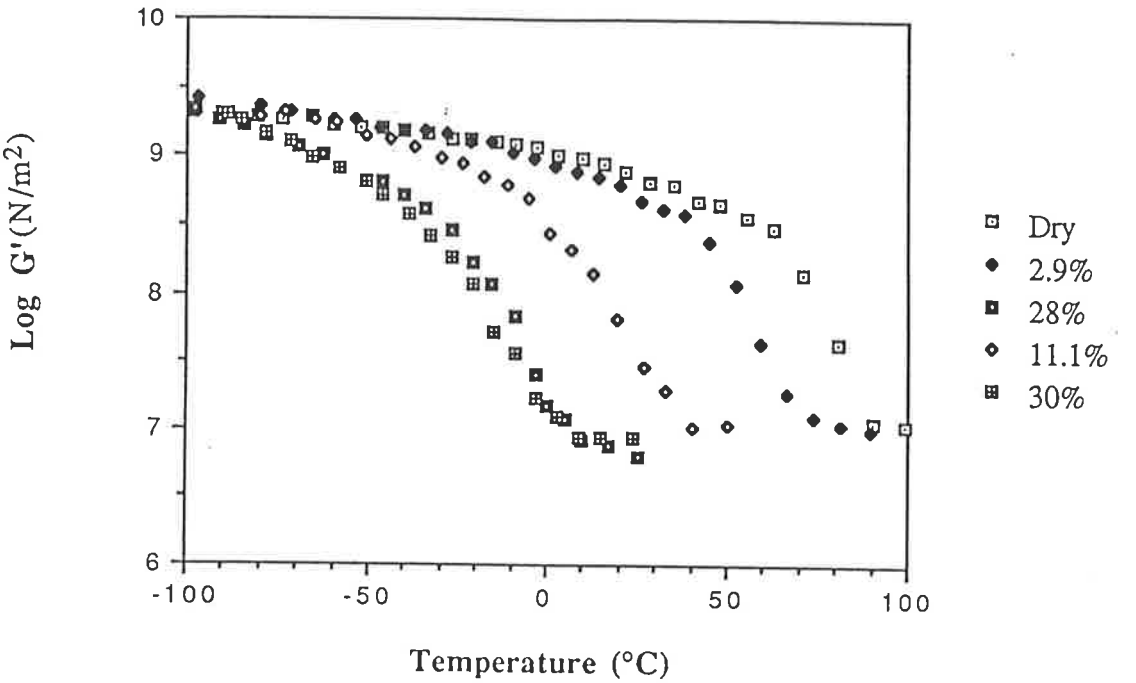

Figure 4.8 Log G'-temperature plots for HEMA copolymerised with 14 mol% P400 at EWCs as listed above.

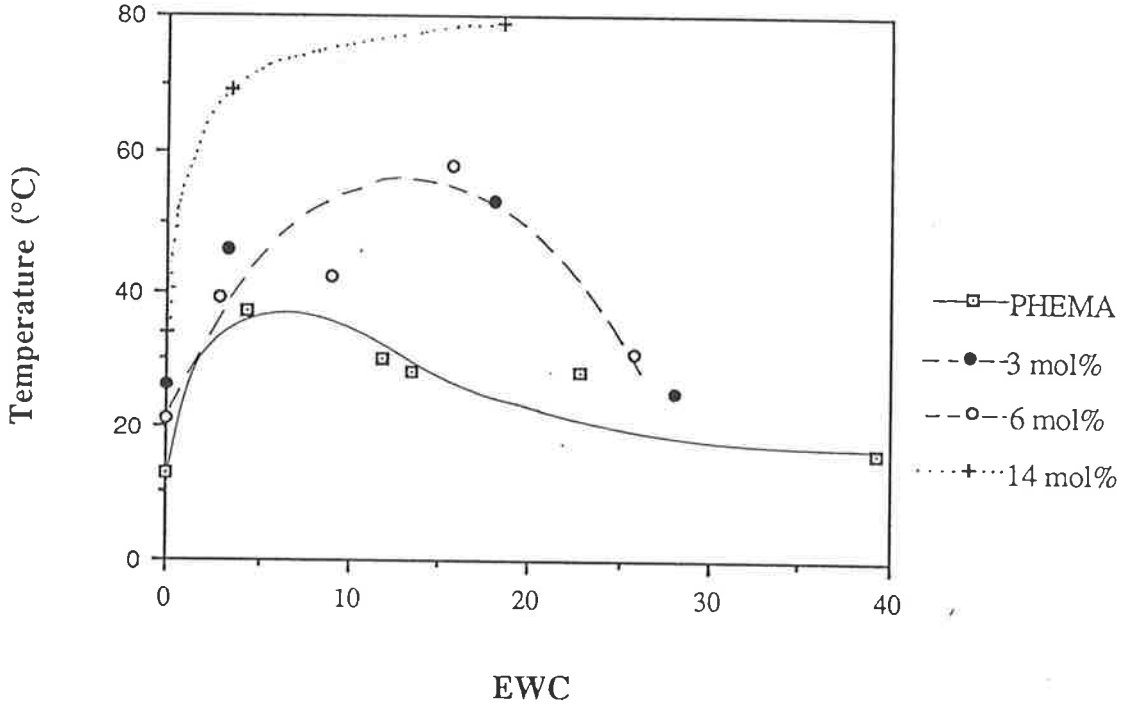

Figure 4.9a Difference in log G" and tan δ peak temperatures for the α transition at different EWCs for HEMA copolymerised with EGDMA in the proportions given above .

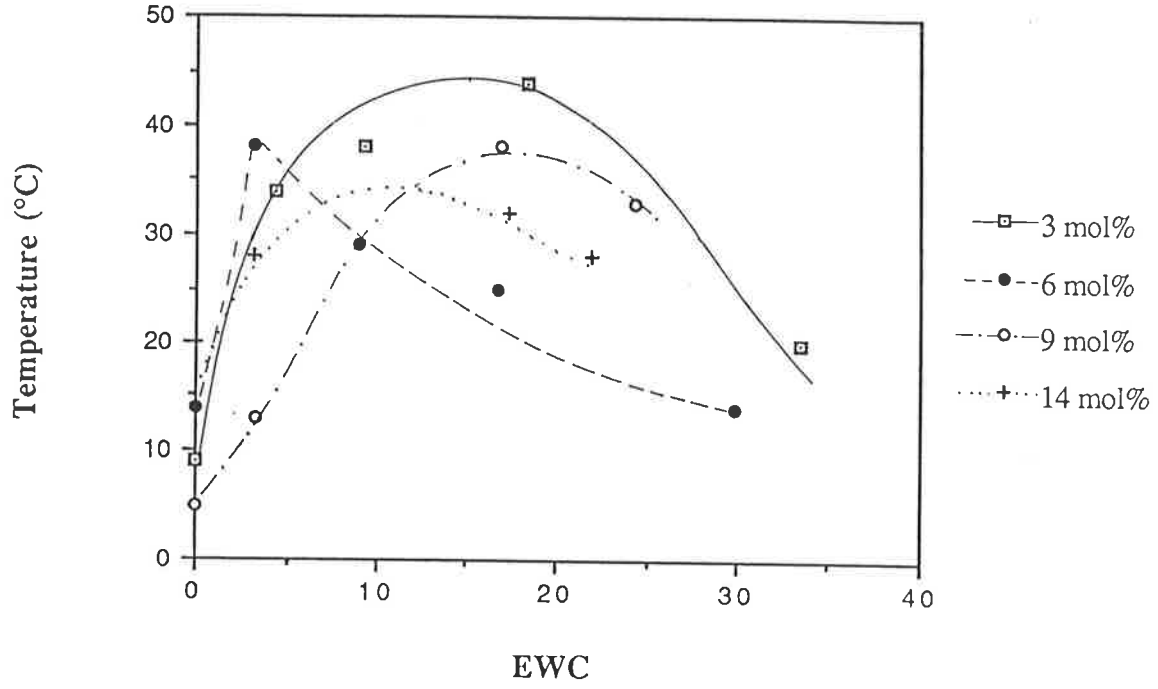

Figure4.9b Difference in log G" and tan δ peak temperatures for the α transition at different EWCs for HEMA copolymerised with TEGDMA in the proportions given above.

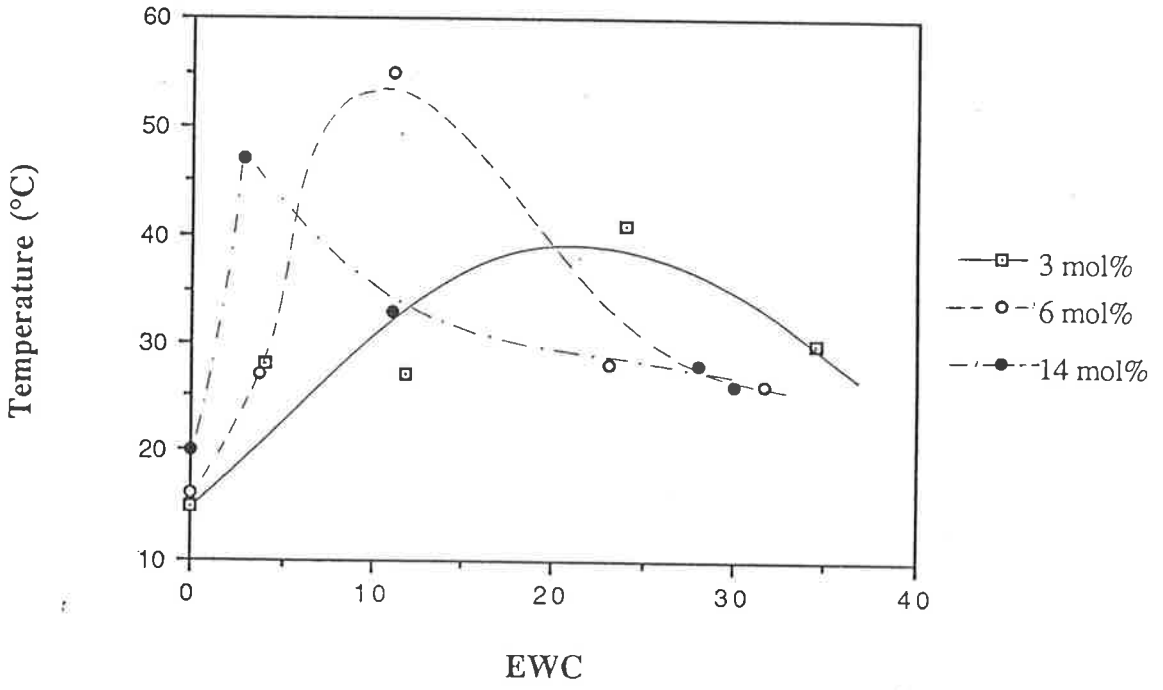

Figure 4.9c Difference in log G" and tan δ peak temperatures for the α transition at different EWCs for HEMA copolymerised with P400 in the proportions given above.

implies that at an intermediate water content the mobile kinetic units which contribute to the tan δ peak height exist in a range of environments greater than that found in either the dry or saturated samples and that there could be some inhomogeneity in the partially hydrated polymers.

It is also apparent form the data presented in Tables 4.1-4 that there is a noticeable temperature difference between the maximum of the loss modulus, log G", and the tan δ maximum for the glass transition region with the loss modulus maximum occurring at the lower temperature. Figures 4.9a-c shows this difference as a function of the EWC. For PHEMA samples this difference is, initially for the dry samples, about 13°C. With increasing EWC this increases to 37 °C at 4.4 %EWC and then decreases to 16°C at full hydration.

The copolymerisation of HEMA with EGDMA cause this difference to be greater, with an initial difference of some 20 - 30 °C for the dry copolymers which increases to around 50°C at intermediate hydration. The TEGDMA and P400 copolymers show much the same trend as found for PHEMA. There is a similarity between the behaviour found here and that observed for the 1/2 peak width of the tan δ glass transition peak.

A similar effect has been noted by Felisberti et al. (8) in a study on copolymers of polystyrene (PS) and polyvinylmethylether (PVME). They found that for samples with low amounts of PS or PVME the difference between the loss modulus maximum and the tan δ maximum was less than 10° C. For intermediate compositions, however, (40 - 70 %PS) the two maxima were separated by 30 - 35 °C. They concluded that the varying distance between the two peaks was an indication that the relaxations related to the glass transition are more complex than in a single component system and that the system studied exhibited thermorheologically complex behaviour. This was further confirmed by measurements made at four different frequencies between 0.1 and 100 rad/s, with the loss modulus peak shifting by about 10°C while the tan δ peak changed by 25 - 30°C. This was

taken as an indication of the occurrence of molecular relaxations with differing rate constants that have different temperature dependencies and therefore indicating that the relaxation behaviour in the glass transition region is thermorheologically complex.

The similarity between their results and the results found here indicate that the polymer water systems studied here may also be exhibiting complex thermorheological behaviour in the glass transition region, which in turn could be due in part to the wide range of environments existing in the partially hydrated polymer, as indicated by the changes in the tan δ peak with different levels of hydration.

The changes in T_g with the addition of EGDMA, TEGDMA, and P400 are given in Tables 4.1-4. The addition of EGDMA causes a substantial increase in T_g, while the addition of P400 causes a similarly noticeable decrease in T_g. This behaviour is understandable given the relative T_gs of the respective crosslinking agents. The behaviour of the P(HEMA/TEGDMA) copolymers, however, is a little more complex. There is a slight initial increase in the T_g up to 6 mole % TEGDMA after which the T_g decreases. Work by Martin et al. (9) on a similar MMA/TEGDMA system found that the T_g was invariant up to the addition of 12.5 mole % TEGDMA. Simon (10), however, also investigated the TEGDMA/MMA system and found that there was an increase in the T_g up to the addition of 11 mole % TEGDMA followed by a subsequent decline in T_g upon the addition of further TEGDMA. It was postulated that this could be due to competition between two competing effects - the crosslinking effect and the copolymer effect. The crosslinking effect meaning that main chain mobility is constricted by the interconnection of the polymethacrylate chains by dimethacrylate units thereby increasing the T_g and the copolymer effect implying that a long oligo - ethylene glycol chain (as in TEGDMA) may be sufficiently flexible to allow local main chain motion to be influenced by the

presence of mobile TEGDMA units. A similar effect may be responsible for the initial increase shown here for P(HEMA/TEGDMA) copolymers.

Attempts to predict changes in the glass transition temperature due to copolymerisation has led to the development of a number of equations which have met with varying success. These are generally developed around either a free volume hypothesis (11-14) or use a statistical mechanical interpretation of composition effects, as with the DiMarzio - Gibbs theory (15-16). Many of these models, however, require the knowledge of a number of other polymer parameters which are often difficult to calculate and are known for only a few systems.

One of the simplest equations developed is the Fox equation (12) (Equation4.1), where it is only necessary to know the respective weight fractions and T_gs of the homopolymers.i.e

$$\frac{1}{T_g} = \frac{w_1}{T_{g1}} + \frac{w_2}{T_{g2}} \qquad \text{Equation 4.1}$$

where w_1 and w_2 represent the weight fractions of homopolymers 1 and 2 and T_{g1} and T_{g2} the respective glass transitions of homopolymers 1 and 2.

Pochan et al. (17) found that Equation 4.2 gave good results for a variety of polymer - polymer, polymer - small molecule and small molecule - small molecule systems. This equation also has the advantage associated with the Fox equation in that it is only necessary to know the weight fractions and T_gs of the homopolymers.

$$\mathrm{Ln}T_g = w_1 \mathrm{Ln}T_{g1} + w_2 \mathrm{Ln}T_{g2} \qquad \text{Equation 4.2}$$

It has been shown, however, that this equation, and the Fox equation are special cases of an equation developed by Couchman (18-19) to predict the T_gs of compatible polyblends assuming the continuity of extensive thermodynamic properties such as entropy and volume at T_g.

$$\mathrm{Ln}\ T_g = \frac{w_1 \Delta Cp_1 \mathrm{Ln}T_{g1} + w_2 \Delta Cp_2 \mathrm{Ln}T_{g2}}{w_1 \Delta Cp_1 + w_2 \Delta Cp_2} \qquad \text{Equation 4.3}$$

where the Cpi are the heat capacities and Δ denotes transition increments. In this case ΔCp represents the change in heat capacity between the glassy polymer and the rubbery polymer. If $\Delta Cp \times T_g$ = constant then the Fox equation results and if $\Delta Cp_1 = \Delta Cp_2$ then Equation 4.2 results. This equation is valid as long as the T_gs of the two components are not too different in temperature. However, with systems where the T_gs have well separated temperatures it is not possible to assume that the ΔCp_i are independent of temperature. Instead Ellis and Karasz (20) assumed that the ΔCp_i are inversely proportional to temperature and used this assumption on an epoxy/water system and found this gave reasonable results. Equation 4.3 then becomes,

$$T_g = \frac{w_1 \Delta Cp_1 T_{g1} + w_2 \Delta Cp_2 T_{g2}}{w_1 \Delta Cp_1 + w_2 \Delta Cp_2} \qquad \text{Equation 4.4}$$

ΔCp values can be obtained from DSC thermograms from the change in specific heat measured before and after the glass transition (Chapter Five). Unfortunately it was not possible to measure the T_g of EGDMA by DSC as it is very high and there is a tendency for the polymer to decompose before T_g is reached and TEGDMA also does not show a T_g with DSC measurements (10). Therefore it was only possible to use Equation 4.4 (this equation was used in preference to equation 4.3 as PHEMA and P400 have well separated T_gs) with the P(HEMA/P400) system. Values for ΔCp of 0.14 ± 0.01 $Jg^{-1}K^{-1}$ and 0.80 ± 0.01 $Jg^{-1}K^{-1}$ were used for PHEMA and P400 respectively The T_g of EGDMA was taken as the value given by Martin et al. (9) of 460°C, which was calculated from copolymer work with MMA. The T_gs of TEGDMA and P400 were taken from work by Simon (10), who also used a torsion pendulum, to be 388K and 268 K respectively.

The experimental and theoretical T_gs for the copolymers are given in Table 4.5a

TABLE 4.5a

Comparison of T_gs predicted by the Fox Equation and Equation 4.2 with experimental values obtained from Torsion Pendulum measurements for copolymers of HEMA with EGDMA, TEGDMA and P400. Also given are the calculated values for the P(HEMA/P400) system using Equation 4.4.

OED	EGDMA			TEGDMA			
% cross linker	3%	6%	14%	3%	6%	9%	14%
Expt T_g	137	143	158	127	129	119	124
Fox Eqn	134	144	164	125	124	123	122
Eqn 4.2	137	150	176	125	124	123	122

OED	P400		
% cross linker	3%	6%	14%
Expt T_g	111	109	84
Fox Eqn	106	89	12
Eqn 4.2	109	89	66
Eqn 4.4	74	48	22

The success of the Fox equation in predicting the T_g of the EGDMA/HEMA copolymers, compared to the results obtained for the other copolymers is probably due to the fact that the T_g of the homopolymer of EGDMA was one that had been calculated by extrapolation from copolymer work and therefore the crosslinking effect would have been largely taken into account. For the other copolymers both equations predict substantially lower T_gs than obtained experimentally with Equation 4.2 giving better results for the P400 system than the Fox Equation. When Equation 4.4 is used, however, as with the P400/HEMA copolymers, substantially different

T_gs are predicted which must clearly set limits on the validity of this treatment even if crosslinking effects are taken into account.

The effect of a plasticiser on the T_g of a polymer has been modelled by a number of people using a variety of methods, including isofree volume (21), isoviscous flow (22), viscous flow (23) and active groups treatments (24). Many of these attempts have resulted in Equation 4.5;

$$T_g = T_{gp} - Bm_2 \qquad \text{Equation 4.5}$$

where B is a constant, T_{gp} is the polymer T_g and m_2 is the weight fraction of plasticiser. Unfortunately this has been found to apply over only a low range of plasticiser concentration (25). Numerous other equations have also been developed, but again as with the case for copolymers, it is difficult to determine some of the parameters required. The Fox equation has also been used and, as remarked before, Pochan et al. (17) obtained some success with Equation 4.2 for small molecule - plasticiser systems.

Again a comparison has been made of the experimentally obtained T_gs with those predicted by the above equations. The T_g of water has been calculated by a number of people (26-29) using a variety of methods including calorimetry and dielectric measurements. The values obtained are in good agreement with each other, giving a T_g of 134-135 K. The value used here was 134K. Equation 4.4 was also applied using $\Delta Cp = 1.94$ $Jg^{-1}K^{-1}$ (25,38).

The results of both equations are presented in Table 4.5b. Generally it is apparent that neither of the equations used are able to adequately predict the change in the glass transition temperature over the whole range of EWCs for any of the polymers. It appears however that the Fox equation is more accurate at intermediate EWCs, while at high EWC it predicts a lower T_g than that usually found, although this could be due to some water loss from the samples, and at low EWCs it tends to overestimate the depression of the

Mole % OED	EWC	Expt Tg	Fox Eqn	Eqn 4.2	Eqn 4.4	Mole % OED	EWC	Expt Tg	Fox Eqn	Eqn 4.2		Mole % OED	EWC	Expt Tg	Fox Eqn	Eqn 4.2
	4.4	107	93	106	22											
	11.9	50	50	77	-47											
0 (PHEMA)	13.5	41	41	70	-56											
	22.8	20	2	38	-87											
	31.7	5	-28	9	-104											
	39.2	0	-48	-13	-112											
	4.2	123	104	118			4.1	95	108	108		3% P400	4.0	104	84	95
3 %E	19.2	56	21	58		3 % T	11.5	53	53	80			12.7	43	37	63
	28.0	14	-12	27			18.4	44	20	54			24.1	23	-7	25
							33.7	4	-33	4			34.5	6	-39	-6
	3.7	134	113	126												
6 % E	11.5	107	62	91			3.4	121	106	116		6%P400	3.7	84	85	94
	15.6	72	40	76		6 % T	11.2	55	55	83			12.5	51	37	62
	25.8	25	-3	38			16.7	26	28	62			23.2	4	-6	27
							29.9	2	-15	23			31.6	-2	-31	1.3
	3.8	150	124	139												
14%E	8.5		89	117			3.6	111	94	104		14%	3.3	63	65	73
	15		50	89		9 % T	15.9	40	27	57			12.3	27	23	43
	18.5	83	33	74			23.3	19	-2	32			25.0	-3	-21	6
													29.7	-6	-34	-6
							3.2	106	101	110						
						14%T	9.9	63	59	83						
							17.3	31	23	56						
							21.9	20	5	40						

TABLE 4.5b Comparison between experimental and theoretical T_gs for PHEMA and copolymers of HEMA with EGDMA, TEGDMA and P400 at varying stages of hydration. E, and T represent EGDMA and TEGDMA respectively.

glass transition temperature. This particularly apparent for the PHEMA/water system where the Fox equation is reasonably accurate at intermediate water concentrations. A comparison of the Equations 4.1 and 4.2 for this system is given graphically in Figure 4.10. Equation 4.2 tends to be more accurate at both high and low water concentrations, but not at intermediate EWCs.

It is again obvious that the application of Equation 4.4 does not provide a reasonable estimate of the T_g depression due to water. It predicts T_gs in some cases of nearly 100°C less than those actually found. As mentioned previously Ellis and Karasz (20) found that it gave good results for epoxy/water systems, however, this could be due to the substantially greater depression of the glass transition temperature found in these systems with a drop typically of some 20 °C/wt% of water. The drop in T_g for the PHEMA/water system here was, at most, 6°C/wt % of water for an 11.9%EWC sample, and was generally less than this.

4.2.2. Theoretical Calculation of G'

It has been found by Katz (30), using EGDMA, tri-EGDMA and TEGDMA, and others (31) that for dimethacrylate/MMA copolymers the laws of ideal rubber elasticity are largely obeyed. It should therefore be possible to predict the modulus of the rubbery plateau occurring in the log G' curve after T_g for the crosslinked PHEMA copolymers using the equation of state for rubbery polymers (32), Equation,4.6

$$G=\frac{\rho RT}{M_c} \qquad \text{Equation 4.6}$$

where G is the shear modulus (N/m2) at temperature T(K), M_c is the molecular weight between crosslinks, R is the gas constant and ρ is the density of the copolymer. M_c in similar systems has been calculated by Flory (33) and Lee et al. (34) to be described by Equation 4.7;

$$M_c = \frac{M}{2\varepsilon w} \qquad \text{Equation 4.7}$$

where w is the weight fraction of crosslinker, M is the molecular weight of the crosslinker and ε is the efficiency of the crosslinker. This relation was used by Martin and Shen (35) when examining the MMA/EGDMA system. The crosslinking efficiency has been defined by Schultz (36) as the fraction of divinyl monomers reacted at both ends This has been determined as being 0.45 for EGDMA (36-38) and 0.72 for TEGDMA (31). The density was calculated from previous work on voids (Chapter 3). References 31 and 37 report the crosslinking efficiencies using the definition of Schultz (36) who measured polymer density changes as a function of cure and calculated the number of unreacted groups by assuming that the reaction of a single group caused a molar contraction of 22.5 cm^3. The method used by Martin and Moran (38) to calculate the crosslinking efficiency used infrared/Raman spectroscopy techniques on EGDMA and obtained a value of 0.45 which is similar to the value obtained by Schultz (36).

The results obtained are shown in Table 4.6 using a temperature of T_g + 40°C to calculate the theoretical results.

TABLE 4.6

Comparison between experimentally obtained values for log G'(T_g+40°C) and those calculated using Equation 4.7, for copolymers of HEMA with EGDMA and TEGDMA. E and T represent EGDMA and TEGDMA respectively.

%OED	log G' (T_g+40°C) (calculated)	logG' (T_g+40°C) (experimental)
3 % EGDMA	6.048	6.10
6 % EGDMA	6.352	6.65
14 % EGDMA	6.652	7.20
3 %TEGDMA	6.037	6.38
6% TEGDMA	6.338	6.42
9% TEGDMA	6.635	6.53
14%TEGDMA	6.808	6.93

It is apparent from the table that the theoretical values are slightly less than those found experimentally, however the rate of increase with additional crosslinker is similar. It may be that polar forces between molecular chains cause an increase in the storage modulus which is not taken into account in the equations used above. However, there appears reasonable agreement between the two experimental and calculated values and it seems that the laws of rubber elasticity may be applied to some extent in estimating the storage modulus.

4.2.3 The β Relaxation

A further relaxation can be observed at approximately 30 °C appearing as a shoulder in some cases on the larger T_g peak. This relaxation has been termed the β relaxation. A β peak has been observed in PMMA at 280 K (1) (measured mechanically at 1 hertz). There is varying opinion on the cause of the β peak with two possible explanations put forth. The first that it originates from specific intramolecular motions (1,40-41) while the second is that it could be due to intermolecular interactions (42-45). McCrum et al. (1)believed it was due to the hindered rotation of the -$COOCH_3$ group about the C-C bond linking it to the main chain. Theoretical calculations by Cowie and Ferguson (46) on poly(alkyl methacrylates), poly(alkyl acrylates) and poly(alkyl itaconates) suggest that it could be explained by rotation of the oxycarbonyl unit driven through the quaternary to carbonyl carbon bond although Heijboer et al. (47), also using theoretical calculations, tend to believe, that for PMMA, it is due to the rotation of the alkoxy carbonyl groups. It has been suggested (3) that partial rotation of side - chains COOR groups, sets in at about 280 K if R=CH_3, C_2H_5, C_3H_7 and C_4H_9 (measured mechanically). The higher temperature of the PHEMA $T\beta$ has been attributed (48) to its higher polarity and therefore stronger interactions of the side - chains.

β peaks for dimethacrylates have been found to occur (10) at a similar temperature to that of PHEMA at between 20 °C and 30° C. The β peak in dimethacrylates has been assigned to the localised motion of the oligo - ethylene glycol groups closest to the main chain poly(methacrylate) (10) and has also been thought by Chernova et al. (49) to refer to the commencement of vitrification in the polymer which implies that the β peak is associated with localised OE motions coupled with a main chain motion which is a precursor to large scale motion characteristic of the glass transition.

The β peak for a variety of linear polymers has been found (50) to increase with the addition of water. In some polymers the β peak is unaffected by water, however, as is the case with PMMA with water uptakes of 1% and 2.3% (57). As the β peak for PMMA is presumed to be due to some type of motion of the side chain around the main chain it is surprising that no change was found as there is evidence that water is attached to the carbonyl (52). However other work by Allen et al. investigating the effect of sorbed water on the solid state ^{13}C NMR spectrum of deuterated PMMA (58) suggests that in the early stages of sorption water is in contact with the backbone CD_2 and quaternary carbons and that a more uniform distribution, with water in contact with the other carbons, only occurs later, due possibly to a redistribution of the water or a second slower sorption process. It could be though, that for PMMA the addition of water only effects very localised motions of the side group i.e. those responsible for the γ transition.

The β peak for PHEMA occurs at 37°C on the tan δ - temperature plot. There is no discernible change in either the height or position of this peak on copolymerisation with either EGDMA or TEGDMA for the dry samples probably due to the similar temperatures at which this transition occurs in the various homopolymers. Copolymerisation with P400 did seem to increase the height of the peak although due to the tendency of the β peak to appear as a shoulder to the glass transition peak this could have been due

to the decrease in the temperature of the glass transition peak for copolymers containing appreciable amounts of P400.

The addition of water generally caused an increase in the peak height and a decrease of some 10-15° C for samples of approximately 10 % EWC regardless of copolymer composition. For samples of higher water content the β peak tended to be overlaid by the glass transition peak although a slight shoulder was sometimes evident on the this peak. Bair et al. (50) has determined that it was the change in the amount of unclustered water that correlated with an increase in the height of the β peak, clustered water being bulk like free water capable of freezing. They used DSC and dielectric methods and found that unclustered water moves in association with the chain causing the resultant change in the β peak. The shift to a lower temperature implies that less energy is required for the motion that causes the β transition and that the β transition could be a prelude to the large scale motion occurring at the glass transition.

4.2.4 Subambient Transitions

The low temperature peak observed in the tan δ - temperature plots of the dry polymers has been referred to as the γ transition, characterised by the temperature T_γ. Low temperature relaxations have been noticed between approximately -105°C and -130°C for a variety of dimethacrylates and linear methacrylates(48,53-54). Previous work on PHEMA (48) has given a T_γ of -130 °C and this has been found not to alter as the length of the side chains have been increased, indicating the localised nature of the motion. Gulyatsev et al. (55-56) observed no γ relaxation in ethylene glycol diacrylates and inferred that the γ relaxation was due to methyl rotation. However other studies on PHEA , the acrylate analogue of PHEMA, did observe a T_γ (48).

Kolarik (48) concludes that the γ process is a small scale internal motion of the side chain in linear methacrylates and proposes that the

contributing mechanisms to the γ activation energy in linear methacrylates were internal and other motions within monomer units, the hindrance between side groups due to the bulk and polarity of neighbouring chains and intermolecular attraction of adjacent units. Using model systems to calculate the magnitude of these various contributions led to the conclusion that local internal motions of the side chains are the dominant process resulting in the γ relaxation.

In addition to the low temperature γ relaxation, when a solvent is added to linear methacrylate systems a further low temperature relaxation is found which has been labelled Tdil. Using dynamic mechanical methods at 1 Hz, Gall and McCrum (57) observed such a peak at -82°C for PMMA equilibrated at 50 % relative humidity, and a peak at -104°C for a sample equilibrated in water. Both samples were equilibrated at 23 °C. Martin et al. (9) also found a peak at -100°C for a PMMA/water system.

The growth of Tdil peaks in linear methacrylates has been ascribed to low molecular weight solvents interacting with ester side groups and thereby disrupting the ester groups polymer - polymer bonds. It has been proposed (64) that the solvents on sorption into the methacrylate network disrupt the polar polymer - polymer interactions between chains and replace them with polymer - solvent interactions which allow greater side chain mobility. This explains the slight decrease in Tdil with addition of solvent. They conclude that the greater the diluent volume the more hydrogen bonds disrupted and the lower the temperature required to activate the relaxation. Therefore, as the water or solvent concentration increases there are a greater number of side chains taking part in the motion and consequently there is an increase in the size of the diluent peak.

Janacek and Kolarik further (4) investigated the Tdil peak using a variety of solvents of differing size and polarity. At low concentrations it was found that the type of diluent used had little effect on the size and position of the Tdil peak. At higher concentrations, however, the smaller

polar molecules resulted in a greater conversion of the local T_γ motion into larger scale Tdil motion. This was thought to be due to the smaller molecules being more able to disrupt the polymer - polymer hydrogen bonds than the larger molecules.

The T_γ and Tdil peak temperatures for PHEMA and the various copolymers, obtained from the tan δ - temperature plot , are given in Table 4.7. The respective tan δ - temperature plot are shown in Figures 4.11-14a-c. The variation in peak height of the Tdil peak are shown in Figures 4.15a-c as a function of EWC.

The T_γ peak for dry PHEMA has a maximum at -118°C. This is lower than that observed by Kolarik (48) but that value was calculated from the loss modulus, G"- temperature plot. The logG" plot for PHEMA here gives a value for T_γ of -126°C which is in good agreement with previous values obtained but also indicates that there is again a discrepancy between the tan δ and log G" values, as occurred in the glass transition region. Upon copolymerisation with EGDMA there is a decrease in T_γ to -126°C for the 14 mol% sample. For the TEGDMA and P400 copolymers T_γ decreases to -121°C and -120°C respectively with the incorporation of 14 mol% crosslinker. The peak height did not change to any great extent for the EGDMA copolymers but did increase slightly from 0.038 up to 0.045 for both the 14 mol% TEGDMA and P400 systems

Simon (10) found that the T_γs of TEGDMA and P400 appear at -132°C and -130°C respectively. Berlin et al. (53-54) proposed that T_γ for dimethacrylate systems was associated with conformational internal motion of the pendant oxyethylene chains decoupled from the main chain motion. It appears that a combination of the T_γ processes found in both PHEMA and the OED can cause T_γ for the copolymers to be shifted to some intermediate value.

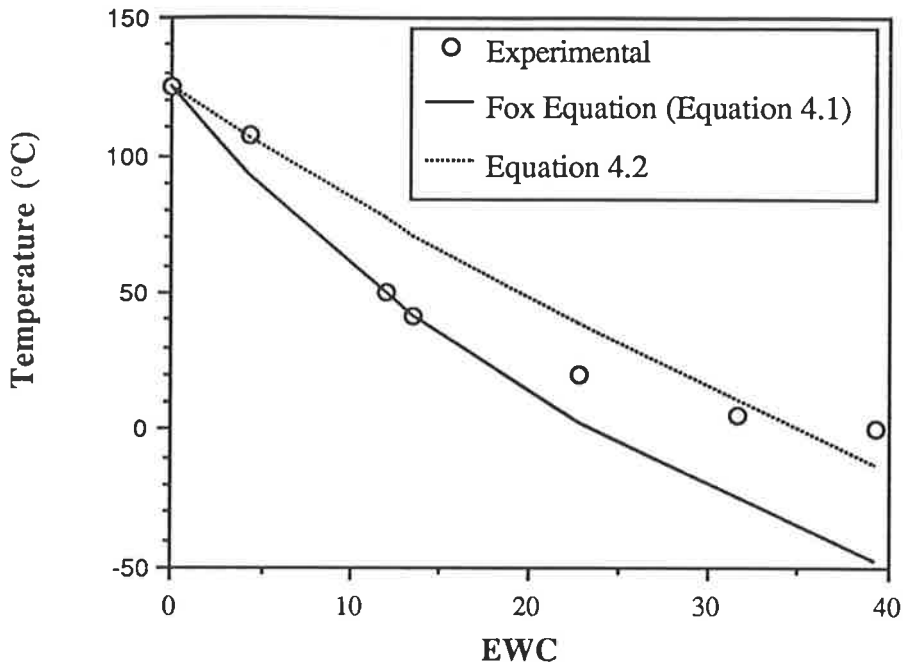

Figure 4.10 Comparison between theoretical and experimental results for the change in T_g of PHEMA due to the sorption of water

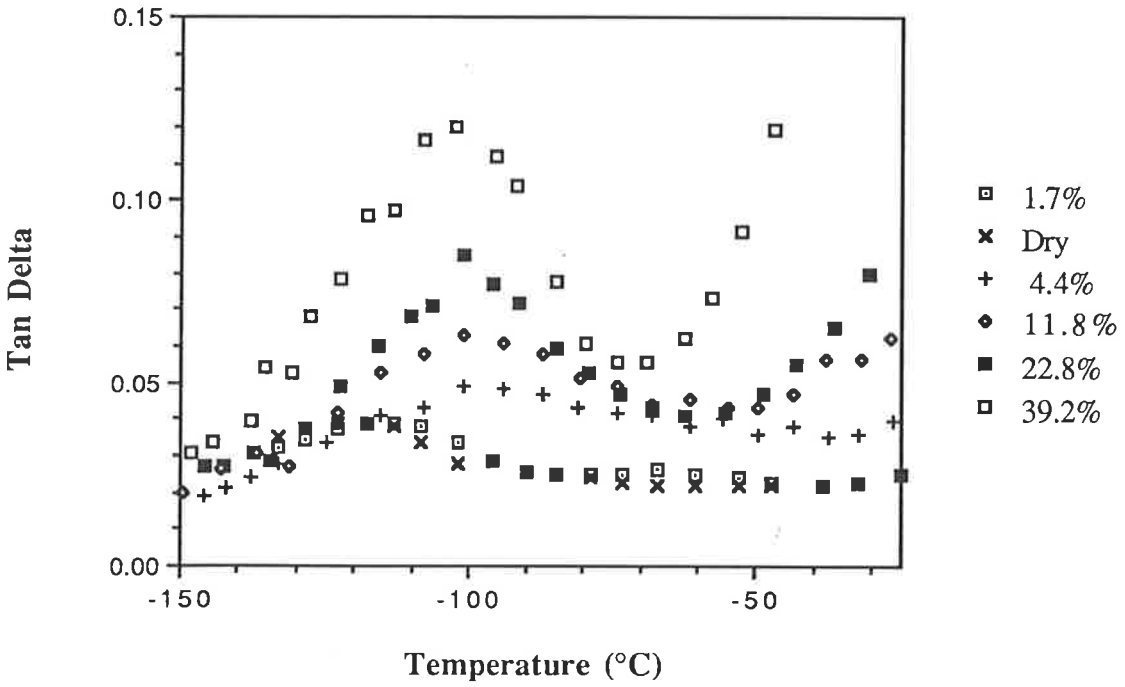

Figure 4.11 Subambient tan δ plots for PHEMA with EWCs as listed above.

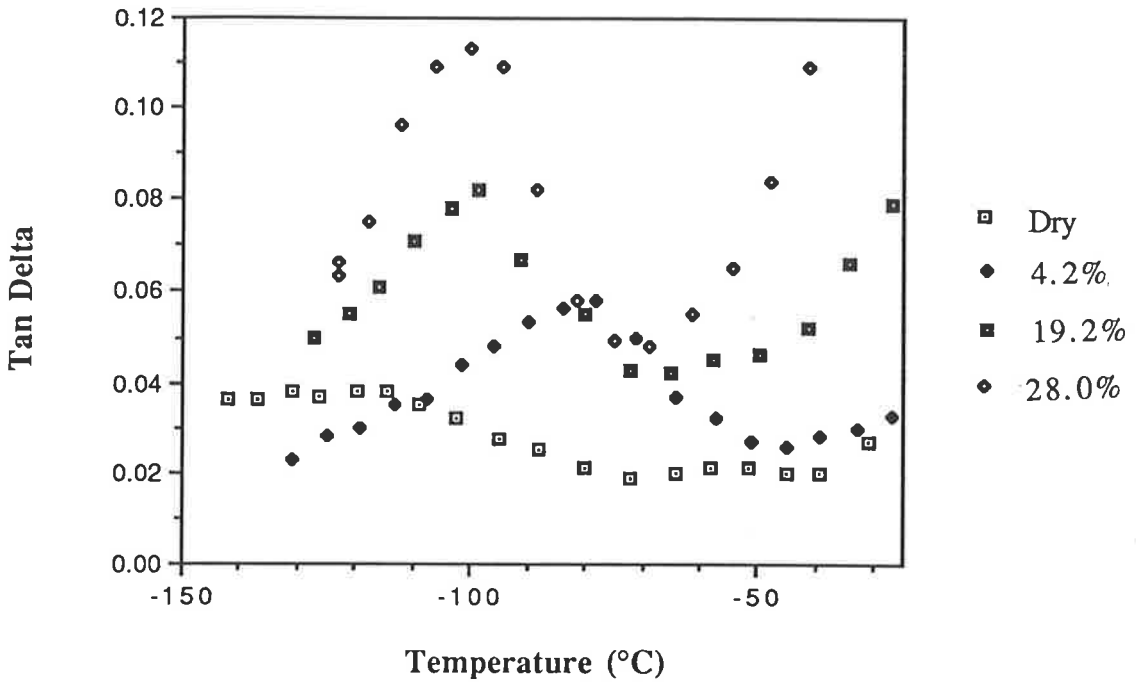

FiFigure 4.12a Subambient tanδ plots for HEMA copolymerised with 3 mol% EGDMA with EWCs as listed above.

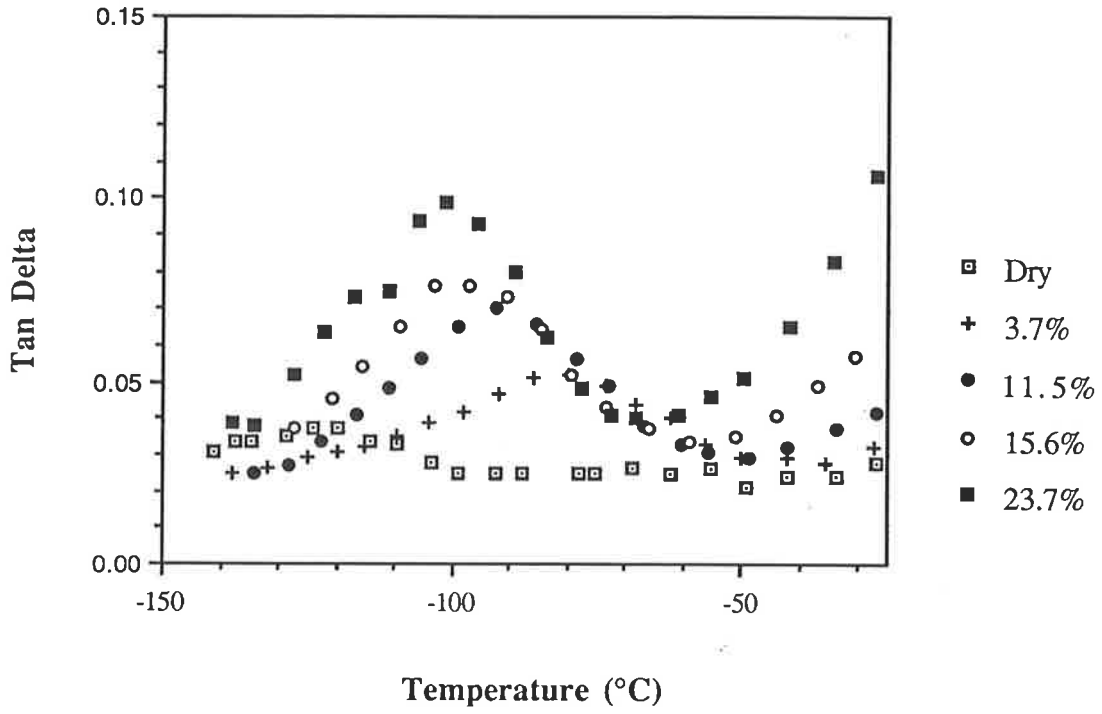

Figure 4.12b Subambient tan δ plots for copolymers of HEMA with 6 mol% EGDMA with EWCs as listed above.

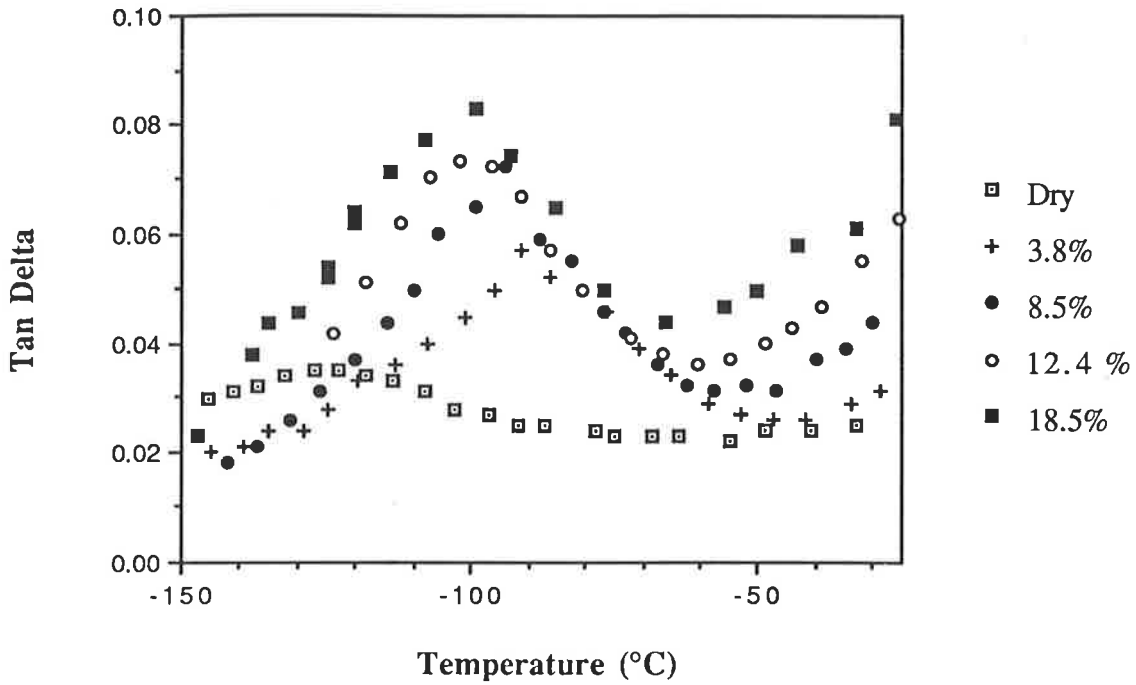

Figure 4.12c Subamient tan δ plots for HEMA copolymerised with 14 mol% EGDMA with EWCs as listed above

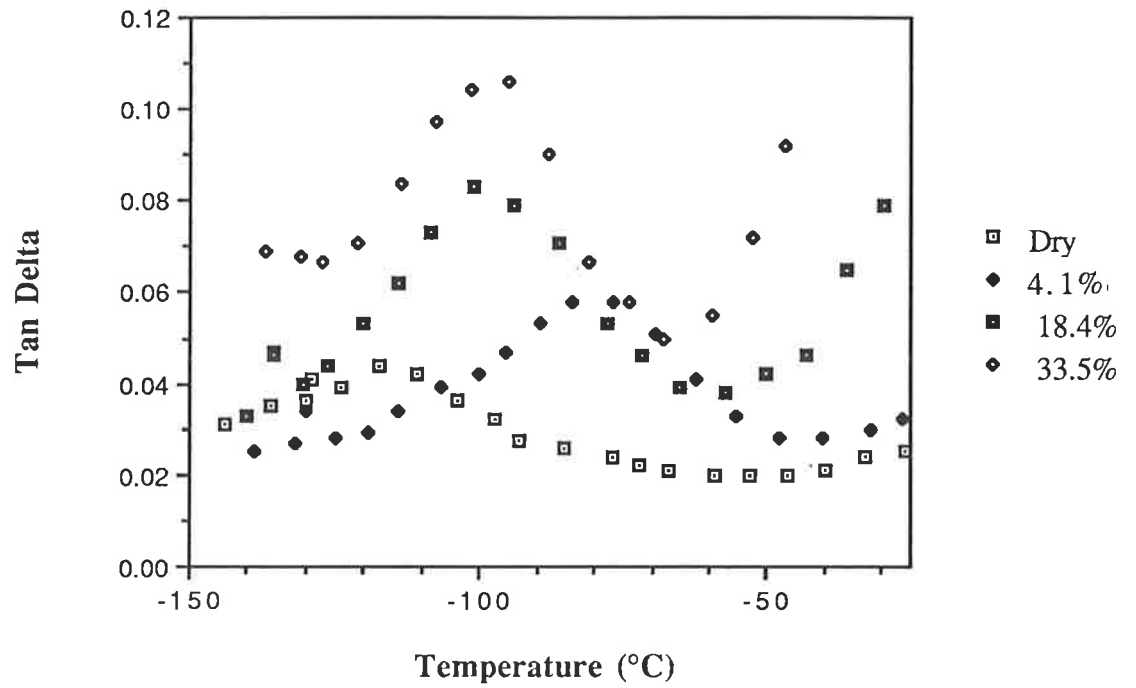

Figure 4.13a Subambient tan δ plots for HEMA copolymerised with 3 mol% TEGDMA with EWCs as listed above.

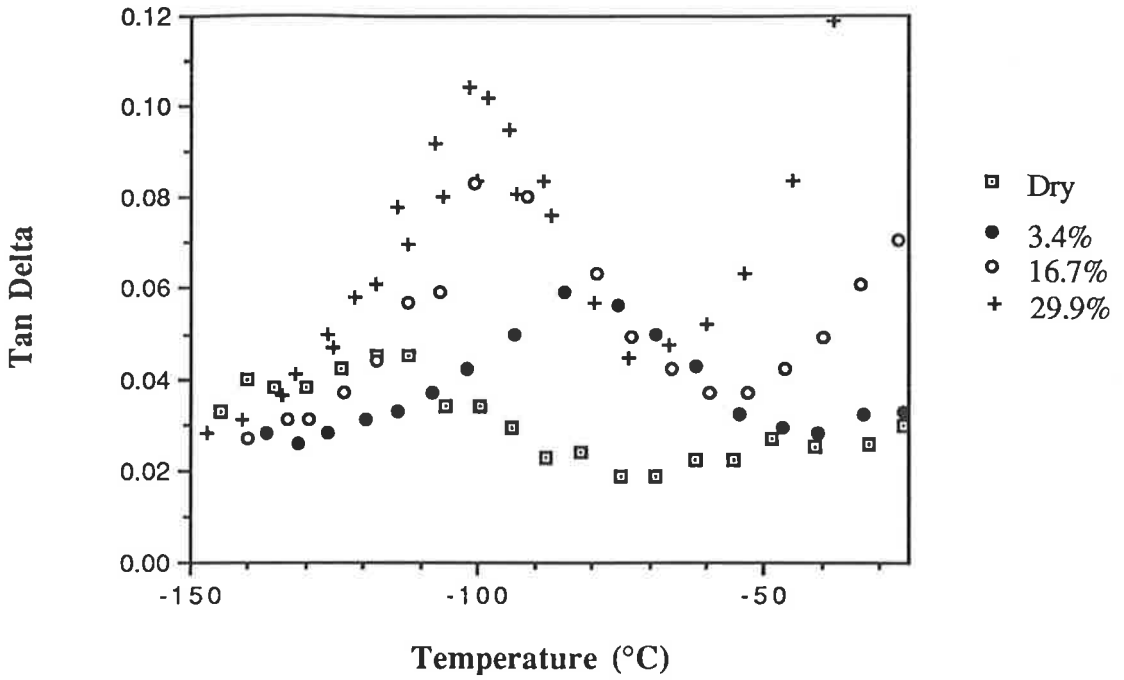

Figure 4.13b Subambient tans δ plots for HEMA copolymerised with 6 mol% TEGDMA with EWCs as listed above.

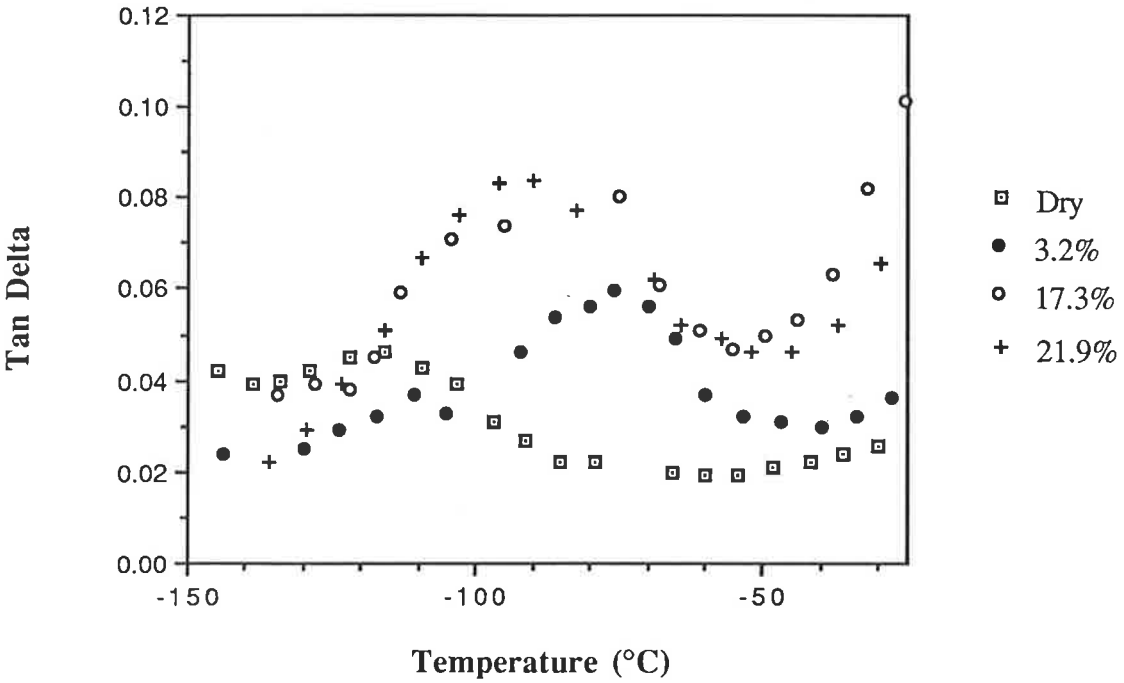

Figure 4.13c Subambient tans δ plots for HEMA copolymerised with 14 mol% TEGDMA with EWCs as listed above.

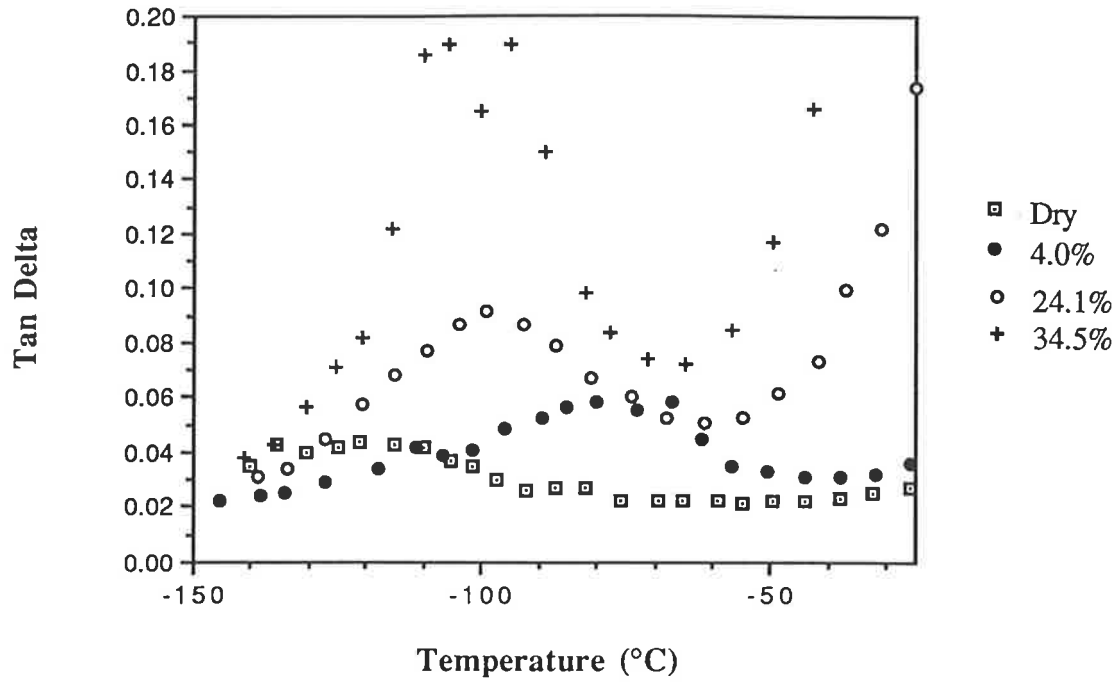

Figure 4.14a Subambient Tans δ plots for HEMA copolymerised with 3 mol% P400 with EWCs as listed above.

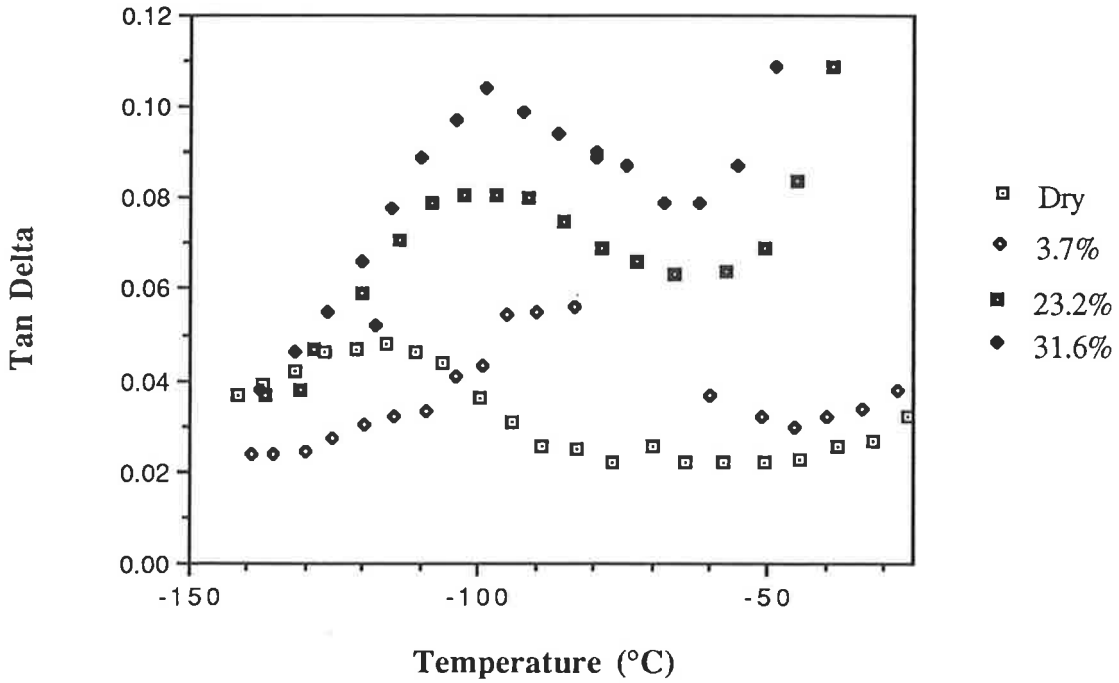

Figure 4.14b Subambient Tans δ plots for HEMA copolymerised with 6 mol% P400 with EWCs as listed above.

TABLE 4.7

Subambient results of the dynamic mechanical testing of PHEMA and its copolymers giving the Tγ and Tdil temperatures (°C). The temperature given for the dry samples is T_γ. For the 1.7%EWC PHEMA sample the lower temperature is T_γ while the higher one is Tdil

	PHEMA						3% EGDMA			
EWC	0	1.7	4.4	11.8	22.8	39.2	0	3.27	18	28
Tdil	-118	-108 -65	-95	-101	-101	-102	-119	-89	-97	-101
OED	6% EGDMA					P14 % EGDMA				
EWC	0	2.84	8.9	16	25.8	0	3.4	10.3	15	18.5
Tdil	-121	-71	-93	-99	-101	-126	-91	-99	-102	-101
OED	3% TEGDMA				6% TEGDMA				14% TEGDMA			
EWC	0	4.4	18.4	33.5	0	3.1	16.7	29.9	0	3.2	19.7	21.9
Tdil	-119	-80	-99	-98	-120	-81	-96	-99	-121	-75	-89	-93
OED	3% P400				6%P400					14% P400		
EWC	0	4.0	24	34.5	0	3.7	11.1	23.2	31.6	0	2.9	28.0	30
Tdil	-120	-73	-98	-100	-120	-72	-83	-90	-96	-121	-75	-89	-93

The addition of even small amounts of water caused the Tdil peak to appear. For a PHEMA sample containing less than 1% water this appeared at -65°C with a slight decrease in T_γ occurring at the same time. At higher EWCs the T_γ peak disappears altogether while the Tdil peak increases in size and gradually shifts to a lower temperature. It can be seen (Figures 4.15a-c) that the increase in height of the Tdil peak is obviously highly dependent on the amount of water present in the polymer.

The copolymerisation of HEMA with P400 caused a shift in Tdil at full saturation with an increase in the peak temperature from that of the PHEMA homopolymer of 8°C for the 14 mol% P400 copolymer. It has been noted (10) that Tdil for the OEDs was dependent on the length of the oligo-ethylene glycol unit, increasing from DiEGDMA to P400 with the TEGDMA and P400 polymers having values of -103°C and - 91°C respectively.

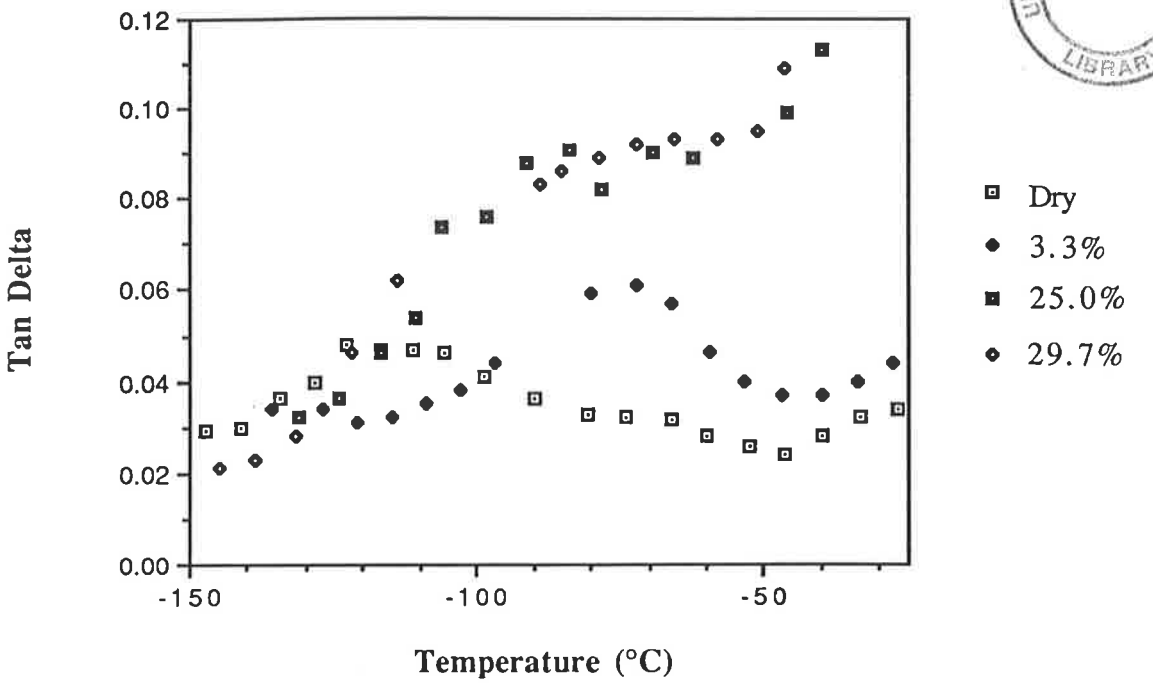

Figure 4.14c Subambient tans δ plots for HEMA copolymerised with 14 mol% P400 with EWCs as listed above.

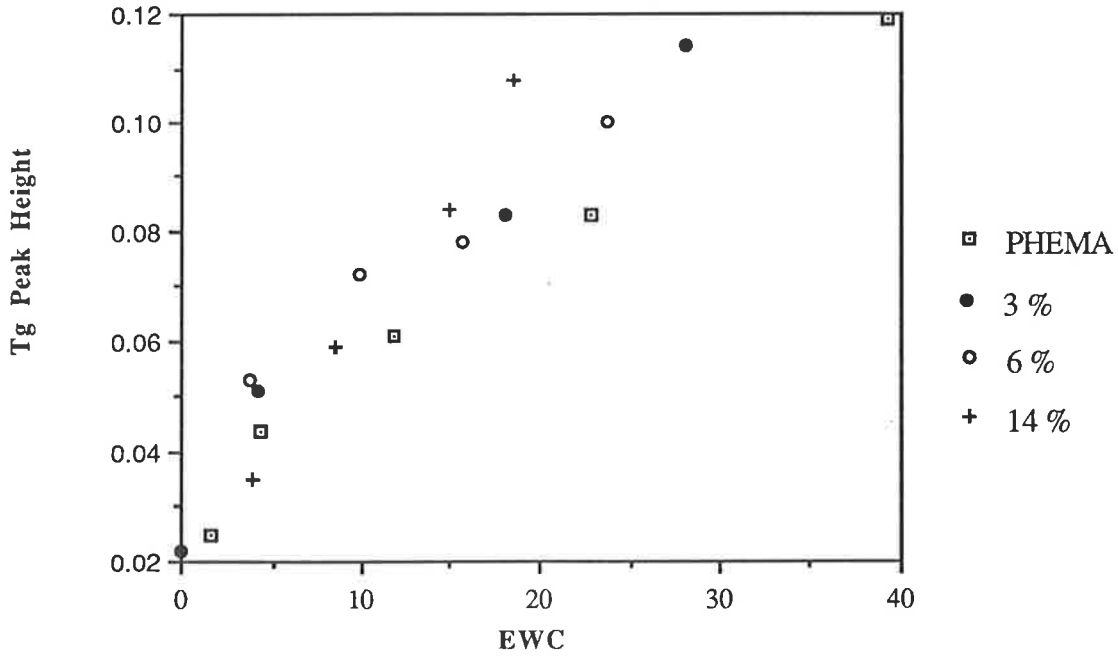

Figure 4.15a Comparison of Tγ peak heights for PHEMA and HEMA copolymerised with EGDMA in the mole ratios given above.

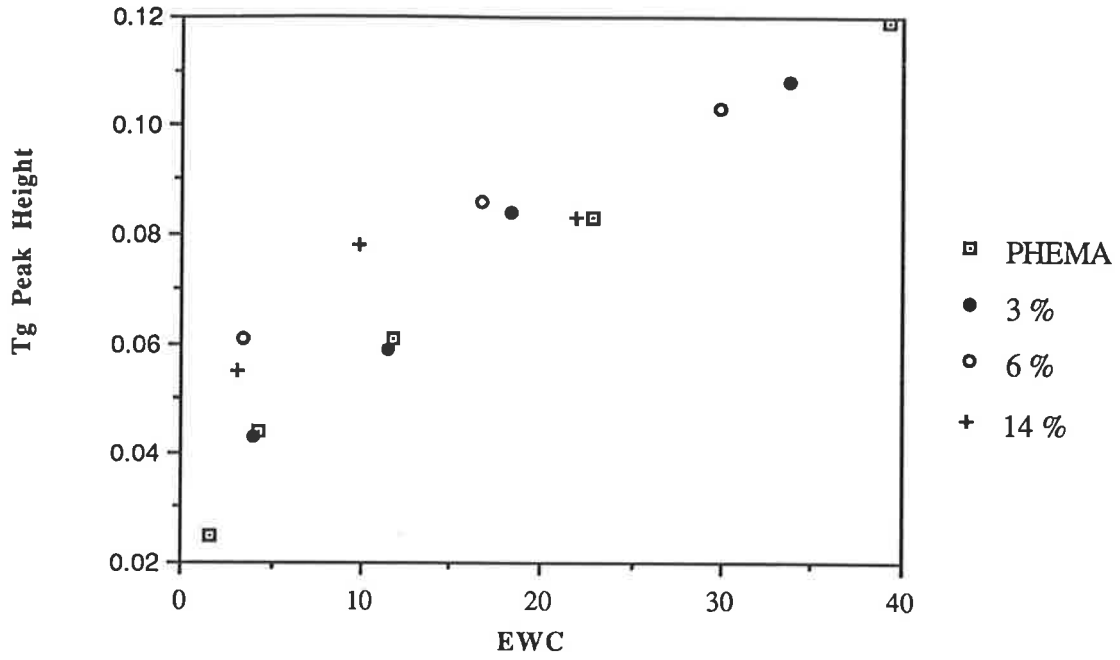

Figure 4.15b Comparison of Tg peak height at different EWCs for PHEMA and HEMA copolymerised with 3, 6 and 14 mol% TEGDMA.

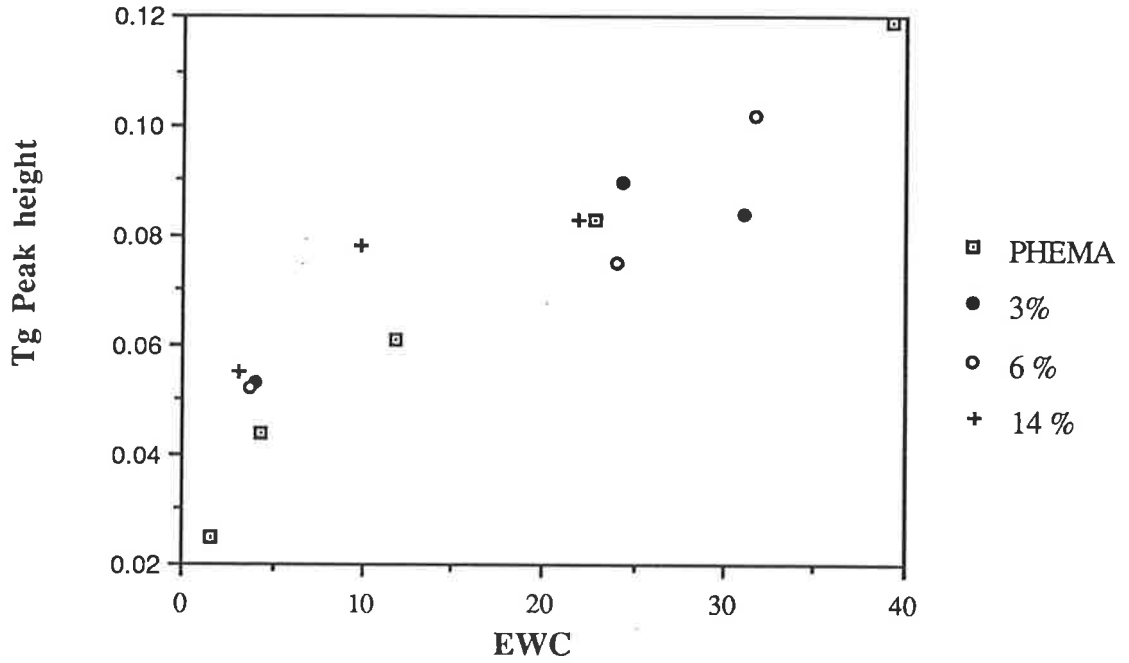

Figure 4.15c Comparison of Tg peak height at different EWCs for PHEMA and HEMA coplymerised with 3, 6 and 14 mol% P400.

It is difficult to tell from the tan δ plots whether the Tdil peaks observed, especially in the case of the P400/HEMA copolymers, are the result of two overlapping peaks resulting from different processes occurring in each of the polymers making up the copolymer or are due to cooperative motions resulting in one distinct Tdil or T_γ peak, as appears to be the case with the T_g transition.

4.3 Summary

The type and degree of OED used in crosslinking the PHEMA hydrogels was found to have a significant effect on the T_g of the resultant copolymer and provides a way in which some measure of control can be achieved over this property. Copolymerisation of HEMA with EGDMA enabled a copolymer to be produced that had a Tg above room temperature but still had a substantial EWC at full hydration. Conversely, copolymerisation with P400 enabled the formation of a copolymer with a Tg below O°C which was not possible for straight PHEMA.

Unfortunately using the equations described here it is not possible to accurately predict the change in T_g on the copolymerisation of HEMA with the OEDs or the effect of water on the T_gs of the polymers studied.

Changes in the height and width at half peak height of the tan δ T_g peak suggest that the mobile kinetic units that contribute to this peak exist in a greater spread of environments at intermediate water contents than for either the dry or fully hydrated polymers.

Sorption of water into any of the copolymers caused the appearance of a low temperature peak that increased with increased EWC. This has been ascribed to water interfering with polymer-polymer interactions and replacing them with water-polymer interactions. Copolymerisation and water sorption appeared to have no great effect on the β peak.

CHAPTER FIVE

DIFFERENTIAL SCANNING CALORIMETRY

5.1 Introduction

The work described in this chapter is an attempt to better elucidate the freezing water behaviour of water in PHEMA hydrogels by examining it under a number of different conditions. Previous measurements (1-2) on the behaviour of freezing water in hydrogels have given differing results in the amounts of freezing water found with, for example, Mardel (2) finding no freezing water present in a copolymer of HEMA containing 40 wt% MMA, while Corkhill et al (1) found between 1 and 2 %for a similar copolymer. Hysteresis effects (1,8) have been noticed in similar studies on hydrogels and the DSC endotherms of freezing water can change depending on the previous history of the sample.

With these results in mind a number of different conditions were employed to investigate the behaviour of water as it freezes in the polymer. In one set of experiments the temperature at which the samples were frozen was varied, keeping the time of freezing constant. In a second set the freezing time of the samples was varied with the temperature kept constant and thirdly the type and amount of crosslinking agent was varied.

It has been assumed here that the enthalpy of melting of the frozen water absorbed into the polymer has not been altered by its incorporation into the polymer structure. While some doubt has been expressed about the validity of this assumption (3-4) it has been shown that the heat of fusion of water swollen in polymers is virtually identical to the heat of fusion of pure water (5-6) and the method used here (Chapter Two) to determine the amount of freezing water is consistent with that employed by others (7-9) and, therefore, enables a comparison to be made between different sets of results, particularly with respect to the copolymer work. It

also seems reasonable to assume that the enthalpy of fusion of water in saturated PHEMA will not be changed, to any great extent, if different freezing cycles are used and so any measured differences will be due to differences in the actual amount of freezing water present.

It should also be noted that water will not be observed in DSC experiments if either the change in heat capacity or the actual amount of water present are too small and fall below the sensitivity of the instrument to detect it.

5.2 Results and Discussion

5.2.1 Variation of Freezing Water With Temperature

One of the first effects that must be taken into account when calculating the percentage of freezing water in the polymer is the differing effects of heating and cooling rates and the immediate history of the sample being scanned. If the sample was allowed to re-equilibrate for 1-2 days under the same conditions (i.e. temperature and relative humidity) it was in before it was run in the DSC, then it was found to give a similar DSC thermogram as its initial scan, indicating that the effects of the scanning procedure on the hydrated sample were reversible. However, to remove any possibility of previous measurements affecting the DSC thermogram fresh samples were used each time and then discarded after use, after first being weighed to detect any possible water loss.

The effect of differing rates of heating can be seen in Figure 5.1a-b. This shows two water melt endotherms, the first (a) from a saturated PHEMA sample that had been cooled rapidly down to - 120°C (at 320 °C/min - the fastest possible cooling rate) , held there for 15 minutes and then scanned while heating at 20°C/min. The resulting thermogram shows a water melt endotherm having two peaks separated by approximately 3°C. The second thermogram (b) is also that of saturated PHEMA which was rapidly cooled to -120°C and held at that temperature for 15 minutes. This

sample, however, was then rapidly heated at 320 °C/min to -20°C and then subsequently scanned. This thermogram shows only a single endothermic water melting peak. It should also be noted that both of these water melt endotherms are much broader than those obtained from water only.

No discernible transitions were observed on the DSC thermogram trace below the water melt endotherms. This differs from the results found with the dynamic mechanical testing in that the low temperature transition, found at approximately -100°C, is not observed here indicating that the DSC is less sensitive to this type of transition. This is confirmed by previous measurements (10) which have shown that DSC appears to be insensitive to events below -40 °C for hydrogels.

The percentage of freezing water found in run 5.1(a) was also greater than that observed for run 5.1(b). This seems to indicate that there is a reordering of the possible environments in which water exists as the sample is heated at the slower rate and also a possible diffusion of water through the sample to areas where more can crystallize.

In order to gain a better understanding of this behaviour the amount of freezing water was measured as a function of temperature with the samples being rapidly cooled to the appropriate temperature, held at that temperature for 15 minutes and then heated at 320°C/min, where necessary, to -20°C and the thermogram recorded at 20 °C/min. A number of different samples were used at each temperature and an average of these taken. The standard deviation found in these and other measurements was usually less than ±5%. The thermogram recording was started at -20°C in order to eliminate problems that occurred with the starting transient when a scan was commenced.

The results are presented in two ways. One gives the amount of freezing water as a percentage of the weight of the total hydrogel while the other gives it as a percentage of the weight of the water in the hydrogel, as given in Figure 5.2.

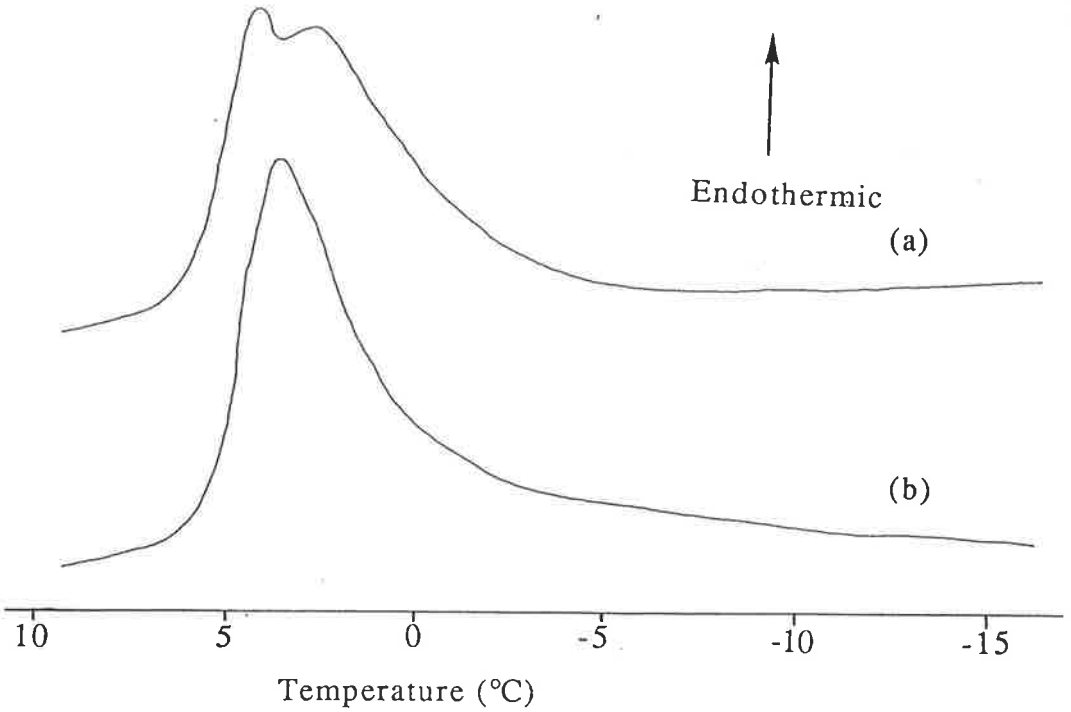

Figure 5.1. Water melt endotherms for saturated PHEMA samples. (a) Sample cooled at 320°C/min to -120°C for 15 minutes and then scanned at 20°C/Min to 15°C. (b) Sample cooled as for (a) but then heated at 320°C/min to -20°C and then scanned at 20°C/min to 15°C.

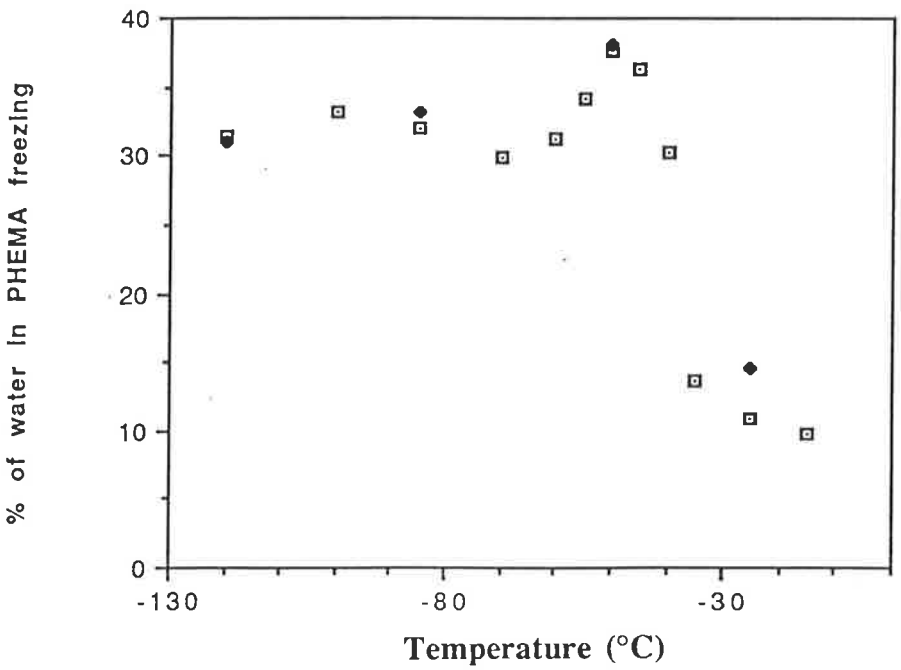

Figure 5.2 Change in the amounts of frozen water found in saturated PHEMA samples frozen at different temperatures for (▫) 15 minutes and (◆) 60 minutes

From Figure 5.2 it can be seen that the percentage of available water that freezes increases as the temperature is decreased from -25°C to -50°C from approximately 11% to 37%, as would be expected. After this, however, there is a decrease in the amount freezing as the temperature is decreased further, until a constant value is achieved after the temperature has fallen below approximately -70°C. At some temperatures additional measurements were made on samples that had been frozen for 60 minutes. Once the temperature had decreased below -50°C, however, the amount of frozen water remained constant, independent of freezing times longer than 15 minutes; between 0°C and -50°C, however, the amount of frozen water measured increased until it had reached a maximum value of 37%, which was the value obtained at -50°C after 15 minutes. In terms of weight percent of the hydrogel this corresponds to approximately 13 % EWC.

Typical thermograms obtained for saturated PHEMA samples are shown in Figure 5.3. From these a number of observations can be made. As the temperature of pre-equilibration of the samples is decreased the water melt endotherm broadens up to about -55°C and it is possible to notice at least two vertices to the endotherm peak. As the pre-equilibration temperature decreases further, however, the peak again becomes more uniform and tends to decrease again in width. This is similar to the effect of temperature cycling noted by Pedley and Tighe (8) in which a second peak in a hydrogel becomes more prominent as the sample is taken through a series of temperature cycles. Pedley and Tighe suggested that there was a continuum of water states existing between those water molecules that were hydrogen bonded to the polymer and water that is unaffected by its polymeric environment and that the change in area under the respective peaks was due to a shift to better crystallization behaviour. If this is true then it seems that this shift can occur while the sample is being heated at 20K/min but that there is insufficient time for a noticeable change to occur when the sample is heated rapidly up to the measuring temperature. The

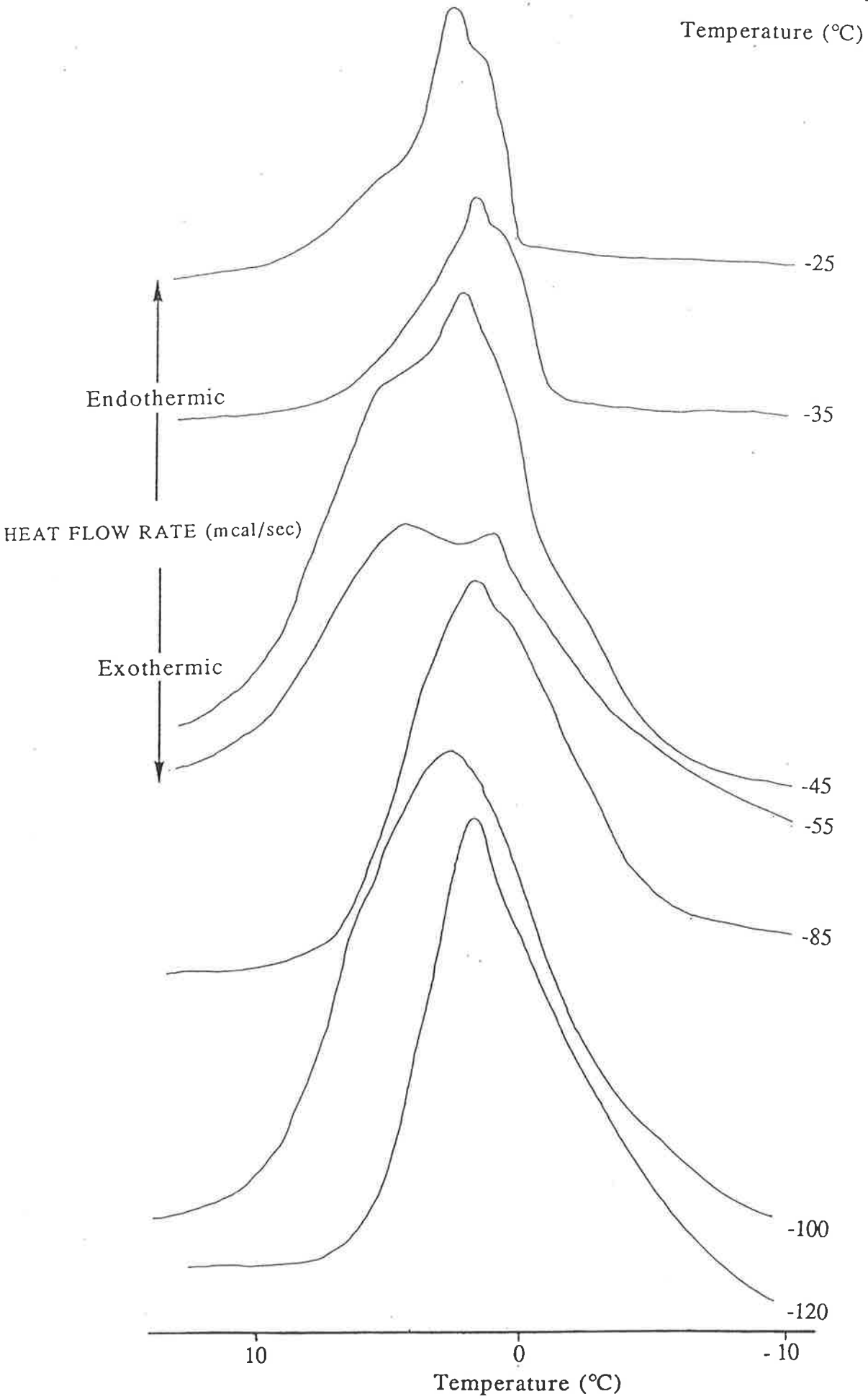

Figure 5.3. Typical melting water endotherms obtained from saturated PHEMA samples frozen for 15 minutes at the temperatures given above.

fact that the peaks observed with the rapid heating cycle from -120°C seem to be independent of the time frozen also suggest that this phemomena is strongly temperature dependent.

From the dynamic mechanical results obtained for saturated PHEMA (Chapter Four, Figure 4.1) it can be observed that for the glass transition peak tan δ values begin to increase somewhere between -70° and -60°C, indicating the beginning of main chain motion. This could explain the decrease in freezing water found as the temperature is decreased below -50°C due to the increasing difficulty of water in diffusing through the polymer as main chain motion decreases.

The temperature at which the water begins to melt (taken as the first deviation from the baseline on the DSC thermogram (as in Figure 2.1a)) also varies. The samples frozen above -35°C having a freezing point depression of about 1°C which tends to decrease further to -4°C to -5°C at -70°C and then remain constant below that temperature.

5.2.2 Variation of Freezing Water With Time.

Isothermal measurements of the amount of freezing water were also made for PHEMA samples at varying freezing times. The first set were carried out at -35°C because the previous measurements showed that at this temperature approximately half the the water had frozen after 15 minutes and, therefore, all the water in the sample that could freeze should have done so after one to two hours. In order for a correlation to be made with the solution NMR work, discussed in the next chapter, the second set of isothermal measurements were made at -15°C. The samples were again cooled as rapidly as possible, and held at their respective temperatures for the appropriate time and the thermograms recorded, with the samples that were frozen at -35°C first being heated rapidly to -20°C . Different samples were used for each measurement to ensure that any possible hysteresis effects would not effect the measurement.

Typical DSC thermograms obtained using the above procedure for the samples frozen at -35°C are shown in Figure 5.4. Similar thermograms were also obtained for those samples frozen at -15°C. It can be seen that there is a distinct change in the appearance of the water melt endotherm as the freezing time increases. After only two minutes the endotherm obtained is a single nearly uniform peak. After 5 minutes the peak has broadened slightly and a shoulder to the main peak can be observed at a lower temperature. From 10 minutes onward it is obvious that two peaks exist, their vertices separated by 2 to 3 °C. There is also the possibility of an additional peak underlying these two, evidenced by the appearance of a further shoulder in the endotherm although this could be an artefact due to the superposition of the other two peaks. This suggests that the change in crystallisation behaviour is also time dependent.

In general there was a depression of the temperature at which freezing commenced of approximately 1°C from that of pure water.

The decrease in the amount of non-frozen water (i.e the increase in freezing water) is shown in Figure 5.5. This could be fitted to a single exponential decay equation of the form

$$W_f = A\exp(\frac{t}{\tau}) \qquad \text{Equation 5.1}$$

where W_f represents the relative amount of freezing water, A is a constant and τ is a time constant which is characteristic of the temperature used. The two values found for τ are 14±0.5 minutes and 25±0.5 minutes for samples frozen at -35°C and -15°C respectively, indicating, as would be expected, that the freezing process occurs more rapidly at lower temperatures.

5.2.3 Variation of Freezing Water With Copolymer Composition

Table 5.1 gives the percentages of freezing water found in PHEMA and the copolymers formed with the OED series, for both saturated samples

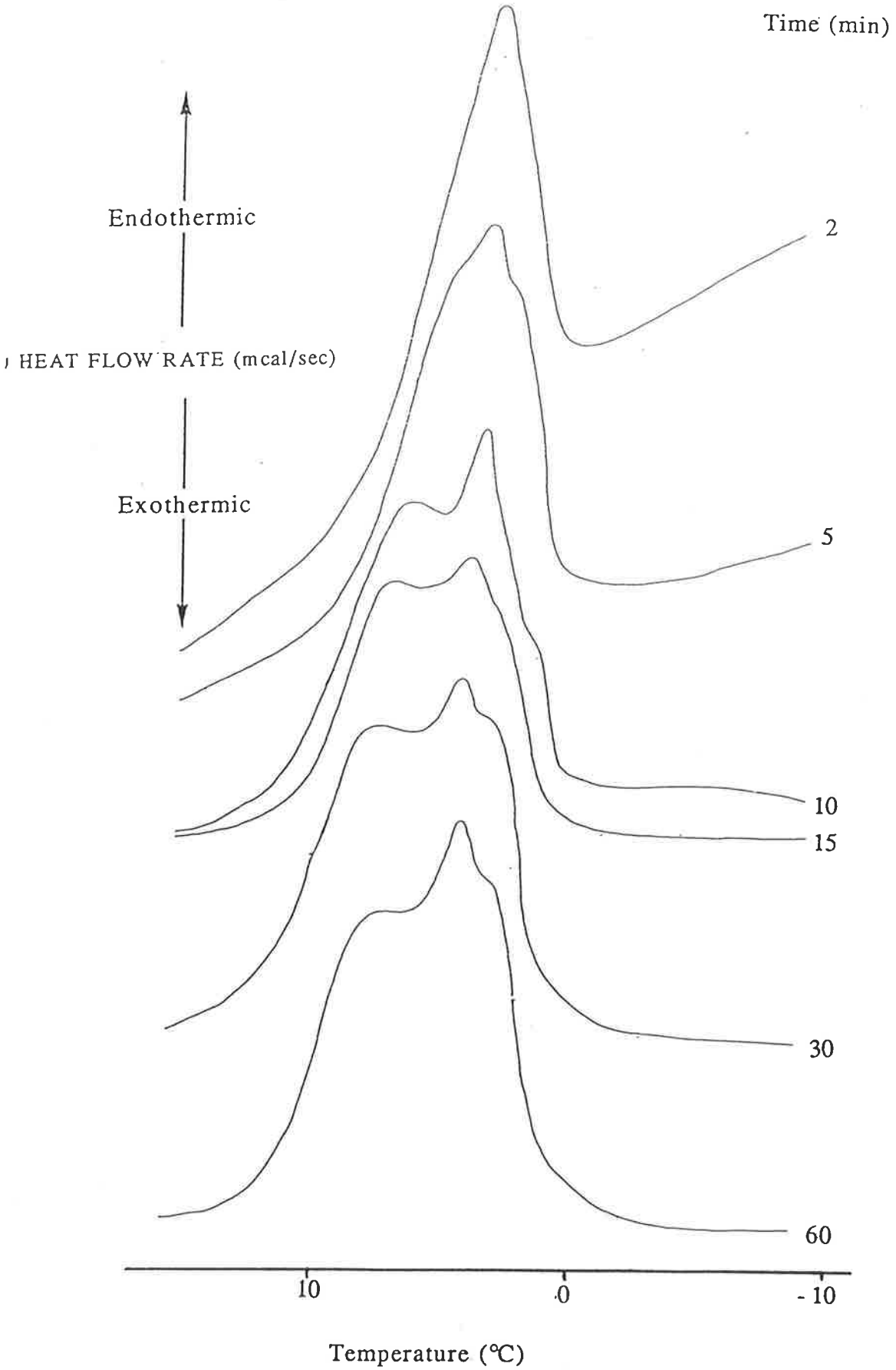

Figure 5.4. Typical melting water endotherms obtained from saturated PHEMA samples held at -35°C for the times given above.

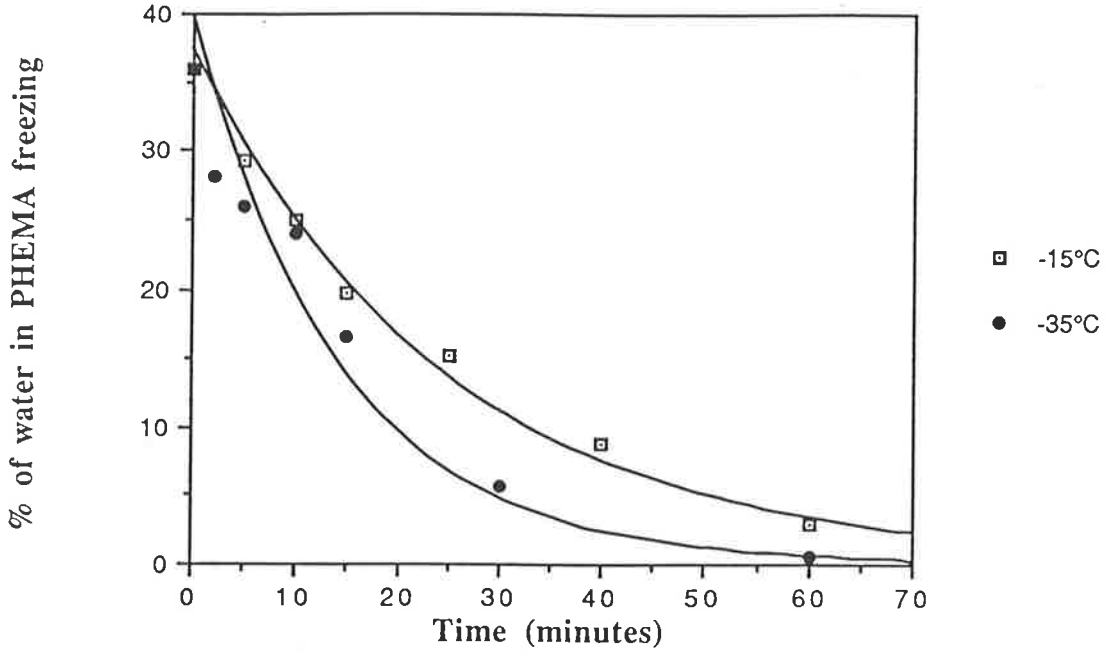

Figure 5.5 Change in the amounts of water found to freeze at -35°C and -15°C as a function of time. The lines are the calculated theoretical fits to Equation 5.1

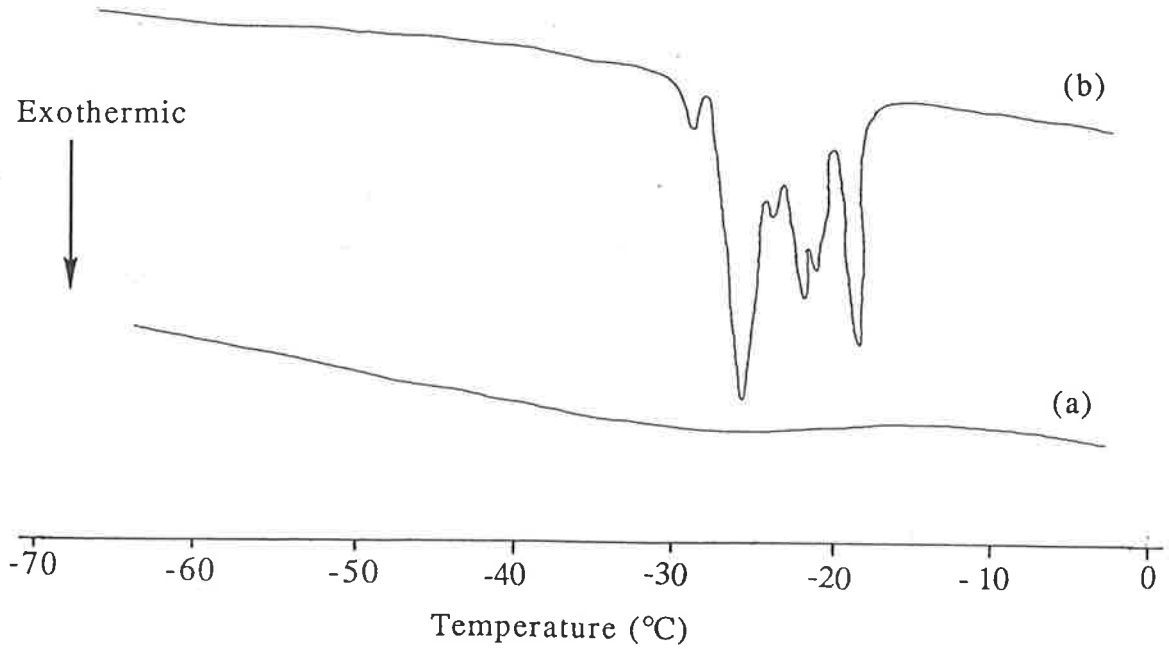

Figure 5.6. DSC thermograms of cooling runs on saturated PHEMA samples (a) Fresh sample and (b) sample that has been heated and cooled repeatedly.

and samples conditioned at 100% relative humidity. Samples conditioned at lower relative humidities did not show any water melting endotherm.. The samples were cooled rapidly to -120°C, allowed to equilibrate for 15 minutes (the previous work on PHEMA showed no change in the amount of freezing water with time after 15 minutes and preliminary experiments on some of the copolymers indicated that this was also the case here), then heated rapidly to -20°C and a thermogram recorded. In some cases a slight freezing water peak was observed but it was not possible to accurately determine the amount of water melting with any great precision and within the experimental error of the method being used. In these cases the amount of freezing water must have been between 0 and 0.1 %.

It can be observed from Table 5.1 that the amount of water freezing in the hydrogels, as a percentage of the total hydrogel weight (column A), decreases with increasing crosslinking concentration, as would be expected as the total water uptake also decreases. The percentage of the water in the polymer that freezes is also indicated (column B). The greatest amount was found for saturated PHEMA at around 33%. The addition of crosslinking agents, however, causes a large decrease and it appears that proportionately much less water in the copolymers is capable of freezing. This decrease is also dependent on the type of crosslinking agent used with the P400 copolymers, in general, showing a much greater proportion of freezing water than the TEGDMA copolymers, a trend that is followed as the molecular weight of the OED decreases.

As has already been noted, no freezing water was observed for samples conditioned below 100% relative humidity. For some samples equilibrated at 100% RH slight water melt peaks for PHEMA and some PHEMA copolymers were observed. These, however, were much smaller than found for fully saturated polymer samples and this seems to indicate that the polymer is hydrated in stages with, in the case of PHEMA, any

additional water absorbed above approximately 30 % EWC becoming free water capable of freezing.

TABLE 5.1

Freezing Water Determination for Copolymers of HEMA with Oligo-(ethylene glycol) Dimethacrylates. The results are given both as a percentage of the total hydrogel weight (A) and as a percentage of the weight of water in the hydrogel (B).

	Polymer equilibrated in water.		Polymer equilibrated at 100% Relative Humidity.	
Mole % OED	A	B	A	B
0 (PHEMA)	13.0	33.2	0.7	2.1
3 % EGDMA	1.9	6.8	0.2	0.8
6 % EGDMA	0.3	1.5	<0.1	<0.1
3 % DiEGDMA	2.2	6.8	0.2	0.9
6 % DiEGDMA	2.0	7.0	<0.1	<0.1
14%DiEGDMA	2.0	9.2	<0.1	<0.1
30%DiEGDMA	0.1	5.4	0	0
3 % TEGDMA	3.1	9.3	0.3	0.9
6 % TEGDMA	1.0	3.4	0.2	0.5
9 % TEGDMA	0.6	2.6	<0.1	<0.1
14 % TEGDMA	0.4	1.9	<0.1	<0.1
30 % TEGDMA	0.2	1.2	0	0
50 % TEGDMA	<0.1	<0.1	0	0
3 %P400	6.2	18.0	0.4	1.1
6 %P400	2.3	7.3	0.2	0.9
14 %P400	1.4	4.8	<0.1	<0.1
30 %P400	0.8	2.8	<0.1	<0.1
50 %P400	0.4	1.4	0	0

5.2.4 Anomalous Water Freezing.

In general, as PHEMA samples were cooled only a broad exothermic trough was found on the thermogram as the water cooled. Similar

thermograms were also found by Smyth et al.(10) on cooling PHEMA. For some hydrogels with higher EWCs sharp exothermic peaks are often noticed (9,14-15) as the water freezes. Quinn et al. (14) found this type of water freezing exotherm for a range of Poly(n-vinyl pyrollidine co MMA) copolymers and similar freezing behaviour has been observed in Sephadex gels (9,15). Pure water cooled in the DSC tended to supercool before eventually freezing and gave a single sharp exothermic peak with all the water freezing at the same time. Supercooling is a common phenomenon and has been noted for water in capillaries, silica and other inorganic materials (11-13) and presumably also occurs in hydrogels.

In addition to this Murase et al.(9) has observed a sharp exotherm appearing, due to water freezing, as some Sephadex gels were heated from subambient temperatures even though exotherms had been noticed as the sample was cooled. This behaviour was found to be dependent on pore size, crosslinking and the cooling rates used. Mardel (2) observed a similar process occurring as a fully hydrated 10 wt%MMA/90wt%HEMA copolymer was heated. This was found to occur only with this particular copolymer ratio.

Figure 5.6 shows two thermograms obtained as samples of saturated PHEMA were cooled. Both thermograms were recorded as the sample was cooled at 20K/min. The first, Figure 5.6(a), shows the cooling thermogram for a previously unfrozen sample showing the broad water freeing exotherm normally noticed. Figure 5.6b, however, shows a cooling thermogram for a PHEMA sample that had already gone through a number of cooling and heating cycles and a number of sharp exothermic peaks can be observed. This behaviour was found only in samples that had been through repeated cycles of cooling and heating (i.e cooled at 20K/min to -100°C and then heated at 20K/min to 20°C with this process repeated at least five times.) and appears to be evidence that the water in the polymer has been restructured in such a way that allows sizable amounts of water to freeze at

the same time. There appeared to be no correlation between the amount of water found in these exotherms and the conditions which it had undergone.

5.2.5 Glass Transition Temperatures

Differential scanning calorimetry can be used to measure the glass transition of polymers as a change in the specific heat generally occurs as the polymer changes from a glassy to a rubbery state. This change is detected by the DSC and from the this the T_g can be calculated (Chapter Two). The ΔCp can also then be calculated for the polymer.

T_gs, however, were often difficult to observe using DSC methods for some of the copolymers both dry and saturated. This can be ascribed to a number of reasons. Firstly, as was seen in the dynamic mechanical work, there is a tendency for the glass transition region to be broadened by the addition of either a crosslinking agent or by the addition of water. This had the effect of causing the DSC thermogram to show an ill defined change in Cp (Figure 6.2) from which it was not possible to measure the T_g. This phenomena usually occurred at intermediate water concentrations (between 10 and 25% EWC), when the mole % crosslinker was between 20%-70% and when both conditions applied. Secondly, some of the copolymers had very high T_gs and tended to decompose before a T_g could be ascertained, particularly those containing a large proportion of EGDMA. Thirdly, the T_g could be difficult to observe if there was not a sufficient change in the specific heat; which seems to be the case for TEGDMA as the DSC trace showed no glass transition, an observation also made by Simon (16).

For these reasons only the T_gs for PHEMA and some of the P(HEMA/P400) copolymers could be measured to any great degree of accuracy and repeatability. The values for these polymers at varying stages of hydration are given in Table 5.2. It should also be noted that the DSC thermograms for the 10% and 18% EWC PHEMA samples show only one glass transition which is strongly supportive of the earlier claim that the

secondary peak observed at high temperature in the torsion pendulum scans was due to water loss, as water loss from the DSC samples was minimal due to the types of pans used and the higher scan rate (20K/Min compared to 2K/min). As before (Chapter Four) both the Fox equation and Equation 4.2 have been applied in order to see if there is reasonable agreement between experimental and calculated values. The difference in the T_gs measured by DSC and those by dynamic mechanical methods can be ascribed to the differing frequencies of testing, which is known to affect the glass transition temperature (17), with the DSC being a static method while the torsion pendulum operated at approximately 1 Hz.

TABLE 5.2

Comparison of theoretical and experimental T_gs calculated using the Fox equation (Equation 4.1) and Equation 4.2.for the P400/HEMA copolymer system.

Mole %P400	EWC	Expt T_g	Fox Eqn	Eqn 4.2	EWC	Expt T_g	Fox Eqn	Eqn 4.2	EWC	Expt T_g	Fox Eqn	Eqn 4.2
0	0	100	100	100	4.5	65	72	83	11.9	47	35	57
3	0	99	84	87	4.0	73	74	84	12.7	46	31	54
6	0	89	70	74	3.74	57	68	76	12.5	33	26	47
14	0	68	45	50	3.3	52	51	58	12.3	21	14	31
30	0	45	23	27								
50	0	23	4	7								
70	0	13	-4	-3								
100	0	-12	-12	-12								

Again it is apparent that neither of the equations used here can predict with any great accuracy the change in T_g due to either copolymerisation of HEMA with P400 or the effect of water plasticising the polymer.

5.2.6 Specific Heat Measurements.

To calculate the change in specific heat before and after the glass transition the DSC was first calibrated with a sapphire standard at the temperature at which the T_g occurred and using the same heating rate and sensitivity as that used when scanning the sample. Values of ΔCp of 0.14 ± 0.02 J g^{-1} K^{-1} and 0.80 ± 0.02 J g^{-1} K^{-1} were obtained for PHEMA and P400 respectively. The low value for PHEMA explains why its is more difficult to obtain well defined T_gs for this polymer (The ΔCp of PMMA has been calculated to be 0.318 J g^{-1} K^{-1} (18) and this gives much more clearly defined T_gs). The higher value obtained for P400 also explains why it was generally possible to obtain good T_gs at all copolymer concentrations with HEMA.

5.3 Summary

The DSC results indicate that copolymerisation of HEMA with any of the OEDs results in a decrease in the bulk or free water that is capable of freezing. They also indicated the necessity of clearly defining the cooling and heatimg procedures used in obtaining water melt endotherms as to some extent the type of endotherm found and the amount of water frozen will vary depending on the method used. The state of the water in the copolymer will also change as a consequence of cooling and heating the sample and in some cases this led to the detection of sharp water freezing exotherms as the sample was cooled.

Attempts to predict changes in T_g in the HEMA/P400 copolymers using Equations 4.1 and 4.2 also met with little success.

CHAPTER SIX

SOLUTION NMR

6.1 Introduction

The use of ^1H NMR techniques make it possible to monitor the behaviour of water in the hydrated polymer. It must be noted, however, that these techniques can only observe water that has some degree of mobility. Water that is constrained from isotropic tumbling, which averages out dipolar interactions, will not be seen as its linewidth will broaden into the baseline. This implies that frozen water or water that is tightly constrained, either by steric hindrance or strong hydrogen bonding to the polymer chain, will not be observed. ^1H NMR, however, has been shown (1-5) to be a useful tool for studying the state of water in solids, which can in turn give information on the overall structure of the hydrogel system.

It was found (6) that the best temperature at which to collect data about the freezing of water in PHEMA was -15°C. At this temperature there was adequate time to collect the initial spectra in the first minutes as the sample reached the required temperature and to follow the first stages of freezing. At temperatures below this the water froze too quickly to be able to collect spectra of the initial freezing process as the ^1H water line broadened into the baseline and adequate spectra could not be resolved in the necessarily short time span required. At -15°C the disappearance of mobile water stopped after four to five hours. In general it was found that the variable temperature probe reached the desired temperature after approximately 30 seconds if the change made was less than 20°C.

The experiments were conducted in a variety of ways on PHEMA and its copolymers with EGDMA, TEGDMA and MMA. In most cases it was desired to see how the water peak area decreased with time at a

constant temperature so the sample was rapidly cooled to -15°C and spectra were collected almost immediately, within 1-2 minutes.

6.2 Results and Discussion

6.2.1(a) PHEMA

The spectra of water in saturated PHEMA are shown in Figure 6.1. This shows some of the spectra collected as the polymer was cooled from 25°C to 5°C in 10°C increments with the samples held at each temperature for 10 minutes. The sample was then cooled rapidly to -15°C and spectra collected at various time intervals, usually starting within 30 seconds of reaching that temperature. Free water has a line width of only a few Hz at room temperature (7) but this increases considerably once it is absorbed into the polymer to a few hundred Hz. As no sharp water peak is observed this indicates that either there is no free and totally unconstrained water in the polymer matrix or what there is is covered by the broad water peak.

The spectrum at 25°C shows an almost uniform single peak but a slight shoulder is noticeable on this peak slightly downfield of it. This becomes more noticeable as the sample is cooled further. There is also an increase in the amount of mobile water indicated by an increase in peak area and the maximum amount of mobile water seems to occur between 0°C and -15°C depending on the cooling cycle used. This could be attributed to the polymer contracting as the temperature decreases forcing water that had previously been constrained in small voids into larger ones and thereby becoming less constrained. Alternatively, it has also been noticed (8) that that the EWC of PHEMA increases as PHEMA is cooled from 25°C to 5°C and the increase in mobile water observed here could be due, in part, to this increase in the ability of the polymer to absorb water with the water present in the polymer being sorbed into different areas giving the molecules greater mobility. At -15°C there is an initial rapid decrease in water over the first 50 minutes but this process then slows. Figure

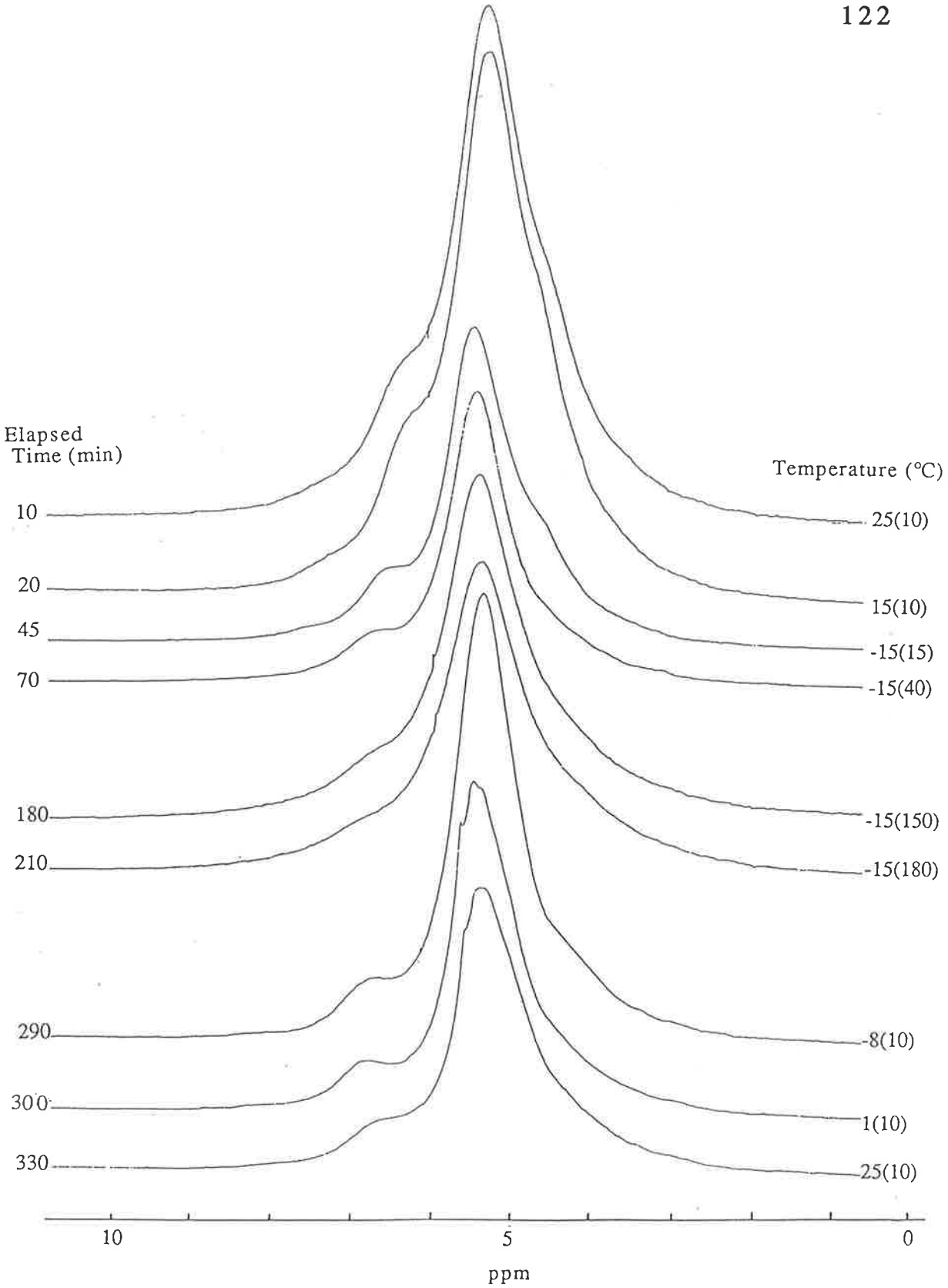

Figure 6.1. ^{1}H NMR spectra of water in PHEMA. The left hand column gives the elapsed time from the start of the experiment while the right hand column represents the temperature at which the spectra were collected with the number in brackets being the time, in minutes, the sample was held at that temperature.

6.2shows the decrease in mobile water at -15°C after normalisation (i.e the amount of mobile water measured at 25°C as the area under the NMR peak, is taken to be one).

Recently Yamada-Nosaka et al.(9) have used proton NMR to study PMMA and PHEMA membranes swollen with water. They observed that when the sheets of polymer were placed in the NMR sample tube rolled into cylinders that the water in both of the polymers showed a splitting of the proton signal with the PHEMA sample giving two peaks, slightly overlapping, of approximately the same intensity, while the water proton signal in the PMMA sample gave three peaks. However, when the polymer sheets were placed in the NMR tube parallel to the external magnetic field each sample gave a sharp signal with the PHEMA sample giving a peak similar to that found here at -15°C after fifteen minutes (Figure 6.1).

Similar results have been reported for cellulose films (10-11). Matsumura et al. (11) reported, from measurements of the angular dependance of the dipolar splitting of water in cellulose acetate films, that splitting was maximal when the surface of the film was perpendicular to the magnetic field. From this they conclude that it is due to the proton-proton dipolar axis of the water tending to be oriented perpendicular to the surface of the film. The NMR tubes here, however, were packed in a random fashion (Chapter Two) and there should have been no preferred orientation. It is also apparent that the secondary peak develops as the temperature is lowered. This apparent splitting of the water proton signal could be due to chemical exchange of protons occurring between the water and the hydroxy group of PHEMA in some domains as the sample cools, causing a shift in the proton resonance. Another possibility is that some of the water in the sample may be sufficiently mobile to still contribute to the overall signal but, as the temperature decreases, it may become slightly oriented either with the magnetic field or internal or external surfaces present in the polymer, sufficiently enough for splitting to occur and produce the

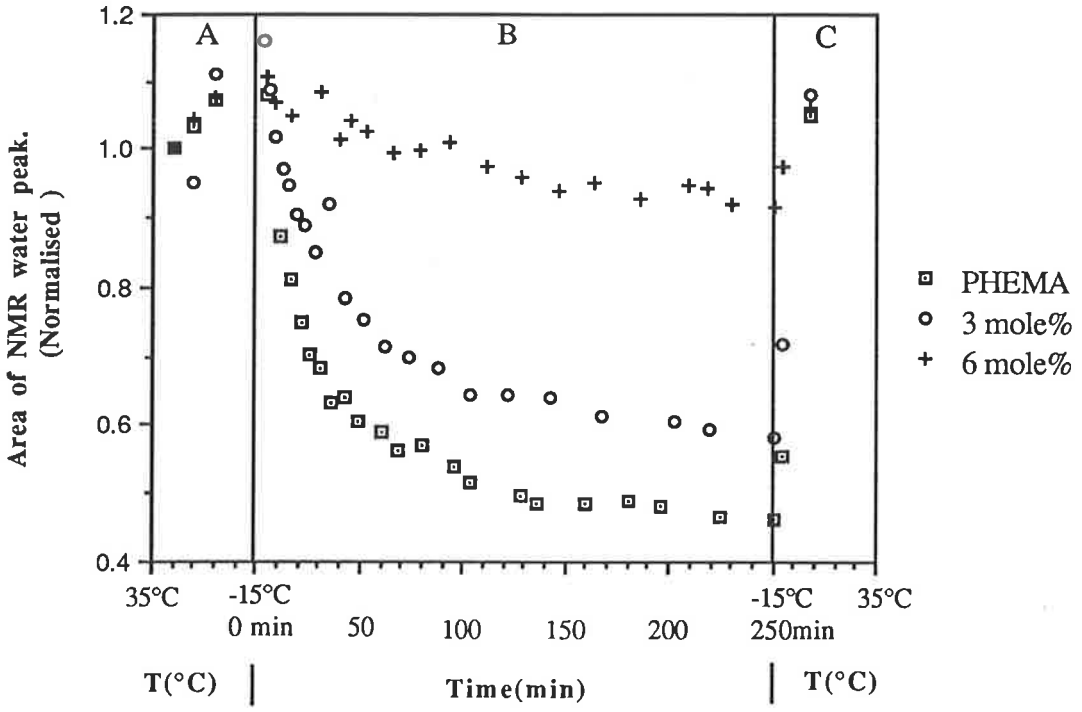

Figure 6.2. The change in the amount of unconstrained water in PHEMA and HEMA copolymers with 3 and 6 mol% EGDMA. Parts A and B give the change as a function of temperature with the sample held at each temperature for 10 minutes while part B gives the change as a function of time at a constant -15°C.

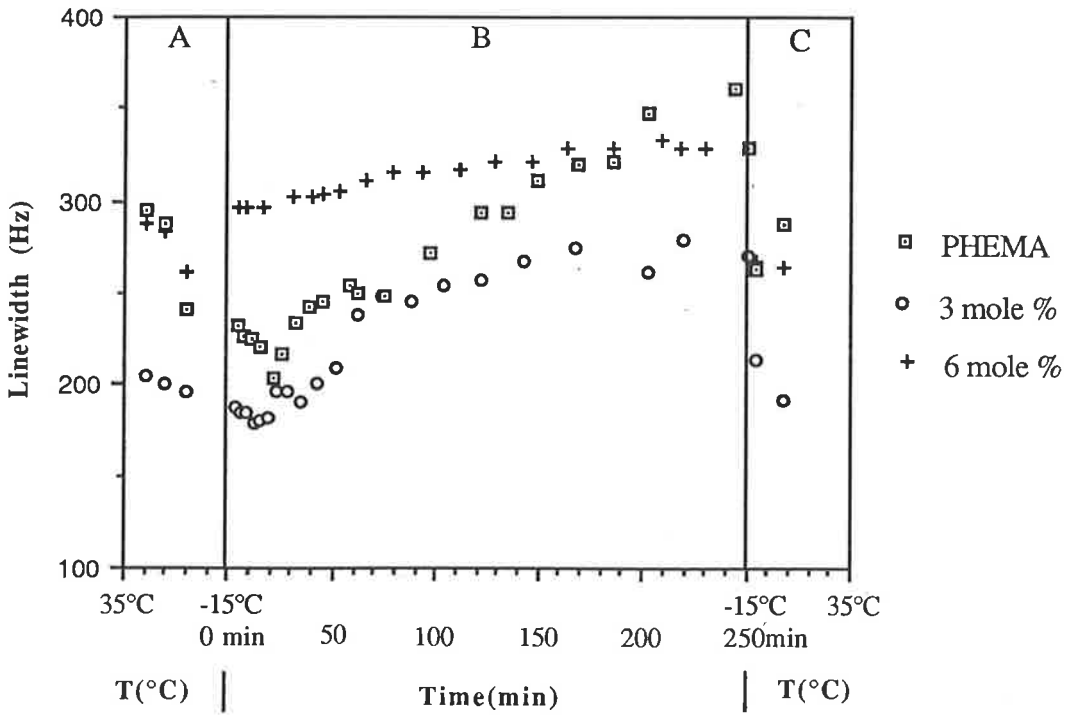

Figure 6.3. The change in the linewidth of water in PHEMA and HEMA copolymers with 3 and 6 mol% EGDMA. Parts A, B and C are as for Figure 6.2.

additional peak. As the water cools further it eventually becomes constrained and no longer contributes to the spectrum. On heating however, it again shows as a shoulder on the main peak which does not disappear, indicating that either its orientation has remained or as it has again become partially mobile it has regained its orientation. As this peak appears before the sample has been heated above the melting point of water it is also apparent that it cannot be due to freezing water.

The increase in mobile water from 25°C to 5°C is of the order of 10%. From -15C approximately 55% of the water measured at 25°C becomes constrained over a period of approximately four hours until little further change occurs.The decrease in unconstrained water (Figure 6.2) at -15°C over time was modelled using a two exponent equation, Equation 6.1;

$$W_t = A\exp(\frac{-t}{T_S}) + B\exp(\frac{-t}{T_L}) \qquad \text{Equation 6.1}$$

where W_t is the amount of water at time t, A and B are constants and T_S and T_L are time constants describing the rate of disappearance of unconstrained water over time.

This gave a good fit to the data and seems to imply that initially there are two types of water being detected by the NMR in the saturated polymer. It is possible to estimate, from the constants A and B, the amount of water in each phase by assuming that A+B represents the total amount of water being measured. From these results approximately 43 % of water is in a phase characterised by the shorter time constant, T_S with a value of 21.5 minutes while the other 57% is in a phase with a time constant, T_L, of approximately 762 minutes. This indicates that the first type is disappearing much more rapidly than the majority and accounts for the initial steep decrease of water indicated in Figure 6.2.

In order to see which type, if any, belonged to water that was freezing the temperature was raised to -8°C (Due to a tendency of the variable temperature probe to initially overshoot the desired temperature by 1 or 2 °C and possible freezing point depressions noticed in the DSC work this was taken to be the closest possible temperature attainable without the possibility of some of the frozen water melting) and the sample left to equilibrate for 10 minutes. From Figure 6.2 it can be seen that the amount of water measured increased to just under 60% of the initial value. This seems to imply that the remaining 40% was water that had frozen. This corresponds well with the amount found in the phase characterised by T_S and seems to indicate that the short time constant T_S water is water that is freezing. When the temperature was raised to 1°C all the water reappeared (Figure 6.2). Similar results were also found on heating the copolymers.

The disappearance of water characterised by T_L could be due to water either diffusing into regions where it becomes trapped and unable to tumble freely or becoming increasingly constrained due to shrinkage of the polymer or regions of the polymer, which could in turn be driven by the expansion of water that is freezing in other areas of the polymer.

The fractions of water in the slow and fast phases along with their respective time constants are tabulated in Table 6.1 as well as the results obtained from the other copolymer systems described in further detail below.

The linewidth, given here in hertz, at half peak height of the water rotn resonance gives some idea of the molecular mobility of the water molecules although there is some slight temperature dependence with the line width decreasing with temperature, but this would not account for the large scale changes observed here. The linewidth decreases (Figure 6.3) from 25°C to 5°C by about 20 % which seems to indicate that water is becoming more mobile as the temperature drops. From -15°C the line width increases with time in an almost linear fashion until it reaches a

plateau after about four hours. Again, however, as the temperature is raised to -8°C there is a large decrease in the line width indicating a freeing up of the water molecules. This is in agreement with the observation that the amount of constrained water is strongly dependent on the temperature at which the measurement takes place.

Sung et al. (12) used pulse NMR to study PHEMA and Poly(HEMA/TEGDMA) copolymers of varying water content, varying from 10 wt% to 50 wt%, and measured both their spin lattice relaxation T_1 and their T_2 values at 34 °C calculating the T_2 value from the linewidth at half maximum absorption as was done here. As would be expected they found that the T_2 values increased as the amount of water increased, indicating the water was in a more mobile environment, the values they obtained, however, are much larger than those observed for saturated PHEMA here. They found values ranging from 5 ms for the 10 wt% sample up to 35 ms for the 50 wt% samples. For comparable PHEMA/water samples here the T_2 value (using Equation 2.3) was only of the order of 1.6 ms at 25 °C. The difference is probably due mostly to the higher operating temperature at which their measurements were made. They also reported no signs of dipolar splitting of the water signal which is also probably due to the higher temperature at which spectra were collected.

6.2.1(b) HEMA/EGDMA Copolymers.

Similar experiments to those described above were performed on copolymers of HEMA with 3 and 6 mol% EGDMA

The spectra obtained for these two copolymers are shown in Figures 6.4a and 6.4b. For the 3 mol% EGDMA copolymer it can be seen that again there is a shoulder evident on the main water peak similar to that of the pure PHEMA sample. This peak, however, disappears more rapidly than that of the homopolymer and is no longer discernible after 35 minutes. The 6 mol% EGDMA sample shows no trace of a shoulder and gives only a

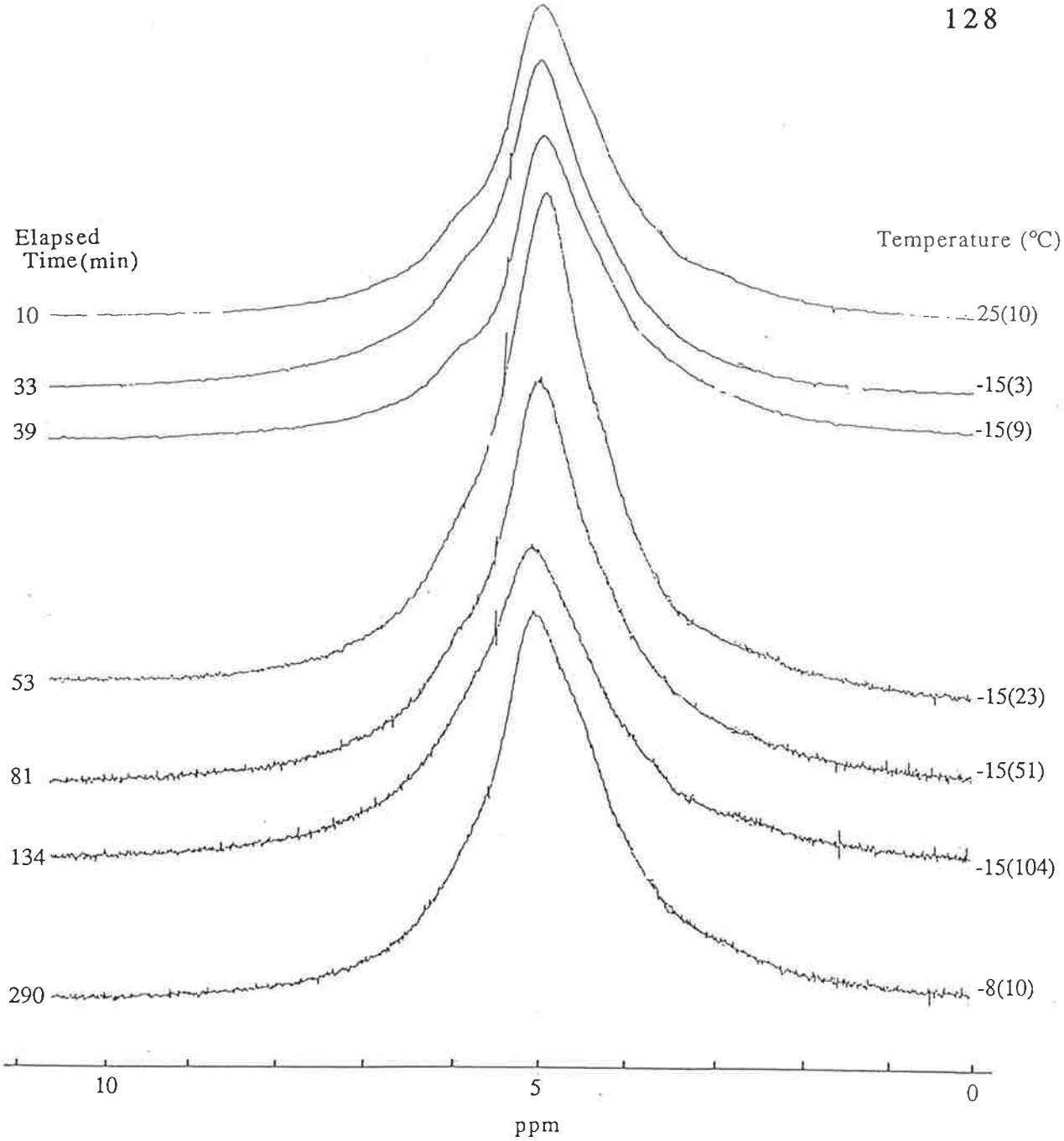

Figure 6.4(a). ^{1}H NMR spectra of water in HEMA copolymerised with 3 mol% EGDMA.. The left hand column gives the elapsed time from the start of the experiment while the right hand column represents the temperature at which the spectra were collected with the number in brackets being the time, in minutes, the sample was held at that temperature.

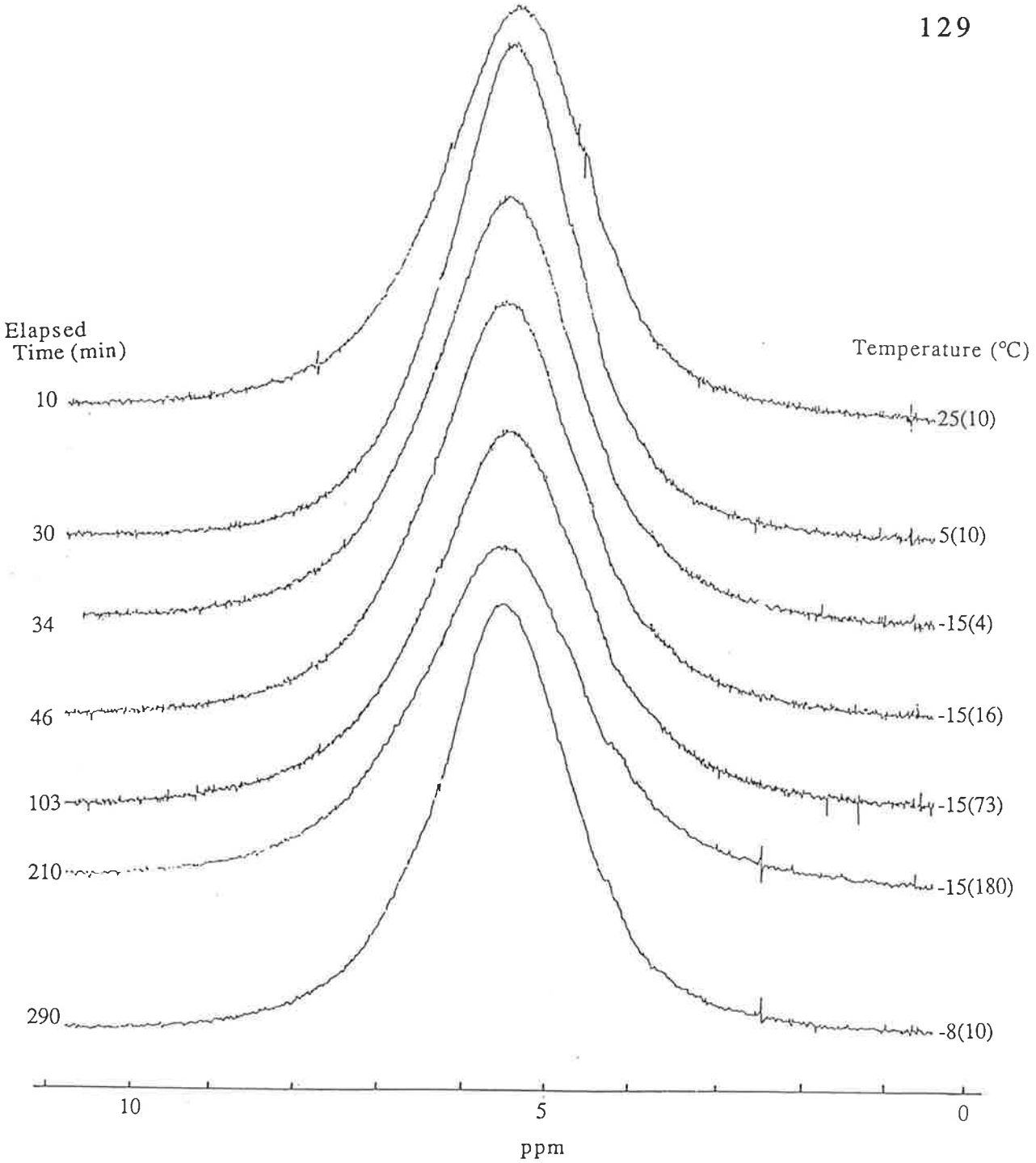

Figure 6.4(b). ^{1}H NMR spectra of water in HEMA copolymerised with 6 mol% EGDMA. The left hand column gives the elapsed time from the start of the experiment while right hand column represents the temperature at which the spectra were collected with the number in brackets being the time, in minutes, the sample was held at that temperature.

single uniform peak. This, however, might not imply that water exists in only one environment but that only one type is visible as there could be other peaks indiscernible beneath the main peak.

The decrease in mobile water is shown in Figure 6.2 for both copolymers and is compared to the result obtained for the PHEMA homopolymer. It can be seen from this that the 3 mol% EGDMA copolymer shows a similar biexponential disappearance of water but that less of the water that was measured initially eventually becomes constrained. For the 3 mol% EGDMA copolymer this decrease is to 59 % of the 25°C value while the 6 mol% EGDMA sample decreases to 95 % of its 25°C value. The proportion of water found in the T_S phase is 39 % while 61 % resides in the long T_L phase with values of T_S and T_L of 22.4 and 1040 minutes respectively. The data from the 6 mol% EGDMA sample could only be fitted to a single exponential indicating that the majority of the water resides in the long T_L water phase with a time constant of 1530 minutes - twice as long as that of the PHEMA /water system and half as long again as that of the 3 mol% EGDMA copolymer, indicating little or no freezing water present in the sample.

The linewidths calculated for the 3 mol% and 6 mol% EGDMA samples are shown in Figure. 6.3. From this it can be observed that while initially the linewidth for PHEMA and its copolymers with EGDMA are similar there is a much sharper decrease in linewidth for the 3 mol% EGDMA sample. The linewidth of this copolymer, while increasing initially at the same rate as the homopolymer levels off earlier and in fact does not increase to the same extent as the linewidth of the water in the homopolymer. The 6 mol% EGDMA sample shows only a slight initial decrease in linewidth and then remains fairly constant, increasing only slightly with time compared to the other systems. While the linewidth of the 6 mol% EGDMA copolymer is initially greater than the water/PHEMA sample the linewidth of the latter actually becomes greater than that of the

the 6 mol% EGDMA copolymer at long freezing times. When the temperature is increased there is a corresponding decrease in the linewidths of all samples.

6.2.1(c) TEGDMA/HEMA Copolymers

The spectra obtained from HEMA copolymerised with 3 mol% and 6 mol% TEGDMA are shown in Figures 6.5a and 6.5b.

The decrease in mobile water over time for both copolymers is shown in Figure 6.6. Unlike the previous 6 mol%EGDMA/HEMA copolymer both of these show a biexponential decay in the amount of water detected with the 3 mol% TEGDMA sample decreasing to 60 % of its original 25°C value while water in the 6 mol% TEGDMA copolymer decreases to approximately 69 % of its 25°C value. The 3 mol% TEGDMA sample had percentages of water in each of the two phases of 36% and 64% for the phases characterised by T_S and T_L respectively with time constants for T_S of 30.4 minutes and T_L of 930 minutes. For the 6 mol% TEGDMA sample the respective proportions of water in the fast and slow disappearing phases were 23.2% and 76.8 % with T_S and T_L being 28 and 844 minutes respectively.

The change in linewidth with time and temperature is shown in Figure 6.7. It can be seen that the 3 mol% TEGDMA sample shows a considerably narrower linewidth at all times than that of water in the homopolymer. The linewidth increases monotonically until a plateau is reached after approximately 180 minutes. The 6 mol% TEGDMA sample has a linewidth that shows a similar pattern to that of the homopolymer but again it is slightly narrower at all stages. Increasing the temperature after over 250 minutes at -15°C also produces a similar reversal in the linewidth but it does not increase to its initial value. It can be noted that for the 3 mol% TEGDMA copolymer that even after 3 hours at -15°C the linewidth was still less than the value initially obtained at 25°C.

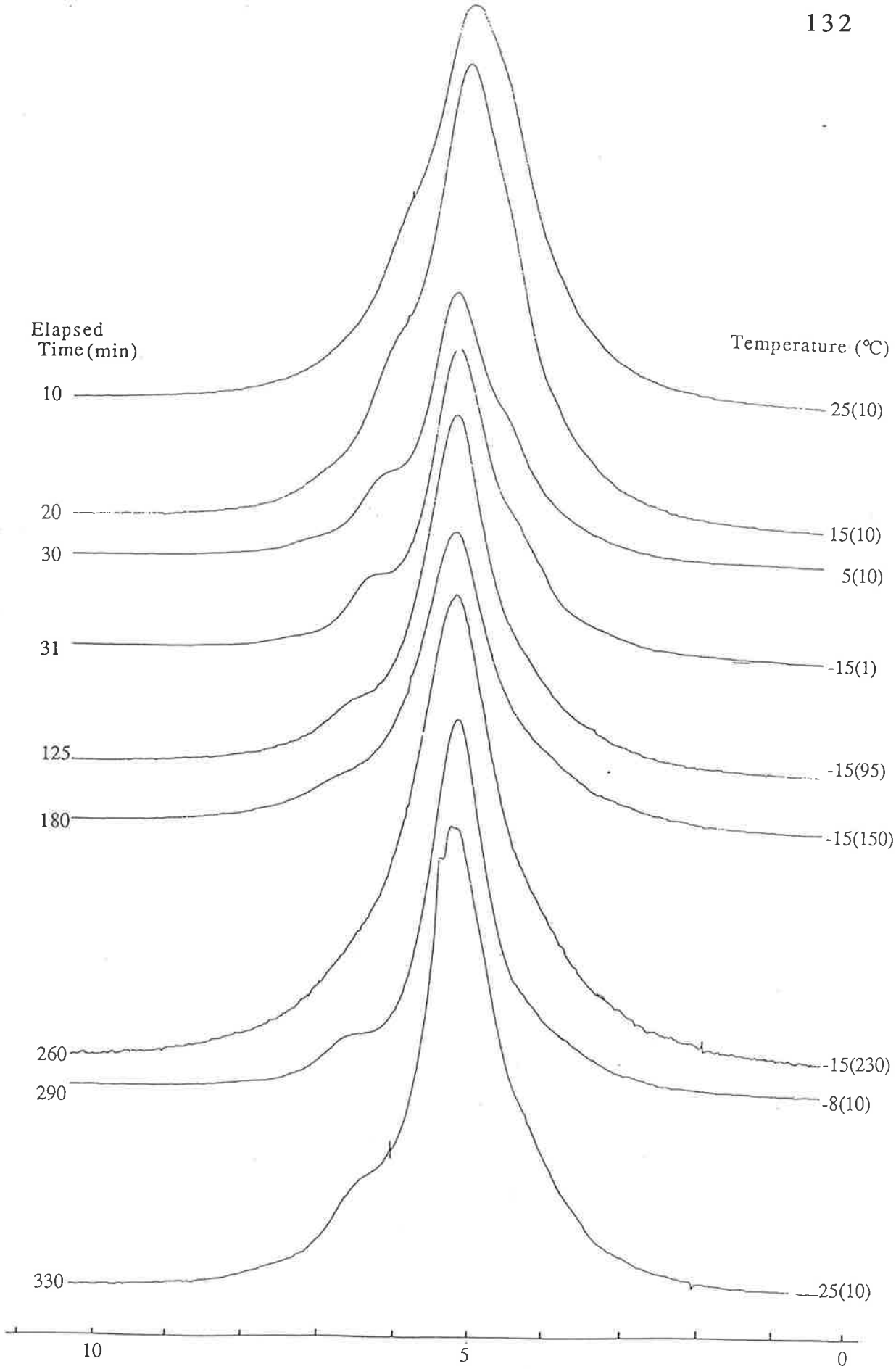

Figure 6.5(a). ^{1}H NMR spectra of water in HEMA copolymerised with 3 mol% TEGDMA The left hand column gives the elapsed time from the start of the experiment while the right hand column represents the temperature at which the spectra were collected with the number in brackets being the time, in minutes, the sample was held at that temperature.

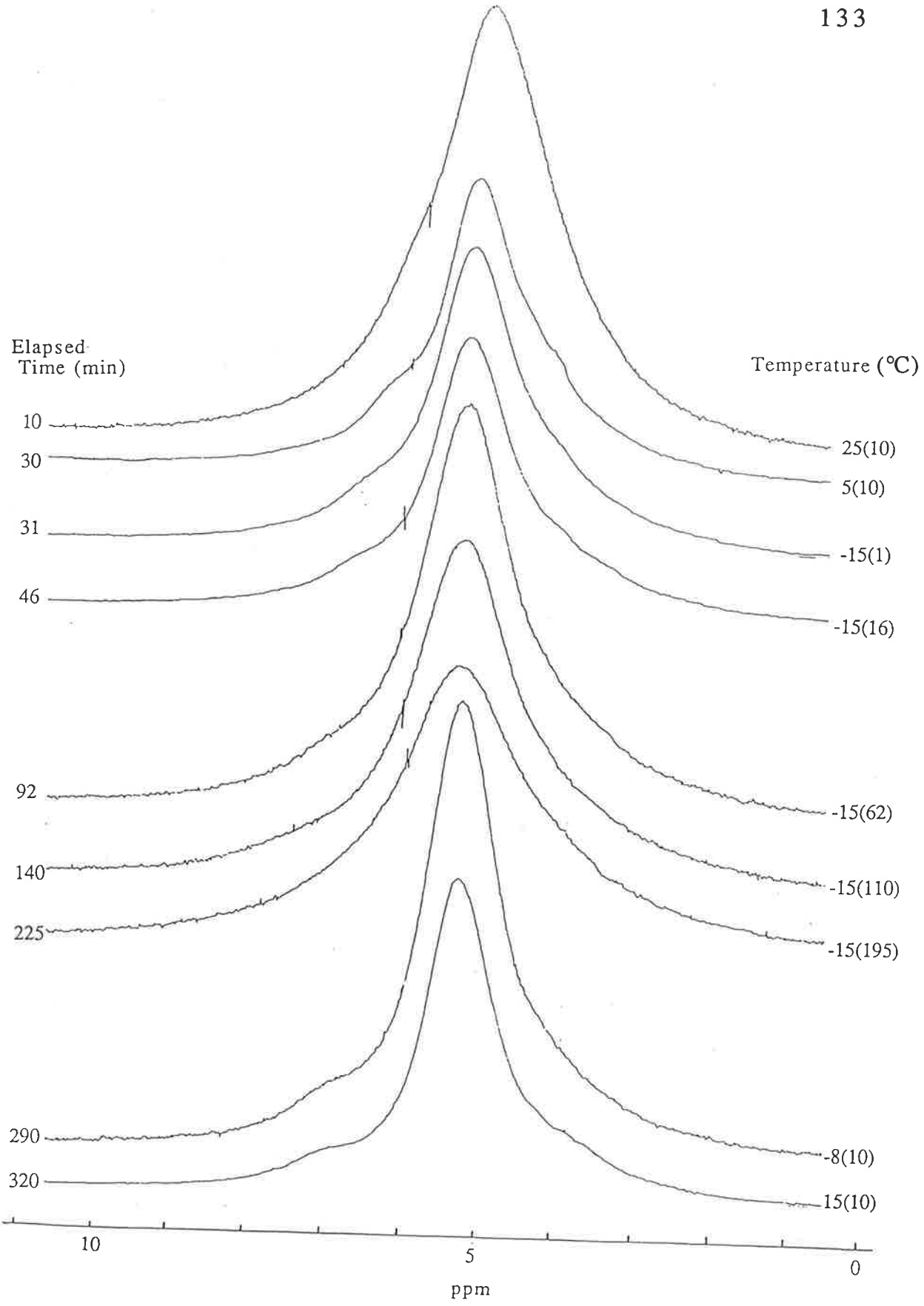

Figure 6.5(b). ^{1}H NMR spectra of water in HEMA copolymerised with 6 mol% TEGDMA The left hand column gives the elapsed time from the start of the experiment while the right hand column represents the temperature at which the spectra were collected with the number in brackets being the time, in minutes, the sample was held at that temperature.

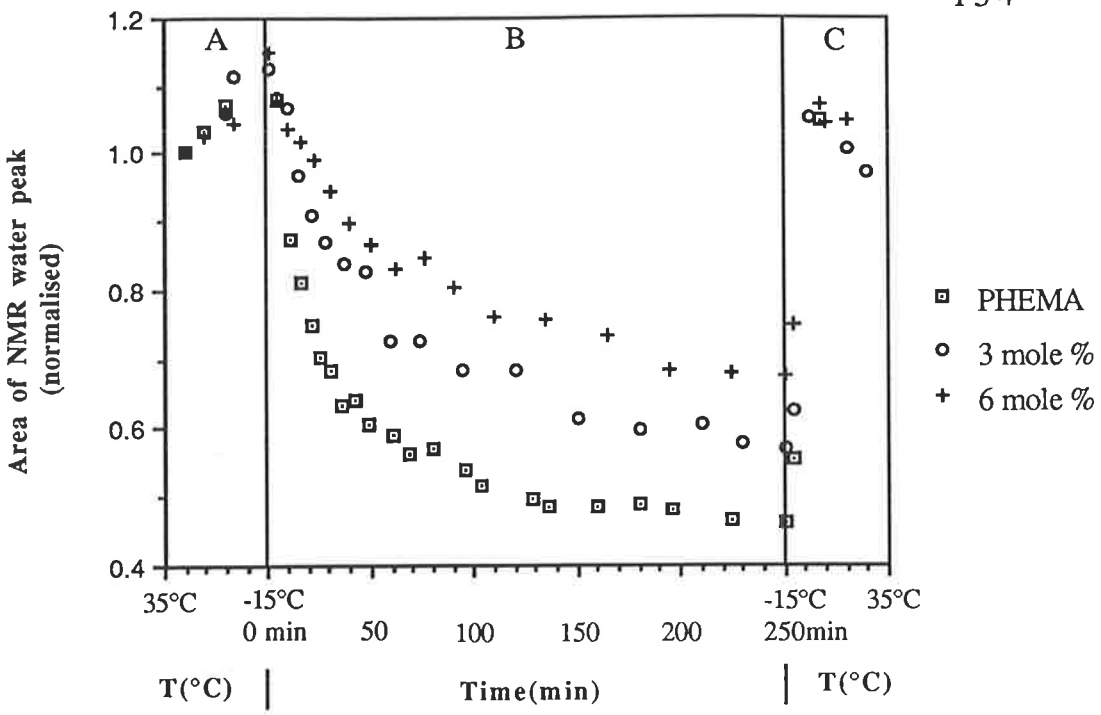

Figure 6.6. The change in the amount of unconstrained water in PHEMA and HEMA copolymers with 3 and 6 mol% TEGDMA. Parts A, B and C are as for Figure 6.2.

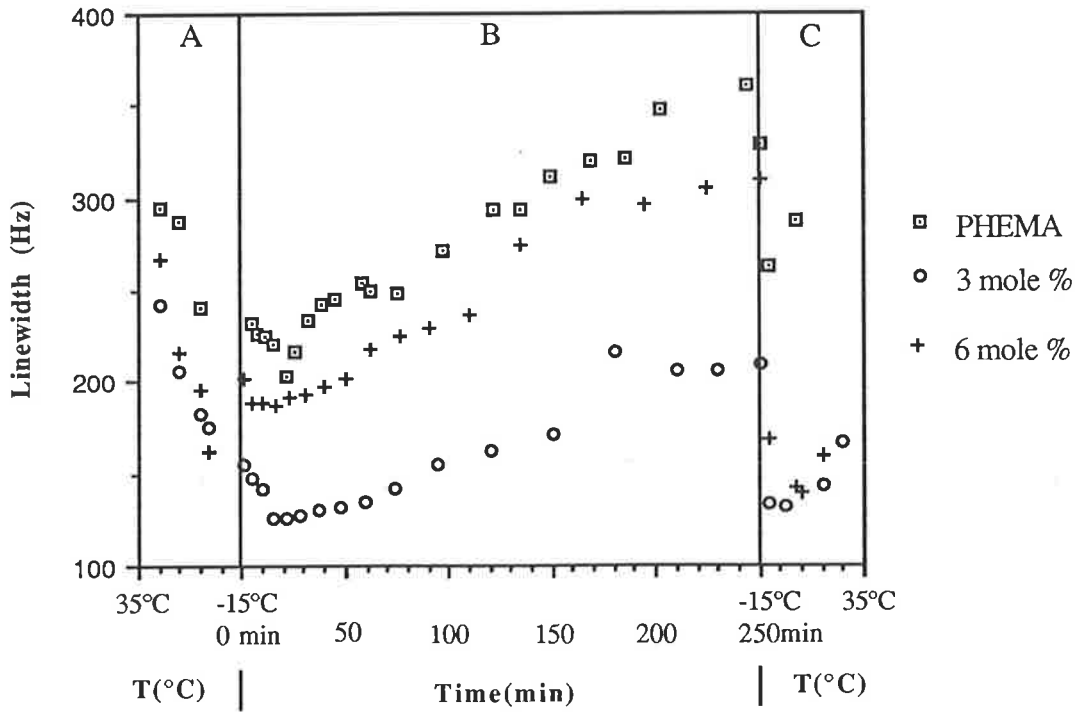

Figure 6.7. The change in the linewidth of water in PHEMA and HEMA copolymers with 3 and 6 mol% TEGDMA. Parts A, B and C are as for Figure 6.2.

6.2.1(d) MMA/HEMA Copolymers

The spectra obtained from the 10 and 20 wt% MMA copolymers are shown in Figures 6.8a and 6.8b.

The decrease in mobile water is shown in Figure 6.9. Both the copolymers show a biexponential decay in the water as the sample is frozen at -15°C. The decrease after approximately four hours, after which time it had levelled off, was to 60% and 85 % of the 25 °C level for the 10 and 20 wt% MMA copolymers respectively. The 10 wt% MMA sample showed a similar distribution to the 3 mol% EGDMA copolymer with 40.4% and 59.6% in the slow and fast phases with time constants T_S and T_L of 24.1 and 1193 minutes respectively. For the 20 wt% MMA sample the respective proportions in the slow and fast phases were 13.1 % and 86.9% with T_S and T_L being 21.9 and 1228 minutes respectively.

The changes in linewidth with time and temperature is shown in Figure 6.10. From this it is apparent that the 20 wt% MMA sample shows a similar line broadening behaviour to that of the homopolymer. The 10 wt% MMA copolymer gives a linewidth that is much narrower at all stages in the freezing process. Again there is a sharp decrease in linewidth for both samples when the temperature is increased to -8°C.

Table 6.1 indicates that the proportion of water found in the two phases is dependant not only on the EWC of the fully saturated polymer, but also the type of copolymer used and the amount of crosslinking.

The fact that water in some of the copolymers exhibit linewidths narrower than that of water in PHEMA under comparable conditions seems to indicate that while PHEMA has a much higher EWC and a greater proportion of freezable water (from the DSC measurements) the water being measured in PHEMA appears to be more constrained. This may be indicative of a smaller pore or void size in PHEMA compared to the copolymers due to the slightly higher density found for PHEMA than for

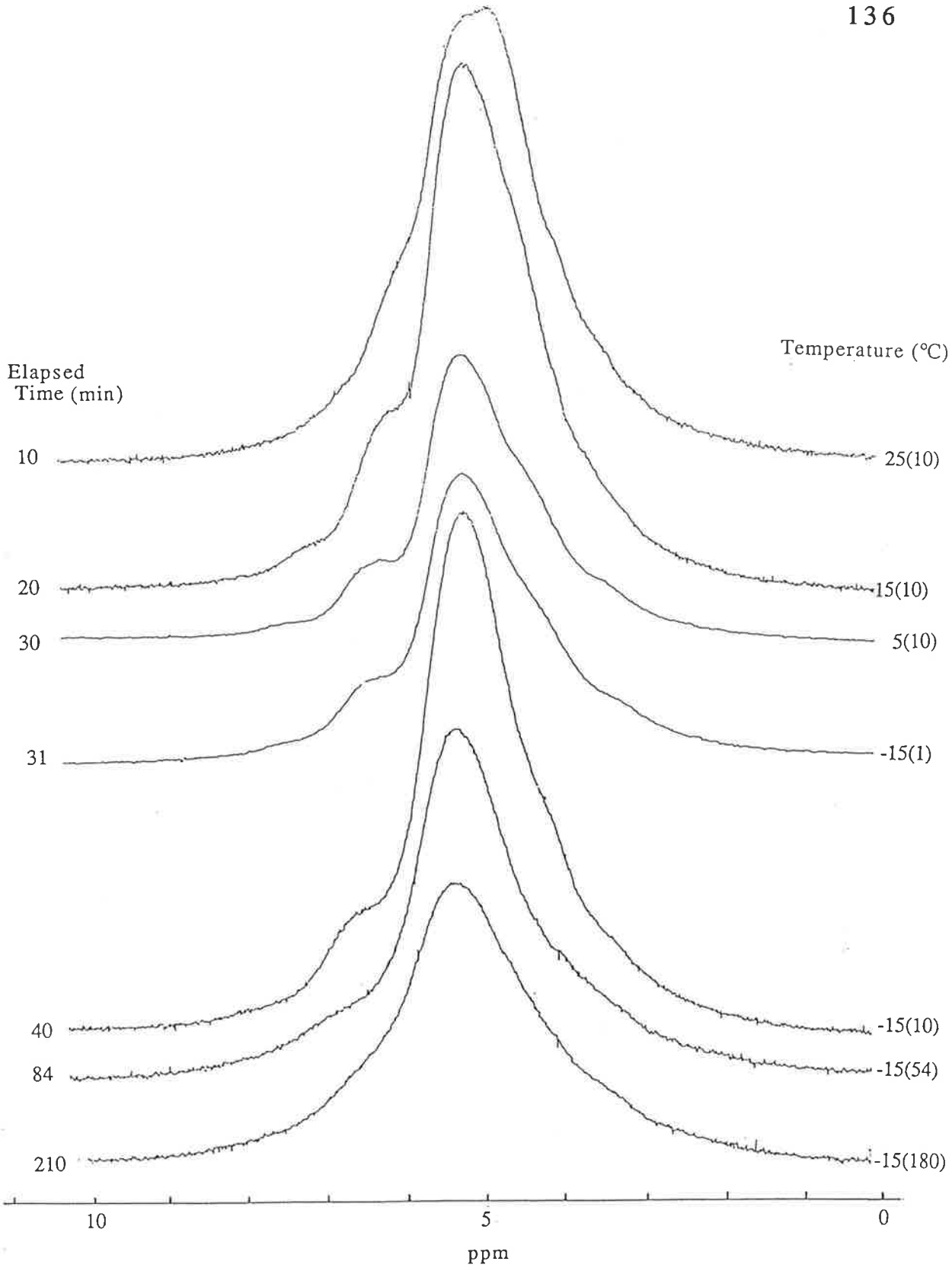

Figure 6.8(a). ^{1}H NMR spectra of water in HEMA copolymerised with 10 wt% MMA The left hand column gives the elapsed time from the start of the experiment while the right hand column represents the temperature at which the spectra were collected with the number in brackets being the time, in minutes, the sample was held at that temperature.

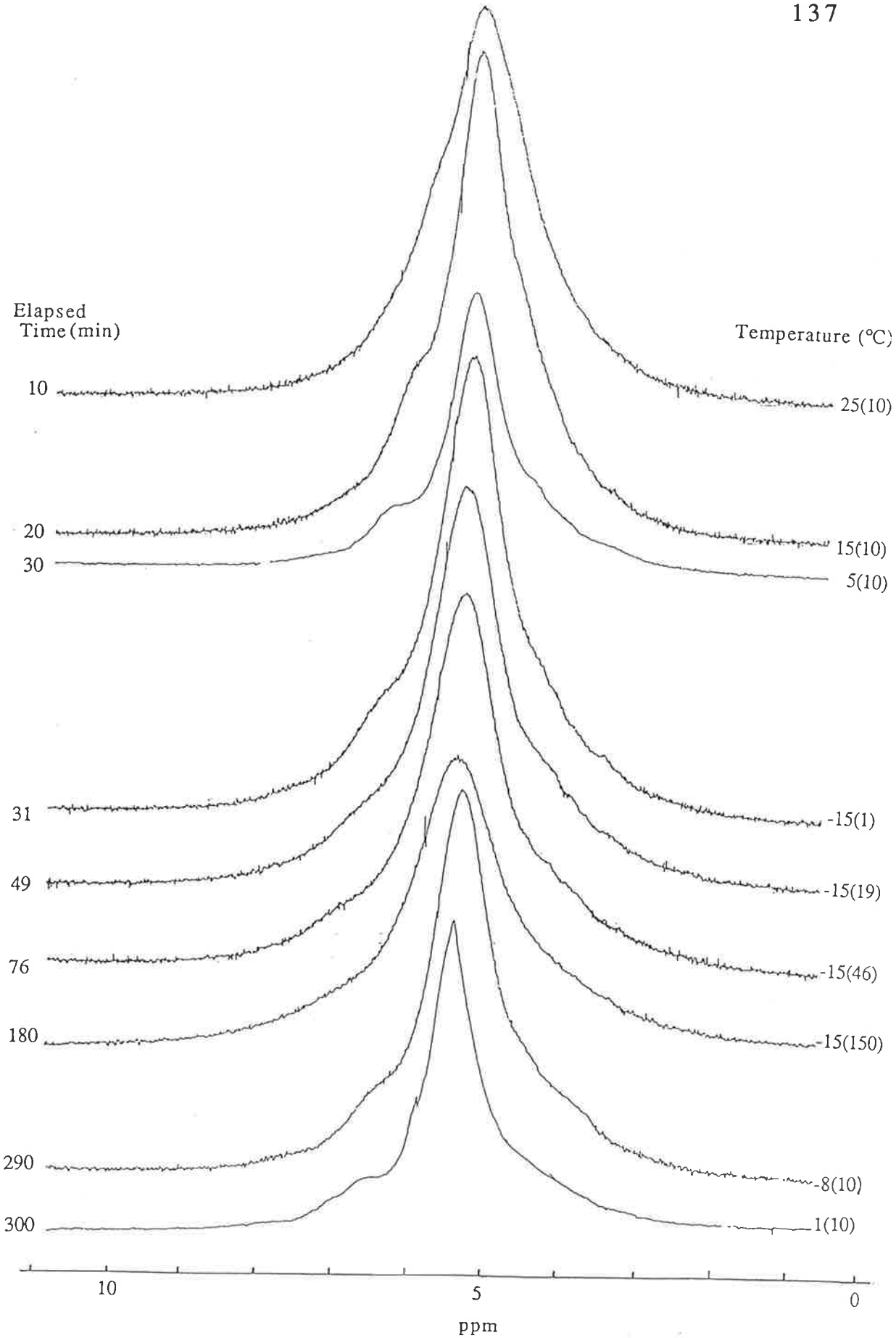

Figure 6.8(b). ^{1}H NMR spectra of water in HEMA copolymerised with 20 wt% MMA The left hand column gives the elapsed time from the start of the experiment while the right hand column represents the temperature at which the spectra were collected with the number in brackets being the time, in minutes, the sample was held at that temperature.

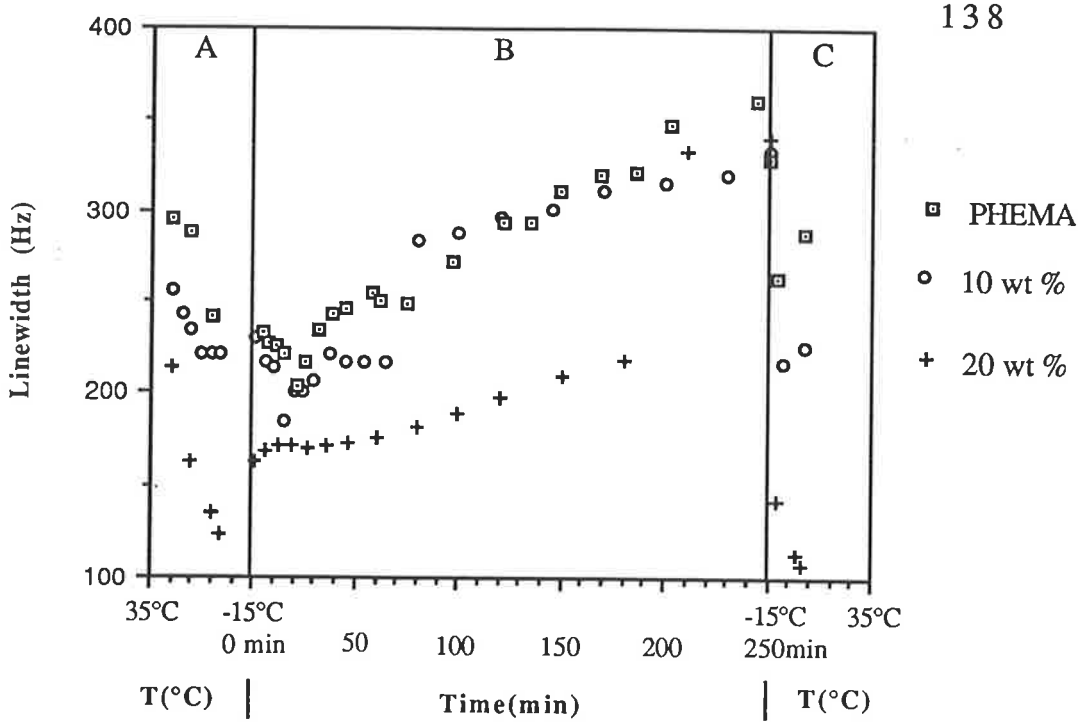

Figure 6.9. The change in the amount of unconstrained water in PHEMA and HEMA copolymers with 10 and 20 mol% MMA. Parts A,B and C are as for Figure 6.2.

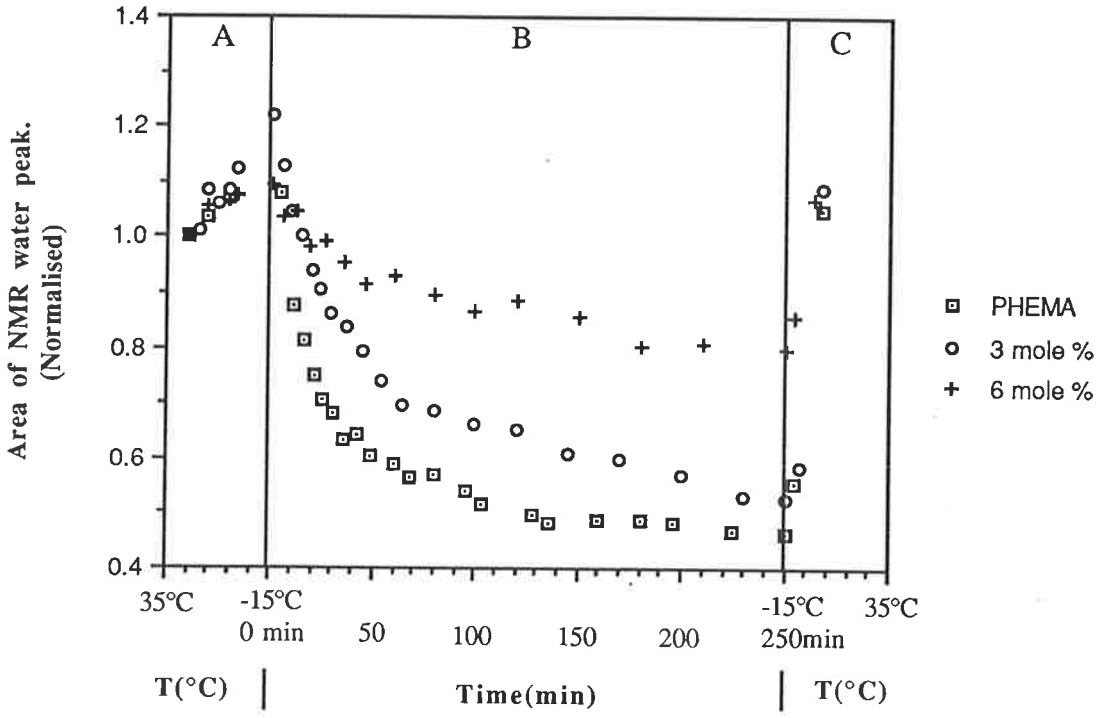

Figure 6.10. The change in the linewidth of water in PHEMA and HEMA copolymers with 10 and 20 mol% MMA. Parts A,B and C are as for Figure 6.2.

the copolymers,(Chapter Three) indicating closer packing of molecular chains.

TABLE 6.1

Percentages of water found in the two phases, A and B, characterised by T_S and T_L respectively according to Equation 6.1 for copolymers of HEMA with MMA,EGDMA and TEGDMA. Also given are standard errors calculated by the data fitting program.

% Copolymer	EWC	A	B	T_S·(min)	T_L (min)
0(PHEMA)	39.2	42.7±0.5	57.3±0.8	22±1	762±7
10%MMA	32.1	40.4±0.6	59.6±0.8	24.1±0.1	1190±10
20%MMA	24.5	13.1±0.4	87±2	22±1	1230±10
3%TEGDMA	33.7	35.7±0.6	64±1	30±2	929±8
6%TEGDMA	29.9	23.1±0.4	77±1	28±1	844±9
3% EGDMA		38.9±0.7	61±1	22.4±0.7	1039±9
6% EGDMA	23.7		100		1530±12

6.3 Correlation With DSC Results

From the DSC results given previously (Chapter Five) it was possible to calculate the amount of freezing water in the polymer. It is therefore possible using the values obtained for the relative proportions of freezing water in the polymer to calculate, in conjunction with the ^1H NMR, the proportions of mobile and constrained water in the polymers if it is assumed that the water in the phase represented by the short time constant T_S is freezing water. This is supported by the DSC measurements made at constant temperatures, in particular those made at -15°C which were fitted to a single exponential decay and gave a time constant of 25 minutes - similar to the T_S value found here (Section 5.2.2). The results are given in Table 6.2. No results are given for the Poly (6 mol% EGDMA/HEMA) copolymer as it was not possible to fit the NMR data to

Equation 4.1. This is probably due to the relatively small amount of freezing water present in the polymer as also indicated by the DSC measurements. The EWCs and freezing water contents of the copolymers of HEMA with 10 and 20 wt% MMA were obtained from results obtained by Mardel (13).

TABLE 6.2

Correlation of DSC and ^1H NMR results showing the percentage of water found in the different environments. Constrained water refers to water that is not detected by ^1H NMR. Mobile water refers to water that is initially unconstrained but does not freeze.

Mole % OED	Type of Water		
	Frozen	Mobile	Constrained
PHEMA	37%	50%	13%
3% EGDMA	7%	11%	82%
3% TEGDMA	9%	17%	74%
6% TEGDMA	3.4%	11.3%	85.3%
10% MMA	20.3%	29.9%	49.8%
20%MMA	3.9%	25.9%	70.2%

From the results given above it is apparent that PHEMA contains both the greatest percentage of freezing water and the least percentage of water that is constrained. The calculated percentages of the three different types of water correspond to 0.6 molecules of water per HEMA repeat unit of constrained water, 2.3 molecules of water /HEMA molecules of mobile water and 1.7 molecules per HEMA molecule of freezing water. The addition of a crosslinking agent had the effect of both decreasing the relative amounts of freezing water but also caused a large increase in the amounts of constrained water thereby resulting in less mobile water. The addition of a linear copolymer in the form of MMA did not have as great as an effect on either the amounts of frozen water (13) or the amounts of

constrained water even though the 20 wt % MMA/HEMA copolymer had a lower EWC than any of the crosslinked copolymers (apart from the 6 mol% EGDMA copolymer).

This compares well with the results found by Corkhill et al.(14), also using DSC techniques, for PHEMA of 2.8 molecules of non-freezing water per repeat unit compared to the 2.9 molecules of water found above (0.6 + 2.3). The much smaller percentage of constrained water found in PHEMA compared to the copolymers could be due to its greater EWC. The fact that less than one water molecule per polymer repeat unit is found to be constrained may imply that even water molecules that are hydrogen bonded to the polymer may be sufficiently mobile to be detected by ^1H NMR - in part assisted by the mobility of the polymer chains themselves, which could also explain the rapid increase in constrained water found upon copolymerisation as being due to an increase in T_g as well as there existing a more sterically confined environment. In addition the wider linewidths found for the PHEMA/water system compared to the other copolymers could be due to a greater proportion of the water being measured in this system, some of which may be only slightly mobile enough to be detected while for the other copolymers water molecules in similar environments are totally constrained.

6.4 Summary

The reduction in the amount of unconstrained water over time measured at -15°C by ^1H NMR indicated the prescence of at least two types of water in the polymer. One being water that freezes and the other unconstrained water that does not freeze but some of which does become constrained over time as the sample is frozen. These two types of water could be characterised by two time constants, T_S and T_L, with T_S representing the freezing water and being between 20 and 30 minutes and T_L being between 700 and 1500 minutes and characterising the time taken

for the unconstrained water to become constrained. The freezing water was also found to decrease on copolymerisation of HEMA with the OEDs and MMA.

In conjunction with the DSC results it was possible to assign water to three disinct regions- freezing water, water that does not freeze but is unconstrained and constrained water. Copolymerisation of HEMA with any of the OEDs was found to cause a large increase in the amount of constrained water but this increase was not as great when HEMA was copolymerised with linear MMA suggesting that the increase in constrained water is primarily due to crosslinking.

CHAPTER SEVEN

SOLID STATE NMR

7.1 Introduction

PEMAS NMR techniques, as described in Chapter Two, were used to measure the $T_{1\rho}(C)$ relaxation times of PHEMA, both dry and hydrated to different EWCs, and a range of dry and hydrated copolymers of PHEMA with EGDMA and MMA. T_{SL} and $T_{1\rho}(H)$ measurements were also made on a number of these polymers.

7.2 Results and Discussion

The PEMAS ^{13}C NMR spectrum of dry PHEMA is shown in Figure 7.1. The peak assignments are given based on previous assignments from PEMAS spectra of PMMA, PEGDMA and PTEGDMA (1-4) and the liquid spectra of HEMA (5).

The effect of absorbed water on the spectrum of PHEMA can be seen in Figure 7.2. This shows the spectrum of PHEMA with an EWC of 39% The number of scans used in acquiring this spectrum is approximately ten times that required for the dry sample but it can be seen that the spectrum shows considerably less resolution with a poor signal to noise ratio. As the EWC increases the acrylate CH_2 peak becomes less prominent and in some cases, at extremely high water content, becomes indistinguishable from the background noise and it is not possible to obtain T_{SL} or $T_{1\rho}(C)$ times for that carbon. Standard deviations, as determined from the DATAFT program (6), also increased significantly due to the decrease in resolution. As the PHEMA and PHEMA copolymer samples were run as powders and the spinning rate of the rotor was of the order of 3000 Hz there was also a problem due to water being desorbed from the more highly saturated samples if measurements were made over a lengthy

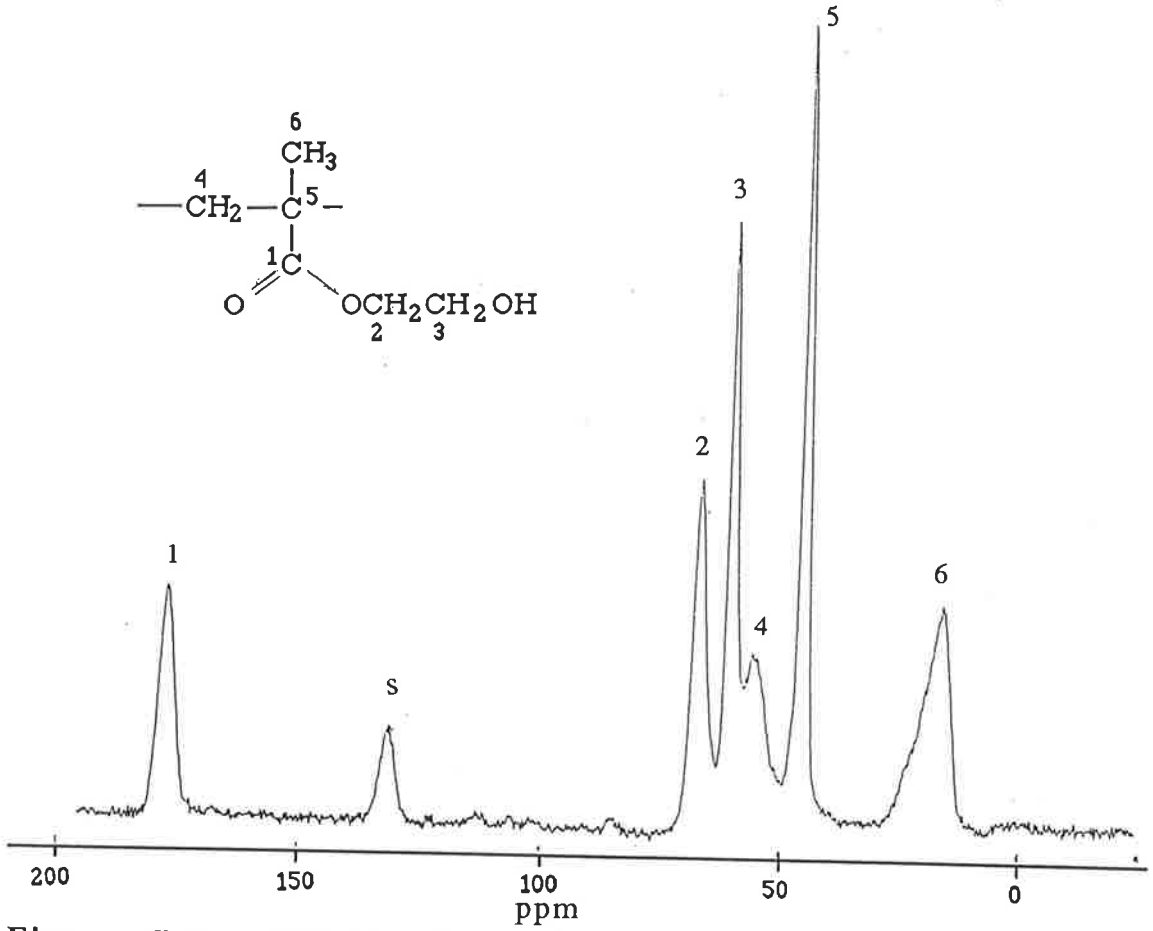

Figure 7.1 PEMAS ^{13}C NMR spectrum of dry PHEMA. Peak assignments are given above and s refers to spinning sidebands.

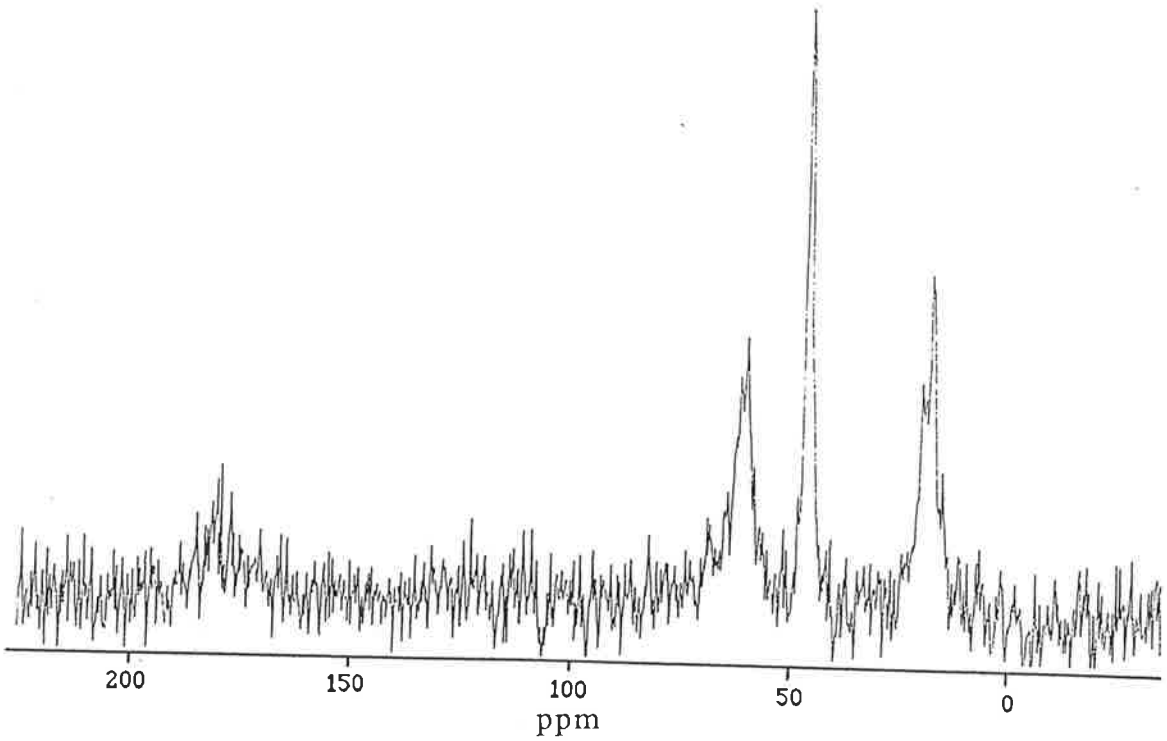

Figure 7.2 PEMAS ^{13}C NMR spectrum of fully hydrated PHEMA. The number of scans used in collecting this spectrum was approximately ten times those used for the spectrum shown in Figure 7.1.

period of time (three to four hours) and so it was necessary to achieve a balance between increasing the resolution and minimising water loss. Therefore the acquisition of data was limited to approximately three hours. This was sufficient time to achieve good resolution on all peaks, except the acrylate CH_2, and to minimise water loss in even the most saturated samples to less than 5% of the total water present. The EWCs referred to later are the initial EWCs of the samples.

The decrease in resolution due to absorbed water is probably due to the increased chain mobility of the polymer due to the plasticising effect of the water which will reduce the static dipolar interactions necessary for efficient cross polarisation. There is also a decrease in the actual amount of PHEMA in the rotor due to the presence of absorbed water.

7.2.1 $T_{1\rho}(C)$ Dispersions

A plot of the intensity vs time for the quaternary carbon of dry PHEMA is shown in Figure 7.3. The experimental data was fitted to Equation 7.1 using the DATAFT program.(6)

$$I_{OBS}=\sum_{i=1}^{n} I_i \exp\left(\frac{-\tau}{T_{1\rho}(C)_i}\right) \qquad \text{Equation 7.1}$$

where I_{OBS} is the observed intensity, τ the delay time, I_i are pre exponential factors and $T_{1\rho}(C)_i$ various relaxation times. Figure 7.3 shows the results obtained for the quaternary carbon of dry PHEMA and the attempted fit of Equation 7.1 to the data with n=2. It was generally found that the best fit was to a double exponential (n = 2) equation in most cases. Attempts to fit the data with n > 2 resulted in increased standard deviations and increasing difficulty in achieving a fit as the number of experimental parameters rose.

The fit of the data to a multi-exponent equation indicates the possibility of a multiplicity of relaxation times (7). This has been noted in $T_{1\rho}(C)$ measurements made on a number of different polymers (8-10). Dickinson (8) et al. found biphasic decay of carbon intensities with α,ω dihydroxypoly(propylene oxide) (PPO) cross-linked with tris (4-isocyanatophenyl) thiophosphate, (TIPTP) although they found only single exponential decay for linear poly urethanes. Other work on glass filled poly amide 6 composites(9) and model urethane elastomers (10) also found biphasic decay which was attributed to soft and hard phases or segments in the polymers. Schaefer et al. (12), however, has noticed that a dispersion of $T_{1\rho}(C)$ relaxation times exists in some glassy polymers that are nominally homogeneous, single phase systems as well as, as might be expected, for mixed phase systems in which the different component phases have significantly different motional properties described by significantly different relaxation times. This is ascribed to the inherent dynamic heterogeneity of the polymer glass. Schaefer (12) proposes that the local flexibility of a main chain carbon is not only dependent on the configuration of the repeating units nearest to it in the chain but also on more distant units in the chain by connected pair-wise interactions. This produces a pronounced heterogeneity in dynamic environments in which a given carbon may be in any of a multiplicity of different states which leads to a range of relaxation times.

These interactions are presumed to be primarily intrachain in nature but there is some evidence (12) of interchain steric interactions as well and Schaefer et al. propose that some of the short relaxation time components of the $T_{1\rho}(C)$ dispersion can be assigned to more disordered regions of the glass. As PHEMA is an amorphous glassy polymer at room temperature it can be assumed that the short $T_{1\rho}(C)$ times can be assigned to the dynamic heterogeneity in the polymer rather than the existence of two distinctly different phases. Unfortunately it was not possible here to place any

significance on the short relaxation times as the standard deviations calculated were often of the order of the relaxation time itself and as the polymer became more rubbery the frozen configurations and conformations, which give rise to the $T_{1\rho}(C)$ dispersion can more rapidly interconvert which, at high water content meant that, in some cases, only a single exponential fit was required and no short $T_{1\rho}(C)$ observed. It is also not possible to place any relevance on the relevant intensities observed as both the magnitude and intensity of the $T_{1\rho}(C)$ decay may be affected by spin diffusion and therefore the component intensities of such systems bear no direct relationship on the number of resonant nuclei contributing to the individual decay terms (9).

7.2.2(a) $T_{1\rho}(C)$ Times For PHEMA at Varying EWCs.

The $T_{1\rho}(C)$ relaxation times for wet and dry PHEMA are given in Table 7.1 along with their standard deviations. All errors cited are standard deviations estimated from the r.m.s. deviation of fit. In some cases, particularly at high EWC it was not possible to obtain a reasonable fit of the data to either a single or double exponent equation.

Repeat runs on samples with the same EWC showed a difference between measurements of less than 10%. When more than one measurement was made the average value was used.

It can be seen from Table 7.2 and Figure 7.4 that the quaternary and carbonyl carbons show the greatest change in $T_{1\rho}(C)$ times with increasing hydration. From dry to fully hydrated the carbonyl value decreases to approximately one-seventh of its original, with a twelve fold decrease in the quaternary.The acrylate CH_2 decreases by a factor of two up to 18 % EWC, which is a slightly greater decrease than the carbonyl or quaternary carbons but at EWCs higher than this it was not possible to resolve this carbon adequately enough to be able to measure its $T_{1\rho}(C)$. The two hydroxy ethyl carbons have nearly identical relaxation times and

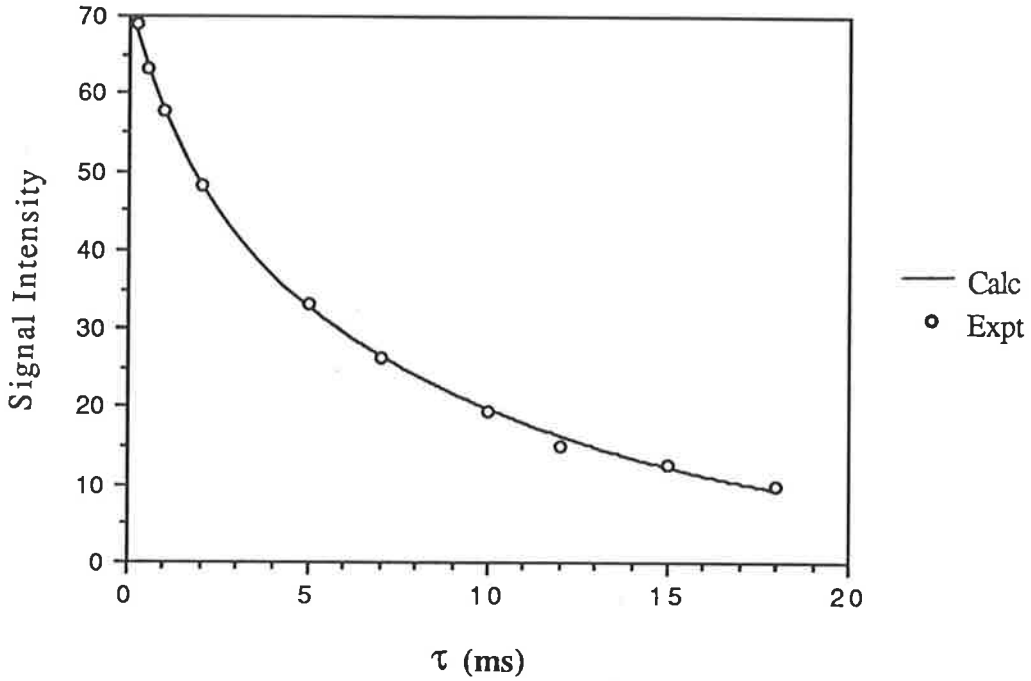

Figure 7.3. Fit of $T_{1\rho}(C)$ experimental data to Equation 7.1 for the quaternary carbon of dry PHEMA.

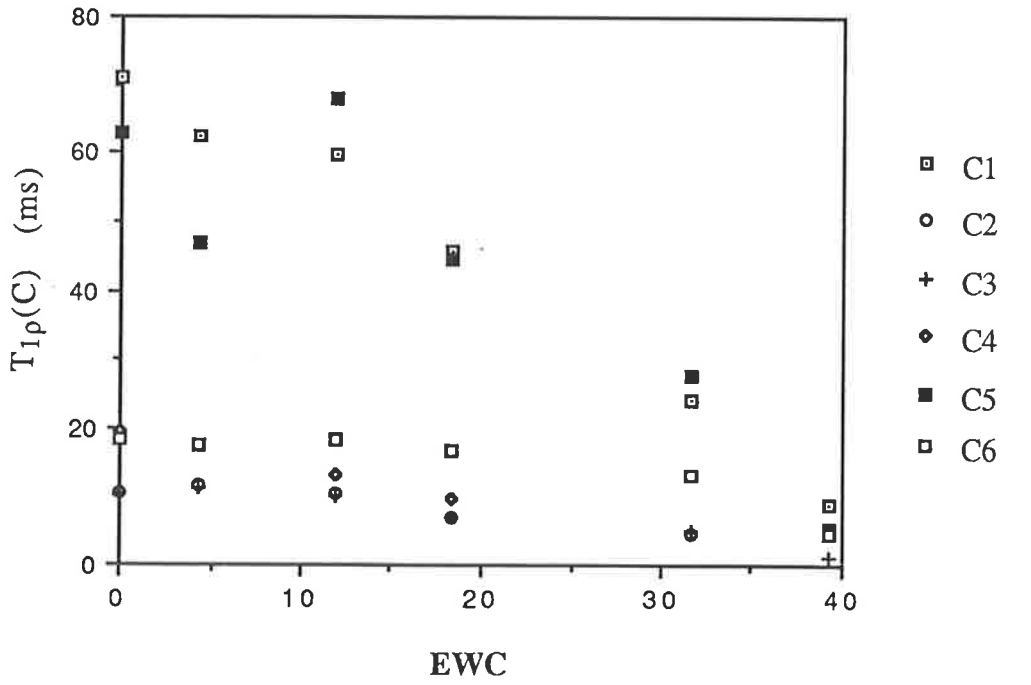

Figure 7.4 $T_{1\rho}(C)$ times for PHEMA at different EWCS. C1-C6 are as designated by Table7.1.

decrease at similar rates. The $T_{1\rho}(C)$ of the α-methyl remains nearly unaffected by the increasing water content up to 18% EWC but then decreases to approximately a quarter of its original value at full hydration.

TABLE 7.1

$T_{1\rho}(C)$ times for PHEMA with varying EWC. C1-C6 refer to the carbonyl, β-hydroxy ethyl, α-hydroxy ethyl, acrylate CH_2, quaternary and α-methyl carbons respectively as indicated in Figure 7.1.

	$T_{1\rho}(C)$ (ms)					
EWC	C1	C2	C3	C4	C5	C6
0	70.9 ±5.2	10.7 ±0.8	10.54 ±0.5	19.37 ±1.3	62.91 ±5.0	18.24 ±1.1
4.4	62.3 ±7.6	11.7 ±0.7	11.18 ±0.6	17.7 ±1.1	46.85 ±5.4	17.75 ±0.9
11.9	59.7 ±3.4	10.43 ±0.5	10.3 ±0.5	13.2 ±1.4	67.98 ±4.5	18.49 ±0.8
18.4	45.5 ±8.1	6.99 ±0.9	6.89 ±0.7	9.81 ±1.4	44.3 ±3.7	16.65 ±1.6
31.7	24.2 ±5.3	4.83 ±4.0	5.2 ±1.0	*	27.8 ±3.6	13.4 ±1.3
39.2	9.1 ±3.3	*	1.18	*	5.34 ±1.3	4.83 ±1.4

*-not possible to fit the data to the relevant equation.

One factor that must be taken into account when evaluating $T_{1\rho}(C)$ measurements is that both spin-spin and spin-lattice processes can contribute to the relaxation mechanism (12,13,15-17). The spin-lattice relaxation is related to the molecular dynamics of the polymer system, the spin-spin process, however, is caused by fluctuations in dipole fields generated by changes in the spin state of protons close to carbons and is therefore not influenced by molecular dynamics. The possibility of spin-spin processes influencing the $T_{1\rho}(C)$ times occurs due to the necessity of the carbon field being close to the local dipolar fields in order to be sensitive to mid kHz motions. Flemming et al. (17-18) measured the T_1

and $T_{1\rho}(C)$ times at a number of relaxation frame to frequencies and temperatures and found for polypropylene and PMMA systems at subambient temperatures that spin-spin interactions dominate the relaxation process. Schaefer and others, however, conclude (12-15) that for amorphous polymers, such as polystyrene, PMMA, poly(phenylene oxide), poly(ethylene terephthalate) and polycarbonate, that, at room temperature, the $T_{1\rho}(C)$ is dominated by spin-lattice like processes and can therefore be taken as an indication of the molecular mobility of the carbon atoms in the polymer. This conclusion seems to be supported in this case as the $T_{1\rho}(C)$ times decrease as the sample becomes increasingly rubbery with a concomitant increase in mid kHz motions which enables a more efficient relaxation of the ^{13}C magnetisation and therefore a shorter relaxation time.

It has also been observed that the α-methyl group may dominate the relaxation of other functional groups (17-18). Flemming et al. found a minima in T_1 and $T_{1\rho}(C)$ times due to α–methyl rotation and reorientation which suggests that the methyl group dominates the relaxation of other functional groups in the polymer. This hypothesis does not seem to be supported by these results. There is a significant decrease in the quaternary and carbonyl values by nearly a factor of ten while the methyl group remains largely unaffected. Other work by Allen et al. (20) also fails to notice the methyl group dominating the relaxation. They found that as TEGDMA cures $T_{1\rho}(C)$ lengthened by seven fold at the quaternary, four fold at the methyl, 3 fold at CH_2O and doubled at the inner CH_2O and conclude that the drastic effects observed with $T_{1\rho}(C)$ relaxation of other groups is not a manifestation of changes in α–methyl motion, which could be due to α-methyl rotation being not greatly affected by changes in network mobility in the frequency range (60 kHz) and therefore cannot be responsible for changes in the other groups.

Measurements made by Belfiore (19) have found that added plasticiser acts by releasing mid kHz components of group mobility of

polycarbonate while the addition of antiplasticisers such as diphenyl phthalate caused little change in T_g. The addition of diluents such as dibutyl phthalate caused the T_g to decrease with a concomitant decrease in $T_{1\rho}(C)$ in the 50-60 kHz range. While $T_{1\rho}(C)$ did decrease with increasing EWC, and therefore decreasing T_g, no large scale effect was noted here until the T_g of the hydrated polymer fell below the operating temperature of the NMR probe (298 K). This is in agreement with the measurements made by Dickinson et al. (8) on cross-linked PPO and poly urethanes and seems to indicate that the sensitivity of NMR to local and small motions makes the T_g measured by NMR difficult to compare with a T_g measured by more mechanical means.

It must be noted, however, that when looking at $T_{1\rho}(C)$ it is not possible from looking at the magnitude of $T_{1\rho}(C)$ alone to distinguish between small amplitude motions in tune with the frequency of the observational window or large amplitude motions somewhat out of tune. This implies that if qualitative comparisons are to be made between results the measurements must be made at similar spin lock frequencies.

7.2.2(b) $T_{1\rho}(C)$ Times for HEMA/EGDMA Copolymers

A series of copolymers of HEMA with EGDMA were prepared as described previously (Chapter Two). The ^{13}C PEMAS spectrum of PHEMA with 14 mol% EGDMA is shown in Figure 7.5. A comparison of this with the spectrum of PHEMA (Figure 7.1) shows no discernible difference between the two spectra due to the coincidence of the EGDMA peaks with those of PHEMA. The only group in EGDMA which does not occur in PHEMA is the oxyethylene group whose resonance is overlaid by that of the α–hydroxy ethyl carbon.

The $T_{1\rho}(C)$ times are given in Table 7.2. From this and Figure 7.6 it can be seen that there is a general increase in $T_{1\rho}(C)$ for all moeities with an increasing amount of crosslinking. The carbonyl and quaternary carbons

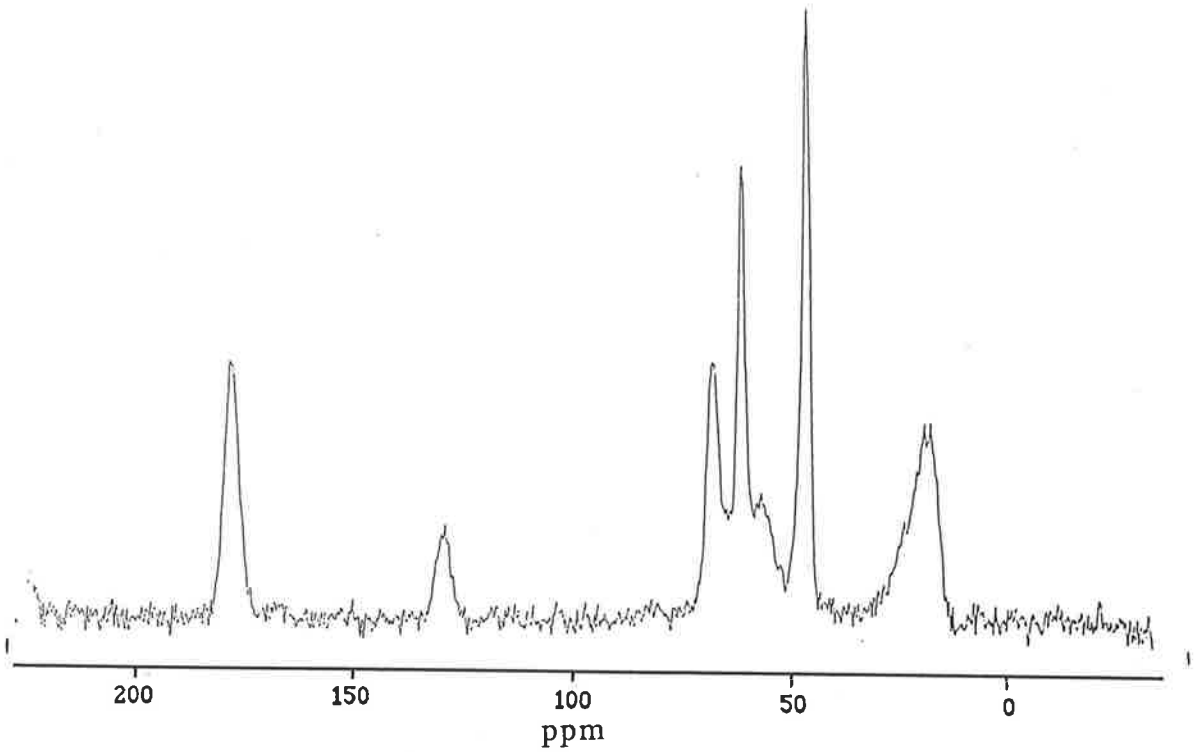

Figure 7.5 PEMAS ^{13}C NMR spectrum of a dry copolymer of HEMA with 14 mol% EGDMA. Peak assignments are the same as given for PHEMA (Figure 7.1)

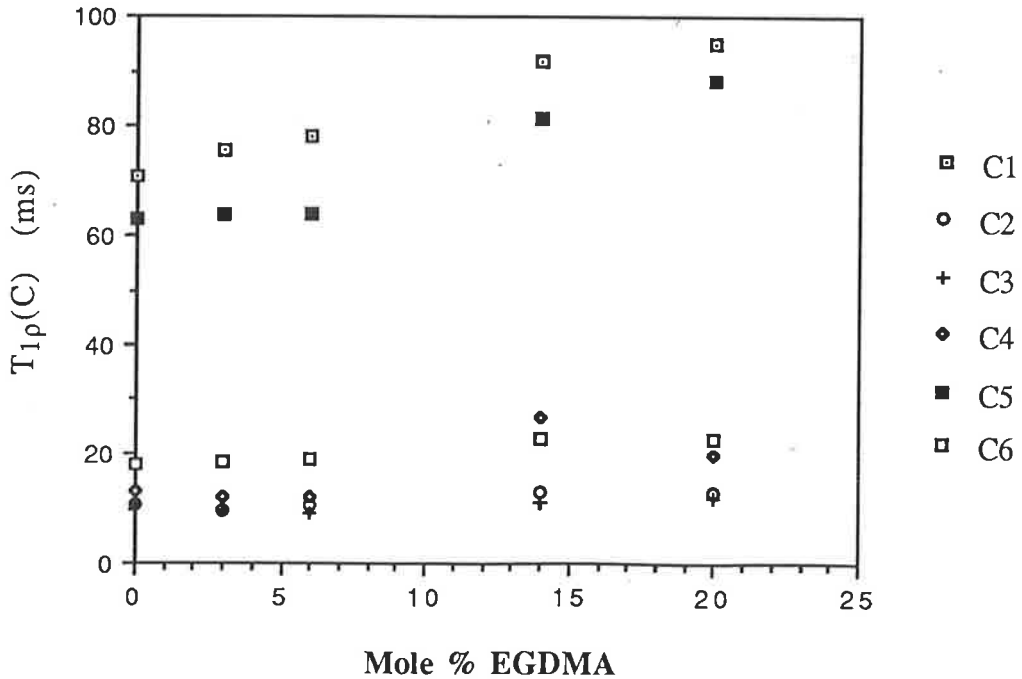

Figure 7.6 Change in $T_{1\rho}(C)$ times for copolymers of HEMA with EGDMA. C1-C6 as before.

show an increase with the addition of 14 mol% EGDMA of approximately 35 % and 40 % respectively from the homopolymer values. There is also a large increase in the acrylate CH_2 value which, when taken into account with the increase in the quaternary carbon seems a strong indication of a considerably stiffer, less mobile polymer backbone. The hydroxy ethyl and α–methyl carbons all increase slightly. Attempts to fit the data to a three exponent equation to investigate the possibility of distinct hard and soft phases developing due to the addition of EGDMA did not succeed (i.e In general a fit to the data could not be found,but if one was found the standard errors were generally a number of orders of magnitude greater then the calculated relaxation times). This could be taken as an indication that the copolymers are homogeneous.

TABLE 7.2
$T_{1\rho}(C)$ times for PHEMA crosslinked with EGDMA. C1-C6 as before.

	$T_{1\rho}(C)$ (ms)					
Mole% EGDMA	C1	C2	C3	C4	C5	C6
0	70.9 ±5.2	10.7 ±0.8	10.5 ±0.5	13.1 ±1.3	62.9 ±5.0	18.2 ±1.1
3	75.8 ±4.3	9.9 ±0.6	9.7 ±0.7	12.0 ±1.0	64.0 ±4.8	18.6 ±2.2
6	78.1 ±10.6	10.8 ±0.5	9.2 ±0.4	12.1 ±0.9	63.7 ±6.7	19.2 ±2.8
14	91.9 ±10.2	12.9 ±1.2	11.1 ±0.4	27.1 ±4.4	81.7 ±5.6	23.1 ±1.3
20	95.0 ±11.2	13.3 ±1.0	12.2 ±0.7	20.1 ±2.1	88.2 ±±10.8	22.8 ±3.4

These increases in the relaxation times, particularly in the main chain carbons, seem to point to a damping of molecular motion in the frequency range observed which is consistent with the observed increase in T_g with the addition of EGDMA. Extrapolation of these results to 100%

EGDMA gives an approximate $T_{1\rho}(C)$ for the carbonyl of 140 ms. This is considerably greater than that observed by Simon (2) of 68 ms also at 60 kHz. It has been suggested, however, that the $T_{1\rho}(C)$ of EGDMA is retarded by the presence of residual trapped monomer, which could be between 10-15%. This is supported by the fact that Poly(TEGDMA) while being more flexible (20), has little or no residual unsaturation and has a carbonyl $T_{1\rho}(C)$ of 140 ms

7.2.2(c) $T_{1\rho}(C)$ Times for HEMA /EGDMA Copolymers of Varying EWCs

The $T_{1\rho}(C)$ relaxation times were measured for a series of partially hydrated copolymers of HEMA with 6 mol% and 14 mol% EGDMA. The resulting values are given in Tables 7.4 and 7.5 and graphically in Figures 7.7 and 7.8.

For the 6 mol% EGDMA sample the carbonyl and quaternary again show the most significant effect with a five fold decrease of the carbonyl and a halving of the quaternary $T_{1\rho}(C)$ from dry to full saturation with a sharp initial decrease from dry to 5% EWC. The hydroxy ethyl carbons also show a decrease to approximately one third of the original value and there is a slight decrease in the α-methyl group. The acrylate CH_2 only decreases noticeably after the EWC increases past 10 % but, again, the lack of resolution possible with this peak could make this value doubtful.

The 14 mol%% EGDMA sample again shows a sharp initial decrease in the $T_{1\rho}(C)$ times from dry to 6 % EWC. After this decrease there was little change in the carbonyl, quaternary, α–methyl and hydroxy ethyl carbons with only small further decreases occurring. The largest change noticed was in the acrylate CH_2 which decreased to approximately a third of the initial dry value.

Again it can be seen that, apart from the initial decrease, there is little change in the relaxation times until the T_g of the sample drops below the temperature at which the measurement is taking place (25 °C). The 6

mol % EGDMA sample also has a T_g of 25°C (measured by the Torsion Pendulum, Chapter Four) at full saturation and therefore is noticeably rubbery at the probe temperature and this is reflected in the decrease in the $T_{1\rho}(C)$ times while the 14 mol% EGDMA sample has a T_g that is well above the probe temperature (83°C) and shows little decline in the measured $T_{1\rho}(C)$s

TABLE 7.3

$T_{1\rho}(C)$ times for HEMA copolymerised with 6 mol% EGDMA at differing EWCs. C1-C6 as before.

	$T_{1\rho}(C)$ (ms)					
EWC	C1	C2	C3	C4	C5	C6
0	78.1 ±10.6	10.8 ±0.5	9.2 ±0.4	12.1 ±0.9	63.7 ±6.7	19.2 ±2.8
3.7	44.4 ±3.2	8.2 ±0.3	8.4 ±0.5	9.4 ±1.1	35.6 ±3.0	16.0 ±0.8
11.5	46.6 ±7.6	7.7 ±0.8	8.7 ±0.9	12.0 ±1.9	37.6 ±2.9	16.6 ±1.7
23.7	15.9 ±2.4	3.4 ±0.8	3.6 ±0.8	2.6 ±1.8	32.7 ±1.4	15.8 ±1.7

TABLE 7.4

$T_{1\rho}(C)$ times for HEMA copolymerised with 14 mol% EGDMA and at different EWCs. C1-C6 as before.

	$T_{1\rho}(C)$ (ms)					
EWC	C1	C2	C3	C4	C5	C6
0	91.8 ±10.2	12.9 ±1.2	11.1 ±0.4	27.0 ±4.4	81.6 ±5.6	23.1 ±1.3
3.8	58.2 ±5.5	10.8 ±0.6	9.2 ±0.6	20.9 ±1.7	56.3 ±5.8	18.6 ±1.6
8.5	*	8.9 ±0.5	9.2 ±0.5	9.8 ±1.0	58.2 ±4.3	19.6 ±0.9
12.4	42.7 ±7.1	7.3 ±0.5	8.3 ±0.8	8.2 ±0.8	44.7 ±3.7	20.6 ±1.1
18.5	45.6 ±7.4	8.2 ±0.5	9.0 ±0.4	9.8 ±1.0	48.5 ±3.1	16.8 ±2.0

*-not possible to fit data to equation

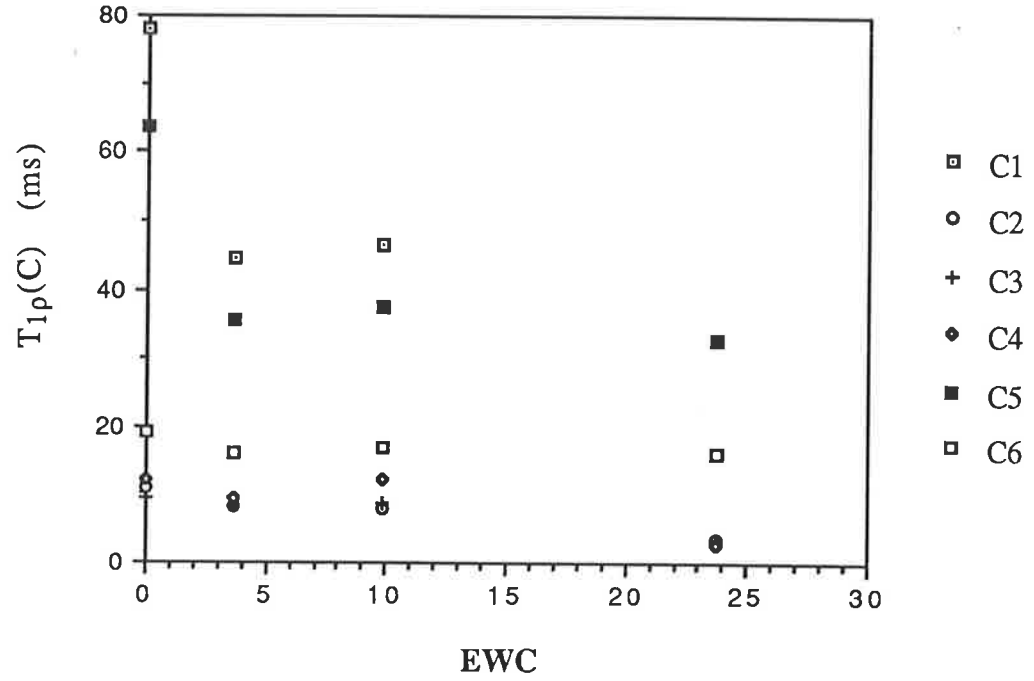

Figure 7.7 Change in $T_{1\rho}(C)$ times for HEMA copolymerised with 6 mol% EGDMA at differing EWCs. C1-C6 as before.

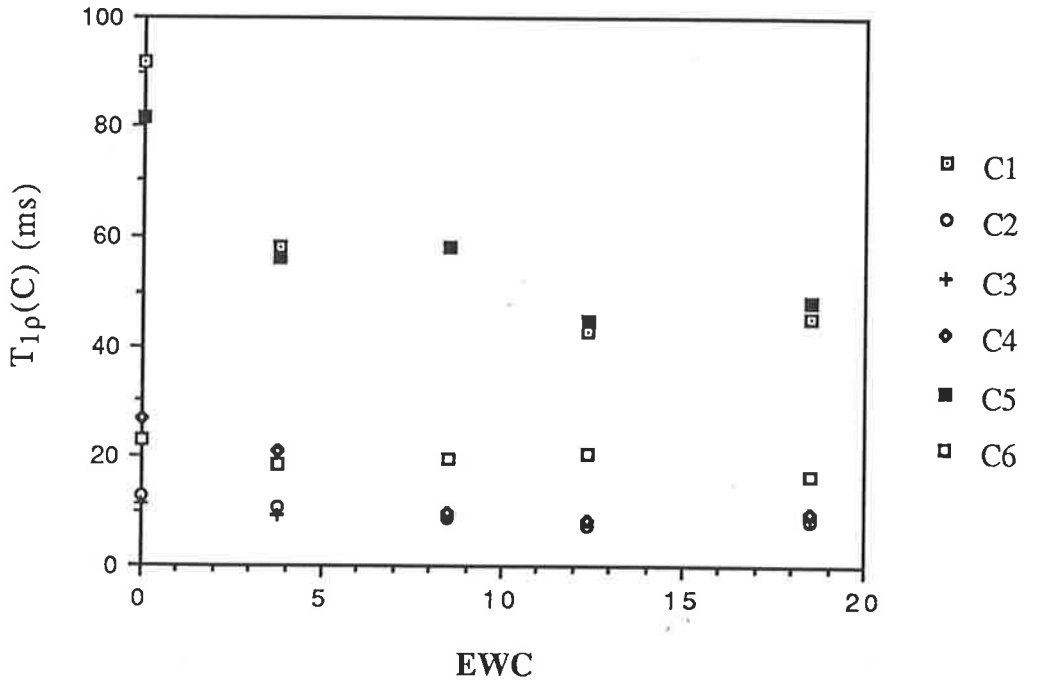

Figure 7.8 Change in $T_{1\rho}(C)$ times for HEMA copolymerised with 14 mol% EGDMA at differing EWCs. C1-C6 as before.

A comparison of the $T_{1\rho}$(C)s for the different functional groups of PHEMA and HEMA copolymerised with 6 and 14 mol% EGDMA can be seen in Figures 7.9a-f. From these it is apparent that the major differences occur in the initial dry $T_{1\rho}$(C)s while the partially hydrated polymers show similar $T_{1\rho}$(C)s with larger differences occurring only when the PHEMA and 6 mol% EGDMA/HEMA samples become fully saturated. The drop in $T_{1\rho}$(C) noticed initially could be due to water plasticising local regions of the polymer chain while not having as great an effect on the bulk properties, such as T_g, until much greater quantities have been absorbed which emphasises the localised nature of the motions that the PEMAS ^{13}C NMR relaxation techniques detect (8).

7.2.2(d) $T_{1\rho}$(C) Times for HEMA/MMA Copolymers of Varying EWCs

$T_{1\rho}$(C) measurements were made on copolymer of PHEMA containing 14 mol% MMA in order to see what effect a hydrophobic non crosslinking copolymer might have. The spectrum of the dry copolymer can be seen in Figure 7.10. As with the previous spectrum of EGDMA/HEMA it can be seen that there is no difference in the observed spectrum.as the carbons of PMMA peaks are identical to those of the acrylate part of PHEMA. The results obtained are shown in Table 7.5.

The results given are similar to those obtained for PHEMA apart from the acrylate CH_2. The carbonyl and quaternary carbons again show a significant decrease from dry to full saturation. The hydroxy ethyl and α–methyl carbons show no great change. The acrylate CH_2 , however, is about three times greater than in PHEMA and a third as large again than the copolymer with 14 mol% EGDMA and decreases to 25 % of its dry value at full saturation. Again the decrease in $T_{1\rho}$(C) occurs largely upon the sample T_g dropping below or nearing the measuring temperature (the T_g of 25 % EWC 20 % MMA/HEMA copolymer is 25°C (11)).

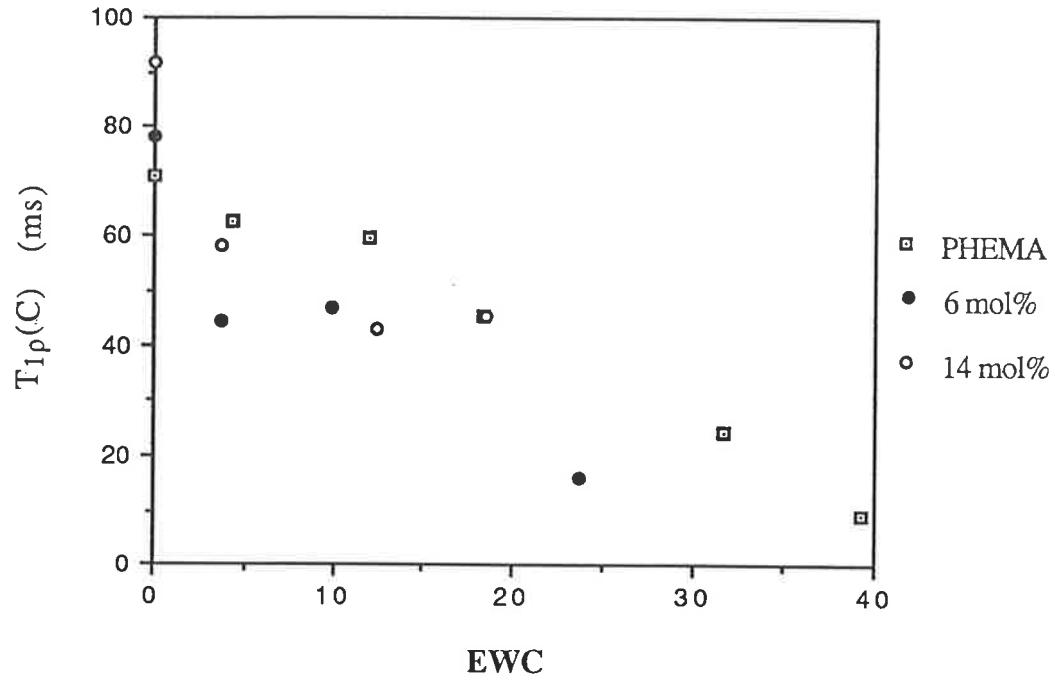

Figure 7.9a Comparison of $T_{1\rho}(C)$ times for the carbonyl of PHEMA and HEMA copolymerised with 6 and 14 mol% EGDMA at different EWCs.

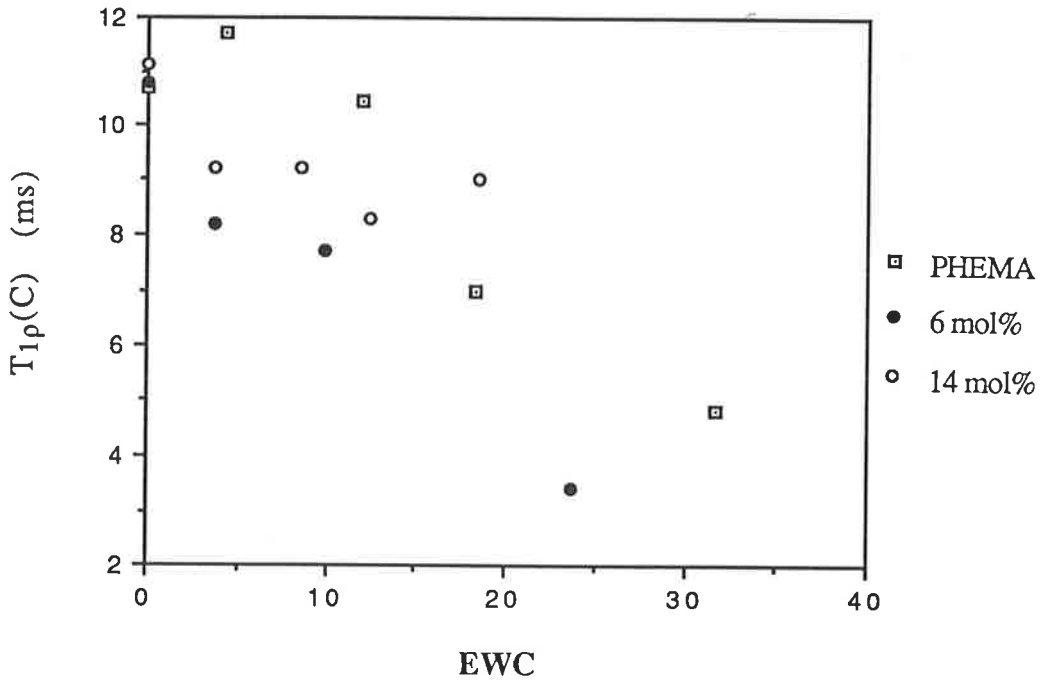

Figure 7.9b Comparison of $T_{1\rho}(C)$ times for the β-hydroxy of PHEMA and HEMA copolymerised with 6 and 14 mol% EGDMA at different EWCs.

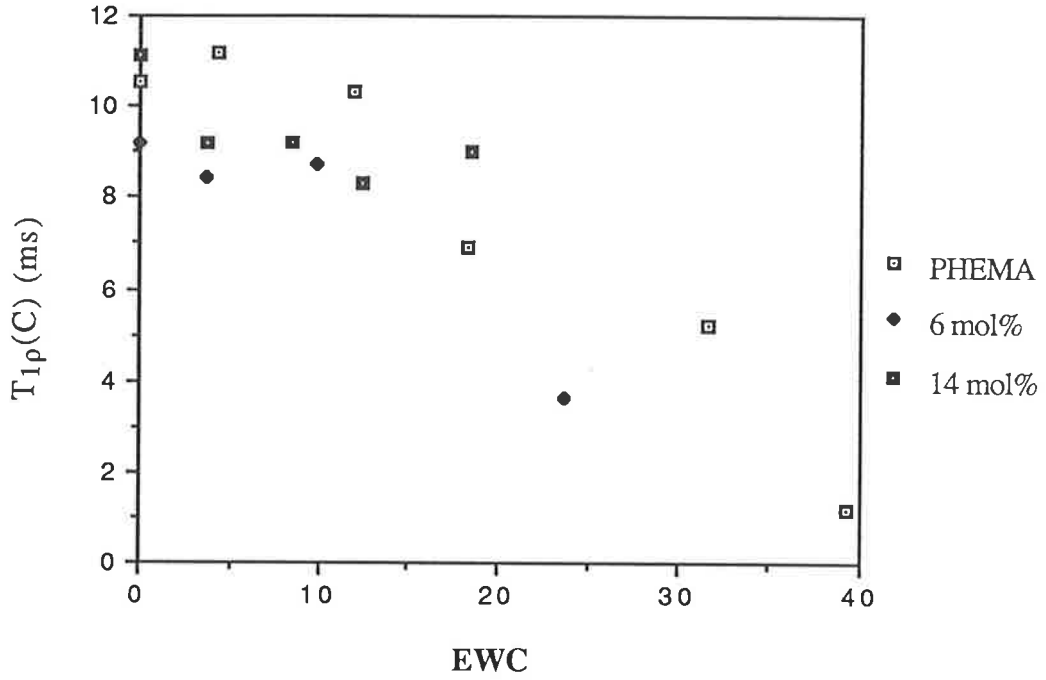

Figure 7.9c Comparison of $T_{1\rho}$(C) times for the α-hydroxy of PHEMA and HEMA copolymerised with 6 and 14 mol% EGDMA at different EWCs.

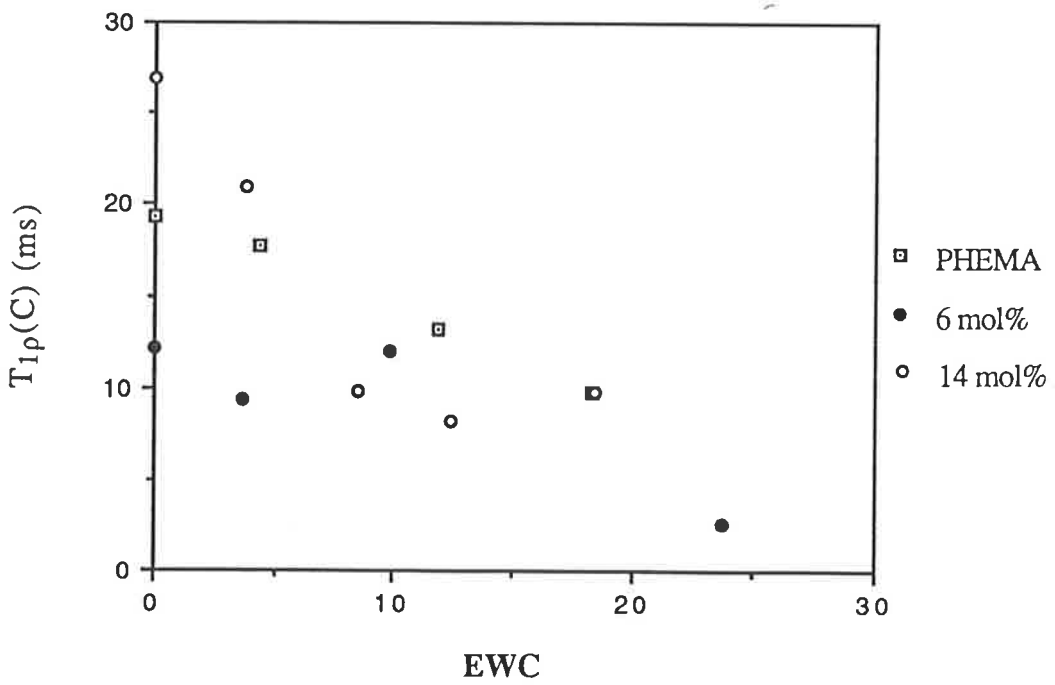

Figure 7.9d Comparison of $T_{1\rho}$(C) times for the acrylate CH_2 of PHEMA and HEMA copolymerised with 6 and 14 mol% EGDMA at different EWCs.

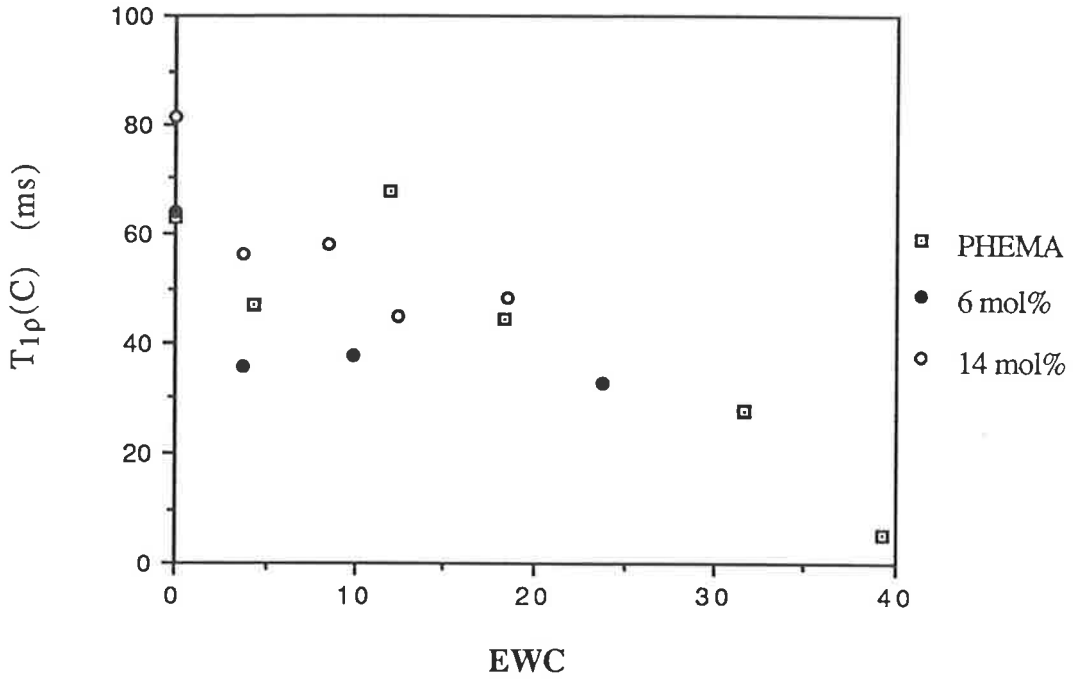

Figure 7.9e Comparison of $T_{1\rho}(C)$ times for the quaternary of PHEMA and HEMA copolymerised with 6 and 14 mol% EGDMA at different EWCs.

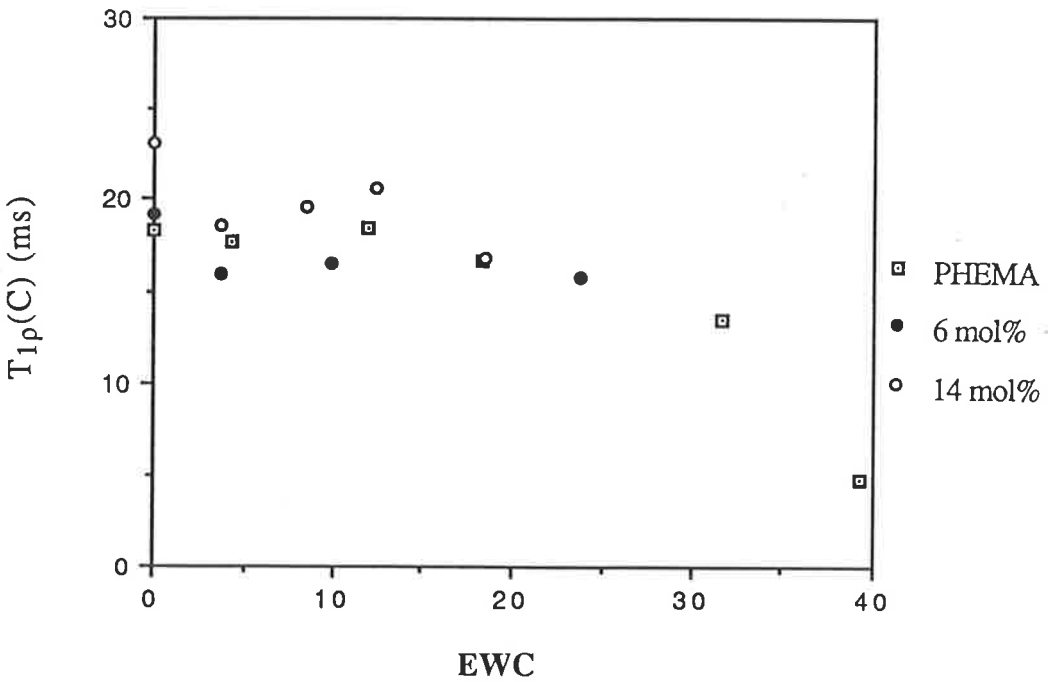

Figure 7.9f Comparison of $T_{1\rho}(C)$ times for the α-methyl of PHEMA and HEMA copolymerised with 6 and 14 mol% EGDMA at different EWCs.

TABLE 7.5

$T_{1\rho}(C)$ times for HEMA copolymerised with 20 wt% MMA. C1-C6 as before.

	$T_{1\rho}(C)$ (ms)					
EWC	C1	C2	C3	C4	C5	C6
0	48.4 ±5.2	9.3 ±1.3	8.07 ±0.5	39.3 ±4.9	64.1 ±5.3	19.15 ±1.05
4.3	89.2 ±5.8	8.8 ±0.7	8.2 ±0.6	51.5 ±11.4	63.9 ±4.2	19.9 ±1.0
10.2	46.8 ±5.1	9.6 ±1.0	9.0 ±0.5	28.3 ±4.1	53.9 ±5.1	17.8 ±2.2
25.0	3.6 ±5.7	11.6 ±7.6	14.3 ±5.9	8.5 ±6.6	59.9 ±5.7	

7.2.5(a) T_{SL} Times for PHEMA at Varying EWCs

The T_{SL} times for wet and dry PHEMA, calculated using Equation 2.3, are shown in Table 7.6 and Figure 7.11. The fit between experimental results for the quaternary carbon of dry PHEMA and this equation is shown in Figure 7.12. This equation was found to provide a good fit to the experimental data.

The major factors affecting cross polarisation are:

1. The number of directly bonded protons. The greater the number of protons the more efficient the cross polarisation indicated by a shorter T_{SL}
2. The motion of the carbon groups which will disturb the dipolar interactions and reduce cross polarisation, thereby lengthening T_{SL}, which in turn implies that T_{SL} is a measure of static motion.

In general it is proposed that T_{SL} times decrease roughly in the order (22);

non-protonated carbons>methyl carbons>protonated aromatic methine carbons>methylene carbons>methyl carbons (static).

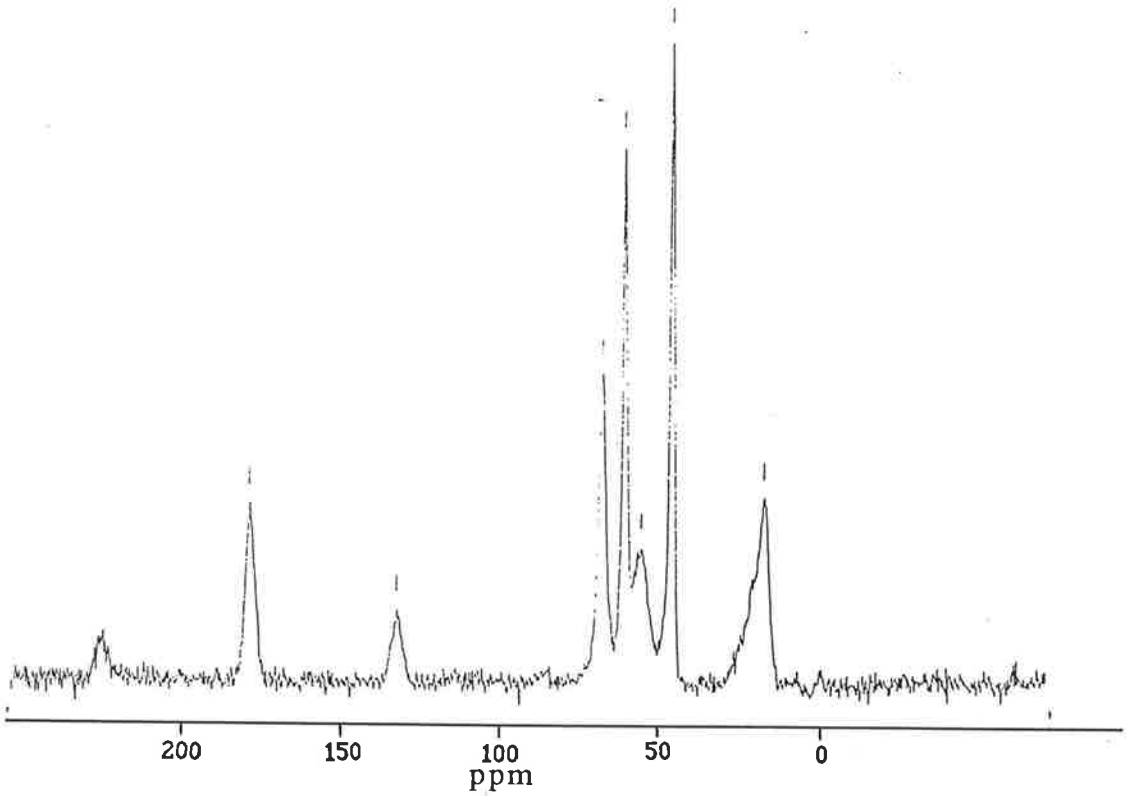

Figure 7.10 PEMAS ^{13}C NMR spectrum of a dry copolymer of HEMA with 20 wt% MMA. Peak assignments are the same as given for PHEMA (Figure 7.1)

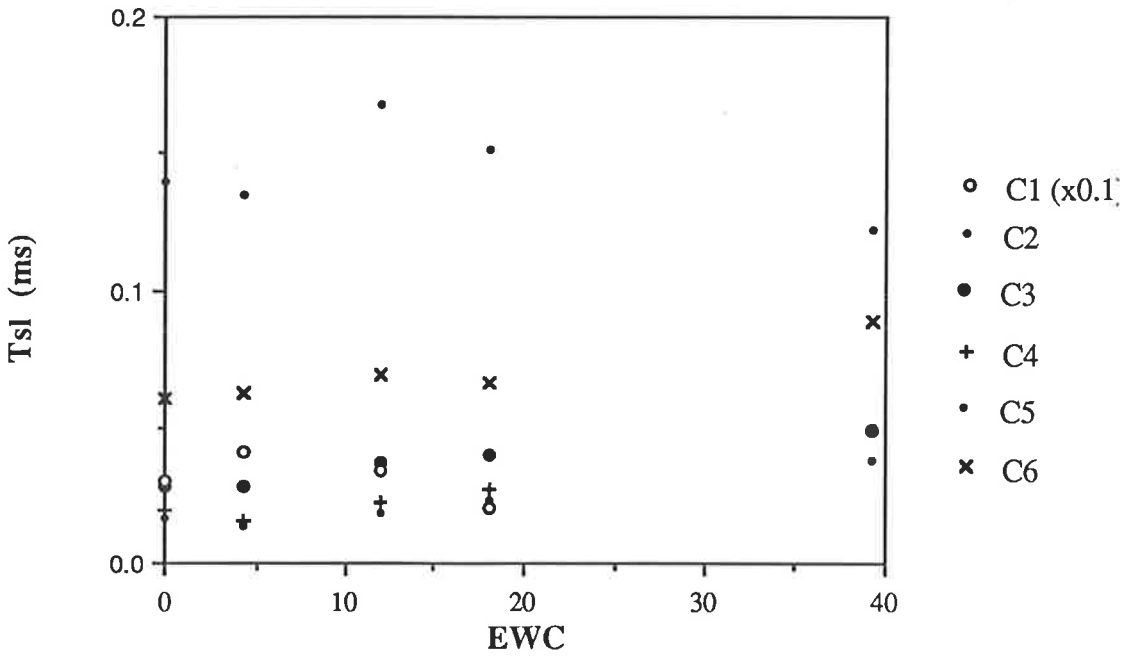

Figure 7.11 Change in T_{SL} times of the carbons of PHEMA at different EWCS. C1-C6 as before. The carbonyl (C1) T_{SL} value has been reduced by a factor of ten.

TABLE 7.6

T_{SL} times obtained from PHEMA samples of different EWCs. C1-C6 as before.

	T_{SL} (ms)					
EWC	C1	C2	C3	C4	C5	C6
0	0.30 ±0.04	0.017 ±0.004	0.028 ±0.003	0.020 ±0.004	0.139 ±0.009	0.060 ±0.005
4.4	0.41 ±0.08	0.014 ±0.006	0.028 ±0.004	0.015 ±0.008	0.135 ±0.009	0.063 ±0.003
11.9	0.34 ±0.05	0.019 ±0.003	0.037 ±0.002	0.023 ±0.003	0.17 ±0.01	0.069 ±0.005
18.4	0.21 ±0.02	0.023 ±0.002	0.040 ±0.003	0.028 ±0.002	0.15 ±0.01	0.066 ±0.009
39.2	*	0.038 ±0.008	0.049 ±0.006	*	0.12 ±0.03	0.089 ±0.007

*- not possible to fit data to the relevant equation

From the values presented in Table 7.6 it is seen that this is true for the PHEMA carbon T_{SL} times. The carbonyl T_{SL} is approximately two to three times that of the quaternary initially, which could be due to cross polarisation of the quaternary by the α-methyl group as it has been noted that the cross polarisation of the quaternary is dependent on the protons of other groups (12,21-22). The β-hydroxy ethyl CH_2 and acrylate CH_2 have similar values while the α-hydroxy ethyl CH_2 is approximately 1.5 times greater, which could be due to greater mobility. The rotation and reorientation of the α-methyl group gives it its relatively high value compared to the other protonated carbons.

The addition of water has the largest effect on the carbonyl with an almost 50% decrease in T_{SL} from dry to full hydration. Since the polymer is becoming more rubbery and molecular motion is increasing this is the reverse of the trend expected. Therefore it seems this decrease must presumably be due to an increase in neighbouring protons even though the interaction falls off in the inverse sixth power of the interatomic separation

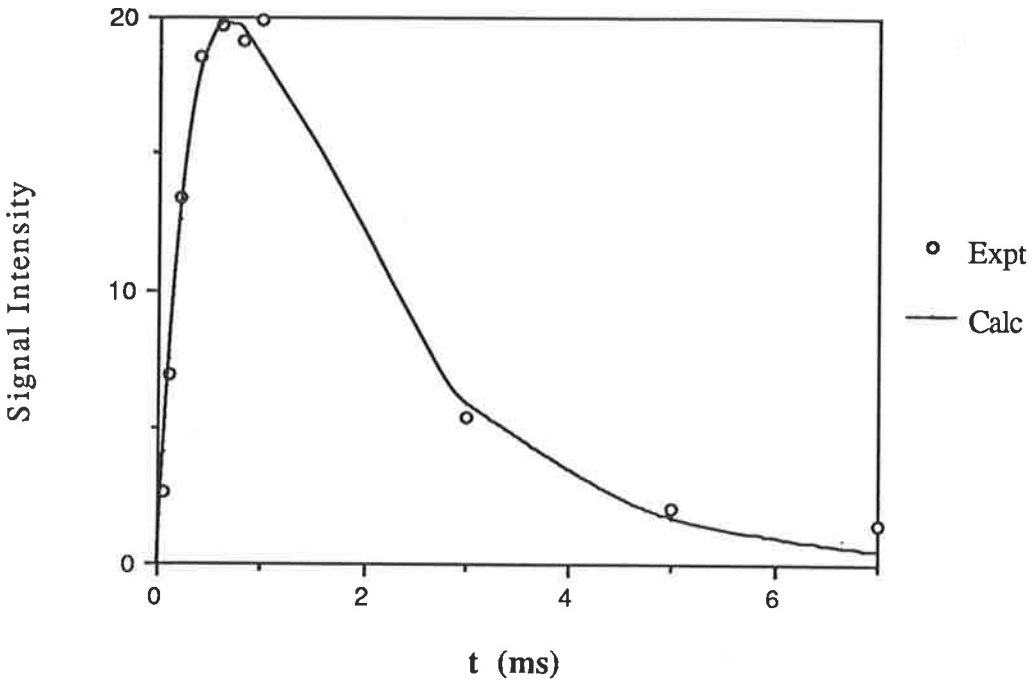

Figure 7.12 Fit of experimental T_{SL} times to those calculated using Equation 2.3.

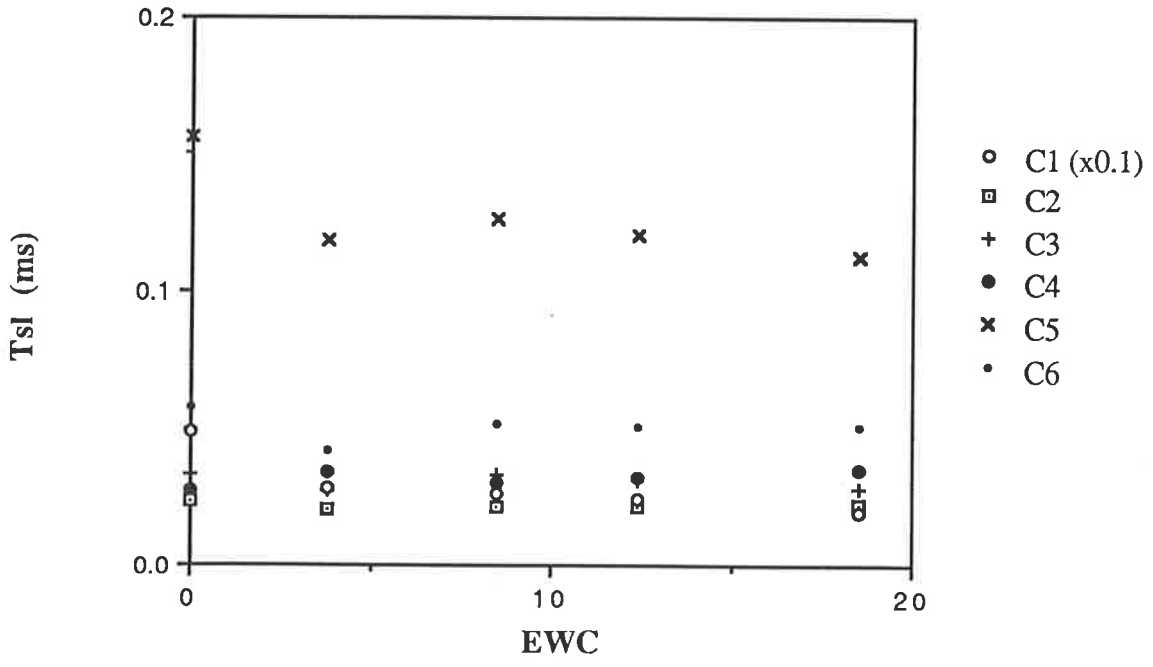

Figure 7.13 Change in T_{SL} times of the carbons of HEMA copolymerised with 14 mol% EGDMA at different EWCs. C1-C6 as before. The carbonyl (C1) T_{SL}has beeen reduced by a factor of ten.

(22). This seems to indicate that water must become closely bound to the carbonyl group. It is also apparent that there is an initial increase in T_{SL}. This is presumably due to an increase in mobility and indicates that water cannot be bound initially to the carbonyl.

The water seems to have little or no effect on the quaternary within the given standard deviations The α-hydroxy ethyl carbon nearly doubles at full saturation and the β-hydroxy ethyl more than doubles from its dry value along with marked increases in the acrylate CH_2. The CH_3 undergoes only a slight increase. These increases are to be expected as molecular motion increases with increasing plasticisation with a resultant decrease in cross polarisation efficiency.

7.2.5(b) T_{SL} Times for Crosslinked PHEMA

T_{SL} measurements were made on copolymers of PHEMA with 14 mol% EGDMA. The results are shown in Table 7.5 and Figure 7.13.

TABLE 7.7

T_{SL} times for HEMA copolymerised with 14 mol% EGDMA. C1-C6 as before.

	T_{SL},(ms)					
EWC	C1	C2	C3	C4	C5	C6
0	0.49 ±0.04	0.023 ±0.002	0.033 ±0.002	0.027 ±0.003	0.156 ±0.007	0.058 ±0.004
3.8	0.28 ±0.02	0.020 ±0.003	0.027 ±0.003	0.034 ±0.004	0.118 ±0.007	0.042 ±0.006
8.5	0.27 ±0.02	0.021 ±0.003	0.033 ±0.002	0.030 ±0.002	0.126 ±0.005	0.052 ±0.008
12.4	0.24 ±0.03	0.021 ±0.003	0.031 ±0.003	0.032 ±0.004	0.120 ±0.007	0.051 ±0.005
18.5	0.20 ±0.03	0.022 ±0.004	0.028 ±0.004	0.035 ±0.003	0.112 ±0.006	0.051 ±0.007

A comparison of the results for the dry 14 mol% EGDMA copolymer and of those for dry PHEMA show that there is little difference between the

two sets of values. Again the absorption of water has the most significant effect on the carbonyl which decreases by over 50 % at full hydration. The hydroxy ethyl carbons and α-methyl carbon values do not vary greatly. The acrylate CH_2 increases slightly from dry to fully hydrated and there is a slight decrease in the quaternary carbon value

A.A Parker et al. (23) have measured the T_{SL} times of plasticised and neat Poly(vinyl butyral-co-vinyl alcohol) PVB and a number of other systems and found that it was possible to measure to T_{SL} for each of the carbons indicating the existence of biphasic behaviour in these polymers. Although they made use of a different pulse sequence to measure the T_{SL} times, work on CR-39 (24) and poly urethanes(25) using the same pulse sequence used in this study has indicated the possibility of two phases. Attempts made here to fit the data to a two T_{SL} equation and assuming that there was only one $T_{1\rho}(H)$ however were not successful and this may be taken as some evidence that the systems studied were mainly single phase systems.

7.2.5(c) $T_{1\rho}(H)$ Times for PHEMA and P(HEMA/EGDMA)

$T_{1\rho}(H)$ times are obtained in the process of calculating T_{SL} from Equation 2.2. The measured $T_{1\rho}(H)$s obtained from each carbon are generally averaged by spin diffusion with other protons and are therefore not indicative of proton relaxation at that particular carbon but are more representative of the relaxation of the whole proton "pool".It was noticeable, however, that the $T_{1\rho}(H)$ value of the carbonyl was usually 50 to 100 percent greater than the other $T_{1\rho}(H)$ times. A similar difference in values was observed by Hjertberg et al. (26) in $T_{1\rho}(H)$ measurements on TRIM. This slower decay of the magnetisation of the carbonyl carbons indicates that these are in fact less influenced by proton spin - spin processes and that, therefore, the carbon relaxation in the rotating frame should be equally well dominated by spin lattice relaxation and is thus a

good indication of the molecular dynamics of the carbonyl group. The values shown in Tables 7.8 and 7.9 for hydrated PHEMA and HEMA copolymerised with 14 mol% EGDMA respectively are the average values obtained from all moeities, except the carbonyl which is given separately, at a particular EWC.

TABLE 7.8

$T_{1\rho}(H)$ times for PHEMA. Given separately are the $T_{1\rho}(H)$ for the carbonyl and the average of the $T_{1\rho}(H)$s obtained at the other carbons

EWC	0	4.4	11.9	18.4	39.2
$T_{1\rho}(H)(C=O)$	1.6 ±0.2	2.3 ±0.3	1.4 ±0.2	1.6 ±0.2	*
$T_{1\rho}(H)$	1.43 ±0.09	1.78 ±0.14	0.83 ±0.07	0.66 ±0.06	0.90 ±0.09

* not possible to fit the data to the relevant equation.

The results for 14 mol% EGDMA/HEMA copolymer are shown in Table 7.9

TABLE 7.9

$T_{1\rho}(H)$ times for HEMA copolymerised with 14 mol% EGDMA. Given separately are the $T_{1\rho}(H)$ for the carbonyl and the average of the $T_{1\rho}(H)$s obtained at the other carbons

EWC	0	3.8	8.5	12.4	18.5
$T_{1\rho}(H)(C=O)$	2.5 ±0.3	2.9 ±0.3	2.3 ±0.2	2.4 ±0.2	2.8 ±0.3
$T_{1\rho}(H)av$	1.2 ±0.1	1.3 ±0.1	0.98 ±0.08	1.00 ±0.07	1.03 ±0.09

It can be seen that there is little variation in $T_{1\rho}(H)(C=O)$ within the given error parameters with only a slight decrease in both the PHEMA and crosslinked PHEMA values as the EWC increases. The average $T_{1\rho}(H)$ of the remaining carbons for the PHEMA sample, however, shows a noticeable decrease with increasing EWC with a drop of approximately 50 %. This seems to indicate that an increase in mid kilohertz motions has occurred which is again consistent with the observed fall in the T_g with increasing EWC. For the 14 mol% EGDMA copolymer it appears that there is a decrease but it is within the bounds of the errors given so it is difficult to say whether it is due to increases in molecular motion or not.

7.2.6 T_{SL} and $T_{1\rho}(H)$ FOR PMMA

T_{SL} Experiments were carried out on a range of partially hydrated PMMA samples. The results obtained are given in Table 7.10. It can be seen that the values obtained are of the same order of those for PHEMA and the PHEMA copolymers but direct comparisons cannot be made as these results were produced under slightly different conditions with a different spin lock frequency (69 kHz compared to 60 kHz used before) and a slower sample spinning speed (2.8 kHz compared to 3.5 kHz).

TABLE 7.10

T_{SL} times for PMMA at different EWCs. C1-C4 refer to the carbonyl, acrylate CH_2, quaternary and α-methyl carbons respectively.

	T_{SL} (ms)			
EWC	C1	C2	C3	C4
0	0.55 ±0.33	0.16 ±0.07	0.19 ±0.09	0.17 ±0.08
0.25	0.52 ±0.29	0.079 ±0.006	0.20 ±0.02	0.11 ±0.01
0.43	0.44 ±0.18	0.056 ±0.003	0.23 ±0.03	0.09 ±0.01
0.61	0.37 ±0.11	0.060 ±0.004	0.19 ±0.02	0.097 ±0.009
1.08	0.30 ±0.07	0.055 ±0.002	0.217 ±0.009	0.098 ±0.008
1.56	0.87 ±0.71	0.076 ±0.006	0.21 ±0.03	0.122 ±0.007
1.88	0.28 ±0.08	0.062 ±0.004	0.22 ±0.03	0.090 ±0.007

PMMA absorbs considerably less water than any of the polymer systems previously studied and, therefore, any effect water has on the T_{SL} times should have been much less. From the times in Table 7.10 and Figure 7.14 it can be seen, however, that the carbonyl shows a noticeable

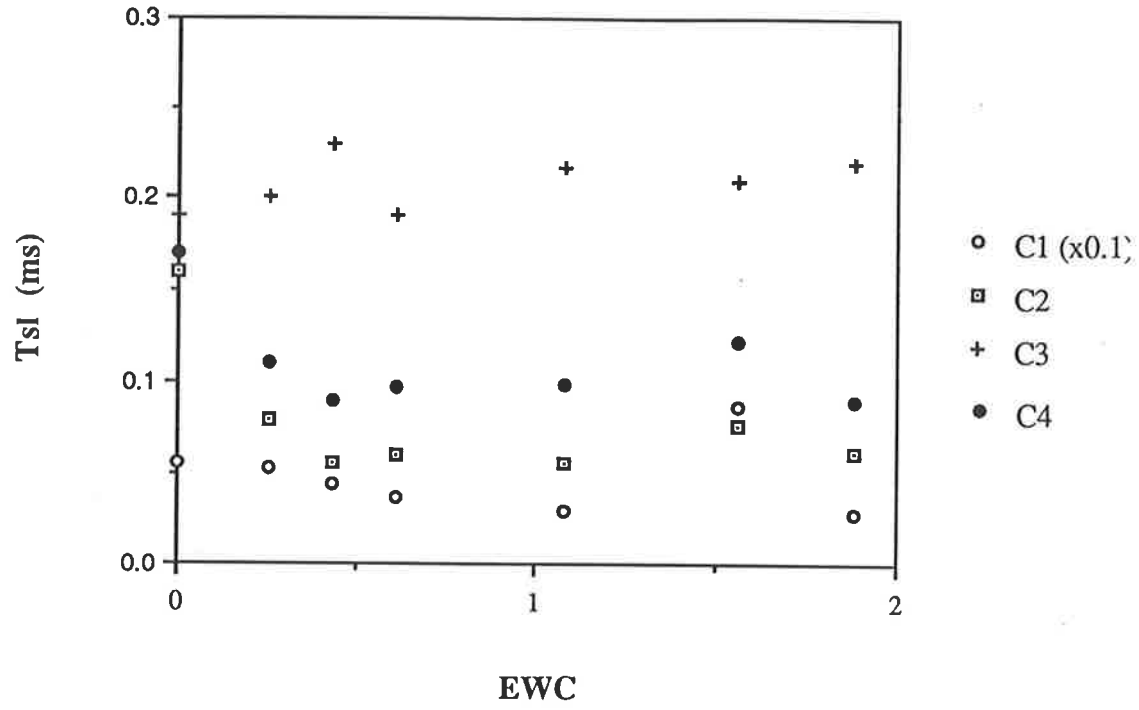

Figure 7.14 Change in T_{SL} times of the carbons of PMMA at different EWCs. C1-C4 are designated in Table 7.10.

decrease from dry to fully hydrated. There is little or no effect on the other carbon groups. The decrease in the carbonyl T_{SL} value is opposite to any expected effect due to an increase in molecular motion resulting from the plasticising effect of water. As T_g of the fully saturated sample decreases by only 20 K from the dry value of 373K (27-28) and the polymer is still glassy at the probe temperature it seems that the major effect of the water is to provide protons which enable the carbonyl to cross polarise more rapidly which seems to indicate that the carbonyl groups must have water closely hydrogen bonding to it which is in agreement with other predictions (29)

The $T_{1\rho}(H)$ proton results calculated for wet and dry PMMA are shown in Table 7.11. As with the PHEMA results the given times are the average obtained for all moieties, except the carbonyl which is given separately, at a particular EWC. The carbonyl again was greater than the other $T_{1\rho}(H)$ calculated at other carbons and there was also a drop in the averaged $T_{1\rho}(H)$ of the other carbons which leads to similar conclusions reached for the previous measurements made with the PHEMA samples.

Table 7.11

$T_{1\rho}(H)$ times for PHEMA. Given separately are the $T_{1\rho}(H)$ for the carbonyl and the average of the $T_{1\rho}(H)$s obtained at the other carbons

EWC	0	0.25	0.43	0.61	1.08	1.56	1.88
$T_{1\rho}(H)(C=O)$	2.6 ±0.8	1.8 ±0.6	1.7 ±0.4	2.0 ±0.4	2.7 ±0.5	1.6 ±0.5	2.9 ±0.6
$T_{1\rho}(H)av$	1.8 ±0.6	1.55 ±0.09	1.35 ±0.09	1.5 ±0.1	1.58 ±0.05	1.4 ±0.1	1.59 ±0.09

7.3 Summary

The $T_{1\rho}(C)$ times measured for the various copolymers indicated that water seemed to have the most noticeable effect on the carbonyl and quaternary carbons with the greatest decrease in $T_{1\rho}(C)$ being noticed when the sample Tg was near to or below that of the measuring temperature of the NMR probe. The $T_{1\rho}(C)$ times for dry copolymers of HEMA with EGDMA

also varied with EGDMA contant, increasing with the increasing T_g of the copolymer.

The T_{SL} times for the PHEMA samples of different EWC seemed to indicate that there was some association of water with the carbonyl group early in the hydration stage as evidenced by a decrease in the T_{SL} times for the carbonyl as the EWC increased from 4.4 % to full hydration. Similar decreases were also noted in the T_{SL} times for the carbonyls of HEMA crosslinked with 14 mol% EGDMA and for PMMA.

CHAPTER EIGHT

CONCLUSION

The physical and mechanical properties of the hydrogels studied here were all significantly affected by the frequency of crosslinks and also to some extent by the size of the crosslinking agent used.

It was found that the sorption kinetics were appreciably dependent on the sorption conditions (i.e samples equilabrated at certain relative humidities or in water) and the amount and types of crosslinking used. Samples equilibrated at 33% RH and in water had sorption kinetics that could be described by Ficks law (Section 3.3.1 and 3.3.2). At 79% and 100% RH, however, there was some deviation from Ficks laws. At 79% RH this deviation was greatest for copolymers of HEMA containing between 14 and 70 mol% OED(Section 3.3.3). At 100% RH the sorption behaviour is more complicated and no particular trend was observable for any of the HEMA/OED copolymer systems. It appeared, however, that for PHEMA, sorption seemed to follow Case II diffusion with water uptake being linear with time (Section 3.3.4). It was still possible , however, to obtain good fits to Equation 3.2 up to $M_t/M_\infty=0.85$.

The change in sorption kinetics, as indicated by the change in n_s values calculated from Equation 3.5, could be explained using the diffusional Deborah number, De, with changes in the ratio of the characteristic relaxation time to the characteristic diffusion time causing changes in the sorption kinetics. The changes in the relaxation time would be dependent on the flexibility of the OED used and the degree of crosslinking, while the change in characteristic diffusion time could be dependent on the hydrophilicity of the OED which, for the OEDs used here, are both dependent on the length of the oxyethlyne chain.

It would appear, in general, that any advantage gained as sorption approaches Case II diffusion (i.e. a more rapid uptake of water as the sorption kinetics change from a square root function of time to a linear function of time) is negated by the decrease found in sorption coefficient D_s as the percentage of OED in the copolymer increases. While this is not the case with P400/HEMA copolymers a further problem arises with the use of this particular OED due to the tendency of the copolymers to break up on drying.

Desorption tended to occur in a similar manner for all copolymer samples regardless of their initial water content, and a good fit could generally be obtained to Equation 3.2 in all cases.

Dynamic mechanical measurements indicated the plasticising effect of water on PHEMA and its copolymers with a drop in T_g for the PHEMA homopolymer of 125°C from dry to wet. From changes in the height and width of the tan δ peak at T_g it seems that at intermediate water contents the mobile kinetic units which contribute to the peak height and width are arranged in a spread of environments (Section 4.2.2) suggesting some inhomogeneity in the polymer/water system at intermediate EWCs. As the amount of water increases, however, uniformity is again approached as evidenced by the increase in height and decrease in width of the tan δ peak at T_g.

It was found to be possible, to some extent, to be able to control the T_gs of the hydrogels by choosing the type and amount of OED used as a copolymer. Attempts to predict changes in T_g by using the various equations mentioned in Chapter Four met with varied success. The Fox equation was found to give reasonable results for the PHEMA/water system up to approximately 18 % EWC (Figure 4.10) after which it overestimated the decrease in T_g as the EWC increased; a fault that also occurred with the other equations used and the other copolymer systems studied. This could be due to the beginning of the formation of a bulk water phase.

The addition of water was also found to initially cause an increase in the temperature difference found between the high temperature tan δ and log G" peaks which decreased as the polymers became fully hydrated (Section 4.2.2). This was ascribed to thermorheologically complex behaviour of these systems and could possibly originate in inhomogeneity in the hydrogel at intermediate EWCs.

Copolymerisation of HEMA with OEDs seemed to have only a small effect on the low temperature $T\gamma$ and T_{dil} peaks and on the T_β peak.

The changes in the molecular relaxation parameter, $T_{1\rho}(C)$, for PHEMA indicated that initially, as the EWC rose from 0 to 18%, only the carbonyl and, to some extent, the quaternary carbons showed any noticeable decrease as the T_g of the polymer decreased. Above this, however, there was a noticeable decrease in all the $T_{1\rho}(C)$ times of all carbons measured. This seems to correspond to the EWC at which the sample T_g would have been near to that of the measuring temperature indicating that large scale main chain motion was mainly responsible for the drop in the $T_{1\rho}(C)$ times of the carbons. A similar response was also noted from the HEMA copolymers with EGDMA, with a decrease occurring initially at only the quaternary and carbonyl moeities, with decreases in the remaining carbons only after the T_g of the sample reached or neared the measuring temperature. For the dry EGDMA/HEMA copolymers the $T_{1\rho}(C)$ times seemed to be sensitive to the increase in T_g caused by an increase in EGDMA content of the copolymer.

The effect of water on the T_{SL} values of PHEMA and HEMA copolymerised with 14 mol% EGDMA was generally most noticeable at the carbonyl. For PHEMA there was an initial increase in the carbonyl T_{SL} value as the EWC increased from 0 to 4.4%, which can probably be ascribed to greater molecular motion making cross polarisation more difficult (Section 7.2.5). As the EWC increases, however, the T_{SL} time of the carbonyl starts to decrease which could indicate that there are an

increasing number of protons in close proximity to the carbonyl group making cross polarisation of that group more efficient. An EWC of 11.9% corresponds to approximately one molecule of water per repeat unit of the polymer. As the carbonyl T_{SL} starts to decrease from 4.4% EWC it would seem that, while the hydroxy group is presumably the preferential point of contact for water molecules, there is some early close association of water with the carbonyl groups.

The T_{SL} times for the carbonyls of the EGDMA/HEMA copolymer and for PMMA showed no initial increase and decreased immediately on sorption of water. While this would be expected for PMMA with the carbonyl group being the most polar in the polymer, it suggests that for the 14 mol% EGDMA/HEMA copolymer water almost immediately comes into close contact with the carbonyl group, possibly due to steric reasons caused by the crosslinking.

DSC measurements indicated that approximately 33-37% of the water present in saturated PHEMA was capable of freezing, depending on the method used. The addition of as little as 3 mol% OED had the effect of drastically reducing the amount of water that was found to freeze although a large proportion of this reduction could be ascribed to the lower EWC found on copolymerisation. It appears for the copolymers in general that water in excess of ≈30% EWC was bulk-like water capable of freezing.

The ^1H NMR results indicated that as the water was frozen at -15°C at least two types of environment were involved. One part that eventually froze and another that remained unconstrained and unfrozen. Using the results obtained from both the DSC and ^1H NMR measurements it was possible to estimate the relative proportions of water existing in different environments within the polymer (Section 6.3). For saturated PHEMA only a relatively small amount (≈13%) of water appears to be constrained and not observable by ^1H NMR. However, it was found that even with the addition of small amounts of EGDMA or TEGDMA there was a large increase in the

amount of constrained water found, probably due to the network structure formed on copolymerisation. This is supported by the fact that copolymerisation with MMA did not result in such a large increase in constrained water.

The DSC and ^1H NMR results in conjunction point to at least three types of environments in which water exists in PHEMA and its copolymers. (1) closely bound, constrained water which is not detected by ^1H NMR measurements, (2) unconstrained water that eventually freezes and (3) unconstrained water that does not freeze. The last category could possibly be split further as some unconstrained water appears to become constrained over time. The first type of water is presumably water that is strongly hydrogen bonded to the polymer, most probably to the hydroxy group initially and then to the carbonyl, or water that has become physically constrained in the polymer, while the second forms a secondary hydration shell around the hydrogen bonded water. The third type is freely diffusable bulk like water that is capable of freezing.

While copolymerisation of HEMA with crosslinking OEDs modifies the sorption properties of the network, the glass transition and properties dependent upon T_g, any improvement in these properties tends to be offset by a decrease in the EWC of the hydrogel and free water present, or by a tendency for some of the HEMA/OED copolymers to break up on drying, which is especially the case for the P400 copolymers.

REFERENCES

CHAPTER ONE

1. O.Wichterle and D.Lim, *Nature*, **165**, 117 (1960).

2. O.Wichterle and D.Lim, U.S. Pat. 2,976,576 (Mar. 28,1961).

3. M.Rosenberg, P.Bartl and J.Lesko, *J. Ultrastruct. Res.*, **4**, 298 (1960).

4. L.Allen, *Polym. Prepr.*, **15**, 395 (1974).

5. B.D.Ratner and A.S.Hoffman, in *Hydrogels for Medical and Related Applications*, Vol. 31, J.D.Andrade Ed.,ACS Symposium Series, American Chemical Society, Washington D.C., 1976,1.

6. D.E.Gregonis, C.M.Chen and J.D.Andrade, in *Hydrogels for Medical and Related Applications*, Vol. 31, J.D.Andrade Ed.,ACS Symposium Series, American Chemical Society, Washington D.C., 1976, 88.

7. J.Kolarik, *Adv. Polym. Sci.*, **46**, 119 (1982).

8. J.Kolarik and J.Janacek, *J. Polym. Sci.*, A-2, **10**, 11 (1972).

9. S.M.Aharoni and S.F.Edwards, *Macromolecules*, **22**, 3361 (1989).

10. M.F.Refojo, "Contact Lenses," in *Encyclopaedia of Polymer Science and Technology*, Wiley, New York, 1976; Supplement Vol.1, pp195-219.

11. T.A.Jadwin, A.S.Hoffman and W.R.Vieth, *J. Appl. Polym. Sci.*, **14**, 1339 (1970).

12. J.Kopecek and J.Vacik, *Coll. Czech. Chem. Commun.*, **38**, 854 (1973).

13. A.S.Hoffman, M.Modell and P.Pan, *J. Appl. Polym. Sci.*, **14**, 285 (1970).

14. B.D.Ratner and I.F.Miller, *J. Biomed. Mater. Res.*, **7**, 353 (1973).

15. J.Vacik, M.Czakova, J.Exner, J.Kalal and J.Kopecek, *Coll. Czech. Chem. Commun.*, **42**, 2786 (1977).

16. J.Kopecek, J.Vacik and D.Lim, *J. Polym. Sci.*, A-1, **9**, 2801 (1971).

17. M.Tollar, M.Stol and K.Kliment, *J. Biomed. Mater. Res.*, **3**, 305 (1969).

18. J.N.LaGuerre, H.Kay, S.M.Lazarus, W.S.Calem, S.R.Weinberg and B.S.Levowitz, *Surg. Forum*, **19**, 522 (1968).

19. S.M.Lazarus, J.N.LaGuerre, H.Kay, S.R.Weinberg and B.S.Levowitz, *J. Biomed. Mater. Res.*, **5**, 129 (1971).

20. G.M.Zenter, J.R.Cardinal and S.W.Kim, *J. Pharm. Sci.*, **67**, 1347 (1978).

21. G.M.Zenter, J.R.Cardinal and S.W.Kim, *J. Pharm. Sci.*, **67**, 1352 (1978).

22. R.Langer and J.Folkman, *Nature*, **263**, 797 (1976).

23. Y.K.Sung, S.W.Kang and U.S.Kim, *J. Busan Natl. Univ.*, **29**, 27 (1980).

24. S.Sevcik, J.Stamberg and P.Schmidt, *J. Polym. Sci.*, **C16**, 821 (1967).

25. J.Stamberg and S.Sevcik, *Coll. Czech. Chem. Commun.*, **31**, 1009 (1966).

26. M.Frommer and D.Lancet, *J. Appl. Polym. Sci.*, **16**, 1295 (1972).

27. M.Frommer, M.Shporer and R.Messalem, *J. Appl. Polym. Sci.*, **17**, 2263 (1973).

28. M.Shporer and M.Frommer, *J. Macromol. Sci.,Phys.*, **B10**, 529 (1974).

29. Y.K.Sung, D.E.Gregonis, M.S.Jhon and J.D.Andrade, *J. Appl. Polym. Sci.*, **26**, 3719 (1981).

30. M.S.Jhon and J.D.Andrade, *J. Biomed. Mater. Res.*, **7**, 509 (1973).

31. H.B.Lee, M.S.Jhon and J.D.Andrade, *J. Colloid. Interface Sci.*, **51**, 225 (1975).

32. A.S.Hoffman, M.Modell and P.Pan, *J. Appl. Polym. Sci.*, 13, 2223 (1969).

33. R.A.Nelson, *J. Appl. Polym. Sci.*, **21**, 645 (1977).

34. M.Froix and R.A.Nelson, *Macromolecules*, **8**, 726 (1975).

35. K.Nakamura, T.Hatekeyama and H.Hatakeyama, *Polymer*, **24**, 871 (1983).

36. T.Hatakeyama, A.Yamauchi and H.Hatakeyama, *Eur. Polym. J.*, **20**, 61 (1984).

37. Y.Taniguchi and S.Horigome, *J. Appl. Polym. Sci.*, **19**, 706 (1975).

38. M.N.Sarbolouki, *J. Appl. Polym. Sci.*, **17**, 2407 (1973).

39. A.Higuchi and T.Iijima, *Polymer*, **26**, 1833 (1985).

40.R.E.Dehl, *Science*, **170**, 738 (1970).

41. M.Aizawa and S.Suzuki, *Bull. Chem. Soc. Japan*, **44**, 2967 (1971).

42. M.Aizawa, J.Mizuguchi, S.Suzuki, S.Hayashi, T.Suzuki, N.Mitomo and H.Toyama, *Bull. Chem. Soc. Japan*, **45**, 3031 (1972).

43. P.H.Corkhill, A.M.Jolly, C.O.Ng and B.J.Tighe, *Polymer*, **28**, 1758 (1987).

44. G.Smyth, F.X.Quinn and V.J.McBrierty, Macromolecules, 21, 3198 (1988).

45. M.F.Refojo and H.Yasuda, *J. Appl. Polym. Sci.*, **9**, 2425 (1965).

46. J.Janacek and J.Hasa, *Coll. Czech. Chem. Commun.*, **31**, 2186 (1966).

47. M.F.Refojo, *J. Polym. Sci., Polym. Chem. Ed.*, **5**, 3103 (1967).

48. B.D.Ratner and I.F.Miller, *J. Polym. Sci., Polym. Chem. Ed.*, **10**, 2425 (1972).

49. J.H.Collett, D.E.M.Spillane and E.J.Pywell, *Polym. Prepr.*, **28**, 141 (1987).

50. M.Iavsky and W.Prins, *Macromolecules*, **3**, 415 (1970).

51. K.Dusek and B.Sedlacek, *Eur. Polym. J.*, **7**, 1275 (1971).

52. D.G.Pedley and B.J.Tighe, *Br. Polym. J.*, **11**, 130 (1979).

53. G.P.Simon, PhD Thesis, University of Adelaide, (1986).

54. C.Carfagna, C.Migliaresi, L.Nicolais and A.Sacerdoti, *Polym. Sci. Technol*, (Plenum), **23**, 311 (1983).

55. L.F.Allen, *Polym. Prepr.*, **15(2)**, 395 (1974).

56. M.B.Huglin and D.C.F.Yip, *Makromol. Chem., Rapid Commun.*, **8**, 237 (1987).

57. M.F.Refojo, *J. Appl. Polym. Sci.*, **9**, 3417 (1965).

58.C.M.Walker and N.A.Peppas, *J. Appl. Polym. Sci.*, **39**, 2043 (1990)

59. N.M.Franson and N.A.Peppas, *J. Appl. Polym. Sci.*, **28**, 1299 (1983).

60. C.C.R.Robert, P.A.Buri and N.A.Peppas, *J. Appl. Polym. Sci.*, **30**, 301 (1985).

61. A.M.North, Molecular Behaviour and Development of Polymeric Materials, (Edited by A.Ledwith and A.M.North), p368, Chapman and Hall, London (1974).

REFERENCES
CHAPTER TWO

1. G.F. Cowperthwaite, J.J.Foy, M.A. Malloy, in *Biomedical and Dental Applications of Polymers*, C.G. Geblen and F.F. Koblitz, Eds. Plenum Press, New York, 1981,pp. 397.

2. J.E. Moore, in *Chemistry and Properties of Crosslinked Polymers*, S.S. Labena, Ed., Academic Press, New York, 1977,pp.535.

3. M.Atsuta and D.T. Turner, *J. Polym.Sci.,Polym.Phys.Ed.*, **20**, 1609 (1982).

4. D.J. Bennett, *Honours Thesis*, University of Adelaide, (1985).

5. P.E.M.Allen, G.P.Simon, D.R.G.Williams and E.H.Williams, *Eur. Polym. J.*, **22**, 549 (1986).

6. P.E.M.Allen, G.P.Simon, D.R.G.Williams and E.H.Williams, *Macromolecules*, **22**, 809 (1989).

7. S.Hagias, Private Communication.

8. G.P.Simon, *PhD Thesis*, University of Adelaide,1986.

9. J.Perry (Ed), *Chemical Engineers Handbook*, McGraw-Hill Book Company, New York (1934).

10. R.C.Weast and S.M.Selby (Eds), *Handbook of Chemistry and Physics*, The Chemical Rubber Company,Ohio (1966).

11. L.S.A.Smith and V.Schmitz, *Polymer*, **29**, 1871 (1988).

12. J.M.G.Cowie and R.Ferguson, *Macromolecules*, **22**, 2307 (1989).

13. T.V.Tan, *PhD Thesis*, University of Adelaide,1981.

14. G.P. Simon, *Honours Thesis*,University of Adelaide, 1981.

15. J.G.Williams, *Sources of Error in a Free Oscillation Torsion Pendulum*, Department of Defence, Report 647, Melbourne, (Jan.1976).

16. E.Becker, *Anal. Chem.*, **51(12)**, 2050 (1979).

17. J.Schaeffer, E.O.Stejskal, R.Buchdal, *Macromolecules*,**10(2)**,38,(1977)

18. A.N.Garroway, W.B.Moniz and H.A.Resing, *ACS Symp. Ser.*, **103**,67 (1979).

19.M.E.Gal, G.R.Kelly and T.Kurucsev, *J. Chem. Soc, Faraday Trans. II*, **69**, 395 (1973).

20. D.T.Turner, *Polymer*, **23** 197 (1982).

REFERENCES
CHAPTER THREE

1. J.W.McBain, *Phil. Mag.*, **18**, 916 (1909).

2.D.Machin and C.E.Rogers, Encyclopedia of Polymer Science and Technology, H.F.Mark, N.G.Gaylord and N.M.Bikales Editors, Wiley Interscience, New York (1970).

3. J.Crank, *The Mathematics of Diffusion*, Oxford University Press, London (1956)

4. A.J.Kovacs, *J.Chim. Phys*, **45**, 258 (1948).

5. D.Fujita, in *Diffusion in Polymers*, J.Crank and G.S.Park,Eds., Academic Press, London, 1968,Ch. 3.

6. H.L.Frisch, *Polym. Eng. Sci.*, **20**, 2 (1980).

7. J.S.Vrentas and J.L.Duda, *J. Polym. Sci., Polym. Phys. Ed.*, **15**, 441 (1977).

8. J.S.Vrentas, C.M.Jarzebski and J.L.Duda, *AIChEJ*, **21**, 894 (1975).

9. D.E.Gregonis, C.M.Chen and J.D.Andrade, in *Hydrogels for Medical and Related Applications*, Vol. 31, Andrade,J.D.,Eds, ACS Symposium Series, American Chemical Society, Washington,D.C.,1976, 88.

10. N.A.Peppas and N.M.Franson, *J. Polym.Sci. Polym. Phys.Ed.*,**21**,983 (1983).

11. M.F. Refojo, *Cont. Intraoc. Lens Med. J.*,**1**,153 (1975).

12. Hydrogels in Medicine and Pharmacy.PeppasN.AA. and Moynihan

13. A.S.Michaels, W.R.Vieth and J.A.Barrie, *J. Appl. Phys.*, **34**, 1 (1963).

14. W.R.Vieth, C.S.Frangoulis and J.A.Rionda Jr., *J. Colloid Sci.*, **22**, 454 (1966).

15. D.T.Turner, *Polymer*, **23**, 197 (1982).

16. F. Bueche, *J. Polym. Sci.*, **14**, 414 (1954).

17. A.Peterlin, *J. Polym. Sci*, **B3**, 1083 (1965).

18. A.Peterlin, *Makromol. Chem.*, **124**, 136 (1969).

19. T.K.Kwei and H.M.Zupko, *J.Polym.Sci.*,**A2(7)**, 867 (1969).

20. I.N. Razinskaya, B.P.Shtarkman, V.A.Izvokchik, N.Yu.Averbakh, I.M.Monich, *Vsokomol.Soyed.*, **A26(8)**,1617 (1984).

21. J.Shen, C.C.Chen, J.A.Sauer, Abstracts IUPAC, Macro '85, "*Structure and Properties*", Section 4,279, Bucharest (1984).

22. R.J.Young and P.W.Beaumont, *J. Mat. Sci*, **11**, 777 (1976).

23. L.C.E.Struik, *Physical Aging in Amorphous Polymers and Other Materials*, Elsvier, Amsterdam (1978).

24. G.P.Simon, *PhD Thesis*, University of Adelaide, (1985).

25. C.M.Walker and N.A.Peppas, *J. Appl. Polym. Sci.*, **39**, 2043 (1990).

26. J.S.Vrentas, J.L.Duda and A.C.Hou, *J. Appl. Polym. Sci.*, **29**, 399 (1984).

27. M.J.Smith and N.A.Peppas, *Polymer*, **26**, 569 (1985).

28. R.P.Kambour, F.E.Karasz and J.H.Daane, *J. Polym. Sci.*, **4**, 327 (1966).

29. W.V.Titow, M.Braden, B.R.Currel and R.J.Lonergan, *J. Appl. Polym. Sci.*, **18**, 867 (1974).

30. N.Overbergh, H.Berghmans and G.Smets, *Polymer*, **16**, 867 (1974).

31. N.A.Peppas and K.G.Urdahl, *Polym. Bull.*, **16**, 20 (1986).

32. N.M.Franson and N.A.Peppas, *J. Appl. Polym. Sci.*, **28**, 1299 (1983).

33. J.I.Mardel, *Honours Thesis*, University of Adelaide (1989).

34. C.Carfagna, C.Migliaresi, L.Nicolais and A.Sacerdoti, *Polym. Sci. Technol*, (Plenum), **23**, 311 (1983).

35. L.F.Allen, *Polym. Prepr.*, **15(2)**, 395 (1974).

36. M.B.Huglin and D.C.F.Yip, *Makromol. Chem., Rapid Commun.*, **8**, 237 (1987).

37. M.F.Refojo, *J. Appl. Polym. Sci.*, **9**, 3417 (1965).

38. C.C.R.Robert, P.A.Buri and N.A.Peppas, *J. Appl. Polym. Sci.*, **30**, 301 (1985).

39. M.J.Smith and N.A.Peppas, *Polymer*, **26**, 569 (1985).

40. J.E. Moore, in *Chemistry and Properties of Crosslinked Polymers*, S.S. Labena, Ed., Academic Press, New York, 1977,pp.535.

41. M.Atsuta and D.T. Turner, *J. Polym.Sci.,Polym.Phys.Ed.*, **20**, 1609 (1982).

42. D.J. Bennett, *Honours Thesis*, University of Adelaide, (1985).

43. P.E.M.Allen, G.P.Simon, D.R.G.Williams and E.H.Williams, *Eur. Polym. J.*, **22**, 549 (1986).

44. P.E.M.Allen, G.P.Simon, D.R.G.Williams and E.H.Williams, *Macromolecules*, **22**, 809 (1989).

45. J.Kolarik, *Adv. Polym. Sci.*, **46**, 119 (1982).

46. O.Wichterle and R.Chromecek, *J. Polym. Sci.*, **C16**, 1677 (1969).

REFERENCES

CHAPTER FOUR

1. N.G.McCrum, B.E.Read and G.Williams, *Anelastic and Dielectric Effects in Polymeric Solids*, Wiley, London (1967).

2. J.Kolarik and J.Janacek, *J Polym. Sci.*, A-2,**10**,11 (1972).

3. J.Kolarik, J.Polym. Sci., **21**, 2445 (1983).

4. J.Kolarik, *J. Macromol. Sci., Phys.*, **B5**, 355 (1971).

5. G.E.Roberts and E.F.Waite, *The Physics of Glassy Polymers*, R.N.Haward Ed., Wiley, New York,1973:p153.

6. P.E.M.Allen, G.P.Simon, D.R.G.Williams and E.H.Williams, *Macromolecules*,**22**, 809 (1989).

7. A.L.Andrady and M.D.Sefcik, *J. Polym. Sci., Polym.Phys.Ed.*, **21**, 2453 (1983).

8. M.Felisberti, L.L. de Lucca Freitas and R.Stadler, *Polymer*,**31**, 1441 (1990).

9. G.C.Martin, R.K.Mehta and S.E.Lott, *Polym. Prepr.*, **22(2)**, 319 (1981).

10. G.P.Simon, *PhD Thesis*, University of Adelaide, (1985).

11. A.J.Kovacs, *Adv. Polym. Sci.*, **3**, 396 (1963).

12. T.G.Fox, *Bull. Am. Phys. Soc.*, **1**, 123 (1953).

13. M.Gordon and J.S.Taylor, *J. Appl. Chem.*, **2**, 493 (1952).

14. F.N.Kelly and F. Bueche, *J. Polym. Sci.*, L549 (1961).

15. E.A.DiMarzio and J.H.Gibbs, *J. Polym. Sci.*, **A-1**,1417 (1963).

16. E.A.DiMarzio and J.H.Gibbs, *J. Polym. Sci.*, **XL**, 121 (1959).

17. J.M.Pochan, C.L.Beatty and D.F.Pochan, *Polymer*, **20**, 879 (1979).

18. P.R.Couchman, *Macromolecules*, **11**, 1156 (1978).

19. P.R.Couchman, *Macromolecules*, **13**, 1272 (1980).

20. T.S.Ellis and F.E.A.Karasz, *Polymer*, **25**, (1984).

21. H.Fujita and A.Kishimoto, *J. Polym. Sci.*, **28**, 547 (1958).

22. R.F.Boyer and R.S.Spencer, *J. Polym. Sci.*, **2**, 157 (1947).

23. W.Kauzmann and H.Eyring, *J. Amer. Chem. Soc.*, **62**, 3113 (1940).

24. S.N.Zhurkov, *CR. Acad. Sci.,USSR*, **47**, 475 (1945).

25. M.C.Shen and A.V.Tobolsky, *Adv. Chem. Ser.*, **48**, (1965).

26. M.Sugisaki, H.Sugg and S.Seki, *Bull.Chem. Soc. Jpn.*, **41**, 2591 (1968).

27. C.A.Angell, J.M.Sare and E.J.Sare, *J. Phys. Chem.*, **82**, 2529 (1978).

28. R.P.Kambour, C.L.Gruner and E.E.Romagosa, *J. Polym. Sci., Polym Phys. Ed.*, **11**, 1879 (1973).

29. G.P.Johari, A.Hallbrucker and E.Mayer, *Nature*, **330**, 552 (1987).

30. D.Katz and A.V.Tobolsky, *J. Polym. Sci.*, **A2**, 1595 (1964).

31 A.V.Tobolsky, D.Katz, M.Takahashi and R.A.Schaffhauser, *J. Polym. Sci.*, **A2**, 2749 (1964).

32. L.E.Nielsen, *Rev. Macromol. Chem.*, **4**, 69 (1970).

33. P.J.Flory, *Principles of Polymer Chemistry*, Cornell University Press, Ithaca, New York (1953).

34. H.B.Lee and D.T.Turner, *ACS Organic Coatings and Plastics Chem.*, **38(1)**, 311 (1978).

35. G.C.Martin and M.Shen, *Polym. Prepr.*, **20(1)**, 786 (1979).

36. A.R.Schultz, *J. Amer. Chem. Soc*, **80**, 1854 (1958).

37. S.Loshaek, *J. Polym. Sci.*,**15**, 391 (1955).

38. M.B.Moran and G.C.Martin, *Polym. Prepr.*, **24(2)**, 141 (1983).

39. G.P.Johari, *Philos. Mag.*, **35**, 1077 (1977).

40. J.Heijboer, Int. *J. Polym. Mater.*, **6**, 11 (1977).

41. J.M.G.Cowie, *J. Macromol. Sci., Phys.*, B18, 569 (1980).

42. G.P. Johari and M.J.Goldstein, *J. Chem. Phys.*, **53**, 2372 (1970).

43. G.P. Johari and M.J.Goldstein, *J. Chem. Phys.*, **55**, 4245 (1971).

44. G.P. Johari, *J. Chem. Phys.*, **58**, 1766 (1973).

45. G.P. Johari, *J. Chem. Phys.*, **77**, 4619 (1982).

46. J.M.G.Cowie and R.Ferguson, *Polymer*, **28**, 503 (1987).

47. J.Heijboer, J.M.A.Baas, B.van de Graaf and M.A.Hoefnagel, *Polymer*, **28**, 509 (1987).

48. J.Kolarik, *Adv. Polym. Sci.*, **46**, 119 (1982).

49. Z.H.D.Chernova, T.D.Glumova, M.F.Lebedeva, Ye.V.Kruchinina, L.V.Krasner, L.S.Andrianova, S.K.Zakharov, T.I.Burisova and G.P.Beloniskaya, *Vsokomol. Soyed.*, **A23(10)**, 244 (1981).

50. H.E.Bair, G.C.Johnson and R.Merriweather, *J. Appl.Phys.*, **49(10)**, 4976 (1978).

51. J.Shen, C.C.Chen and J.A.Sauer, Abstracts IUPAC, Macro'85, "Structure and Properties", Section 4, 279, Bucharest (1984).

52. C.C.Chen, J.Shen and J.A.Sauer, *Polymer*, **26**, 511 (1985).

53. A.A.Berlin and N.G.Matvejeva, *J. Polym. Sci-Macromol. Rev.*, **15**, 107 (1980).

54. A.A.Berlin, *Vsokomol. Soyed.*, **A20(3)**, 483 (1978).

55. V.N.Gulyatsev, Yu.M.Sivergin, Yu.V.Zelenev, *Plaste. und Kautsch*, **10**, 740 (1971).

56. V.N.Gulyatsev, Yu.M.Sivergin, Yu.V.Zelenev, *Plaste. und Kautsch*, **11**, 802 (1973).

57. W.Gall and N.G.McCrum, *J. Polym. Sci.*, **50**, 489 (1961).

58. P.E.M.Allen, S.Hagias, G.P.Simon, E.H.Williams and D.R.G.Williams, *Polym. Bull.*, **15**, 359 (1986).

59. G.Khozin, A.A.Polyanskii, Yu.M.Budnik and V.A.Voskrenskii, *Vsokomol. Soyed.*, **A24(1)**, 2308 (1982).

60. G.V.Korolev and A.A.Berlin, *Vsokomol. Soyed.*, **A4(11)**, 1654 (1962)

REFERENCES

CHAPTER FIVE

1. P.H.Corkhill, A.M.Jolly, C.O.Ng and B.J.Tighe, *Polymer*, **28**, 1758 (1987).

2. J.I.Mardel, *Honours Thesis*, University of Adelaide (1989).

3. L.D.Kuntz and W. Kauzman, *Adv. Protein Chem.*, **28**, 239 (1974).

4. J.A.Bouwstra, J.C.van Miltenberg, W.E.Roorda and H.E.Junginger, *Polym. Bull.*, **18**, 337 (1987).

5. H.Yasuda, H.G.Olf, B.Crist, C.E.Lamaze and A.Peterlin, in "*Water Structure at the Water-Polymer Interface*," H.H.G.Jellinek,Ed., Plenum Press, New York (1975)..

6. R.A.Nelson, *J. Appl. Polym. Sci.*, **21**, 645 (1977).

7. P.H.Corkhill and B.J.Tighe, *Polymer*, **33**, 1526 (1990).

8. D.G.Pedley and B.J.Tighe, *Br. Polym. J.* ,**11**, 130 (1979).

9. N.Murase, K.Gonda and T.Watanabe, *J. Phys. Chem.*, **90**, 5421 (1986).

10. G.S.Smyth, F.X.Quinn and V.J.McBrierty, *M acromolecules,* **21**, 3198(1988).

11. T.Hori, *Low Temp. Sci. Ser. A*, **A15**, 34 (1956).

12. J.Clifford and G.K.Rennie, *J.Chem. Soc., Faraday Trans 1*, **73**, 680 (1977)

13. F.H.Stillinger, in *Water in Polymers*, S.P.Rowland Ed., Washington, pp11-21 (1980).

14. F.X.Quinn, E.Kampff, G.Smyth and V.J.McBrierty, *Macromolecules*, **21**, 3191 (1988).

15. N.Murase, M.Shiraishi, S.Koga and K.Gonda, *Cryo-Lett.*, **3**, 251 (1982).

16. G.P.Simon, *PhD Thesis*, University of Adelaide (1986).

17. I.M.Ward, Mechanical Properties of Solid Polymers, Wiley-Interscience, London (1971).

18. K.Naito, G.E.Johnson, D.L.Allara and T.K.Kwei, *Macromolecules*, **11**, 1260 (1978).

REFERENCES
CHAPTER SIX

1. J.Maquet, H.Theveneau, M.Djabourov, J.Leblond and P.Papan, *Polymer*, **27**, 1103 (1986).

2. B.Nystrom, M.E.Moseley, W.Brown and J Roots, *J. Appl. Polym. Sci.*, **26**, 3385 (1981).

3. J.E.Carles and A.M Scallan, *J. Appl. Polym. Sci.*, **17**, 1855 (1973).

4. K.Erdmann and A.Gutsze, *Coll. Polym. Sci.*, **265**, 667 (1987).

5. K.Munn and D.M.Smith, *J. Colloid Interface Sci.*, **119**, 117 (1987).

6. S.Hagias, Personal Communication.

7. E.D.Becker, High Resolution NMR: Theory and Chemical Applications, 2nd Edition, Academic Press (1980).

8. M.F.Refojo and H.Yasuda, *J. Appl. Polym. Sci.*, **9**, 2425 (1965).

9. A.Yamada-Nosaka, K.Ishikiriyama, M.Todaki and H.Tanzawa, *J. Appl. Polym. Sci.*, **39**, 2423 (1990).

10. R.Sporer and A.J.Vega, *J. Polym. Sci.*, **12**, 645 (1974).

11. K.Matsumara, K.Hayamizu, T.Nakane, H.Yanagishita and O.Yamamoto, *J. Polym. Sci.*, **25**, 2149 (1987).

12. Y.K.Sung, D.E.Gregonis, M.S.John and J.D.Andrade, *J. Appl. Polym. Sci.*, **26**, 3719 (1981).

13. J.I.Mardel, *Honours Thesis*, University of Adelaide (1989).

14. P.H.Corkhill, A.M.Jolly, C.O.Ng and B.J.Tighe, *Polymer*, **28**, 1758 (1987).

REFERENCES

CHAPTER SEVEN

1. R.A.Komoroski Ed., *High Resolution NMR Spectroscopy of Synthetic Polymers in Bulk*, VCH: Weihheim (1986).

2. G.P.Simon, *PhD Thesis*, University of Adelaide (1986).

3. D.J.Bennett, *Honours Thesis*, University of Adelaide(1985).

4. P.E.M.Allen, G.P.Simon, D.R.G.Williams and E.H.Williams, *Polym. Bull.*, **11**, 593 (1984).

5. A.B.Clayton, *Honours Thesis*, University of Adelaide (1988).

6. M.E.Gal, G.R.Kelly and T.Kurucsev, *J. Chem. Soc, Faraday Trans. II*, **69**, 395 (1973).

7. M.D.Sefcik, J.Schaefer, E.O.Stejskal and R.A.McKay, *Macromolecules*, **13**, 1132 (1980).

8. L.C.Dickinson, P.Morganelli, C.W.Chu, Z.Petrovic, W.J.McKnight and J.W.Chien, *Macromolecules*, **21**, 338 (1988).

9. T.P.Huijgen, H.Angad Gaur, T.L.Weeding, L.W.Jenneskens, H.E.C.Schuurs, W.G.B.Huysmans and W.S.Veemans, *Macromolecules*, **23**, 3063 (1990).

10. M.D.Meadows, C.P.Christenson, W.L.Howard, M.A.Harthcock, R.E.Guerra and R.B.Turner, *Macromolecules*, **23**, 2440 (1990).

11. J.Mardel, *Honours Thesis*, University of Adelaide (1989).

12. J.Schaefer, E.O.Stejskal and R.Buchdahl, *Macromolecules*, **10**, 384 (1977).

13. J.Schaefer, E.O.Stejskal, T.R.Steger, M.D.Sefcik and R.A.McKay, *Macromolecules*, **13**, 1121 (1980).

14. D.A.Torchia and A.Szabo, *J. Magn. Reson.*, **49**, 109 (1982).

15. J.Schaefer, M.D.Sefcik, E.O.Stejskal and R.A McKay, *Macromolecules*, **17**, 1118 (1984).

16. F.Laupretre, L.Monnerie and J.Virlet, *Macromolecules*, **17**, 1397 (1985).

17. W.W.Flemming, J.R.Lyerla and C.S.Yannoni, *ACS Symp. Ser.*, No.247, 83 (1984).

18. W.W.Flemming, J.R.Lyerla and C.S.Yannoni, *ACS Symp. Ser.*, No. 203, 455 (1983).

19. L.A.Belfiore, P.M.Henricks, D.J.Massa, N.Zumbalyadis, W.P.Rothwell and S.L.Cooper, *Macromolecules*, **20**, 175 (1983).

20. P.E.M.Allen, G.P.Simon, D.R.G.Williams and E.H.Williams, *Macromolecules*, **22**, 809 (1989).

21. J.Schaefer and E.O.Stejskal, *Top. Carbon-13 NMR Spectrosc.*, **3**, 284 (1979).

22. L.B.Alemany, D.M.Grant, R.J.Pugmire, T.D.Alger and K.W.Zilm, *J. Am. Chem. Soc.*, **105**, 2133, 2142 (1983).

23. A.A.Parker, J.J.Marcinko, Y.T.Shieh, C.Shields, D.P.Hendrick and W.M.Ritchey, *Polym. Bull.*, **21**, 229 (1989).

24. J.Matisons, Personal Communication.

25. A.B.Clayton, Personal Communication.

26. T.Hjertberg, T.Hargitai and P.Reinholdsson, 23, 3080 (1990).